METALLOCENE CATALYZED BRANCHED POLYOLEFIN COPOLYMERS

by

MONJA GELDENHUYS

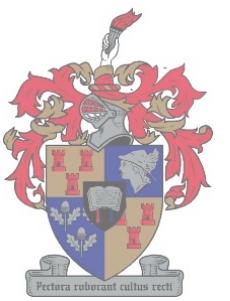

Thesis presented for the degree of

Master of Science (Polymer Science)

at the

University of Stellenbosch

Study Leaders:
Prof. R.D. Sanderson
Dr. R. Brüll

Stellenbosch
December 1999

DECLARATION

I, the undersigned hereby declare that the work contained in this thesis is my own original work and has not previously in its entirety or in part been submitted at any university for a degree.

ABSTRACT

This study concerns the copolymerization of ethylene and propylene with 1-pentene using metallocene-based zirconium catalysts. A thorough study on the background of the copolymerizations of 1-pentene with ethylene and propylene was done.

The metallocene catalyst that was used in the copolymerization of ethylene with 1-pentene was the isospecific *rac*-[ethylene *bis*(1-indenyl)]zirconium dichloride (*rac*-Et(Ind)$_2$ZrCl$_2$) catalyst, and in the copolymerization of propylene with 1-pentene the silylene-bridged catalyst, *rac*-Me$_2$Si(2-MeBenz[e]Ind)$_2$ZrCl$_2$. Methylalumoxane (MAO) was used as cocatalyst in all the polymerizations.

Characterization of these copolymers included determinations of the thermal properties, microstructures, molecular masses and molecular mass distributions. In particular the relationship of the amount of 1-pentene incorporated in the copolymers on the thermal properties was investigated. The short-chain branching of these copolymers was investigated by crystallization analysis fractionation (CRYSTAF).

OPSOMMING

Hierdie studie behels die kopolimerisasie van etileen en propileen met 1-pentene deur van homogene metalloseenkatalisatore gebruik te maak. 'n Deeglike studie oor die agtergrond van die kopolimerisasie reaksies van 1-pentene met etileen en propileen is gedoen.

Die metalloseenkatalisatore wat gebruik is vir die kopolimerisasie van etileen met 1-penteen en propileen met 1-penteen is die isospesifieke *rac*-[etileen *bis*(1-indeniel)] zirkonium dichloried (*rac*-$Et(Ind)_2ZrCl_2$) katalisator en die silileen-gebrugde katalisator, *rac*-$Me_2Si(2\text{-}MeBenz[e]Ind)_2ZrCl_2$, respektiewelik. Metielalumoksaan (MAO) is as ko-katalisator in al die polimerisasie reaksies gebruik.

Karakterisering van die kopolimere het die berekening van die termiese eienskappe, mikrostrukture, molekulêre massas en molekulêre massa verspreidings behels. Daar is veral gekyk na die invloed van die hoeveelheid 1-penteen geïnkorporeer op die termiese eienskappe van die kopolimeer. Die kort-kettingvertakkings van die kopolimere is ondersoek deur die kristallisasie analise fraktioneringstegniek (CRYSTAF).

This thesis is dedicated to

my father Johann and my mother Martie,

for always believing in me, and for their love and support.

ACKNOWLEDGEMENTS

I wish to express my very sincere thanks to:

Prof. R.D. Sanderson, Director of the Institute for Polymer Science, University of Stellenbosch, for his enthusiasm, encouragement and help throughout this study.

Dr. R. Brüll for his encouragement and assistance during this study.

Dr. A.J. van Reenen for all his advice and fruitful discussions held during this study.

Dr. M. Pohlmann and Dr. U. Wahner for their active involvement during the first year of this study.

Polifin for financial support and for chemicals provided for this study.

Dr. F. du Toit, my mentor at Polifin, for his encouragement and assistance throughout this study.

Dawie Joubert, Principal Scientist, Sastech, Sasol, for his advice and for the haze measurements of the propylene/1-pentene copolymers.

Prof. H. Pasch, for the all the GPC and CRYSTAF analyses done during this study.

Deon Bezuidenhout for allowing me to use his laboratories for the preparation of the propylene/1-pentene copolymer films.

Mr. H.S.C. Spies and Mr. J. Greyvenstein for all the NMR analyses done during this study.

Bertus Smit for all his advice and for the infrared spectroscopy analyses done during this study.

Derreck McCauley and Dirk Reyskins for all the melting point determinations carried out for this study.

Dr. M.J. Hurndall for the proof-reading of this thesis.

A word of thanks to all my friends at the Institute for Polymer Science, whithout whom the last two years would not have been the same; **Marcelle Hodgson, Marissa Opperman, Elna Diederiks, Liezel Coetzee, Marietjie Coetzee, Sven Graef, James McCleary, Malan Calitz, André van Zyl, Ewan Sprong and Cor Beyers**.

Also a special word of thanks to my friends who always supported and encouraged me; **Marietjie van der Merwe, Suzanne Hauman, Joelynn Mouton, Suzanne van Niekerk and Roné Stander**.

Jaco, for being my best friend and for making this year very special.

Special thanks for the love and support of my family.

LIST OF FIGURES

CHAPTER 2

CHAPTER 3

CHAPTER 4

CHAPTER 5

CHAPTER 6

LIST OF TABLES

CHAPTER 2

CHAPTER 3

CHAPTER 4

CHAPTER 5

CHAPTER 6

LIST OF CONTENTS

CHAPTER 1

Introduction and objectives

1.1 INTRODUCTION

'Ziegler-Natta catalysts' is a term that describes a large variety of transition metal-based catalysts capable of polymerizing and copolymerizing α-olefins and dienes. The products of these polymerization reactions (poly(α-olefins), polydienes and α-olefin copolymers) are commercially produced in very large volumes and have numerous applications as general-purpose and engineering plastics. Ziegler-Natta catalysts have different active sites and there is poor control of comonomer incorporation, leading to the production of heterogeneous polymers. The products obtained with heterogeneous Ziegler-Natta catalysts are mixtures containing polymer molecules of differing stereoregularity. In the copolymers made with Ziegler-Natta catalysts, the amount of comonomer incorporated and the regular placement of the comonomer along the polymer chain can not be controlled. The comonomer can act as a chain transfer agent and could cause a broad molecular mass distribution.

Metallocene-based catalysts, including the so-called "single-site" catalysts, are bicomponents consisting of group 4 transition metal compounds and cocatalysts. They generate only one kind of active center and therefore are the only catalysts that can be used to control both the molecular mass and the microstructure (tacticity, regioregularity and comonomer distribution) of polyolefins. Their use therefore leads to homogeneous copolymers of narrow molecular mass distributions and it is likely that the metallocene-type catalysts will become of greater importance to the polyolefin industry.

1-Pentene is a major byproduct of the South African Fischer-Tropsch process of SASOL- the process by which synthesis gas (syngas) is manufactured from coal. The use of 1-pentene as a comonomer in the copolymerization of ethylene or propylene could be an excellent way of using this byproduct in a constructive way.

1.2 OBJECTIVES

The main objective of this work was to synthesize and characterize short-chain branched copolymers prepared with metallocene-based catalysts. In particular, the effect of 1-pentene on the properties of ethylene/1-pentene and propylene/1-pentene copolymers was investigated. In order to achieve high molecular mass ethylene/1-pentene and propylene/1-pentene copolymers, the catalysts selected for this study were the ethylene-bridged metallocene *rac*-$Et(Ind)_2ZrCl_2$, and the homogeneous silylene-bridged catalyst *rac*-$Me_2Si(2\text{-}MeBenz[e]Ind)_2ZrCl_2$. Methylalumoxane (MAO) was used as cocatalyst in all the polymerizations. The resultant ethylene/1-pentene and propylene/1-pentene copolymers were characterized by differential scanning calorimetry (DSC), nuclear magnetic resonance (NMR) spectroscopy, gel permeation chromatography (GPC), infrared (IR) spectroscopy and crystallization analysis fractionation (CRYSTAF). The effect of 1-pentene on the properties of these copolymers was investigated as very little has been reported on the copolymerization of ethylene or propylene with odd numbered α-olefins.

1.3 STRUCTURE OF MANUSCRIPT

For the sake of simplicity and economy of words, the wording used in this thesis 'polymers produced by the catalyst $Et(Ind)_2ZrCl_2$' actually means the polymers which were prepared during a reaction in which $Et(Ind)_2ZrCl_2$ was used as catalyst.

Chapter 2 gives a historical and theoretical overview of the research, which has been done on ethylene and propylene copolymers, using different comonomers, with different metallocene catalyst systems.

Chapter 3 describes the copolymerization of ethylene with 1-pentene using the isotactic stereorigid zirconium metallocene $Et(Ind)_2ZrCl_2$, together with the cocatalyst methylalumoxane (MAO). A significant fraction of MAO acts as an impurity scavenger, therefore increasing the activity of the metallocene catalyst. Characterization of these copolymers included determinations of the melting points

(by DSC), microstructure (by NMR spectroscopy), molecular masses and molecular mass distributions (by GPC).

Propylene/1-pentene copolymers were prepared with the $Et(Ind)_2ZrCl_2$/MAO catalyst system. Results of their characterization showed that only low molecular mass copolymers were obtained, as described in Chapter 4. An alternate catalyst system was used in efforts to improve the molecular mass of the propylene/1-pentene copolymers. Chapter 5 describes the synthesis of high molecular mass propylene/1-pentene copolymers with the homogeneous *rac*-$Me_2Si(2\text{-MeBenz[e]Ind})_2ZrCl_2$/MAO catalyst.

The ethylene/1-pentene copolymers, prepared with the $Et(Ind)_2ZrCl_2$/MAO catalyst system, and the propylene/1-pentene copolymers, prepared with the $Me_2Si(2\text{-MeBenz[e]Ind})_2ZrCl_2$/MAO catalyst system, were characterized by a recently developed crystallization technique, crystallization analysis fractionation (CRYSTAF). This is an unique approach to monitor the solution crystallization of a polymer and by monitoring the polymer solution concentration during crystallization, the cumulative and differential short-chain branching (SCBD) of the copolymers can be obtained without the need for the physical separation of fractions.

CHAPTER 2

Metallocene catalyzed ethylene/1-pentene and propylene/1-pentene copolymers: historical and theoretical background

2.1 HISTORICAL BACKGROUND

2.1.1 Introduction

Metallocene catalysts for olefin polymerization were discovered by Breslow and Natta soon after the original discovery of Ziegler Natta catalysts[1, 2]. Metallocene catalysts are bicomponents consisting of group four transition metal compounds and cocatalysts. Titanocenes were the first metallocene catalysts that afforded the synthesis of ethylene copolymers with 1-butene[3] and propylene[4], with a high degree of compositional uniformity. Unfortunately, these catalyst systems are only moderately active, and the molecular masses of the copolymers they produce rapidly decrease with an increase in the α-olefin content[3, 4]. In 1976 German scientists Kaminsky and Sinn developed a new class of metallocene catalysts that exhibit extremely high activity[5, 6, 7]. These catalysts and their subsequent modifications presently compete with Ziegler-Natta catalysts for many commercial applications. The evolution of metallocene catalyst structures for olefin polymerization until 1984 is tabulated in Table 2.1[8]. Since 1985, a rapid, worldwide industrial and academic development began in the field of metallocene catalysts, which continues today.

In the early 1980s Brintzinger and coworkers synthesized racemic ethylene-bridged *bis*(indenyl)zirconium dichloride, $Et(Ind)_2ZrCl_2$, and racemic ethylene-bridged *bis*(4,5,6,7-tetra-hydroindenyl) zirconium dichloride, $Et(H_4Ind)_2ZrCl_2$[9], as well as their titanium analogues, $Et(Ind)_2TiCl_2$ and $Et(H_4Ind)_2TiCl_2$[10], which have both meso and racemic configurations. The sterically rigid chiral $Et(Ind)_2ZrCl_2$ and $Et(H_4Ind)_2ZrCl_2$ catalysts activated with methylalumoxane (or methylaluminoxane, MAO) catalyzed the stereoselective polymerization of propylene with very high activities. This was the first time that isotactic polyolefins were obtained from homogeneous Ziegler-Natta polymerizations. This demonstrated stereochemical control by the chiral *ansa*-indenyl ligands on the transition metal ion in the selection

of one of the two enantiotropic faces (re or si) of a prochiral vinyl monomer in migratory insertion. In 1988 Ewen *et al.*[11] synthesized a C_s-symmetric zirconocene ($[Me_2C(Flu)(Cp)]ZrCl_2$) which produces syndiotactic polypropylene in high quantities.

Table 2.1. Historical developments in the field of metallocene research

1952	Development of the structure of metallocenes (ferrocene) by Fischer and Wilkinson	Ref.12
1955	Metallocene as component of Ziegler-Natta catalysts, low activity with common aluminium alkyls.	Ref.1
1973	Addition of small amount of water to increase the activity ($Al:H_2O$ = 1:0.05 up to 1:0.3) (Reichert, Meyer and Breslow)	Ref.13, Ref.14
1975	Unusual increase in activity by adding water at the ratio $Al:H_2O$ = 1:2 (Kaminsky, Sinn and Motweiler)	Ref.15
1977	Using separately prepared methylalumoxane (MAO) as cocatalyst for olefin polymerization. (Kaminsky and Sinn)	Ref.5
1982	Synthesis of *ansa* metallocenes with C_2 symmetry (Brintzinger)	Ref.3
1984	Polymerization of propylene using a *rac/meso* mixture of *ansa* titanocenes lead to partially isotactic polypropylene. (Ewen)	Ref.11
1984	Chiral *ansa* zirconocenes produce highly isotactic polypropylene (Kaminsky and Brintzinger)	Ref.6

In the field of the copolymerization of linear α-olefins, new possibilities for controlling the properties of copolymers have emerged through the development of homogeneous, chiral metallocene catalysts. Results of early studies revealed that these catalysts polymerize propene and higher α-olefins at a moderately lower rate than ethylene[16-19]. Accordingly, copolymers obtained with these catalysts contain larger fractions of higher olefins than those obtained with heterogeneous catalysts, under comparable conditions[20-27]. Results of later studies, particular by the groups of Zambelli[28-31], Chien[32-37], Soga[38] and Kashiwa[39, 40] showed that copolymers produced by metallocene-based catalysts consist of uniform chains with narrow molecular mass distributions typical of single-site catalysts (see Figure 2.1).

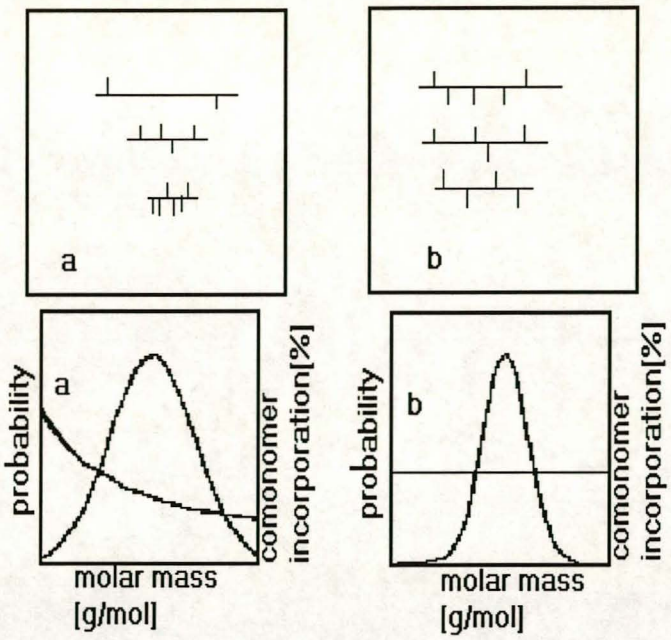

Figure 2.1. Molar mass distribution and comonomer incorporation of multi-site Ziegler-Natta catalysts (a), compared to single-site metallocene based catalysts (b)[41].

(a)Copolymers consist of a complex mixture of homo- and copolymers with comonomers frequently incorporated in the low molar mass fractions, broad molar mass distribution (M_w/M_n = 5-40). (b)Uniform comonomer incorporation, narrow molar mass distribution ($M_w/M_n \approx 2$).

2.1.2 Advantages and disadvantages of metallocene alumoxane catalysts

The major advantages of these homogeneous metallocene alumoxane (MAO) catalysts are:

(a) they have high catalytic activities

(b) small quantities of catalyst are required

(c) they have the ability to polymerize a wide variety of monomers, by suitably changing the ligands around the transition metal

(d) they produce polymers with narrow molecular mass distributions approaching the theoretical value of 2.0 as predicted by the Schultz-Flory mechanism, and

(e) they are able to polymerize α-olefins with almost any desired stereospecificity.

Disadvantages of these catalyst systems are:

(a) decay-type kinetics are evident with ethylene/higher α-olefin mixtures

(b) high Al/Zr ratios are required for obtaining high catalytic activity and a relatively stable kinetic profile

(c) the high cost of methylalumoxane (MAO)

(d) the short shelf lifetime of methylalumoxane

(e) the inability of catalysts to be used in slurry or gas phase processes, and

(f) only poor control can be exercised over polymer morphology.

2.1.3 Ethylene copolymers

Copolymers of ethylene with 1-hexene and 1-octene are important commercial resins. Much research has therefore been done on their copolymerization, using Ziegler-Natta as well as metallocene catalysts[42-45]. Wang *et al.*[46] and Quijada *et al.*[47, 48] compared the activities of metallocene complexes in ethylene/α-olefin copolymerization reactions. Their results showed that bridged metallocene complexes are more active in copolymerization than the nonbridged complexes are. The relative activities of some metallocene complexes can be seen in Table 2.2[49].

Table 2.2. Relative activities of metallocene complexes in ethylene/α-olefin copolymerization reactions[a] [46]

Catalyst	Activity, g/molZr·h·P_M[b]	Weight-average molecular mass(M_w)	Molecular mass distribution (M_w/M_n)	Monomer content C_M, [mol%][c]
Ethylene/1-hexene copolymerization				
Cp_2ZrCl_2	72,700	207,000	2.3	0.54
Ind_2ZrCl_2	154,100	146,000	2.7	1.02
$C_2H_4(Ind)_2ZrCl_2$	421,000	85,000	2.3	1.06
$Me_2Si(Ind)_2ZrCl_2$	341,000	85,000	2.3	1.40
Ethylene/1-octene copolymerization				
Cp_2ZrCl_2	93,600	119,000	2.3	0.51
Ind_2ZrCl_2	147,100	143,000	2.8	0.91
$C_2H_4(Ind)_2ZrCl_2$	532,600	83,000	2.2	1.12
$Me_2Si(Ind)_2ZrCl_2$	546,500	83,000	2.2	1.30

[a]Copolymerization in hexane at 75°C, [α-olefin]: 0.1M, ethylene pressure: 4.0bar, cocatalyst: MAO, [Al]:[Zr] 1000, [Zr] 0.2×10^{-3} - 2×10^{-3}M

[b]Activity calculated per 6.8 bar of ethylene pressure

[c]Monomer content in copolymer

The metallocenes generally used in the synthesis of ethylene copolymers are bridged, unbridged, substituted and half-sandwich complexes. Examples of unbridged and bridged catalysts are shown in Figure 2.2.

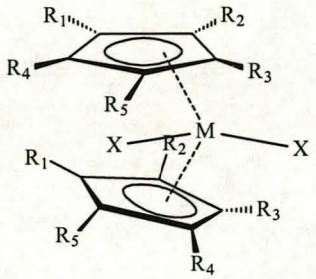

M = Ti, Hf, Zr. **I**

R = H, Methyl, Ethyl

X = Cl, Methyl

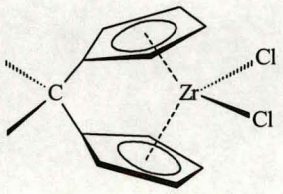

II

Figure 2.2. Schematic representation of unbridged (I) and bridged (II) metallocene catalysts.

The reason for the difference in activities between the bridged and nonbridged complexes is not known, but a possible explanation is an increase in the aperture angle of the two cyclopentadienyl rings in the bridged complexes and the increased accessibility of the zirconium atom in them for approaching olefin molecules[49]. Metallocene catalysts differ significantly from Ziegler catalysts in their abilities to copolymerize higher α-olefins with ethylene, as can be seen from the molecular masses in Table 2.2. The main features of metallocene complexes that affect olefin reactivity are: the type of transition metal (titanium, hafnium or zirconium) in the complex, the type and number of substituents in the cyclopentadienyl groups, and the presence of bridges between the two rings. Table 2.3 shows some examples of metallocene-alumoxane catalyst systems used for the copolymerization of ethylene with olefins.

Table 2.3. Examples of metallocene-alumoxane catalyst systems used for the copolymerization of ethylene with olefins

Catalyst	Comonomer	Reference
$Me_2Si(Ind)_2ZrCl_2$	1-Hexene	50
i-Pr[CpFlu] $ZrCl_2$	1-Hexene	50
$Me_2Si(Ind)_2ZrCl_2$	1-Dodecene	51
i-Pr[CpFlu] $ZrCl_2$	1-Octadecene	51
$C_2H_4(Ind)_2ZrCl_2$	Propene	52
$C_2H_4(Ind)_2ZrCl_2$	1-Hexene	52
$Me_2Si(2\text{-}MeBenz[e]Ind)_2ZrCl_2$	1-Octene	53
$Me_2Si(Ind)_2ZrCl_2$	1-Octene	54
$Me_2Si(2\text{-}MeInd)_2ZrCl_2$	1-Octene	54
$Me_2Si(2\text{-}MeBenz[e]Ind)_2ZrCl_2$	1-Octene	54

MAO used as cocatalyst throughout

2.1.4 Propylene copolymers

Limited information[55-61], compared to ethylene copolymers, is available concerning the copolymerization of propylene with other olefins. Those metallocene systems used for the copolymerization of propylene with α-olefins are shown in Table 2.4[62].

Table 2.4. Examples of metallocene-alumoxane catalyst systems used for the copolymerization of propylene with olefins

Catalyst	Comonomer	Reference
i-Pr[FluCp]$ZrCl_2$	1-Butene	55
$Me_2Si(Ind)_2ZrCl_2$	Ethylene	56
i-Pr(Cp)(Flu) $ZrCl_2$	5-Methyl-2-norborene	57
rac-$Me_2Si(Ind)_2HfCl_2$	Ethylene	58
[9,9'-*i*-$Pr(Flu)_2$] $ZrCl_2$	Ethylene	59
i-Pr(Cp)(Flu) $ZrCl_2$	Norbornene	60
$C_2H_4(Ind\text{-}H_4)_2ZrCl_2$	1-Hexene	61
$C_2H_4(Ind)_2HfCl_2$	1-Hexene	62
$C_2H_4(Ind)_2HfCl_2$	1-Octene	62
$C_2H_4(Ind)_2HfCl_2$	1-Dodecene	62
$C_2H_4(Ind)_2HfCl_2$	1-Hexadecene	62
i-Pr(Cp)Flu$ZrCl_2$	1-Butene	63
$C_2H_4(Ind)_2ZrCl_2$	1-Hexene	64
i-Pr(Cp)(Flu) $ZrCl_2$	Ethylene	65
i-Pr(Cp)(Flu) $ZrCl_2$	1-Butene	65
i-Pr(Cp)(Flu) $ZrCl_2$	1-Pentene	65
i-Pr(Cp)(Flu) $ZrCl_2$	1-Hexene	65
i-Pr(Cp)(Flu) $ZrCl_2$	4-Methyl-1-pentene	65
$Me_2Si(Ind)_2ZrCl_2$	1-Hexene	66
i-Pr[CpFlu] $ZrCl_2$	1-Hexene	67
Me_2Si(2-MeBenz[e]Ind)$_2ZrCl_2$[a]	1-Octene	68

MAO used as cocatalyst throughout, except in [a].

a). SiO_2/MAO used as cocatalyst.

Very little is reported on the copolymerization of ethylene or propylene with odd numbered α-olefins, such as 1-pentene, using metallocene catalysts. In 1997 Naga *et al.*[66] reported on the use of *i*-Pr(Cp)(Flu)$ZrCl_2$ for the preparation of five kinds of syndiotactic poly(propylene-co-olefin) (where olefin = ethylene, 1-butene, 1-pentene, 1-hexene, or 4-methyl-1-pentene).

2.2 REACTION MECHANISM OF THE PREPARATION OF COPOLYMERS PRODUCED BY METALLOCENE CATALYSTS.

2.2.1 Catalyst activation

Spectroscopic evidence[69, 70] is consistent with the assumption that Lewis acidic centers present in MAO are able to accept CH_3^- (or Cl^-) anions from the alkylated metallocene, thus generating a metallocene alkyl cation, the active polymerization species[71,72], and a poorly coordinating counteranion (Figure 2.3)[73].

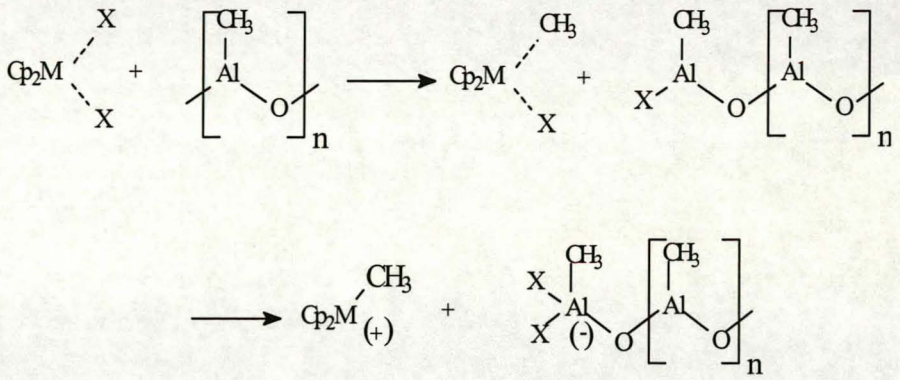

Figure 2.3. Formation of a metallocene alkyl cation (the active species) by the reaction between metallocene and methylalumoxane.

2.2.2 Propagation

The polymerization reaction starts when ethylene or an α-olefin molecule is inserted into the Zr-Me bond[70, 74, 75].

$$Cp_2Zr^+\text{-}Me + CH_2{=}CH_2 \rightarrow Cp_2Zr^+\text{-}CH_2\text{-}CH_2\text{-}CH_3 \qquad (1)$$

During copolymerization, two or more different α-olefin molecules are competitively inserted into the transition metal-carbon bonds of the active centers.

When two α-olefins, CH_2=CH-R' and CH_2=CH-R'', copolymerize, four chain-growth reactions (2-5) should be considered:

$$M\text{-}CH_2\text{-}CHR'\text{-}Polymer + CH_2{=}CH\text{-}R' \rightarrow M\text{-}CH_2\text{-}CHR'\text{-}CH_2\text{-}CHR'\text{-}Polymer \quad (2)$$

$$M\text{-}CH_2\text{-}CHR'\text{-}Polymer + CH_2{=}CH\text{-}R'' \rightarrow M\text{-}CH_2\text{-}CHR''\text{-}CH_2\text{-}CHR'\text{-}Polymer \quad (3)$$

$$M\text{-}CH_2\text{-}CHR''\text{-}Polymer + CH_2{=}CH\text{-}R'' \rightarrow M\text{-}CH_2\text{-}CHR''\text{-}CH_2\text{-}CHR''\text{-}Polymer \quad (4)$$

$$M\text{-}CH_2\text{-}CHR''\text{-}Polymer + CH_2{=}CH\text{-}R' \rightarrow M\text{-}CH_2\text{-}CHR'\text{-}CH_2\text{-}CHR''\text{-}Polymer \quad (5)$$

Reactions (2) and (4) represent homopolymerization growth processes (rate constants k_{11} and k_{22}), and the other two reactions (3) and (5) represent copolymerization processes (rate constants k_{12} and k_{21}). The values of the four rate constants in this reaction scheme are different, which means that the rate of the insertion reaction of a particular α-olefin into the Me-C bond depends not only on the structure of the α-olefin itself, but also on the structure of the last monomer unit attached to the transition metal atom before a given olefin-insertion reaction. In copolymerization reactions, the four rate constants are traditionally grouped into two ratios named reactivity ratios:

$$r_1 = k_{11}/k_{12} \text{ and } r_2 = k_{22}/k_{21}.$$

In copolymerization reactions of ethylene with other α-olefins or propylene with other α-olefins, ethylene and propylene is always much more reactive than the α-olefin, independent of the last monomer unit in the growing chain. Hence the r_1 value is always higher than 1 and the r_2 value is always lower than 1.

The insertion of an α-olefin in the metal-carbon bond may take place in two different ways[73]:

$$Zr\text{-}P + CH_2{=}CH\text{-}CH_3 \rightarrow \begin{cases} Zr\text{-}CH_2\text{-}CH(CH_3)\text{-}P \text{ (1,2 or primary insertion)} \\ Zr\text{-}CH(CH_3)\text{-}CH_2\text{-}P \text{ (2,1 or secondary insertion)} \end{cases} \quad (6)$$

It was proved, by chain-end group analysis, that the 1,2 insertion mode was evident in the isospecific polymerization of olefins with metallocene-based catalysts[28,76]. Isospecific PP, obtained with chiral C_2-symmetric group 4 metallocenes (for example $Et(Ind)_2ZrCl_2$), includes a small number (about 1%) of isolated regioirregular structural units resulting from the 1,2 and 1,3 insertion of the monomer, as follows:

$$-CH_2\text{-}CH(CH_3)\text{-}CH(CH_3)\text{-}CH_2\text{-}CH_2\text{-}CH(CH_3)\text{-} \quad \text{(2,1 insertion)} \quad (7)$$

$$-CH_2\text{-}CH(CH_3)\text{-}CH_2\text{-}CH_2\text{-}CH_2\text{-}CH_2\text{-}CH(CH_3)\text{-} \quad \text{(3,1 insertion)} \quad (8),$$

revealed by the presence of $(CH_2)_2$ and $(CH_2)_4$ groups respectively[31, 77, 78]. The content of the two regioirregularities and their relative proportion depends on the σ-ligands, polymerization temperature, and monomer concentration[79].

2.2.3 Termination

The polymer chains are usually terminated in two reactions, a β-hydride elimination reaction (9) and a chain transfer reaction to ethylene or an α-olefin molecule (10)[75, 79].

$$Cp_2Zr^+\text{-}CH_2\text{-}CH_2\text{-Polymer} \rightarrow Cp_2Zr^+\text{-}H + CH_2{=}CH\text{-Polymer} \quad (9)$$

$$Cp_2Zr^+\text{-}CH_2\text{-}CH_2\text{-Polymer} + CH_2{=}CHR \rightarrow Cp_2Zr^+\text{-}CH_2\text{-}CH_2R + CH_2{=}CH\text{-Polymer} \quad (10)$$

(R is H or an alkyl group)

2.3 FACTORS INFLUENCING COPOLYMERIZATION BEHAVIOR

The structures and properties of copolymers produced with metallocene catalysts can be changed by varying the following factors: (1) type of catalyst used, (2) [Al]/[Zr] ratios, (3) polymerization temperatures, (4) monomer feed ratios and (5) using different cocatalysts. Aspects of these variables are discussed here.

2.3.1. Catalyst used

Copolymerizations of ethylene/α-olefins or propylene/α-olefins with compositions covering the entire range of feasible copolymers ratios, were investigated as a function of metallocenes with different ligands, bridging groups and transition metal centers[36, 43, 47, 48, 53, 80-95]. The non-bridged catalysts are traditionally used in the polymerization of ethylene, whereas the bridged ones are used in the polymerization of propylene and higher α-olefins.

2.3.1.1 Steric control

In stereo- and regioselective metallocene-catalyzed propene polymerization, steric control depends primarily on metallocene structure, especially metallocene symmetry. Only C_2- and some C_1-symmetrical *ansa*-metallocenes produce isotactic polypropylene, whereas C_s-symmetrical metallocenes form either atactic or syndiotactic polypropenes[96, 97]. Metallocenes used in olefin polymerization have been classified on the basis of their symmetry (see Figure 2.4 and Table 2.5).

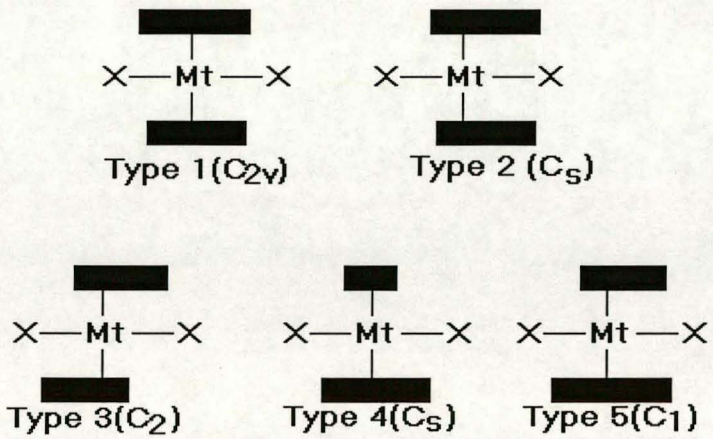

Figure 2.4. Schematic representation of the different metallocene complex structures.

Type 1, C_{2v} symmetry; Type 2, C_s symmetry; Type 3, C_2 symmetry; Type 4, C_s symmetry; Type 5, C_1 symmetry [98].

In Type 1, the two η^5-ligands (represented by shaded rectangles) can be bridged or not; whereas in the other classes they are bridged. In Types 1 and 2, the two active sites occupied by the η^5-ligands are bisected by a horizontal mirror plane and consequently are achirotopic and identical in Type 1 and different in Type 2. In the other types, the two sites are chirotopic; they are related by a two-fold rotation axis in Type 3 and are homotopic (equal). In Type 4, the two sites are related by a vertical mirror plane and are enantiotopic (mirror image to each other). No symmetry elements are present in Type 5, the two sites are diastereotopic (different).

Table 2.5: Relationship between metallocene symmetry and polymer structure [99]

Idealised symmetry	Metallocene type	Examples	Polymer microstructure
C_{2v}	1	Cp_2MCl_2, Cp_2*MCl_2[a]	Atactic
C_s	2	meso-EBIMCl_2[b]	Atactic
C_2	3	rac-EBIMCl_2[c]	Isotactic
C_s	4	$Me_2C(Cp)(Flu)MCl_2$[d]	Syndiotactic
C_1	5	$Me_2C(MeCp)(Flu)MCl_2$[e]	Hemiisotactic

[a]Cp = cyclopentadienyl; Cp* = pentamethylcyclopentadienyl; [b]meso-EBI = meso-ethylene *bis* indenyl; [c]rac-EBI = racemic-ethylene *bis* indenyl; [d]Flu = fluorenyl; [e]MeCp = 3-methylcyclopentadienyl.

2.3.1.2 Molecular mass

The molecular mass of ethylene/propylene copolymers is dependent on the metallocene structure of the catalyst used in the polymerization (see Figure 2.5). Brintzinger[78] and Spaleck[100-102] discovered, almost simultaneously, that benzannelation, and especially the 2-methyl substitution of silylene-bridged *bis*(indenyl)zirconocenes, leads to substantial increases in the molecular masses of propylene copolymers. In the family of silylene-bridged *bis*indenyl zirconocenes, benzannelation clearly promoted the random incorporation of 1-octene. This result was in accord with recent force field modelling studies done by Schneider and Prosenc[54], where benzannelation accounted for substantially lower differences of activation energy of 1-octene insertion subsequent to ethylene insertion or ethylene

subsequent to 1-octene, respectively. Although 2-methyl substitution did not effect randomness, it improved copolymer molar mass at the expense of catalytic activity.

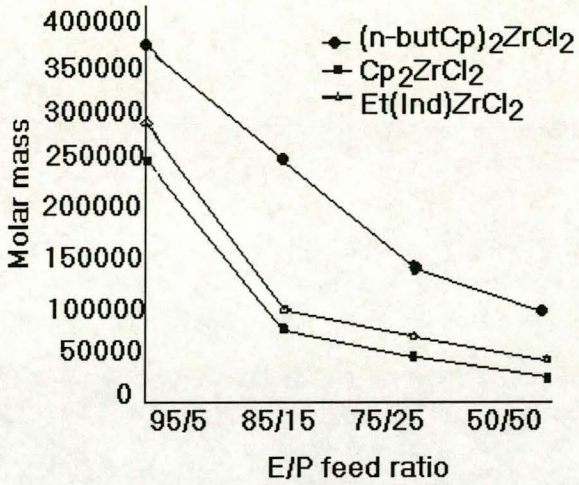

Figure 2.5. Molecular masses of the ethylene/propylene copolymers produced with (n-butylCp)$_2$ZrCl$_2$, Cp$_2$ZrCl$_2$ and Et(Ind)$_2$ZrCl$_2$ catalysts [103].

2.3.1.3 Co-/monomer incorporation

Copolymers obtained with metallocene catalysts contain higher amounts of higher α-olefins than those obtained with heterogeneous catalysts under similar conditions. In heterogeneous catalysts several active centers are present at the catalyst surface, and they show different selectivities towards the bulkier comonomer[65, 104-108]. Subsequently, the copolymers obtained are nonhomogeneous and can be separated into fractions having different compositions. Conversely, the copolymers produced by metallocene-based catalysts consist of chains with uniform monomer composition and narrow molecular mass distribution, typical of single-site catalysts[32-34, 36-40].

Monomer incorporation in the copolymerization of propylene with α-olefins can be promoted by using bridged cyclopentadienyl- or indenyl-ligands. Soga *et al.*[38] and Fink *et al.*[51, 109] reported that the syndiospecific catalyst Me$_2$C(Cp)(Flu)ZrCl$_2$ leads to much higher α-olefin incorporation compared to isospecific and non-stereospecific catalysts. According to Kaminsky *et al.*[42], substituting zirconium for hafnium in the catalyst appears to further improve comonomer incorporation.

2.3.2. [Al]/[Zr] ratios

In 1990 Resconi *et al.*[110] proposed that the actual cocatalyst in the metallocene-MAO system is $AlMe_3$ (TMA) itself, with MAO acting as a soluble carrier-activator of the ion-pair formed upon reaction of the metallocene with TMA[2].

In these catalyst systems the following reaction is believed to take place[111]:

$$Cp_2MX_2 + (\text{-AlMeO-})_n \rightarrow [Cp_2MCH_3]^+[X_2(\text{-AlMeO-})_n]^-$$

Recent findings suggest that MAO serves both as an alkylating agent and as a template for poorly coordinating anions[112-115]. Other studies of metallocenes used for stereoregular α-olefin polymerization showed that polymerization activities, stereoregularities, and polymer molecular masses were strongly dependent on the types of cocatalyst and their concentrations, suggesting strong, structure-sensitive ion-pairing effects[116-118].

The response of zirconocenes to changes in the [Al]/[Zr] ratio and MAO structure can be interpreted in terms of a mechanistic model involving ion pairs (see Figure 2.6) [39, 119, 120].

$$Cp_2MX_2 + nMAO \rightarrow [Cp_2M\text{-}CH_3]^+ \bullet X \bullet [X\text{-}MAO]^- \bullet [MAO]_{n-1}$$

Contact ion pair

$$[Cp_2M\text{-}CH_3]^+ \bullet X \bullet [X\text{-}MAO]^- \bullet [MAO]_{n-1} \rightarrow [Cp_2M\text{-}CH_3]^+ \parallel [X_2\text{-}MAO]^- \bullet [MAO]_{n-1}$$

Solvent separated ion pair

Figure 2.6. Ion-pair model [111].

It is postulated that as the MAO ratio increases, the MAO aggregates become larger, and the cationic species becomes further separated from the anions (see Figure 2.7). This less sterically hindered species is largely responsible for the enhanced activity. The extent of ion pairing is dependent on the structure of the zirconocene composition.

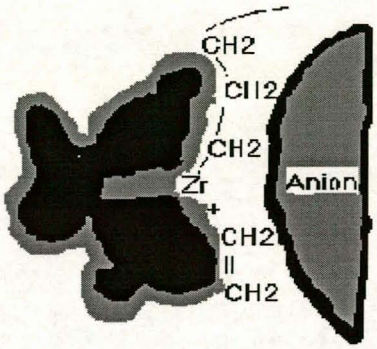

Figure 2.7. Ion-pair effects in metallocene catalysis [111].
The monomer moves through channels to the active site where it joins the growing polymer chain.

With BuCpZr(*bis*(n-butylcyclopentadienyl)zirconium dichloride) and InZ(*bis*(indenyl)zirconium dichloride) catalysts at lower MAO/Zr ratios, some contact ion pairs are formed. As the MAO/Zr ratio increases, these eventually become solvent-separated ion pairs. These "free" cations are responsible for the enhanced activity and improved comonomer response. The "free" cations should facilitate β-hydride elimination by creating a four-centered, coplanar transition state for chain transfer[111].

Weak ion-pair effects with the EBIZ(rac-ethylene*bis*(indenyl)zirconium dichloride) and SIZR-2(rac-dimethylsilylene*bis*(2-methylindenyl)zirconium dichloride) catalysts are postulated, based on the catalyst responses to Al/Zr ratios and changes in MAO structure. With EBIZ as a catalyst the extent of activity enhancement with Al/Zr ratio was much less than with the unbridged InZ[111].

The acceleration of the polymerization rate with metallocene catalysts in the presence of α-olefins may also be related to perturbations of the ion pair at the active site. α-Olefins can function not only as reactants but also as ligands at the active site and, in such a role, serve to reduce the extent of interaction of the cationic zirconium center and the alumoxane counteranion. The chemical nature of the counteranion can have a profound effect on polymerization activity and stereoregularity, with "inert", non-coordinating counteranions providing a route to higher activity[32, 118-120].

The catalytic productivity of the zirconocene-alumoxane catalyst system depends on the [Al]/[Zr] ratios. It is well known that a high excess of MAO is needed to achieve optimum polymerization activity with metallocene catalysts. It is likely that the excess of MAO converts all the metallocene molecules into active centers, but it is also proposed that it reconverts the inactive intermediates which form, into the active species by an alkyl exchange reaction[121]. Both these effects give rise to an increase in the population of active species, which accounts for the increased activity.

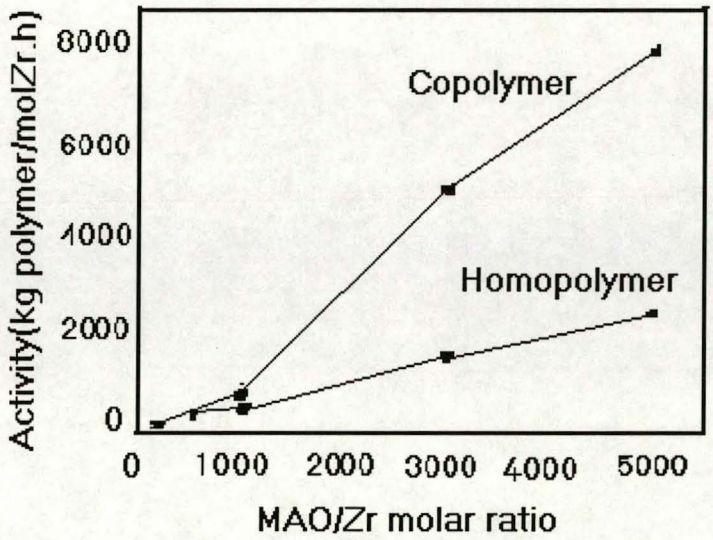

Figure 2.8. The trends in homo- and copolymerization activities obtained with different MAO/Zr ratios [122].

In 1997 Forlini *et al.*[122] showed that there is a high increase in activity for [Al]/[Zr] ratios between 1000 and 3000 (Figure 2.8), but it becomes slower at higher MAO concentrations. A clear increase in molecular masses is also observed in the homo- and copolymerization as the [Al]/[Zr] ratio increases. This indicates that there is an increase in the rate of propagation, which is higher than that of chain termination, due to the higher activity and/or stability of the catalytic complexes in the presence of MAO[122].

It was also found that an increase in the [Al]/[Zr] ratio did not have any influence on the homo- or copolymer microstructure. Therefore, the excess MAO, that leads to an increase in the number of active species and makes the catalyst more active, and

more stable, does not favour the insertion of a certain comonomer above another. (Reactivity ratios remain constant.)

2.3.3 Polymerization temperature

The temperature dependence of the copolymerization parameters of ethylene/propylene copolymers was investigated by Chien and Xu using *rac*-Et[Ind]$_2$ZrCl$_2$[37]. The copolymerization parameter of the bulkier α-olefin increased with increasing temperature. Mühlenbrock and Fink[109] reported temperature-dependent copolymerization parameters for ethylene/1-hexene copolymerization, opposite to those of Chien and Xu[37]. Suhm *et al.*[53] found that an increase in temperature or a decrease in ethylene concentration markedly influenced the copolymer's molecular mass, while for 1-octene incorporation in ethylene/1-octene copolymers it remained constant. They concluded that the solution enthalpy of the different monomers has a potential influence on copolymerization parameters. In the copolymerization of ethylene with 1-hexene or 1-octene, incorporation of 1-octene or 1-hexene increased with decreasing temperature, despite using different metallocenes and transition-metal to aluminium ratios for copolymerization.

2.3.4 Different monomer feed ratios

Koivumäki *et al.*[51] found that with the Me$_2$C(Cp)(Flu)ZrCl$_2$/MAO catalyst, above the [comonomer]/[ethylene] ratio of 1 the polymerization rate of ethylene: (1) increases markedly with 1-hexene, (2) increases slightly with 1-dodecene, and (3) decreases with 1-octadecene. The larger the comonomer the more difficult it is for the ethylene monomer unit to insert itself and the ethylene propagation reaction becomes slower. With the catalyst system *rac*-Et[IndH$_4$]$_2$ZrCl$_2$/MAO, the polymerization rate increased steadily, to a maximum at a [1-octadecene]/[ethylene] ratio of 2. Above this the rate decreased sharply.

Lehtinen *et al.*[123] found that there were no great differences in the incorporation of hexene and hexadecene in the ethylene/hexene and ethylene/hexadecene copolymers. The molar contents in the copolymers remained low, even with very high comonomer

ratios in the polymerization process. This was due to the low activity of the $Et(Ind)_2ZrCl_2$ catalyst used.

2.3.5 Different cocatalysts

MAO is a relatively expensive chemical and Kaminsky-Sinn catalysts require a high concentration of it to achieve high activity. A major improvement towards simpler and cheaper metallocene-based systems will be to use other cocatalysts in the place of MAO. Boron compounds, such as $B(C_6F_5)_3$, NR_3H^+ $B(C_6F_5)_4^-$ and $Ph_3C^+B(C_6F_5)_4^-$, in combination with metallocene dimethyls, can be used as cocatalysts[124-128]. Typically, cationic metallocene complexes can be formed by reactions of perfluorinated triphenylborane or trityltetrakis(pentafluorophenyl) borate:

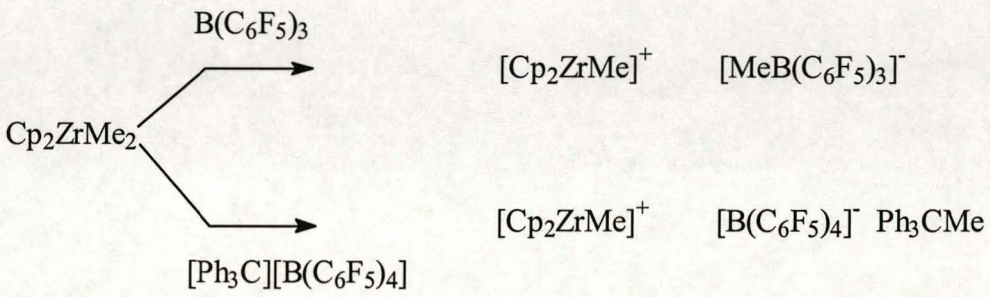

Whereas the ratio of MAO to metallocene needs to be around 5 000:1 for active catalyst systems, the required ratio of borate to metallocene is 1:1. As these systems are not able to scavenge impurities, a large part of the activated catalyst has to be sacrificed for that purpose. Better results have been achieved by adding small amounts of aluminium alkyls (AlR_3) to the borate catalyst system. AlR_3 scavenges impurities and alkylates the metallocene so that the simpler metallocene dichloride can be used[129, 130].

2.4 CONCLUSIONS

On the basis of the information available in the literature, as discussed in this chapter, some conclusions can be drawn, as they relate to this study.

- Bridged metallocene catalysts are more active in the copolymerization of propylene than the non-bridged complexes.
- Little information is available on the copolymerization of copolymers of ethylene or propylene with odd numbered α-olefins, like 1-pentene, using metallocene catalysts.
- Copolymers obtained with metallocene catalysts contain higher amounts of α-olefins than those obtained with heterogeneous catalysts.
- The introduction of α-olefins in the metallocene-catalyzed reaction leads to an acceleration of the polymerization rate.
- A high excess of MAO leads to increased catalytic activity, but since MAO is quite expensive, reducing its required concentration is an important issue to be addressed, especially for industrial application.
- The type of metallocene catalyst used will have an influence on the polymer microstructure, molecular mass and comonomer incorporation.
- A temperature study might be useful as the solution enthalpy of the different monomers at different temperatures has an influence on the copolymerization parameters and therefore the incorporation of the comonomer. Molecular mass is also dependent on the polymerization temperature, with an increasing reaction temperature leading to a decrease in molecular mass.
- The monomer feed ratio could have an influence on the incorporation of the comonomer, but it depends on the catalyst system and the different monomers used.

The catalyst of choice for the copolymerization of ethylene/propylene with 1-pentene is the bridged, stereorigid, C_2-symmetric metallocene ethylene *bis*(indenyl)zirconiumdichloride, **Et(Ind)$_2$ZrCl$_2$**. Toluene was selected for use as solvent and an excess of MAO as cocatalyst. The effect of increasing the amount of

1-pentene in the copolymer on the melting point, molecular mass, molecular mass distribution and microstructure will be investigated.

2.5 REFERENCES

1. Breslow D.S., Newburg N.R., *J. Am. Chem. Soc.*, 1957, **79**, 5072.
2. Natta G., Pino P., Mazzanti G., Giannini U., *J. Am. Chem. Soc.*, 1957, **79**, 2957.
3. Wild F.R.W.P., Zsolani L., Huttner G., and Brintzinger H.H., *J. Organomet. Chem.*, 1982, **232**, 233.
4. Kaminsky W., Miri M., Sinn H., Woldt R., *Makromol. Chem., Rapid. Commun.*, 1983, **4**, 417.
5. Sinn H., Kaminsky W., *Adv. Organomet. Chem.*, 1980, **18**, 99.
6. Kaminsky W., Kulper K., Brintzinger H.H., Wald F.R., *Angew. Chem., Int. Ed. Engl.*, 1985, **24**, 507.
7. Kaminsky W. in *History of Polyolefins*. Seymour, R.B., Cheng T., eds. Plenum Press, New York, 1987, 361.
8. Mashima, K., Nakayama, Y., Nakamura A., *Adv. Polym. Sci.*, 1997, **133**, 1.
9. Matkovsky P.E., Belov G.P., Kissin Y.V., Chirkov N.M., *Vysokomol. Soed.*, 1970, **A12**, 2286.
10. Belov G.P., Belova V.N., Raspopov L.N., Kissin Y.V., Birkenshtein K.A., Chirkov N.M., *Polym J.*, 1972, **3**, 681.
11. Ewen J.A., Jones R.L., Razavi A., Ferrara J.P., *J. Am. Chem. Soc.*, 1988, **110**, 6255.
12. Wilkinson G., Birmingham I.M., *J. Am. Chem. Soc.*, 1954, **76**, 4281.
13. Reichert K.M., Meyer K.R., *Makromol. Chem.*, 1973, **169**, 163.
14. Long W.P., Breslow D.S., *Justus Liebigs Ann. Chem.*, 1975, 463.
15. Andresen A., Cordes H.G., Herwig J., Kaminsky K., Merck A., Mottweiler R., Pein J., Sinn H., Vollmer H.J., *Angew. Chem. Int. Ed. Engl.*, 1976, **15**, 630.
16. Wild F.R.W.P., Wasincionek M., Huttner G., and Brintzinger H.H., *J. Organomet. Chem.*, 1985, **288**, 63.
17. Kaminsky W., Miri M., *J. Polym. Sci., Chem. Ed.*, 1985, **23**, 2151.
18. Kaminsky W., Drögemüller H., *Makromol. Chem., Rapid. Commun.*, 1990, **11**, 89.

19. Heiland K., Kaminsky W., *Makromol. Chem.*, 1992, **193**, 601.
20. Tait P.J.T., Berry I.G., *Comprehensive Polymer Science*, Vol. 4 (Eds.: Eastmond G.C., Ledwith A.,Russo S., Sigwalt), Pergamon Press, Oxford, 1989, **4**, 575.
21. *Encyclopedia of Polymer Science and Engineering* (Eds.: Mark H.F.,Bikales N.B., Overnerger C.G., Menges G.,Kroschwitz J.I.) John Wiley & Sons. New York, 1986, **6**, 429(LLDPE), 522(EPDM).
22. *Encyclopedia of Polymer Science and Engineering* (Eds.: Mark H.F.,Bikales N.B., Overnerger C.G., Menges G.,Kroschwitz J.I.) John Wiley & Sons. New York, 1988, **13**, 500.
23. Guidetti G.P., Busi P., Giulianelli I., Zanneti R., *Eur. Polym. J.*, 1983, **19**, 757.
24. Busico V., Corradini P., De Rosa C., Di Benedetto E., *Eur. Polym. J.*, 1985, **21**, 239.
25. Avella M., Martuscelli E., Volpe G.D., Segre A., Rossi E., Simonazzi T., *Makromol. Chem.*, 1986, **187**, 1927.
26. Davis D.S., *Proc. Annu. Tech. Conf. Reinf. Plast. Compos. Inst. Soc. Plast. Ind.*, 1992, **50**, 628.
27. Zimmerman J., *J. Macromol. Sci.*, 1993, **B32**, 141.
28. Zambelli A., Ammendola P., Grassi A., Longo P., Pronto A., *Macromolecules,* 1986, **19**, 2703.
29. Zambelli A., Longo P., Ammendola P., Grassi A., *Gazz. Chim. Ital.*, 1986, **116**, 731.
30. Zambelli A., Ammendola P. *Gazz. Chim. Ital.*, 1986, **116**, 329.
31. Grassi A., Zambelli A., Resconi L., Albizatti E., Mazzocchi R., *Macromolecules*, 1988, **21**, 617.
32. Chien J.C.W., He D., *J. Polym. Sci. Part A* 1991, **29**, 1585.
33. Chien J.C.W., He D., *J. Polym. Sci. Part A*, 1991, **29**, 1595.
34. Chien J.C.W., He D., *J. Polym. Sci. Part A,* 1991, **29**, 1603.
35. Chien J.C.W., He D., *J. Polym. Sci. Part A*, 1991, **29**, 1609.
36. Chien J.C.W., Nozaki T., *J. Polym. Sci. Part A: Polym. Chem.*, 1993, **31**, 227.
37. Chien J.C.W., Xu B., *Makromol. Chem. Rapid Commun.*, 1993, **14**, 109.
38. Uozumi T., Soga K., *Makromol. Chem.*, 1992, **193**, 823.
39. Tsutsui T., Kashiwa N., *Polym. Commun.*, 1988, **29**, 180.
40. Tsutsui T., Mizuno A., Kashiwa N., *Polymer,* 1989, **30**, 428.

41. Suhm J., Schneider M.J., Mülhaupt R., *J. Molecular Catalysis A: Chem.*, 1998, **128,** 215.

42. Heiland K., Kaminsky W., *Makromol. Chem.*, 1992, **193**, 601.

43. Rossi A., Zhang J., Odian G., *Macromolecules,* 1996, **29**, 2331.

44. Soga K., Kaminaka M., *Macromol. Chem. Phys.*, 1994, **195**, 1369.

45. Soga K, *Polym. Prepr. Japan.*, 1993, **42**, 258.

46. Wang S., Kuntz B.A., Nistola S., Collins S., Harrison D., Coulter I., *MetCon '95*, Houston.

47. Quijada R., Scipioni R.B., Mauler R.S., Galland G.B., Miranda M.S.L., *Polym. Bull.*, 1995, **35**, 299.

48. Quijada R., Dupont J., Lacerda Mirabda M.S., Scipioni R.S., Galland G.B., *Macromol. Chem. Phys.*, 1995, **196**, 3991.

49. Krentsel B.A., Kissin Y.V., Kleiner V.J., Stotskaya L.L., *Polymers and Copolymers of Higher α-Olefins*, Hanser Publications, Munich, Vienna, New York, 1997.

50. Herfert N., Montag P., Fink G., *Macromol. Chem.*, 1993, **194**, 3167.

51. Koivumäki J., Fink G., Seppälä J.V., *Macromolecules,* 1994, **27**, 6254.

52. Lehtinen C., Starck P., Löfgren B., *J. Polym. Sci.: Part A: Pol. Chem.*, 1997, **35**, 307.

53. Suhm J., Schneider M.J., Mülhaupt R., *J. Polym. Sci.: Part A: Polym. Chem.*, 1997, **35**, 735.

54. Schneider M.J., Suhm J., Mülhaupt R, Prosenc M-H., Brintzinger H.H., *Macromolecules,* 1997, **30**, 3164.

55. Tsutsui T., Ishimaru N., Mizuno A., Toyota A., Kashiwa N. *Polymer*, 1989, **30**, 1350.

56. Hirose T., Tsutsui T., Toyota A. (Mitsui Petrochemical Industries, Ltd.) Japanese Kokai 01,173,111, *Chem. Abstr.*, **114**,7423w, 1991.

57. Winter A., Dolle V., Rohrmann J., Antberg M., Boehm L., Walter S., (Hoechst A-G) German Offen.DE 3,914,468, *Chem. Abstr.*, **114**,62977e, 1991.

58. Shiomura T., Sanuma T.A., Kouno M., Inoue N., Fukushima S., Sonobe Y., Mizutani K., Iwantani T., Sugimoto R. (Mitsui Toatsu Chemicals, Inc.), PCT Int. Appl. WO 91,15,523(1991), *Chem. Abstr.*, **116**,4222r, 1992.

59. Schreck M., Winter A., Spaleck W., Kondoch H., Rohrmann J., (Hoechst

A-G) European Patent Appl. EP 433,990, *Chem. Abstr.*, **115**,160011a, 1991.

60. Winter A., Dolle V., Rohrmann J., Spaleck W., Antberg M., (Hoechst A-G), Eur. Patent Appl. EP433,986, *Chem. Abstr.*, **115**,233115z, 1991.
61. Asanuma T., Iwantani T., Sugimoto R., Inoue N., Kouno M., Shiomura T. (Mitsui Toatsu Chemical, Inc.) European Patent Appl. 452,763, 1991, *Chem. Abstr.*, 116,84387P, 1992.
62. Uozumi T., Soga K., Bello A., Perez E., Lacatelli P., Fan Z.Q., Zucchi D., *Polym. Bull.*, 1996, **36**, 249.
63. Arnold M., Henschke O., Knorr J., *Macromol. Chem. Phys.*, 1996, **197**, 563.
64. De Rosa C., Talarico G., Caporaso L., Auriemma F., Galimberti M., Fusco O., *Macromolecules*, 1998, **31**, 26, 9109.
65. Forlini F., Fan Zhi-Qiang, Tritto I., Lacatelli P., Sacchi M.C., *Macromol. Chem. Phys.*, 1997, **198**, 2397.
66. Naga N., Mizunuma K., Sadatoshi H., Kakugo M., *Macromolecules*, 1997, **30**, 2197.
67. Fink G., Ojala T.A., in *Transition Metal Organometallics as Catalysts for Olefin Polymerization,* Kaminsky W., Sinn H., eds. Springer-Verlag, Berlin, 1988, 169.
68. Jüngling S., Koltzenburg S., Mülhaupt R., *J. Polym. Sci.: Part A: Polym. Chem.*, 1997, **35**, 1.
69. Siedle A.R., Lamanna W.M., Newmark R.AA., *Makromol. Chem. Macromol. Symp.*, 1993, **66**, 215.
70. Shista C., Hatorn R.M., Marks T.J., *J. Am. Chem. Soc.*, 1992, **114**, 1112.
71. Jordan R.F., Bajgur C.S., Willet R., Scott B., *J. Am. Chem. Soc.*, 1986, **108**, 7410.
72. Jordan R.F., *Adv. Organomet. Chem.*, 1991, **32**, 325.
73. Edward P. Moore, Jr., *Polypropylene Handbook*, Hanser Publishers, Munich Vienna New York 1996.
74. Tritto I., Li S.X., Sacchi M.C., Lacatelli P., Zannoni G., *Macromolecules,* 1995, **28**, 5358.
75. Rossi A., Zhang J., Odian G., *Macromolecules,* 1996, **29**, 2331.
76. Ewen J.A., *J. Am. Chem. Soc.*, 1984, **106**, 6355.
77. Soga K., Shiono T., Takemura S., Kaminsky W., *Macromol. Chem. Rapid Commun.*, 1987, **8**, 305.

78. Stehling U., Diebold J., Kirsten R., Röll W., Brintzinger H.H., Jüngling S., Mülhaupt R., Langhauser F., *Organometallics,* 1994, **13**, 964.

79. Resconi L., Fait A., Piemontesi F., Colonnesi M., Rychlicki H., Ziegler R., *Macromolecules,* 1995, **28**, 6667.

80. Uozumi S., Soga K., *Macromol. Chem.*, 1992, **193**, 823.

81. Zambelli A., Grassi A., *Macromol. Chem., Rapid Commun.*, 1991, **12**, 523.

82. Tsai W.-M., Chien J.C.W., *J. Polym. Sci., Part A,* 1994, **32**, 149.

83. Soga K., *Macromol. Chem.*, 1989, **190**, 37.

84. Soga K., *Macromol. Chem.*, 1988, **189**, 2839.

85. Usami T., Gotoh Y., Takayama S., *Macromolecules*, 1986, **19**, 2722.

86. Jüngling S., Mülhaupt R., Fischer D., Langhauser F., *Angew. Makromol. Chem.*, 1995, **229**, 93.

87. Koivumäki J., *Polym. Bull.*, 1996, **36**, 7.

88. Arnold M., Henscke O., Knorr J., *Makromol. Chem. Phys.*, 1996, **197**, 563.

89. Soga K., Uozumi S., Nakamura S., Toneri T., Teranishi T., Sano T., Arai T., *Macromol. Chem.*, 1996, **197**, 4237.

90. Benadente R., Josi J.M., Perena M., Bello A., Perez E., Locatelli P., Fan Z.Q., Zucchi D., *Polym. Bull.*, 1996, **36**, 249.

91. Galland G.B., Mauler R.S., De Menezes S.C., Quida R., *Polym. Bull.*, 1995, **34**, 599.

92. Bailey A.L., Tchir L.T., Kale W.J., *J. Appl. Polym. Sci.*, 1994, **51**, 547.

93. Koivumäki J., Lathi M., Seppällä J.V., *Angew. Makromol. Chem.*, 1994, **221**, 117.

94. Koivumäki J., Seppällä J.V., *Macromolecules,* 1994, **27**, 2008.

95. Kaminsky W., *Angew. Makromol. Chem.*, 1986, **146**, 149.

96. Huang J., Rempel G.L., *Polym. Sci.*, 1995, 20, 459.

97. Brintzinger H.H., Fischer D., M lhaupt R., Rieger B., Waymouth R., *Angew. Chem.*, 1995, **107**, 1255.

98. Farina M., Di Silvestro G., Terragni A., *Macromol. Chem. Phys.*, 1995, **196**, 353.

99. Zucchini U., Dall Occo T., Resconi L., *Indian J. Tech.*, 1993, **31**, 247.

100. Spaleck W., Antberg M., Rohrmann J., Winter A., Bachmann B., Kiprof P., Behm J., Herrmann W.A., *Angew. Chem.*, 1992, **104**, 1373.

101. Spaleck W, Kuber F., Winter A., Rohrmann J., Bachmann B., Antberg M., Dolle V., Paulus E.F., *Organometallics*, 1994, **13**, 954.

102. Spaleck W, Antberg M., Dolle V., Klein R., Rohrmann J., Winter A., *New J. Chem.*, 1990, **14**, 499.

103. Lehtinen C., Löfgren B., *Eur. Polym. J.*, 1997, **33**, 115.

104. Locatelli P., Sacchi M.C., Tritto I., *Makromol. Chem., Rapid Commun.*, 1988, **4**, 417.

105. Locatelli P., Sacchi M.C., Tritto I., Forlini F., *Macromolecules*, 1990, **23**, 2406.

106. Sacchi M.C., Shan C., Forlini F., Tritto I., Locatelli P., *Makromol. Chem., Rapid Commun.*, 1993, **14**, 231.

107. Sacchi M.C., Fan Z.Q., Forlini F., Tritto I., Locatelli P., *Makromol. Chem. Phys.*, 1994, **195**, 2805.

108. Fan Z.Q., Forlini F., Tritto I., Locatelli P., Sacchi M.C., *Makromol. Chem. Phys.*, 1994, **195**, 3889.

109. Muhlenbrock P., Fink G., Naturforsch Z., B-A, *J. Chem. Sci.*, 1995, **50b**, 423.

110. Resconi L., Bossi S., Abis L., *Macromolecules*, 1990, **23**, 20, 4489.

111. Karol F.J., Kao S.C., Wasserman E.P., Brady R.C., *New J. Chem.*, 1997, **21**, 797.

112. Tritto I., Sanxi L., Sacchi M.C., Locatelli P., Zannoni G., *Macromolecules*, 1995, **28**, 5358.

113. Tritto I., Sanxi L., Sacchi M.C., Zannoni G., *Macromolecules*, 1993, **26**, 7111.

114. Pieter P.J.J., Van Beeck J.A.M., Van Tol M.F.H., *Macromol. Rapid Commun.*, 1995, **16**, 463.

115. Harlan C.J., Bott S.G., Barro A.R., *J. Am. Chem. Soc.*, 1995, **117**, 6465.

116. Giardello M.A., Eisen M.S., Stern C.L., Marks T.J., *J. Am. Chem. Soc.*, 1993, **115**, 3326.

117. Giardello M.A., Eisen M.S., Stern C.L., Marks T.J., *J. Am. Chem. Soc.*, 1995, **117**, 12114.

118. Chien J.C.W., Song W., Rausch M.D., *J. Polym. Sci., Part A: Polym. Chem.*, 1994, **32**, 2387.

119. Eisch J.J., Pombrik S.I., Zheng G.X., *Organometallics*, 1993, **12**, 3856.

120. Eisch J.J., Pombrik S.I., in *Catalyst Design for Tailor-made Polyolefins*, Soga K., Terrano M., Eds., Kodansha, Tokyo, 1994, p.221 and references therein.

121. Kaminsky W., *Macromol. Symp.*, 1995, **97**, 79.

122. Forlini F., Fan Z.Q., Tritto I., Locatelli P., Sacchi M.C., *Makromol. Chem. Phys.*, 1997, **198**, 2397.

123. Lehtinen C., Starck P., Löfgren B., *J. Polym. Sci., Part A: Polym. Chem.*, 1997, **35**, 307.

124. Yang X., Stern C.L., Marks T.J., *J. Am. Chem. Soc.*, 1991, **113**, 3623.

125. Yang X., Stern C.L., Marks T.J., *J. Am. Chem. Soc.*, 1994, **116**, 10015.

126. Bochmann M., Lancaster S.J., *Organometallics*, 1993, **12**, 633.

127. Chien J.C.W., Tsai W., Rausch M.D., *J. Am. Chem. Soc.*, 1991, **113**, 8570.

128. Herfert N., Fink G., *Makromol. Chem. Rapid Commun.*, 1993, **14**, 91.

129. Idemitsu *European Patent Appl.*, 513 380, 1992.

130. Tsai W., Rausch M.D., Chien J.C.W., *Appl. Organomet. Chem.*, 1993, **7**, 71.

CHAPTER 3

Polymerization and characterization of ethylene/1-pentene copolymers produced with the bridged metallocene *rac*-Et(Ind)$_2$ZrCl$_2$

Summary

An investigation into the effect of varying the amount of comonomer used in the ethylene/1-pentene copolymerization with the isospecific catalyst *rac*-[ethylene *bis*(1-indenyl)]zirconium dichloride (*rac*-Et(Ind)$_2$ZrCl$_2$) was carried out. This was done to investigate the effect of 1-pentene on the melting point, molecular mass, and molecular mass distribution of the ethylene/1-pentene copolymers produced. The copolymers obtained were characterized by differential scanning calorimetry (DSC), gel permeation chromatography (GPC), nuclear magnetic resonance (NMR) spectroscopy and infrared (IR) spectroscopy. A noticeable decrease in the melting point of the copolymers, due to the increased amount of 1-pentene incorporated in the copolymers, was detected.

3.1 INTRODUCTION

The traditional Ziegler-Natta catalysts used in the production of polyolefins have different active sites, leading to poor control of comonomer incorporation and resulting in a mixture of polymer molecules differing greatly in both polymer length and in comonomer distribution.

Very few completely homogeneous Ziegler-Natta catalysts are known, except for the early metallocene-based catalysts[1]. One completely homogeneous vanadium-based catalyst (a combination of V^{3+} acetonate and a dialkylaluminium chloride) has been used to investigate the copolymerization of ethylene with a series of higher α-olefins: 1-butene, 1-pentene, and 1-hexene[2]. These catalysts are, however, not very reactive, but a variety of ethylene/1-pentene and ethylene/1-hexene copolymers with varying compositions were prepared.

The recent introduction of metallocene-based catalyzed polyolefins has been a breakthrough in the polyolefin industry. Metallocenes are a class of compounds in which cyclopentadienyl or substituted cyclopentadienyl ligands are σ-bonded to a metal atom (Zr, Ti or Hf) from group 4. An important step in the development of metallocene catalysed polyolefins for industrial use was Kaminsky's development of a methylalumoxane (MAO) cocatalyst[3], the use of which greatly improved the productivity of metallocene catalysts and enabled them to polymerize higher α-olefins.

Metallocene catalysts differ from the conventional Ziegler-Natta catalysts in that they are "single-site" catalysts. They generate only one kind of active species and, therefore, very homogeneous polymers of narrow molar mass distribution. Based on the function of metallocene structure, it is possible to control stereochemistry, molecular mass, end-groups, and short-chain branching without affecting narrow molecular mass distributions[4-6] of $M_w/M_n \approx 2$.

An advantage of the metallocene-catalyzed ethylene copolymerization is the incorporation of α-olefin comonomers into the polyethene backbone over the entire feasible composition range, from 0 to 100% comonomer content. The comonomers are equally distributed on all chain lengths and also along each chain.

Kaminsky[7] and Ewen[8] have used homogeneous catalysts to copolymerize ethylene with α-olefins. Lehtinen *et al.*[9] found that non-bridged catalysts were not very suitable for the copolymerization of ethylene with higher α-olefins such as 1-hexene and 1-hexadecene. However, the bridged *ansa* stereorigid compound $Et(Ind)_2ZrCl_2$, synthesized by Brintzinger and coworkers[10, 11], was active towards both 1-hexene and 1-hexadecene in ethylene/propylene/α-olefin terpolymerizations.

The *ansa* metallocene catalysts possess very high polymerization activities over a wide range of comonomer feed compositions. We carried out an investigation into the variation of the amount of 1-pentene on ethylene/1-pentene copolymerization with the isospecific catalyst *rac*-[ethylene *bis*(1-indenyl)]zirconium dichloride (*rac*-$Et(Ind)_2ZrCl_2$) (see Figure 3.1), and will report on the effect of the amount of

1-pentene incorporated in the copolymer on the melting point, molecular mass, and copolymer microstructure (comonomer composition).

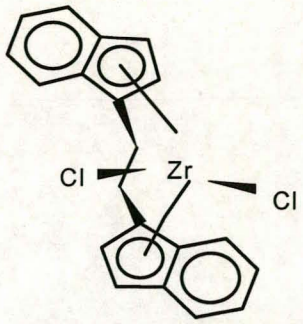

Figure 3.1. $Et(Ind)_2ZrCl_2$

3.2 EXPERIMENTAL

All experiments were carried out in an argon or nitrogen atmosphere, using standard Schlenk techniques. All reagents were adequately dried prior to use because of the moisture and air sensitivity of the catalyst. Glassware, including syringes, was kept in an oven at 95°C prior to use. Toluene was used as solvent in the copolymerization of ethylene with 1-pentene. Analytical grade toluene, obtained from BDH, was refluxed and distilled over sodium and then distilled onto 3Å molecular sieve. Ethylene (polymerization grade, > 99%) was obtained from Fedgas and was used without further purification in the copolymerization of ethylene with 1-pentene. 1-Pentene was obtained from Polifin and refluxed over lithium aluminium hydride ($LiAlH_4$) and afterwards distilled onto 3 Å molecular sieve. The catalyst used in this study was the stereorigid C_2-symmetric metallocene ethylene *bis*(indenyl)zirconiumdichloride, **$Et(Ind)_2ZrCl_2$**. The catalyst was obtained from Strem Chemicals and used as received. Methylalumoxane (MAO) was commercially obtained from Aldrich as a 10 wt% solution in toluene and was used without further purification. The MAO was stored under nitrogen.

3.3 EQUIPMENT

3.3.1 Polymerization equipment

A 75 mL stainless-steel Parr autoclave was used in the ethylene copolymerization. The reactors were equipped with a fitted steal seal ring and a pressure gauge.

3.3.2 Analytical equipment

The copolymers were characterized by DSC, GPC, NMR- and IR-spectroscopy.

3.3.2.1 Differential scanning calorimetry (DSC)

Differential scanning calorimetry (DSC) analyses were carried out with a Du Pont 910 DSC and a Du Pont 9900 Computer/Thermal analyzer, to determine the melting points (T_m) of the copolymers. Samples of the polymers (8-10 mg) were heated in aluminium pans in a nitrogen atmosphere at a rate of 20°C/min, from ambient temperature to 200°C. The samples were allowed to cool down to room temperature and then heated again at the same heating rate. The melting temperatures were obtained from the endothermic curves.

3.3.2.2 Nuclear magnetic resonance (NMR) spectroscopy

The ^{1}H NMR spectra and the ^{13}C NMR spectra of the copolymers were recorded with a Varian VXR 300 spectrometer at 100°C. The samples (60-70 mg) were dissolved in a mixture of 1,2,4,-trichlorobenzene and benzene-d_6 (9:1 volume ratio).

3.3.2.3 Gel permeation chromatography (GPC)

Gel permeation chromatography (GPC) analyses of molecular mass and molecular mass distributions were carried out in 1,2,4-trichlorobenzene at 140°C, using a Waters 150C GPC, with a flow rate of 1.0 mL/min.

3.3.2.4 Photo-acoustic infrared spectroscopy (PAS-IR)

The PAS-IR spectra of the copolymers were recorded on a Perkin Elmer 1600 Infrared Fourier Transform spectrometer (FTIR). The PAS-IR spectra were recorded by means of a photo-acoustic detector system that obviates any sample preparation.

3.4 SYNTHESIS OF COPOLYMERS

3.4.1 Preparation of catalyst

Typically, 4.185 mg of $Et(Ind)_2ZrCl_2$ was weighed and dissolved in 10 mL toluene.

3.4.2 Ethylene copolymerization

Polymerizations were carried out in a 75 mL stainless steel pressure reactor fitted with a magnetic stirring bar. The system was first evacuated and flushed with nitrogen and toluene was then injected. 0.5 mL (2 mol/L) of MAO in 5mL toluene was introduced into a Schlenk tube. The catalyst (1 mL, 25 μmol/L) was added to the Schlenk tube and allowed to stand for 5 min at room temperature to preactivate the catalyst.

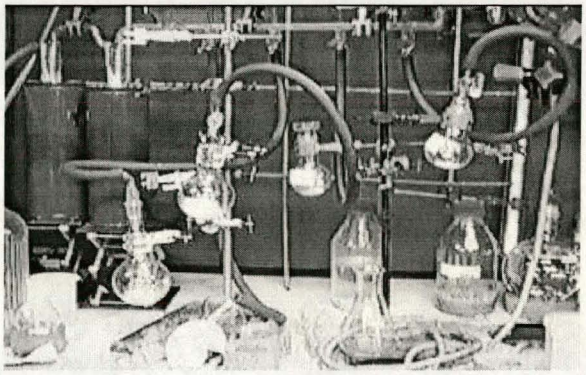

Figure 3.2. The Schlenk-line used in the preparation of the catalyst/cocatalyst/comonomer mixture.

The comonomer, 1-pentene, was then added and the catalyst/cocatalyst/comonomer mixture was charged into the reactor, and the polymerization was initiated by introducing the gaseous ethylene. The total volume of the reaction mixture was 40 mL in all the polymerizations. Figure 3.2 shows the experimental set-up of the Schlenk-line used in the preparation of the catalyst/cocatalyst/comonomer mixture.

The reactor was then charged with 20 MPa ethylene, and placed in a temperature-controlled oil bath, set at 50°C. After 3 hours the reactor was vented, opened and the

copolymer produced precipitated in 200 mL ethanol, acidified with 10 mL 10 wt% aqueous HCl. The copolymer was filtered, and dried at room temperature under vacuum for 6 hours.

A series of copolymerization reactions was carried out using different amounts of 1-pentene (see Table 3.1).

3.5 RESULTS AND DISCUSSION

The results of the copolymerizations of ethylene and 1-pentene with the bridged catalyst, $Et(Ind)_2ZrCl_2$, are shown in Table 3.1. The amount of 1-pentene incorporated in the copolymer, the melting points and the molecular masses of the copolymers produced are summarized.

Table 3.1. Results of ethylene/1-pentene copolymerizations at 50°C

Sample	1-pentene feed(mL)	1-pentene (mol %) [b]	Yield (g)	T_m [c](°C)	M_w [d] (g/mol)	M_n [e] (g/mol)	M_v [f] (g/mol)	M_w/M_n
EtPn0 [a]	0	0	3	137	154 840	51 270	141 400	3.1
EtPn1	1	1.5	3.9	127.74	126 400	36 650	113 100	3.5
EtPn4	4	5.2	4.8	118.15	111 200	26 260	97 460	4.2
EtPn10	10	2.6	3.3	104.66	127 200	62 430	116 000	2.0
EtPn20	20	45.3	12.7	92.01	172 700	23 320	133 100	7.4

[a]See experimental section for polymerization conditions. [b]Content of comonomer in copolymers determined by ^{13}C NMR spectroscopy. [c]Melting peak temperatures obtained from DSC analyses. [d]The weight-average molecular masses of the polymers were determined from GPC analyses, using polystyrene standards. [e]The number-average molecular masses of the polymers were also determined from GPC analyses. [f]The viscosity-average molecular masses of the polymers were determined from GPC analyses, using polystyrene standards.

3.5.1. Melting points

The copolymers were analyzed by DSC to determine their melting points and percent crystallinities. Basically the criterion for crystallization is that the free energy of the crystalline phase must be lower than the free energy of the liquid phase. The assembling of a group of molecules in liquid to form a crystal gives rise to the evolution of heat, the heat of fusion (ΔH_f). Since this change in energy is the result of the tighter association bonds between the molecules in the crystal than those in the

liquid, it is clear that ΔH_f will be large whenever strong intermolecular bonding is possible. A polymer molecule in the molten state has very few restrictions on its possible positions, and it is able to assume nearly all the configurations possible without regard to the orientation of surrounding chains. Therefore the entropy is much higher than in the crystalline material, where the molecules are constrained in many ways. Since a system seeks the highest entropy, entropy alone favors the liquid state. The change in free energy as liquid changes to crystal is given as

$$\Delta G_f = \Delta H_f - T\Delta S_f$$

At the melting point T_m, the crystals and liquids are at equilibrium, and hence $\Delta G_f = 0$. The melting temperature is therefore given by

$$T_m = \Delta H_f / \Delta S_f$$

The ability of a polymer to crystallize depends upon the structural regularity of the chain configuration. Substantial numbers of structural irregularities or heterogeneities can be present in the polymer, and these to a large extent control and determine the percent crystallinity in a sample. The effects of surface energy, chain ends, and short-chain branching lead to a lowering of the T_m.

The effect of copolymerization on the melting point and the crystallinity is not simple. The difficulty encountered with the measurement of copolymers is associated with the fact that the melting range of copolymers is very wide, and it is very difficult to determine where the last bit of crystallinity disappears. Therefore we report the end of melting, the offset temperature as well as the melting peak temperature of the copolymers, as the thermodynamic melting temperature is the end of melting, while the conventional method is the offset temperature or the melting peak temperature.

The offset temperature for melting (T_m) was determined by the conventional interpolation method as illustrated in Figure 3.4. The values of enthalpies of the transition, λH_m, were evaluated from the peak area by taking a base line of the peak and calculating the area of the peak as illustrated in the Figure 3.4. The relative amount of crystalline structure (i.e. % crystallinity) can be directly determined from the DSC melting endotherm by comparing the measured heat of fusion (ΔH_f) with that for a standard of known crystallinity. The enthalpy of fusion of a perfect

polyethylene crystal was taken as 290 J/g[12]. The melting points, heats of fusion and the amount of crystallinity of the ethylene/1-pentene copolymers are listed in Table 3.2.

Table 3.2. Results of DSC analyses of ethylene/1-pentene copolymers

Sample	1-Pentene feed(mL)	1-Pentene (mol %)	Onset of melting tempera-ture	Melting peak tempera-ture Tm[a] (°C)	End of melting tempera-ture	Heat of fusion ΔH_f(J/g)	Crystalli-nity m_{co}[b](%)
EtPn1	1	1.5	120	127	129	125.9	43.4
EtPn4	4	5.2	114	118	120	86.1	29.7
EtPn10	10	2.6	95	104	109	61.6	21.2
EtPn20	20	45.3	78	92	99	6.5	2.3

[a]Final temperature of melting peak. [b]Calculated from heat of fusion of samples and heat of fusion, assuming 290 J/g for enthalpy of perfectly crystalline polyethylene.

There is a definite decrease in the melting point of the copolymer with increasing 1-pentene content, except for sample EtPn10, which can be due to impurities that was present when the reaction was carried out (see Figure 3.3).

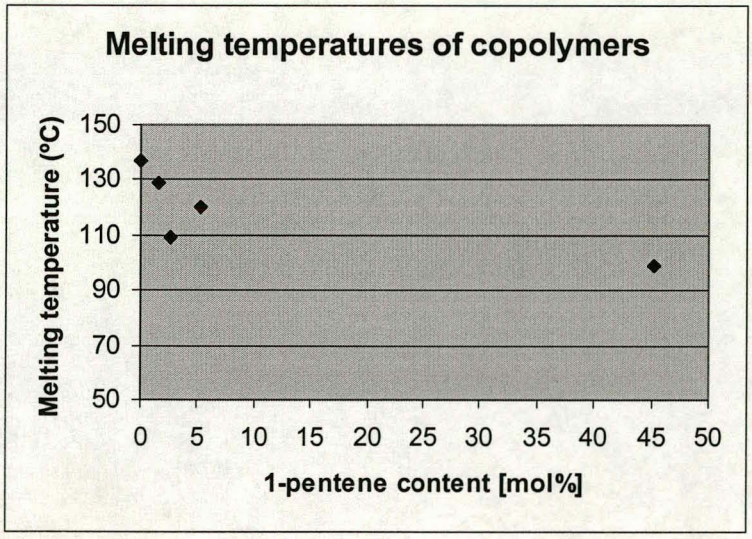

Figure 3.3. Melting temperatures of ethylene/1-pentene copolymers as a function of 1-pentene content.

The DSC traces of samples EtPn1 and EtPn10 are given in Figures 3.4 and 3.5. Sample EtPn10 has a higher amount of 1-pentene incorporated (2.6% 1-pentene) than does sample EtPn1 (1.5% 1-pentene), as calculated from results of NMR spectroscopy analysis. The differences between the two DSC melting endotherms are the broadness of the melting peaks and the temperatures of the melting points. The melting temperature of sample EtPn10 (2.6% 1-pentene) was much lower than that of sample EtPn1 (1.5% 1-pentene), and in both samples a shoulder on the lower temperature side could be seen. That feature is typical for a linear low-density polyethylene (LLDPE) with low branch content[13]. According to Sequela and Rietsch[14, 15], even small amounts of branches are not able to enter the crystalline phase, resulting in small crystal size and imperfection. Both of these cause a lower melting temperature and also lower crystallinity. Thus, the introduction of 1-pentene into the polymeric chain creates a discontinuity that sharply reduces the crystallization tendency. The results are a reduction in the rate of crystallization, a lower level of crystallinity, and therefore a reduction in the melting point, all related to the less-perfect structure of the chains.

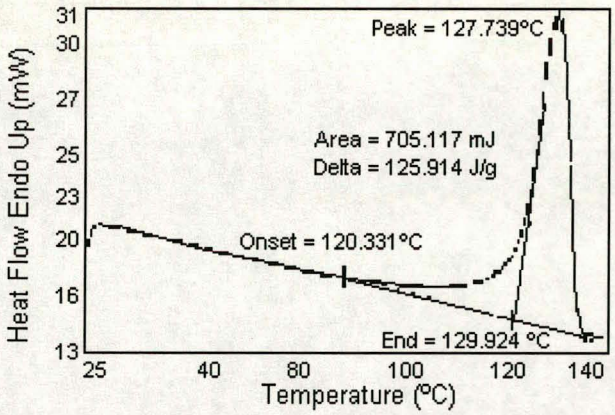

Figure 3.4. DSC curve of an ethylene/1-pentene copolymer, sample EtPn1 (1.5% 1-pentene), showing the melting endotherm.

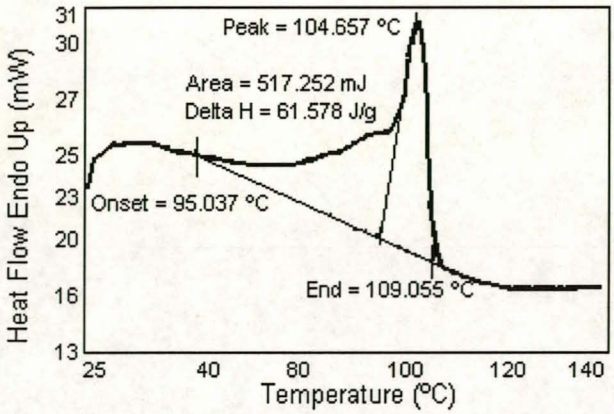

Figure 3.5. DSC curve of an ethylene/1-pentene copolymer, sample EtPn10 (2.6% 1-pentene), showing the melting endotherm.

The very broad melting endotherm of EtPn10 corresponds to those of earlier reported zirconium-based copolymers[9, 16] and the shape of the DSC curve is similar to those of some commercial Ziegler-Natta based linear, very low density polyethylenes (VLLDPE) polymers[17]. Molecules of ethylene/α-olefin copolymers with very low α-olefin contents (as seen in sample EtPn1 (1.5% 1-pentene)), have longer sequences of ethylene units. These nearly linear ethylene blocks form crystals, the same as in an ethylene homopolymer. If a copolymer is compositionally homogeneous, all its molecules have approximately the same composition. With an α-olefin content of up to 2%, the average lengths of the ethylene blocks are relatively short and these blocks form thin lamellae that melt at relatively low temperatures. On the other hand, any copolymer with pronounced compositional heterogeneity is a mixture containing copolymer molecules with a broad range of compositions, from practically linear macromolecules with high molecular masses to low molecular mass macromolecules with higher α-olefin contents (as seen in sample EtPn10, 2.6% 1-pentene incorporation). This leads to a very broad melting peak. Therefore we can use DSC to evaluate the compositional uniformity of ethylene/α-olefin copolymers, although only on a semi-quantitative level.

3.5.2 Molecular mass and molecular mass distributions

Figures 3.6 and 3.7 show the mass distributions of molar mass, w(log M), against the molar masses of the two samples, EtPn1 (1.5% 1-pentene) and EtPn20 (45.3% 1-pentene).

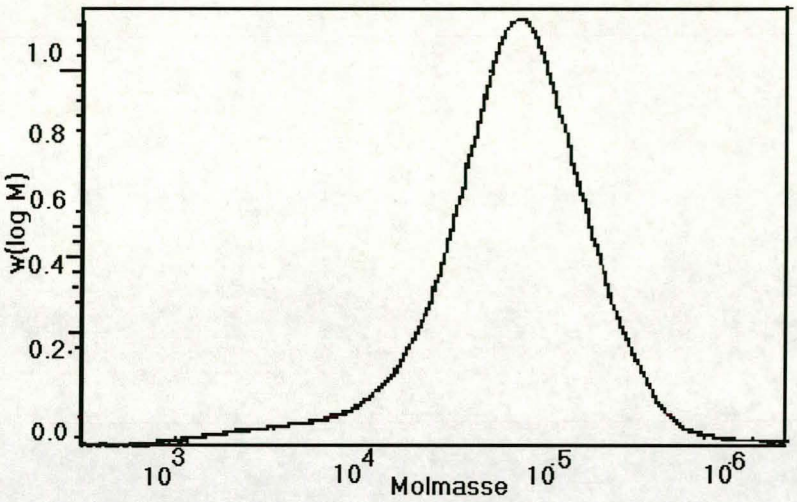

Figure 3.6. The distribution of the molar mass, w(log M), against the molar mass of the sample EtPn1 (1.5% 1-pentene).

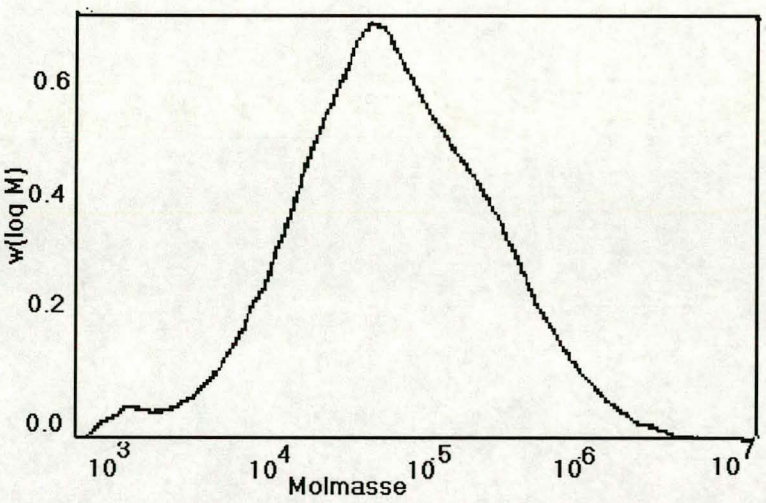

Figure 3.7. The distribution of the molar mass, w(log M), against the molar mass of the sample EtPn20 (45.3% 1-pentene).

The weight-average molecular mass of polyethylene was 154 840 g/mol, which decreased with the introduction of 1-pentene. With a molar content of 5%, the molar mass decreased to 111 200 g/mol. When the incorporation of 1-pentene was higher than 40% the molar mass increased to 172 700 g/mol. Copolymers with this high

amount of 1-pentene were sticky and viscous. They were difficult to handle and their processibility was poor.

The polydispersities of the copolymers also increased with increasing 1-pentene content. The polydispersities varied from 3.5 (polyethylene) to 7.4 in the copolymer containing 45% 1-pentene. A polydispersity of 7.4 is very high and not representative of a metallocene catalyst (see Figure 3.8). The explanation for the broad molar mass distribution of the copolymer could be the formation of more active sites in the catalyst[18]. The molecular masses of the polymers produced by the different active sites are different and lead to the broad molecular mass distribution[19]. A graphic representation of the molar mass distribution of the ethylene/1-pentene copolymers is shown in Figure 3.8.

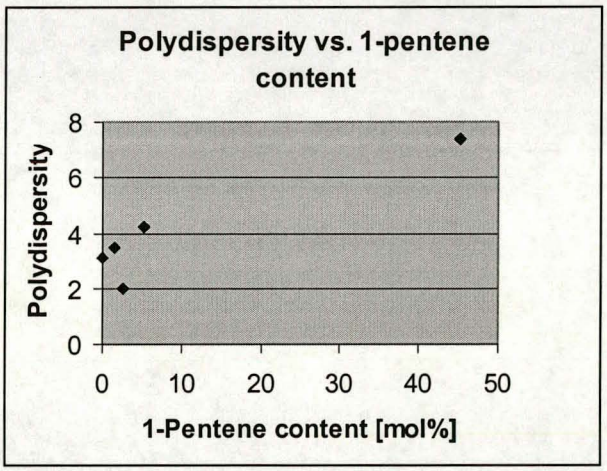

Figure 3.8. Polydispersities of ethylene/1-pentene copolymers as a function of 1-pentene content.

3.5.3 Photo-acoustic infrared spectroscopy (PAS-IR)

Using the photo-acoustic detector in conjunction with the Perkin Elmer FTIR, no sample preparation was required. The PAS-IR spectra of the copolymers were recorded and compared. The expected spectral characteristics can be predicted from the copolymer structure.

For polyethylene ($-CH_2CH_2CH_2CH_2CH_2-$) the following absorption bands are expected for the $-CH_2$ groups:

- Crystalline bands (729 cm^{-1})
- C-H stretch vibrations, both symmetrical (2940–2915 cm^{-1}) and asymmetrical (2870–2840 cm^{-1}),
- $-CH_2$ scissor vibrations[15] (deformation) at 1480-1440 cm^{-1} and
- $-CH_2CH_2-$ skeletal -C-C- vibrations[20] at 745-735 cm^{-1}.

The PAS-IR spectrum of polyethylene (EtPn0) can be seen in Figure 3.9.

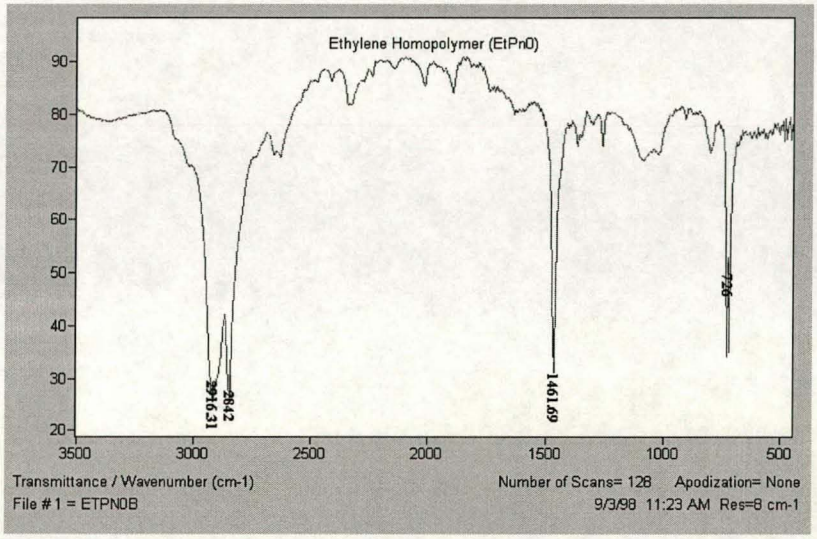

Figure 3.9. PAS-IR spectrum of polyethylene (EtPn0, 0% 1-pentene).

The only difference between the abovementioned and the ethylene/1-pentene copolymer

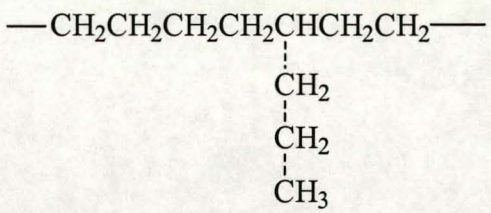

is the presence of the methyl group and the –CH- group. The latter gives only a very weak –C-H- stretching vibration in the region 2900-2880 cm^{-1}, while the presence of the methyl group gives the following vibrations:

- –C-H- stretching vibrations at 1465-1440 cm^{-1} (symmetric, but probably hidden by $-CH_2-$ scissor vibration) and at 1390-1370 cm^{-1} (asymmetric). The latter is the band that is commonly used to indicate the presence of methyl groups[21], and can

be compared with the CH_2CH_2-scissor vibration to indicate the amount of methyl groups present in the structure.

- n-propyl groups will cause a vibration in the region 745-735 cm^{-1}, but this is in the same region as the CH_2CH_2 vibrations that we see for the ethylene homopolymer (confirmed by the presence of a band at 732 cm^{-1})[20].

The PAS-IR spectra of samples EtPn10 (2.6% 1-pentene) and EtPn20 (45.3% 1-pentene) are shown in Figures 3.10 and 3.11.

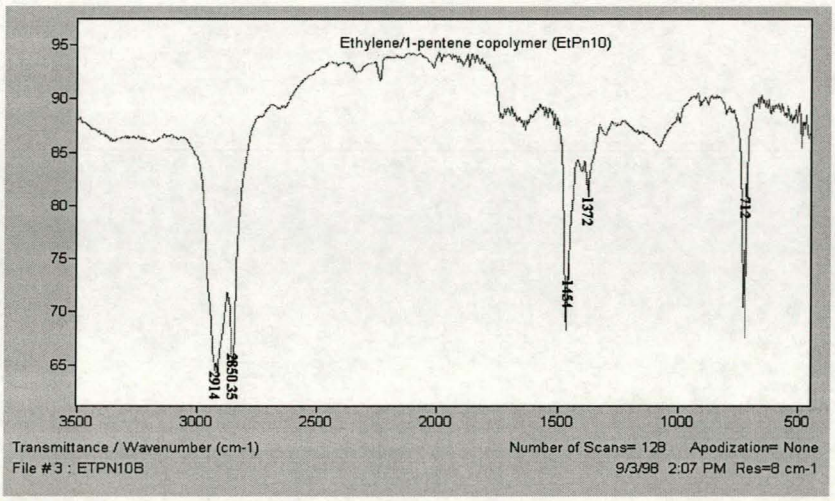

Figure 3.10. PAS-IR spectrum of an ethylene/1-pentene copolymer, sample EtPn10 (2.6% 1-pentene).

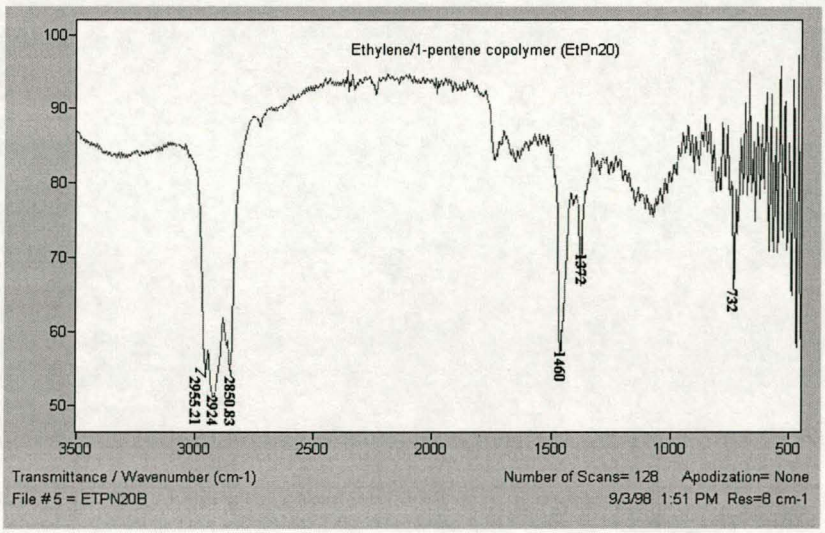

Figure 3.11. PAS-IR spectrum of an ethylene/1-pentene copolymer, sample EtPn20 (45.3% 1-pentene).

If we compare the spectra of EtPn10 and EtPn20 (Figures 3.12 and 3.13), differences can be seen in the following areas: 3000cm^{-1}, 1400cm^{-1}and 1200cm^{-1}.

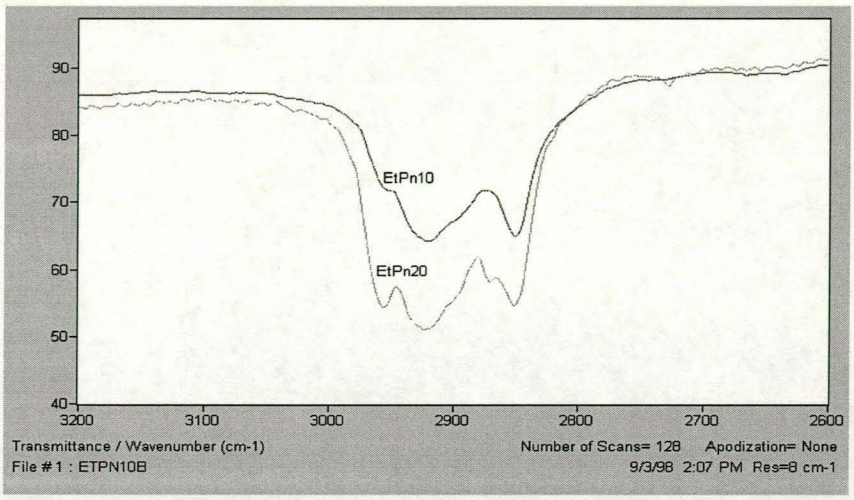

Figure 3.12. Comparison of PAS-IR spectra of EtPn10 (2.6% 1-pentene) and EtPn20 (45.3% 1-pentene) in the range 3200 to 2600 cm^{-1}.

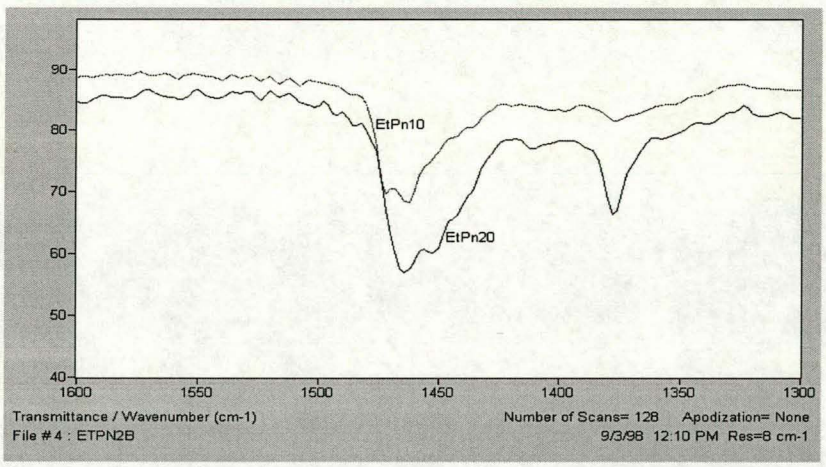

Figure 3.13. Comparison of PAS-IR spectra of EtPn10 (2.6% 1-pentene) and EtPn20 (45.3% 1-pentene) in the range 1600 to 1300 cm^{-1}.

In the 2800 cm^{-1} region there is a slight shoulder on the band at 2924 cm^{-1} for the copolymer EtPn20. This is due to the asymmetric –C-H- stretching vibrations of the –CH- group, which could indicate a much higher amount of 1-pentene units in the copolymer. The band at 1450 cm^{-1} also becomes larger in the spectrum of the copolymer EtPn20. As the $-CH_2-$ scissor vibration hides the symmetric –C-H- stretching vibrations of the methyl groups, this increase in the band could be due to a

higher amount of methyl groups in the copolymer. This is confirmed by the band at 1374 cm^{-1}, due to the asymmetric –C-H- stretching vibrations of the methyl group, which are not visible in the case of the copolymer EtPn10. In conclusion, although PAS-IR cannot indicate the precise amount of 1-pentene incorporated in the case of ethylene/1-pentene copolymers, it will give an indication of the presence of 1-pentene in the copolymer.

3.5.4 Microstructure of polyethylene and ethylene/1-pentene copolymers

^{13}C NMR spectroscopy can be used to investigate the microstructure of ethylene copolymers with respect to comonomer sequence distribution. It can also be used to determine ethyl, propyl and butyl branches concentrations independently of the saturated end-groups. ^{13}C NMR spectroscopy therefore has a distinct advantage over corresponding infrared measurements because the latter technique can only detect methyl groups, irrespective of whether the methyl groups belongs to a butyl branch or chain end. Short-chain branches can be introduced into polyethylenes in a controlled manner by copolymerizing ethylene with α-olefins. In this study we looked at the branches formed when 1-pentene was introduced into ethylene copolymers with a metallocene/MAO catalyst system. The catalyst used in this study was $Et(Ind)_2ZrCl_2$.

3.5.4.1 Polyethylene

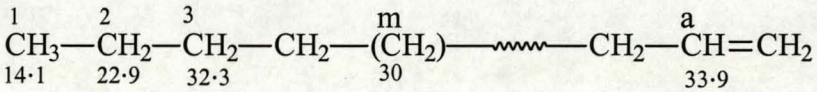

An examination of the ^{13}C NMR spectrum of a completely linear polyethylene, containing both terminal olefinic and saturated end-groups, shows only 5 resonances. The major resonance at δ(30)ppm is ascribed to equivalent, recurring methylene carbons, designated as 'm' (see above), which are four or more positions distant from an end group or a branch. Resonances at δ(14.1), δ(22.9) and δ(32.3)ppm are carbons 1, 2 and 3, from the saturated, linear end group. The resonance at δ(33.9)ppm is ascribed to an allylic carbon, designated as 'a', from a terminal olefic end-group[22].

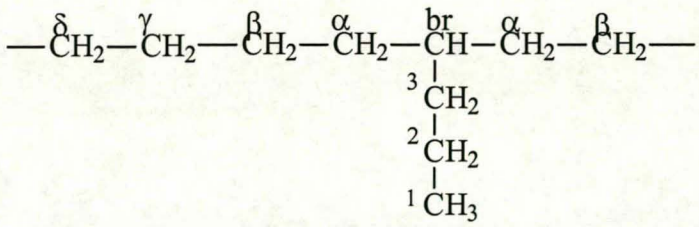

Figure 3.14. Carbon assignment scheme used for branched polyethylene.

The nomenclature used to designate the polymer backbone and side-chain carbons in ethylene/α-olefin copolymers as used in the discussion of ^{13}C NMR spectroscopy, is shown in Figure 3.14[23]. The distinguishable backbone carbons are designated by Greek symbols, while the side-chain carbons are numbered consecutively, commencing with the methyl group and ending with the methylene carbon bonded to the polymer backbone.

In the ^{13}C NMR spectrum of polyethylene obtained from $Et(Ind)_2ZrCl_2$/MAO (spectrum shown in Figure 3.15) the only signals that could be seen were the signals at δ(30.3)ppm and δ(28.9)ppm. The signal at δ(30.3)ppm is due to the methylene carbons of the polyethylene backbone and the signal at δ(28.9)ppm could be ascribed to the methylene carbons of an ethyl branch near the chain ends. Due to the absence of a signal at δ(10.94)ppm for the methyl group of the ethyl branch, as well as the absence of a signal for the methine carbon at δ(39.86)ppm[24], the assignment of the peak at δ(28.9)ppm is inconclusive.

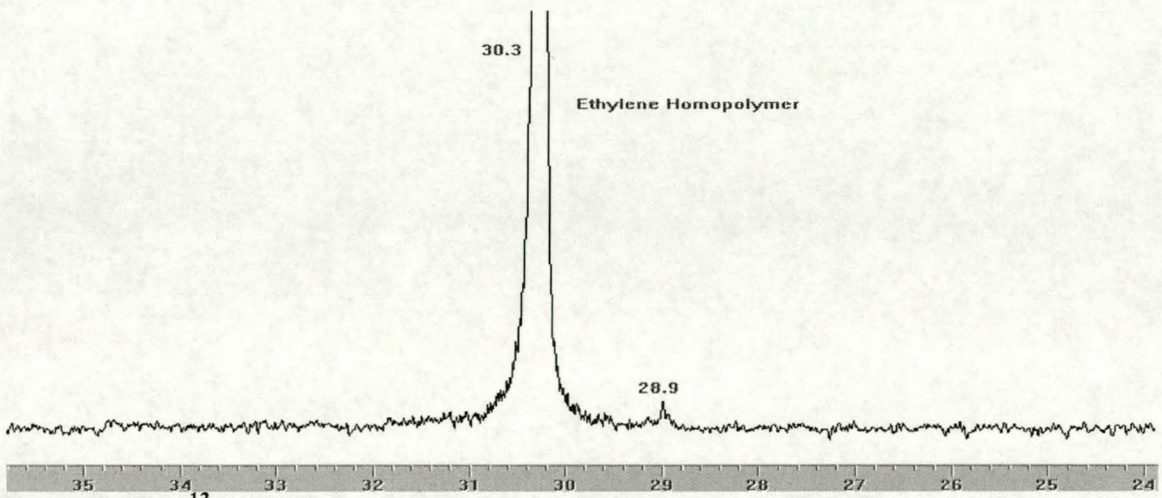

Figure 3.15. ^{13}C NMR spectrum of polyethylene (sample EtPn0).

Solvent: 1,2,4-trichlorobenzene:benzene-d_6 (9:1 volume ratio), temperature: 100°C.

3.5.4.2 Ethylene/1-pentene copolymers

After the introduction of a comonomer (for example 1-pentene) into the polyethylene chain, more ^{13}C NMR peaks can be seen. Confirmation of assignments of the chemical shifts, as well as their multiplicities, could be determined by using the attached proton test (APT) experiment, without any great loss in sensitivity. In the APT spectrum, the ^{13}C signals are converted into negative and positive signals[25]. CH_3- and CH-carbon atoms are characterised by negative amplitudes, while the CH_2- and C-carbon atoms are characterised by positive amplitudes. Figure 3.16 shows the APT ^{13}C NMR spectrum of an ethylene/1-pentene copolymer (EtPn4, 5.2% 1-pentene).

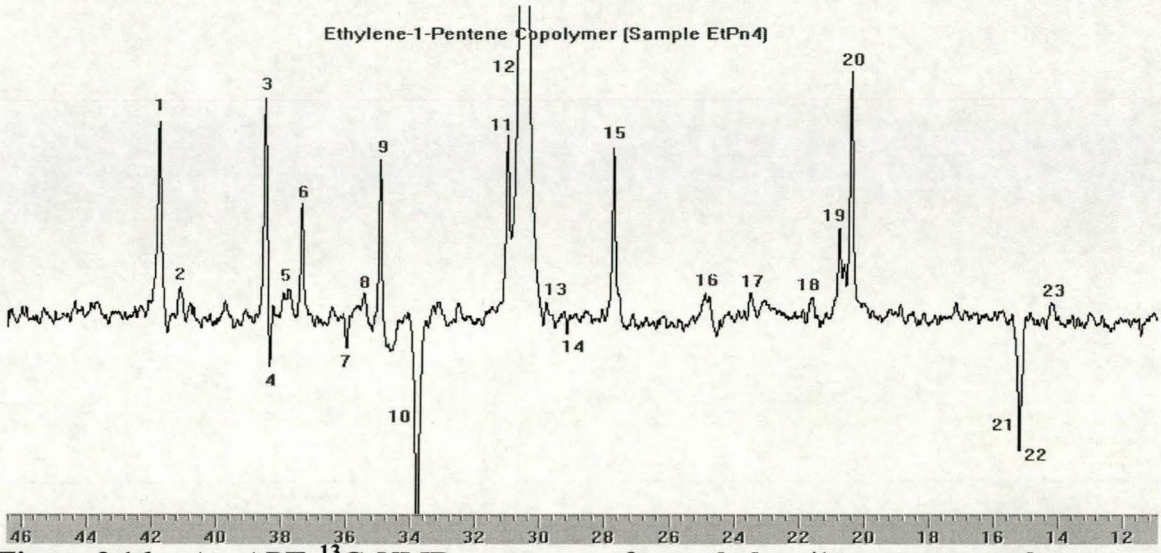

Figure 3.16. An APT ^{13}C NMR spectrum of an ethylene/1-pentene copolymer (sample EtPn4, 5.2% 1-pentene).

Solvent: 1,2,4-trichlorobenzene:benzene-d_6 (9:1 volume ratio), temperature: 100°C.

From the APT spectrum it can be seen that the peaks numbered 4, 7, 10, 14, 21 and 22 have negative amplitudes and are resonances ascribed to CH_3- and CH-carbon atoms. The rest of the peaks have positive amplitudes and are ascribed to CH_2- and C-carbon atoms. Proposed assignments of these peaks will be given in Table 3.3.

Figure 3.17 shows the ^{13}C NMR spectrum of an ethylene/1-pentene copolymer (EtPn1, 1.5% 1-pentene).

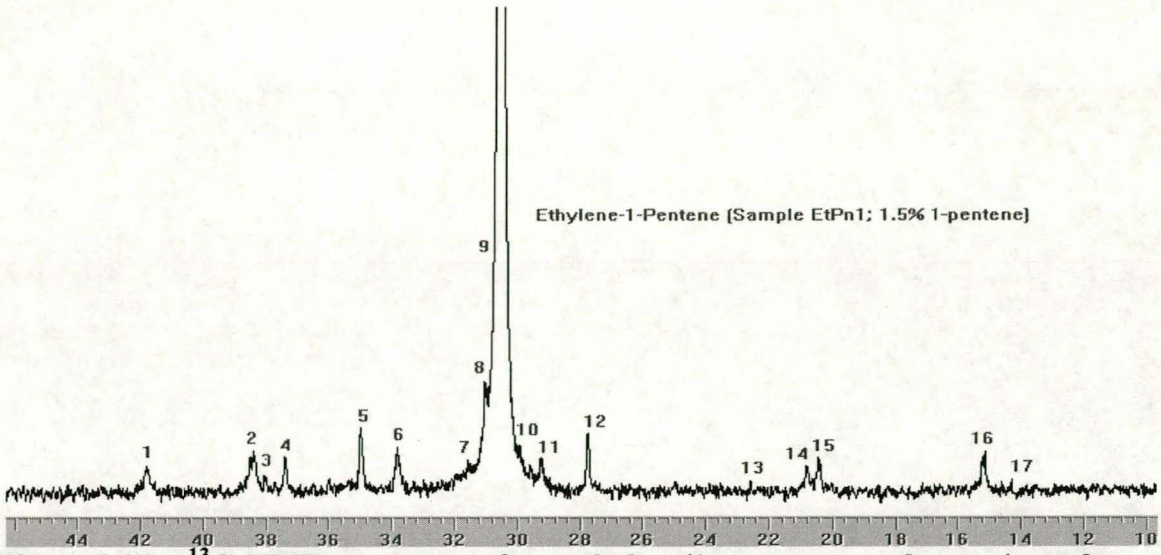

Figure 3.17. ^{13}C NMR spectrum of an ethylene/1-pentene copolymer (sample EtPn1, 1.5 % 1-pentene).

Solvent: 1,2,4-trichlorobenzene:benzene-d_6 (9:1 volume ratio), temperature: 100°C

The amount of 1-pentene incorporated was measured by calculating the ratio of the integrated signals of the $^{2}CH_2$ δ(20.44)ppm signal with that of the backbone carbons δ(30.05)ppm. Many problems can arise if the proper experimental parameters are not used in the analysis of polyolefins with the use of NMR. Problems include the independent specification of the correct pulse NMR experimental conditions, instrumental sensitivity, peak assignments, requirements for quantitative analysis, and conformation of internal consistency among these assignments[24]. Many problems arise when nonequilibrium magnetization data is acquired. For instance, short-pulse repetition rates selectively saturate carbons having the longest relaxation times and lead to the conclusion that branch types associated with such carbons are quantitatively reduced or are not present. Even if all the resonances can be identified they will contain very little useful quantitative information.

Figures 3.18, 3.19 and 3.20 contain the ^{13}C NMR results for the ethylene/1-pentene copolymers with 2.6%, 5.2 % and 45% 1-pentene incorporated in the copolymer. The solvent used in the recording of ^{13}C NMR spectra was a mixture of 1,2,4-trichlorobenzene and benzene-d_6 (9:1 volume ratio). Table 3.3 contains the experimental results and the calculated assignments[24, 26-28] of the different signals of the ethylene/1-pentene copolymers.

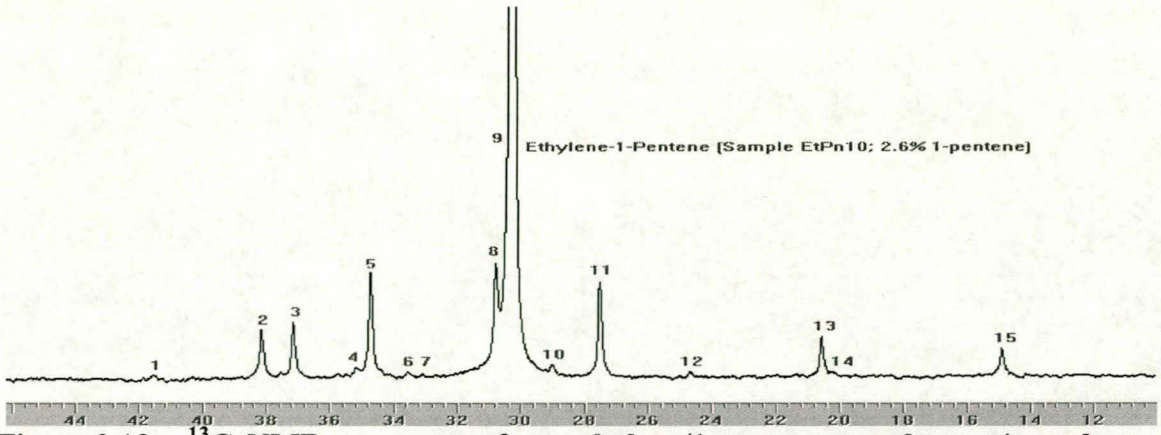

Figure 3.18. ^{13}C **NMR spectrum of an ethylene/1-pentene copolymer (sample EtPn10, 2.6 % 1-pentene).**

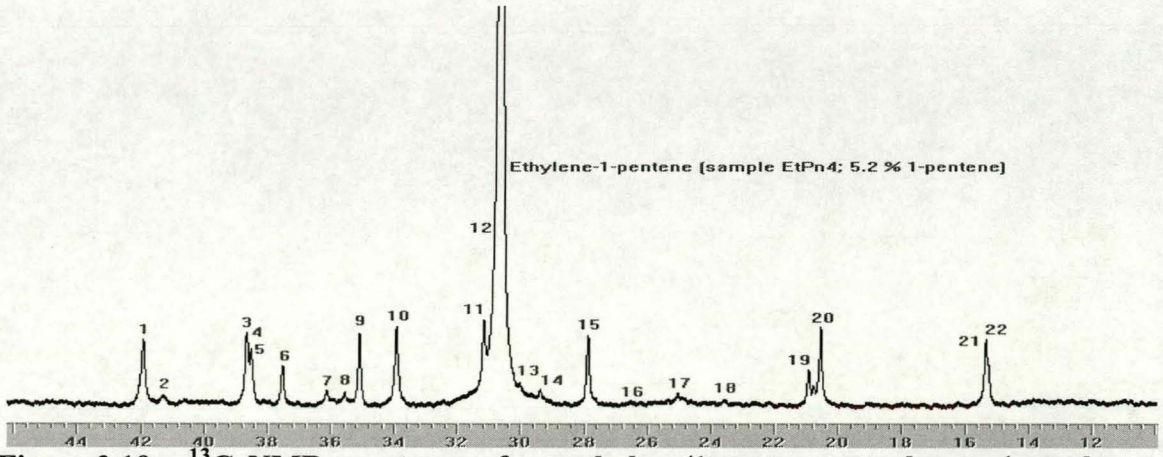

Figure 3.19. ^{13}C **NMR spectrum of an ethylene/1-pentene copolymer (sample EtPn4, 5.2% 1-pentene).**

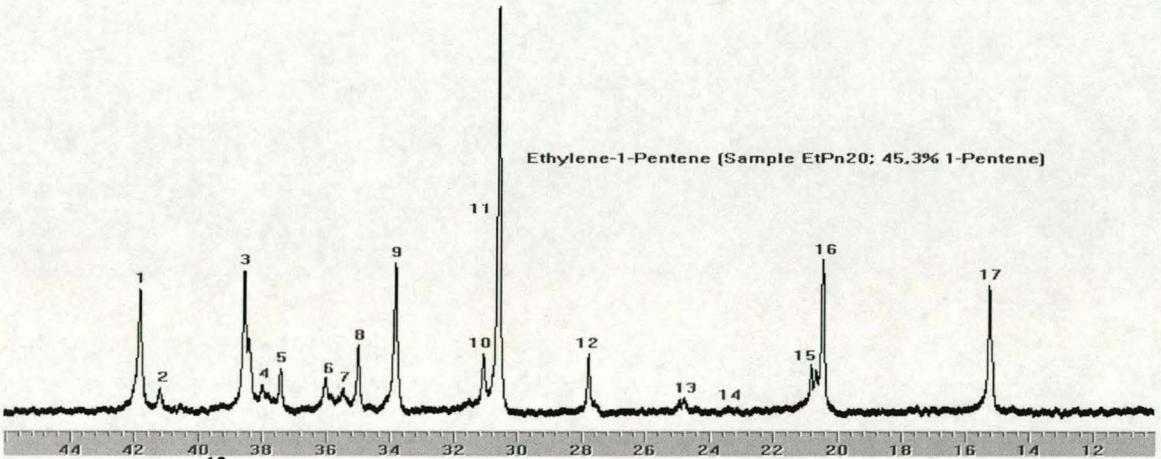

Figure 3.20. ^{13}C **NMR spectrum of an ethylene/1-pentene copolymer (sample EtPn20, 45% 1-pentene).**

Table 3.3. ^{13}C NMR spectra signal assignment of ethylene/1-pentene copolymers

EtPn1		EtPn10		EtPn4		EtPn20			
Sig-nal	Observed δ(ppm)[a]	Sig-nal	Observed δ(ppm)[a]	Sig-nal	Observed δ(ppm)[a]	Sig-nal	observed δ(ppm)[a]	Calculated δ(ppm)[b]	Carbon Assignment[c]
1	41.75	1	41.92			1	41.804		
		2	41.24	1	41.54	2	41.16		
2	38.52	3	38.68			3	38.54		
		4	38.61			3-4	38.3		
3	38.38	5	38.47	2	38.17	4	37.99	39.7	^{br}CH
4	38.06	6	36.11	3	37.16	5	37.39	39.4	^{3}CH
		7	35.5	4	35.22	6	36.01		CH
		8	35.16			7	35.46		
5	34.97	9	33.95	5	34.77	8	35.00	36.8	$^{a}CH_2$
6	33.81	10	31.18	6	33.55	9	33.81	34.4	
7	31.56			7	33.09				
8	31.05	11	30.71	8	30.79	10	31.4	30.4	$^{\gamma}CH_2$
9	30.05	12	30.64	9	30.32	11	30.59	30	CH_2 backbone
10	29.97	13	30.03						
11	29.22	14	29.36	10	28.93			29.2	β-CH_2 saturated end group
12	27.77	15	27.87	11	27.51	12	27.74	27.3	$^{\beta}CH_2$
		16	26.52						
		17	25.04	12	24.69	13	24.75		
13	22.59	18	23.55			14	23.42	22.9	β-CH_2 saturated end group
14	20.81	19	20.92			15	20.8	20.6	methyl branch
15	20.44	20	20.58	13	20.58	16	20.43	20.3	$^{2}CH_2$
16	15.15	21	15.38	14	20.17			14.6	$^{1}CH_3$
17	14.27	22	15.31	15	14.19	17	15.24	14.4	$^{1}CH_3$

[a]Solvent 1,2,4-trichlorobenzene: benzene-d_6 (9:1 volumer ratio), temperature 100°C

[b] (ppm) values obtained from literature, reference 24.

[c]Carbon numbering scheme used for branched polyethylene described in Figure 3.14.

The ratio between the intensities of the $^{2}CH_2$ carbon δ(20.44)ppm of the propyl branch and the backbone carbons δ(30.05)ppm is used to calculate the amount of 1-pentene incorporated in the ethylene/1-pentene copolymers. Table 3.4 shows the relative intensities of the signals at δ(20.44)ppm ($^{2}CH_2$ carbons) and at δ(30.05)ppm (backbone carbons), used to calculate the amount of 1-pentene incorporated in each copolymer.

Table 3.4. Relationships between the intensities of the $^{2}CH_2$ carbons at δ(20.44)ppm and the backbone carbons at δ(30.05)ppm

Copolymer	Intensities of $^{2}CH_2$ carbons at δ(20.44)ppm	Intensities of backbone carbons at δ(30.05)ppm	Mole % 1-pentene in copolymer
EtPn1	107.32	1.63	1.5%
EtPn10	114.84	3.10	2.6%
EtPn4	32.35	1.68	5.2%
EtPn20	3.09	1.4	45.31%

3.5.4.3 Short-chain branching of ethylene/1-pentene copolymers

The samples EtPn1, EtPn10 EtPn4 and EtPn20 all exhibit a resonance at δ(20.58 ± 0.15)ppm. This corresponds to the expected resonance of the C-2 carbon of the propyl branch group (δ(20.85)ppm described in the literature[24].

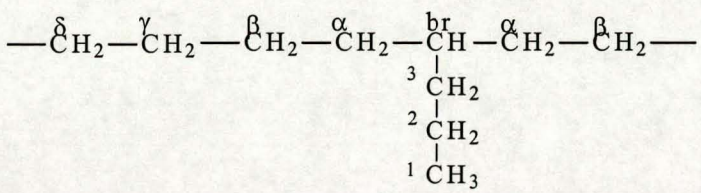

Both the C-3 carbon of the propyl branch and the methine backbone carbon (^{br}CH) should contribute signals in the region of δ(37)ppm. There is an asymmetric peak of relatively large intensity here but the various contributing carbons cannot be individually recognized. The Grant and Paul[29] substituent parameters predict a difference of δ(0.81)ppm between the methyl resonance and the C-2 carbon of a propyl branch. Similarly, the Lindeman-Adams[30] parameters predict a difference of δ(0.57)ppm. The methyl carbon of the propyl branch ($^{1}CH_3$) resonates at

δ(14-15)ppm.

Ethyl branches are usually characterised by the presence of the following resonances:

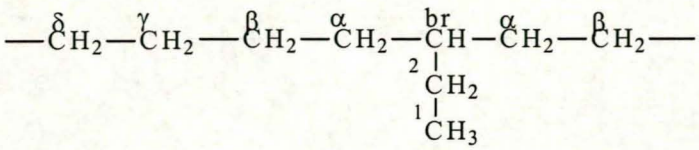

a)The resonance of the methine carbon groups of the ethyl branch (^{br}CH) is usually a low-intensity signal at δ(39.86)ppm.

b)The C-2 carbon groups of the ethyl branch is normally found at δ(27.15 ± 0.04)ppm[24].

c)The α-carbon groups adjacent to the ethyl branch ($^{\alpha}CH_2$) should resonate in the region of δ(34)ppm.

d)The methyl carbon ($^{1}CH_3$) groups of the ethyl branch, always observed when ethyl branches are present, would resonate at δ(10.94)ppm[24].

Though the signals at δ(41)ppm, δ(35.16)ppm, and δ(27.77)ppm are observed, the resonance of the methyl carbon is <u>not</u> observed. Thus there is no evidence of ethyl branches in these samples (neither isolated nor adjacent to each other).

Butyl branches are characterised by resonances at δ(38.27)ppm, δ(23.34)ppm and δ(14.00)ppm, due to the C-4 and C-2 methylene carbons and the C-1 methyl carbon of

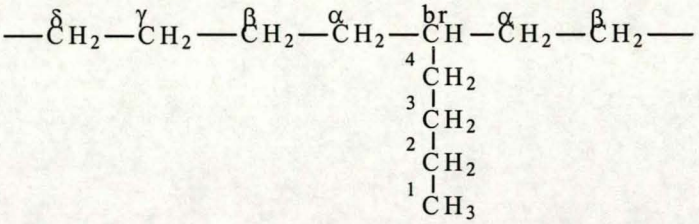

the butyl branch[24]. However, it is only the resonance at δ(23.34)ppm, due to the 2-methylene carbon, which could indicate the presence of the butyl branch. This resonance can be found in samples EtPn10 (peak 18) and EtPn20 (peak 14). As can be seen from Figures 3.19 and 3.20, the resonances of these signals are of low intensity and difficult to identify.

The literature reports that amyl branches in branched polyethylene show a unique resonance at approximately δ(32.7-32.4)ppm. This shift is attributed to the C-3

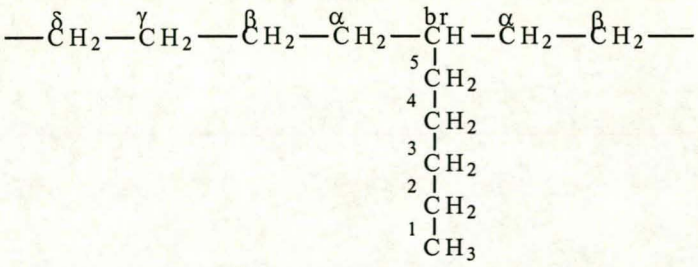

carbon of the amyl branch[24]. In addition, in the C-3 region, the signal at δ(22.85)ppm represents a composite contribution from the C-2 methylenes of amyl and longer chains. In samples EtPn4 and EtPn20, in which there is a higher 1-pentene content compared to samples EtPn1 and EtPn10, the presence of these branches can not be identified with certainty.

It can be concluded that not all the ^{13}C NMR signals can be assigned to specific types of branches with certainty.

3.6 CONCLUSIONS

High molecular mass ethylene/1-pentene copolymers (M_w between 111 000 g/mol and 172 200 g/mol) were obtained with the $Et(Ind)_2ZrCl_2$/MAO catalyst system. The presence of propyl branches, evident in ^{13}C NMR analysis, indicates that copolymerization took place. Increasing the amount of 1-pentene in the feed resulted in an increase of 1-pentene incorporated in the copolymer. The melting point, as well as percent crystallinity, of the ethylene/1-pentene copolymers decreased with increasing 1-pentene content. The molecular mass distribution of the ethylene/1-pentene copolymers was narrow (typical for copolymers formed in reactions with metallocene catalysts) but increased with increasing 1-pentene content.

3.7 REFERENCES

1. Beilov G.P, Belova V.N., Raspopov L.N., Kissin Y.V., Brikenstein K.A., Chirkov N.M., *Polym. J.*, 1992, **3**, 681.

2. Krentsel B.A., Kissen Y.V., Kleiner V.J., Stotskaya L.L., *Polymers and Copolymers of Higher α-Olefins*, Hanser Publishers, Munich, 1997, p.278.
3. Sinn H., Kaminsky W., *Adv. Organomet. Chem.*, 1980, **18**, 99.
4. Aulbach M., K ber F., *Chem. Z.*, 1994, **28**, 197.
5. Huang J., Rempel G.L., *Polym. Sci.*, 1995, **20**, 459.
6. Brintzinger H.H., Fischer D., M lhaupt R., Rieger B., Waymouth R., *Angew. Chem.*, 1995, **107**, 1255.
7. (a)Kaminsky W. and Miri M., *J. Polym. Chem.*, 1985, **23**, 2151.,
   (b)Kaminsky W. and Schlobohen M., *Makromol. Chem. Macromol. Symp.*, 1986, **4**, 103.,
   (c)Kaminsky W., in *Transition Metal Catalysed Polymerizations*, R.P. Quirk, Ed. Harwood, New York, 1983, p. 25.,
   (d)Drögemüller H., Heiland K., Kaminsky W., *Transition Metals and Organometallics as Catalysts for Olefin Polymerizations*, Kaminsky W. and Sinn H., Eds. Springer-Verlag, Berlin, 1987, p. 303.
8. Ewen J.A., in *Catalytic Polymerization of Olefins*, Keii T. and Soga K., Eds., Kodansha, Tokyo, 1986, p. 271.
9. Lehtinen C., Starck P., Löfgren B., *J. Polym. Sci.: Part A: Pol. Chem.*, 1997, **35**, 307.
10. Wild F.R.W.P., Zsolani L., Huttner G., and Brintzinger H.H., *J. Organomet. Chem.*, 1982, **232**, 233.
11. Wild F.R.W.P., Wasincionek M., Huttner G., and Brintzinger H.H., *J. Organomet. Chem.*, 1985, **288**, 63.
12. Koivumäki J., Seppällä J.V., *Eur. Polym. J.*, 1994, **30**, 10, 1111.
13. Mirabella F., Jr., Ford E.A., *J. Polym. Sci.: Polym. Phys. Ed.*, 1987, **25**, 777.
14. Sequela R., Rietsch F., *J. Polym. Sci.: Polym. Lett.*, 1988, **23**, 415.
15. Sakurai K., MacKnight W.J., Lohse D.J., Schulz D.N., Sissano J.A., *Macromolecules*, 1994, **27**, 4941.
16. Starck P., Lehtinen C., Löfgren B., *Die Angewandte Makromol. Chemie*, 1997, **249**, 115.
17. Starck P., *Polym. Int.*, 1996, **40**, 122.
18. Lehtinen C., Löfgren B., *Eur. Polym. J.*, 1997, **33**, 115.
19. Usami T., Gotoh Y., Takayama S., *Macromolecules*, 1986, **19**, 2722.

20. Baker B.B., Bonesteel Jr. J.K., Keating M.Y., *Thermochimica Acta*, 1990, **166**, 53.

21. Blitz J.P., McFaddin D.C., *J. Appl. Polym. Sci.*, 1994, **51**, 13.

22. Campbell D., *Polymer Characterization: physical techniques*, London: Chapman and Hall, 1989.

23. Bailey A.L., Kale L.T., Tchir W.J., *J. Appl. Polym. Sci.,* 1994, **51**, 547.

24. Axelson D.E., Levy G.C., Mandelkern L., *Macromolecules*, 1979, **12**, 1, 41.

25. Cheng H.N., *Macromolecules*, 1991, **24**, 4813.

26. Hsieh E.T., Randall J.C., *Macromolecules*, 1982, **15**, 353.

27. Rossi A., Zhang J., Odian G., *Macromolecules*, 1996, **29**, 2331.

28. Peng Y.X., Cun L.F., Dai H.S., Liu J.L., *J. Polym. Sci. Part A: Polym. Chem.*, 1996, **34**, 903.

29. Grant D.M., Paul E.G., *J. Am. Chem. Soc.*, 1904, **86**, 2984.

30. Lindemann L.P., Adams J.Q., *Anal. Chem.*, 1971, **43**, 2984.

CHAPTER 4

Copolymerization of propylene/1-pentene with the isotactic stereorigid zirconium metallocene catalyst system *rac*-Et(Ind)$_2$ZrCl$_2$/MAO

Summary

The copolymerization of propylene/1-pentene using a methylalumoxane-activated metallocene catalyst, the isospecific catalyst *rac*-[ethylene*bis*(1-indenyl)]zirconium dichloride] (*rac*-(EBI)ZrCl$_2$), was performed in toluene. The influence of polymerization temperature, variation of the Al/Zr molar ratio and the use of different monomer feed ratios on the amount of comonomer incorporation, melting points, molecular masses, molecular mass distributions, and on the microstructure of the copolymers, was investigated. The peak melting point of the copolymers decreased with increasing 1-pentene content in the copolymer. The weight-average molecular mass of the copolymers obtained was in the range of 20 000-30 000 g/mol which is too low for industrial use, but interesting for academic research. The highest amount of 1-pentene incorporated and the higher molecular mass was found in copolymers prepared in reactions carried out at lower temperatures. Narrow molecular mass distributions were found, owing to the properties of the metallocene catalyst. The propylene/1-pentene copolymers were analysed by DSC, GPC, NMR- and IR-spectroscopy.

4.1. INTRODUCTION

Metallocene catalysts offer new possibilities for controlling the properties of copolymers of linear α-olefins, extending beyond the capabilities of classical heterogeneous catalysts. Metallocene catalysts generally have the advantage of producing polymers with equally distributed comonomer in the polymer backbone and with narrow molecular mass distribution.

Kaminsky[1] and coworkers[2-4] found that combinations of metallocenes with oligomeric methylalumoxane (MAO) form ethylene polymerization catalysts[4] which have extremely high activities. They have however, little activity for propylene polymerization or produce only atactic polypropylene[5]. Brintzinger and coworkers[6, 7] synthesized ethylene *bis* (tetrahydroindenyl) (Et[$IndH_4$]$_2$) and ethylene *bis* (indenyl) (Et[Ind]$_2$) ligands and the corresponding dichlorozirconium compounds with these ansa-ligands: (Et[$IndH_4$]$_2$)$ZrCl_2$ and Et[Ind]$_2ZrCl_2$. (Et[$IndH_4$]$_2$)$ZrCl_2$ and Et[Ind]$_2ZrCl_2$, activated with MAO, were found to catalyze the stereospecific polymerization of propylene[8-11].

Much research has been carried out on ethylene/propylene copolymerization with metallocene catalysts[12-17]. Product properties can be varied by changing the polymerization temperature or the comonomer concentration. Copolymers with propylene concentrations ranging from 10 to 90 wt% have been produced[18-20]. Other comonomers for propylene were 1-butene[21], 1-hexene[22], 1-octene[23] and norbornene[24].

In this work we studied the influence of various reaction parameters used in the copolymerization of propylene and 1-pentene with the homogeneous metallocene catalyst Et[Ind]$_2ZrCl_2$ on the resultant copolymer properties. The process parameters investigated were: polymerization temperature, the Al/Zr molar ratio and the effect of increasing comonomer content. The polymer properties of interest were the melting point, molecular mass of the polymer and intrinsic viscosity. Molecular mass distributions, with GPC analyses, and the microstructure, with NMR analyses, of the samples were also determined.

4.2 EXPERIMENTAL

The experimental conditions were as described previously (Section 3.2) except that here polymerization grade propylene (> 99.5%) was purchased from Messer Fedgas and purified by passing through three columns containing BASF catalysts R3-11G and R3-12 and molecular sieve of 3Å obtained from Polifin (see Figure 4.1).

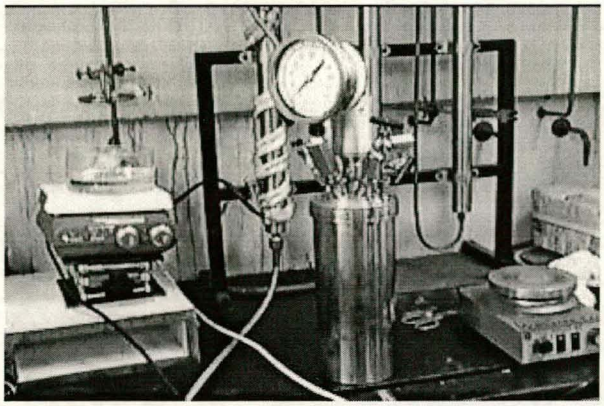

Figure 4.1. Experimental apparatus used in the copolymerization of propylene with 1-pentene: reactor, purification columns and temperature-regulated oil bath.

4.3 EQUIPMENT

4.3.1 Polymerization equipment

Two different reactors were used in the polymerization of propylene with 1-pentene. In the first series, a small 75 mL thermostable stainless-steel autoclave was used and in the second and third series of propylene copolymerizations, a 350 mL, teflon-sealed, stainless-steel Parr reactor was used. The small reactor was equipped with a fitted steal seal ring and the larger reactor with a teflon seal ring. Both reactors had a pressure gauge.

4.3.2 Analytical equipment

The copolymers were characterized by DSC, GPC, NMR- and IR-spectroscopy. A description of the analytical equipment and the methods used are given in Section 3.3.2.

4.4 SYNTHESIS OF COPOLYMERS

The copolymerization of propylene with 1-pentene was carried out in three separate series. After the first series of reactions in which an [Al]:[Zr] ratio of 2000:1 was used in

the small reactor, a larger reactor, was used for the second series. This was done to overcome the problem of the small amount of product formed. In the second series, the [Al]:[Zr] ratio was 10 000:1 and the temperature of the reaction was increased from 50°C to 60°C. The third series was carried out to investigate the influence of the reaction temperature on the copolymer properties. For this the temperature was increased to 80°C.

4.4.1 Series 1

The following series of copolymerization reactions was carried out using different amounts of 1-pentene.

Polymerization was carried out in a 75 mL stainless steel pressure reactor fitted with a magnetic stirring bar. The system was first evacuated, flushed with nitrogen and then 10 mL toluene were introduced. A Schlenk tube was filled with 1 mL (2 mol/L) MAO in 5 mL toluene. The catalyst solution (1 mL, 10^{-4} mol/L) was added to the Schlenk tube and preactivated for 5 min by standing at room temperature. The [Al]:[Zr] ratio used in this series was 2000:1. The comonomer, 1-pentene, was added and then the catalyst/cocatalyst/comonomer mixture was introduced into the reactor, and the polymerization was initiated by introducing the monomer. The total volume of the reaction mixture for all the polymerizations was 10 mL. Finally, the reactor was charged with propene until the pressure in the reactor was 1 MPa.

The reactor was placed in a temperature-controlled oil bath, set at 50°C. After 3 hours the reactor was vented, opened and the copolymer produced was precipitated in 200 mL ethanol, acidified with 10 mL 10 wt% aqueous HCl. The copolymer was filtered, and then dried at room temperature under vacuum for 6 hours.

4.4.2 Series 2

In series 2 five different reactions were carried out with different amounts of 1-pentene in the reaction mixture. The catalyst concentration was 25 μmol/L. In these copolymerizations the [Al]:[Zr] ratio was changed from 2 000:1 (series 1) to 10 000:1.

This series was carried out in a larger reactor (350 mL); the total volume of the reaction mixture was now 40 mL instead of the 10 mL.

The procedure followed was the same as described in Section 4.4.1. The introduction of propylene into the reactor was done in an icebath, to increase the solubility of the propylene in the toluene. Propylene has a negative temperature dependence of solubility in toluene, as shown by Wang[25] (see Figure 4.2). The reaction temperature of this series was 60°C.

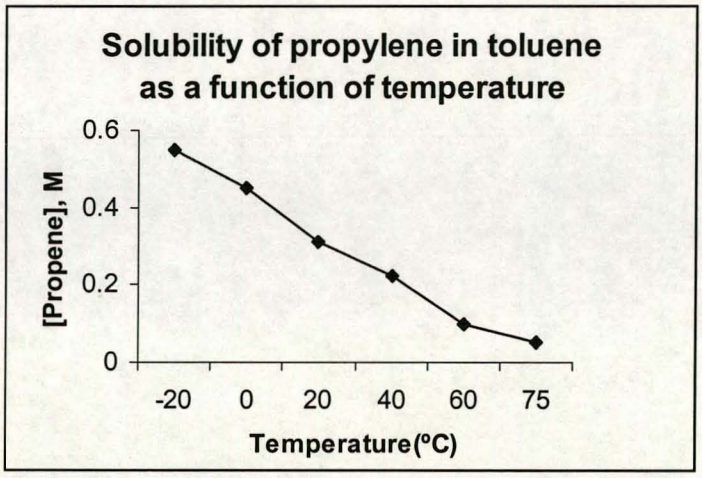

Figure 4.2. The solubility of propylene in toluene as a function of temperature [26].

4.4.3 Series 3

The same procedure was followed as in Section 4.4.2, but the temperature of the copolymerization reactions was changed to 80°C.

4.5 SUMMARY OF COPOLYMERIZATION REACTIONS

A summary of the reactions conditions for the copolymerizations of propylene with 1-pentene in the series 1, 2 and 3 are tabulated in Table 4.1.

Table 4.1 Reaction conditions of propylene/1-pentene copolymerizations carried out with $Et(Ind)_2ZrCl_2$

	PROPYLENE/1-PENTENE COPOLYMERS		
	Series 1	**Series 2**	**Series 3**
Reactor size	75 mL	350 mL	350 mL
[catalyst] (mol/dm^{-3})	10^{-4}	9.5×10^{-4}	9.5×10^{-4}
[Al]:[Zr]	2000:1	10 000:1	10 000:1
Polymerization temperature T_p(°C)	50°C	60°C	80°C
Time (min)	180	180	180
Pressure (reactor)	1 MPa	1 MPa	1 MPa

4.6 RESULTS AND DISCUSSION

Polymerization conditions, polymer yields, and copolymerization data for the copolymerization of propylene with 1-pentene are presented in Table 4.2.

Table 4.2. Polymerization conditions, catalyst yields, and copolymerization data for the propylene/1-pentene copolymerization reactions

Sample	[Al]:[Zr]	T_p(°C)	1-Pentene feed content (mol %)	1-Pentene content in copolymer (mol %)[c]	Polymer yield(g)
Series 1[a]					
Mg05	2000:1	50	3.8	1.9	2.7
Mg02	2000:1	50	10.7	3.8	3.4
Mg01	2000:1	50	30	13.7	2.1
Series 2[b]					
Mg33	10000:1	60	0	0	3.0
Mg36	10000:1	60	2.8	2.1	14.8
Mg14	10000:1	60	6.3	2.7	6.7
Mg34	10000:1	60	11.8	8.7	12.6
Mg35	10000:1	60	15.7	7.1	9.0
Series 3[b]					
Mg37	10000:1	80	0	0	6.9
Mg41	10000:1	80	3.5	0.5	35.5
Mg39	10000:1	80	5.8	0.8	19.2
Mg38	10000:1	80	12.6	4.4	28.5
Mg40	10000:1	80	20.6	9.9	16.2

[a]Polymerization conditions: solvent toluene, [Al] 2 mol/L, [Zr] 10^{-4} mol/L, time 3 hours.

[b]Polymerization conditions: solvent toluene, [Al] 2 mol/L, [Zr] 25 ℓmol/L, time 3 hours.

[c]Content of 1-pentene in copolymers determined by ^{13}C NMR spectroscopy.

4.6.1 Melting points

All the copolymers were analyzed by DSC to determine their melting points and crystalline content. The melting temperature was obtained as described in Section 3.5.1. We report the offset temperature, peak melting temperature and the end of melting. The offset temperature of melting (T_m) was determined by the conventional interpolation method[27] as illustrated in Figure 4.5. The value of enthalpy of the transition, ΔH_f, was also evaluated from the peak area by taking a base line as illustrated in the Figure 4.5. The measured enthalpy of fusion (ΔH_f) was converted to the degree of crystallinity (m_c/m_o) by taking the ratio of the measured heat of fusion (ΔH_f) to that of a standard of known crystallinity. The heat of fusion of a perfect polypropylene crystal, used in the determination of the crystallinity, was taken as 209 J/g[28, 29]. The amounts of 1-pentene incorporated, the melting points, heats of fusion and percentage crystallinities of the propylene/1-pentene copolymers are summarized in Table 4.3.

Table 4.3. Results of DSC analysis of propylene/1-pentene copolymers

Sample	1-Pentene (mol %)	Offset of melting temperature	Melting peak temperature T_m[a] (°C)	End of melting temperature	Heat of fusion ΔH_f(J/g)	Crystallinity m_c/m_o[b] (%)
Mg05	1.9	116	123	128	62	29.7
Mg02	3.8	98	112	121	33	15.8
Mg01	13.7	90	104	110	12	5.7
Mg33	0	129	137	140	57	27.3
Mg36	2.1	114	126	131	44	21.1
Mg14	2.7	116	124	128	23	11.0
Mg35	7.1	94	103	110	20	9.6
Mg34	8.7	84	98	108	11	5.3
Mg37	0	132	140	142	30	14.4
Mg41	0.5	105	116	123	19	9.1
Mg39	0.8	101	113	120	27	12.9
Mg38	4.4	88	102	111	24	11.5
Mg40	9.9	61	77	96	10	4.8

[a]Final temperature of melting peak. [b]Calculated from heat of fusion of samples and heat of fusion of perfectly crystalline polypropylene, assuming 209 J/g for ethalpy of perfectly crystalline polypropylene.

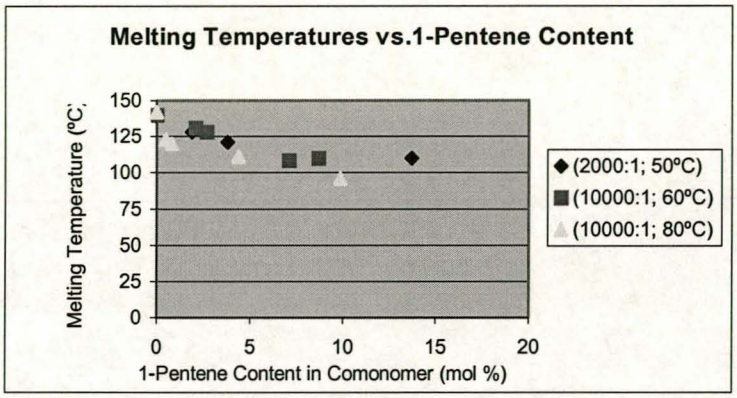

Figure 4.3. Effect of the content of 1-pentene on the melting point of the propylene/1-pentene copolymers.

The melting temperatures of the copolymers decrease as the 1-pentene content in the copolymer is increased (Figure 4.3). This in accordance with the theory[29] that the introduction of a comonomer into a polymeric chain creates a discontinuity that sharply reduces the crystallization tendency, comparable to a reduction in stereoregularity in homopolymers. The results are a reduction in the rate of crystallization, a lower level of crystallinity (Figure 4.4) and a reduction in the melting point, all related to the resultant less perfect structure of the chains. Figure 4.3 shows the melting points of the copolymers as a function of their 1-pentene content and Figure 4.4 shows the percentage crystallinity as a function of their 1-pentene content.

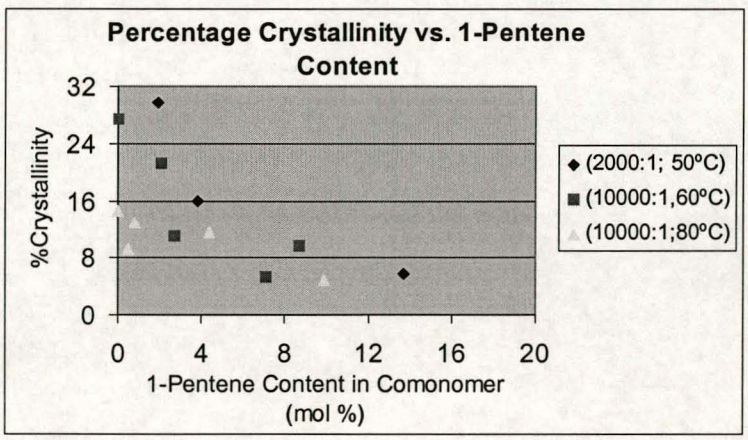

Figure 4.4. Effect of the content of 1-pentene on the crystallinity of the propylene/1-pentene copolymers.

The differential scanning calorimetry (DSC) traces of the following samples are shown in Figures 4.5-4.8:

4.5) sample Mg36, 2.1% 1-pentene;

4.6) sample Mg35,7.1% 1-pentene;

4.7) sample Mg37, 0% 1-pentene, and

4.8) sample Mg38, 4.4% 1-pentene.

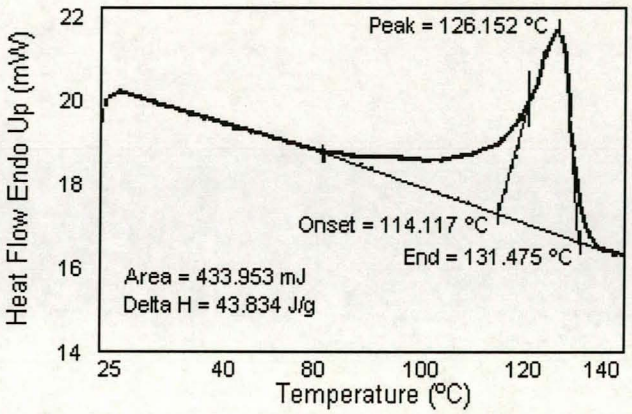

Figure 4.5. DSC trace of propylene/1-pentene copolymer (Mg36), showing the melting endotherm (2.1% 1-pentene).

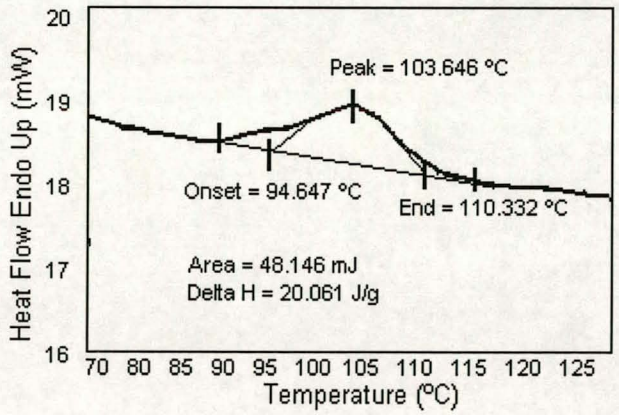

Figure 4.6. DSC trace of propylene/1-pentene copolymer (Mg35), showing the melting endotherm (7.1% 1-pentene).

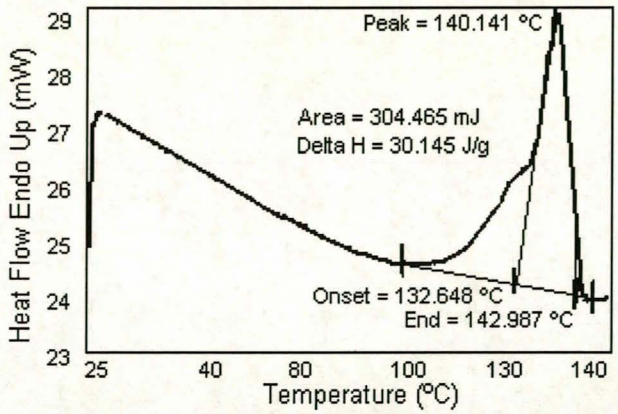

Figure 4.7. DSC trace of propylene/1-pentene copolymer (Mg37), showing the melting endotherm (0% 1-pentene).

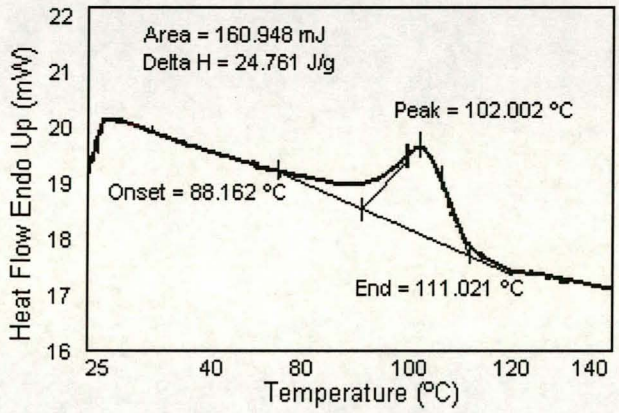

Figure 4.8. DSC trace of propylene/1-pentene copolymer (Mg38), showing the melting endotherm (4.4% 1-pentene).

The observed reduction in melting point from polypropylene (Mg37) to the propylene/1-pentene copolymer (Mg38) with 4.4% 1-pentene is related to the comonomer content. The propylene/1-pentene copolymers show single endotherms and in some cases melting curves with an additional shoulder in the lower temperature range. The broad peak found in sample Mg38 (4.4% 1-pentene) (see Figure 4.8) is due to the compositional heterogeneity of the copolymer. Any copolymer with pronounced compositional heterogeneity contains crystallizable sequences with a broad range of compositions, depending on the placement of pentene units along its chain. This leads to the very broad melting peak indicative of different fold lengths in the crystallites.

4.6.2. Molecular mass and molecular mass distributions

The molecular masses of all the polymers prepared with metallocene catalysts are very sensitive to reaction temperature: an increase in temperature leads to a decrease in molecular mass[30-33]. The molecular masses and polydispersities of all propylene/1-pentene copolymers, as determined by GPC analyses, are presented in Table 4.4.

Table 4.4. Molecular mass and molecular mass distributions of propylene/1-pentene copolymers

Sample	1-Pentene content (mol %)	Weight-average molecular mass M_w(g/mol)	Number-average molecular mass M_n(g/mol)	Viscosity-average molecular mass M_v(g/mol)	Molecular mass distribution M_w/M_n
Mg05	1.9	29 610	7 222	26 730	4.1
Mg02	3.8	26 650	7 378	23 610	3.6
Mg01	13.7	30 980	6 630	27 690	4.7
Mg33	0	47 050	20 740	43 000	2.3
Mg36	2.1	34 050	11 320	30 380	3.0
Mg14	2.7	46 661	24 260	43 540	1.9
Mg34	8.7	33 230	14 770	30 630	2.2
Mg35	7.1	49 010	23 070	45 530	2.1
Mg37	0	57 300	26 490	52 770	2.2
Mg41	0.5	19 230	4 158	16 090	4.6
Mg39	0.8	22 721	8 778	20 470	2.6
Mg38	4.4	24 030	7 406	21 540	3.2
Mg40	9.9	25 590	9 952	23 200	2.5

Generally the weight-average molecular masses of the copolymers were quite low, in the range 19 000 to 49 010 g/mol. The copolymer with the highest molecular mass was obtained at a reaction temperature of 60°C and an Al/Zr ratio of 10 000:1. This was confirmed by our results. The same trend was observed for the viscosity-average molecular mass. Viscosity-average molecular mass increases as the reaction temperature decreases. Pietikäinen *et al.*[14] investigated this for ethylene/propylene copolymers.

A distinct increase in molecular mass was observed when the Al/Zr ratio was increased from 2 000:1 to 10 000:1. This indicates that an increase of the rate of propagation occurs which is higher than that of chain termination, due to the higher activity and/or stability of the catalytic complexes in the presence of an excess of MAO.

It is reported that metallocene-MAO systems are inherently unstable. Their decomposition leads to methane evolution and the formation of a Zr-CH_2-Al species[30]:

$$>Zr\text{-}CH_3 + CH_3\text{-}AlO_2< \rightarrow >Zr\text{-}CH_2\text{-}AlO_2< + CH_4$$

Bimetallic Zr-CH_2-Al species produced in this reaction is not catalytically active and the number of polymerization centers is therefore reduced. However, the active centers can be regenerated with an excess of MAO[30]

$$>Zr\text{-}CH_2\text{-}AlO_2< + CH_3\text{-}AlO_2< \rightarrow >Zr\text{-}CH_3 + >O_2Al\text{-}CH_2\text{-}AlO_2<$$

An excess of MAO is therefore the reason for the increased activity of the catalyst and leads to copolymers with higher molecular mass.

The polydispersities of all the copolymers were in the range 2-4.7. From our results, no dependence of reaction temperature or Al/Zr ratio on MWD could be detected, but Rieger *et al.*[34] have reported that MWD is narrower at higher Al/Zr ratios and Pietikäinen *et al.*[14] showed that polydispersity increased with increasing temperature.

Figures 4.9 and 4.10 show the mass distribution of molar mass, w(log M), against the molar mass of two different samples, Mg35 (7.1% 1-pentene) and Mg41 (0.5% 1-pentene).

From Figures 4.9 and 4.10 it can be seen that the GPC curves of the copolymers have a characteristic shape, predicted by Flory's distribution law. The molecular mass distributions of such copolymers do not change with polymerization time. The molecular mass at the maximum corresponds to the weight-average molecular mass of the polymer. It can also be seen that Mg41 has a much broader molecular mass distribution (4.6) than that of Mg35 (2.1).

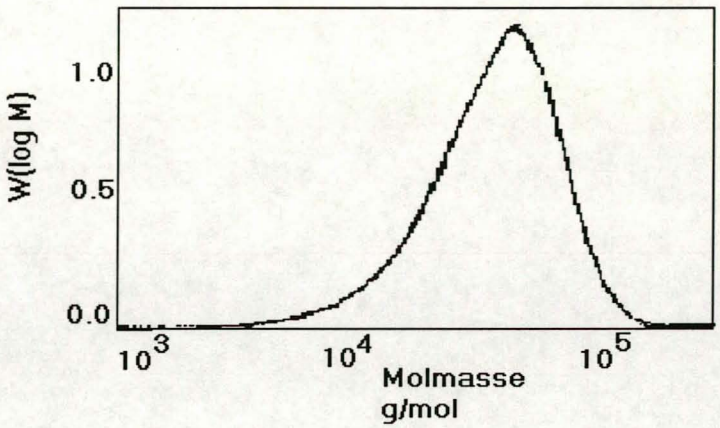

Figure 4.9. The distribution of the molar mass, w(log M), against the molar mass of the sample Mg35 (7.1% 1-pentene).

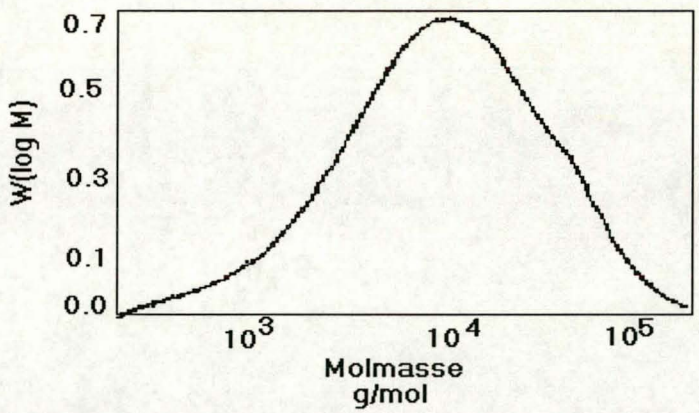

Figure 4.10. The distribution of the molar mass, w(log M), against the molar mass of the sample Mg41 (0.5% 1-pentene).

4.6.3 Photo-acoustic infrared spectroscopy (PAS-IR)

Infrared (IR) spectroscopy is a relatively simple, fast and potentially quantitative analytical technique. Infrared spectroscopy is frequently used to analyze short chain

branching. Useful information regarding the types of unsaturation present in copolymers can also be gained from the application of infared spectroscopy[35].

In the case of polypropylene

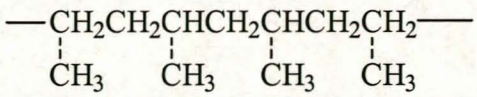

the following IR bands are present: Kissin and coworkers[36, 37] proposed three IR indices for the measurement of isotacticity [973 cm^{-1} for 5 meso units (5 isotactic units next to each other), 998 cm^{-1} for 11-12 meso units, and 841 cm^{-1} for 13-15 meso units]. The ratio A_{998}/A_{973} was said to measure the macrotacticity; the ratio A_{998}/A_{1460} was proposed as a measure of spectral degree of isotacticity. The 973 cm^{-1} band has been attributed to PP's head-to-tail sequence of repeat units and to the presence of short isotactic helices. McRae *et al.*[38, 39] and others[40] have found a band at 935 cm^{-1} which is specific for methyl branches. The presence of the –CH- group gives vibrations at 1465-1449 cm^{-1} (symmetric –C-H- stretching vibrations) and at 1390-1370 cm^{-1} (asymmetric –C-H- stretching vibrations).

The three types of unsaturation, which can occur in polypropylene, and their corresponding IR absorptions, are:

- $R_1R_2C{=}CH_2$: external vinylidene at 1645 cm^{-1} and 890 cm^{-1}

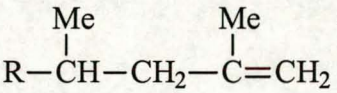

- $R\text{-}CH{=}CH_2$: terminal vinyl at 910 cm^{-1}

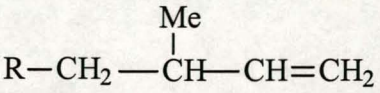

- internal double bonds at 1665 cm^{-1}

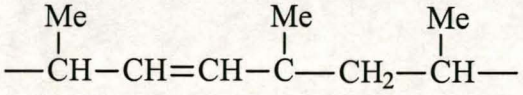

Three types of olefinic end groups, transvinyl (ν = 965 cm^{-1}), vinyl (ν = 910 cm^{-1}) and vinylidene (ν = 888 cm^{-1}) can be present in propylene copolymers.

Figure 4.11 shows the PAS-IR spectrum of polypropylene (Mg33, 0% 1-pentene), in which all these groups, except for the vinyl endgroup, are present.

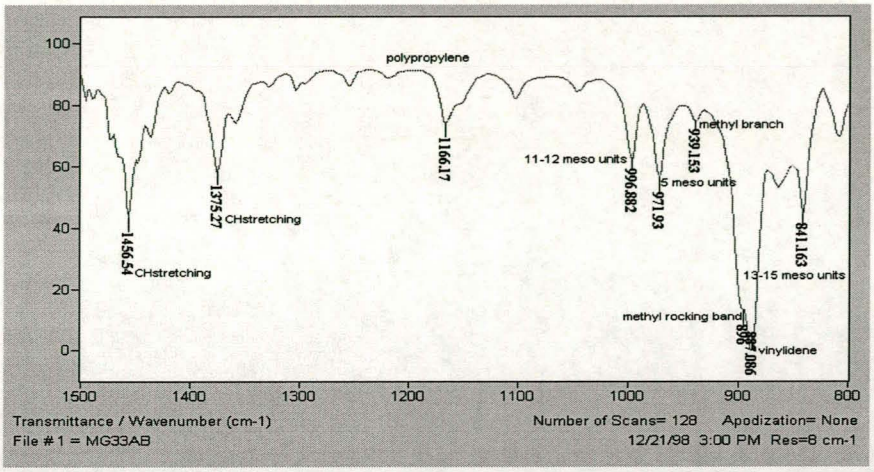

Figure 4.11. PAS-IR spectrum of polypropylene (sample Mg33, 0% 1-pentene)

Upon the introduction of 1-pentene into the polymer, the resultant copolymer will comprise the unit:

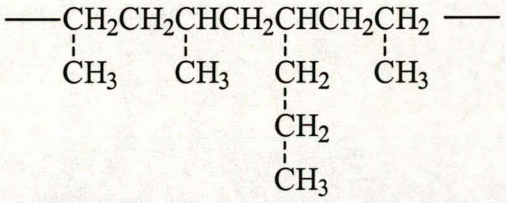

Figure 4.12 shows an overlay of the spectra of samples Mg33 (homopolymer) and Mg34 (8.7 % 1-pentene). As can be seen, the only difference between the IR spectra of the homopolymer and the propylene/1-pentene copolymer is the presence of an n-propyl branch, which will cause a vibration in the region 745 – 735 cm^{-1}. A band at approximately 890 cm^{-1} has been assigned to a methyl rocking mode for branches larger than ethyl[39-41].

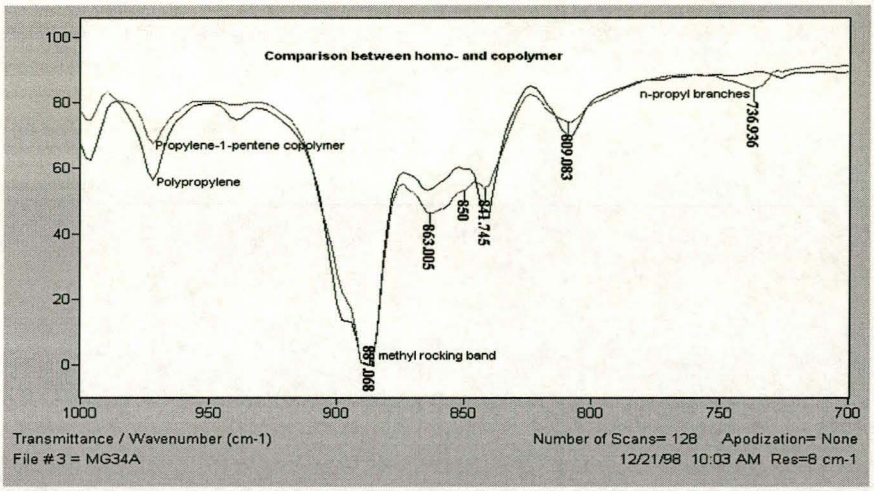

Figure 4.12 Comparison of PAS-IR spectra of Mg33 (polypropylene) and Mg34 (8.7 % 1-pentene).

A definite increase in the intensity of the band at 736 cm^{-1} can be seen. Closer consideration of the PAS-IR spectra in Figure 4.12 revealed that the existence of transvinyl end groups would be difficult to detect in the propylene/1-pentene copolymer as this band overlaps with the vibration of propylene units. Both IR spectra had signals at 972 cm^{-1}, which could be due to transvinyl end groups. The signals at 888 cm^{-1} (due to vinylidene end groups), and at 910 cm^{-1} (due to the vinyl end groups), could overlap with the signal of the methyl rocking of the propylene units. Therefore it is difficult to make any conclusions from the IR spectra about the end groups present in the propylene copolymers, although the spectra of samples Mg38 (4.4% 1-pentene) and Mg40 (9.9% 1-pentene) have bands at 888 cm^{-1} and 972 cm^{-1}. Sample Mg40 (9.9 % 1-pentene) shows a small signal of the vinylidene end group at 888 cm^{-1} and a large signal at 972 cm^{-1}.

The PAS-IR spectra of sample Mg38 (4.4% 1-pentene) and sample Mg40 (9.9 % 1-pentene) are shown in Figures 4.13 and 4.14. The only bands in the IR spectra of these samples in the 745-735 cm^{-1} region, is a broad band at 808 cm^{-1}. Due to the overlapping of these signals, the IR spectra of the propylene/1-pentene copolymers cannot indicate the amount of 1-pentene in the copolymers.

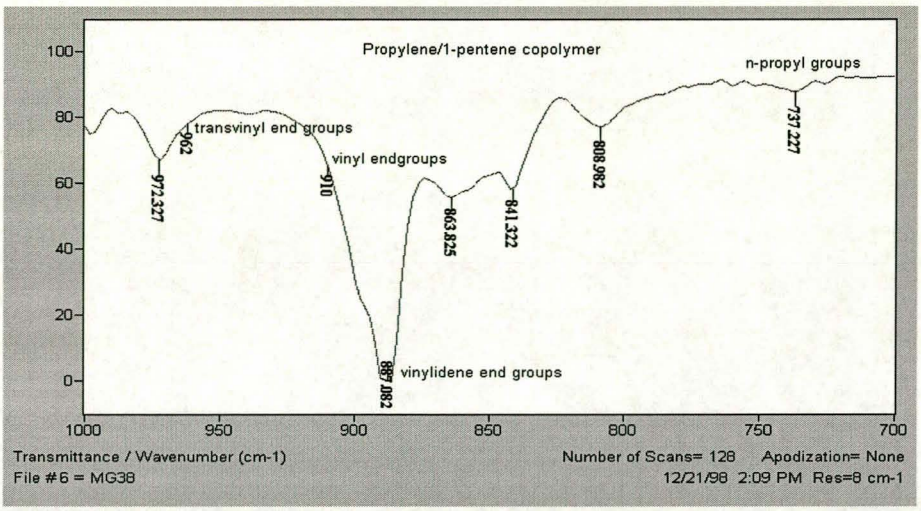

Figure 4.13. PAS-IR spectrum of propylene/1-pentene copolymer (sample Mg38, 4.4% 1-pentene).

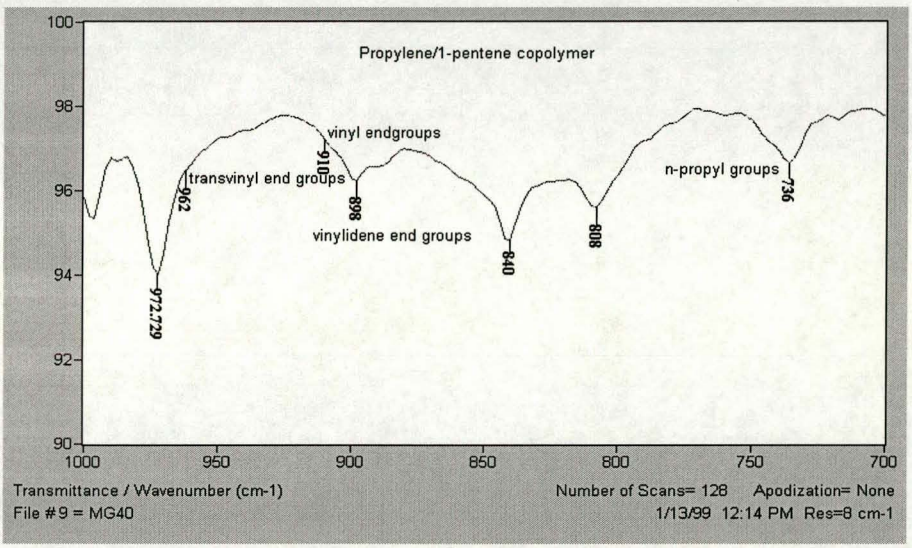

Figure 4.14 PAS-IR spectrum of propylene/1-pentene copolymer (sample Mg40, 9.9 % 1-pentene).

4.6.4 Microstructure of propylene/1-pentene copolymers

4.6.4.1 Polypropylene

The ^{13}C NMR spectrum of polypropylene (sample Mg37) is shown in Figure 4.15.

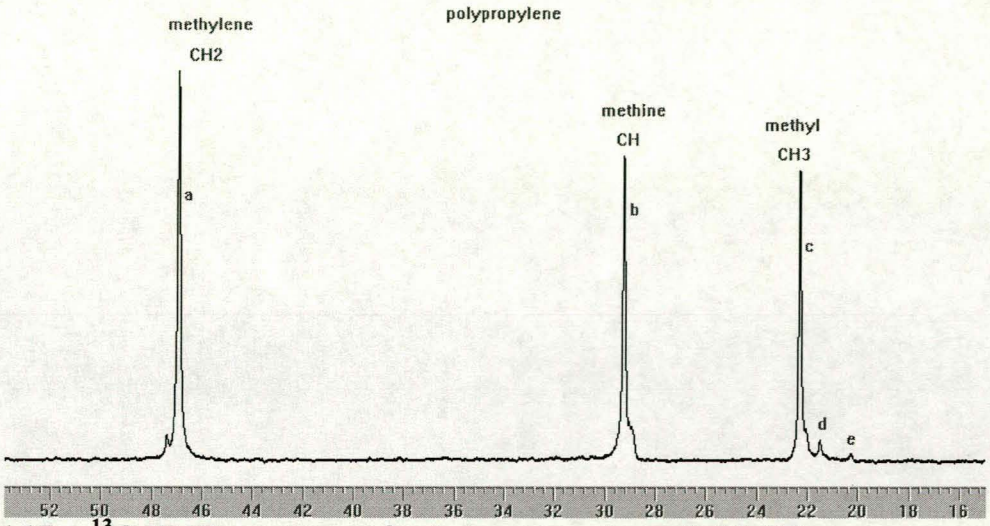

Figure 4.15. ^{13}C NMR spectrum of polypropylene (sample Mg37).

Solvent 1,2,4-trichlorobenzene:benzene-d_6(9:1 volume ratio), temperature 100°C.

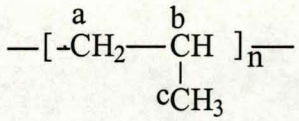

I

The ^{13}C NMR spectrum of the polypropylene **(I)** sample Mg37 contains three signals which can be identified as those of the methyl carbons (δ(22.3)ppm), of the methine carbons (δ(29.1)ppm), and of the methylene carbons (δ(46.0)ppm)[42]. (The chemical shifts are reported with respect to an internal 1,2,4-trichlorobenzene standard.) The methyl region exhibits by far the greatest sensitivity. Assuming stereochemical shifts of the methyl pentads are grouped together according to the central triad sequences *mm*, *mr* and *rr*, from low to high field[43], at least ten resonances can be assigned to the unique pentad[44] sequences, observed in the order *mmmm*, *mmmr*, *rmmr*, *mmrr*, *mmrm*, *rmrr*, *mrmr*, *rrrr*, *rrrm* and *mrrm*. In the ^{13}C NMR spectrum of the polypropylene sample

Mg37 not all of these pentad sequences can be identified (see Figure 4.16). The assignments of the observed resonances are given in Table 4.5.

Table 4.5 ^{13}C NMR assignments for isotactic polypropylene

Resonance no.	Shift[a], ppm	Shift[b], ppm	Stereochemical Resonance[c]
a	46.0	45.72-47.42	methylene carbons
b	29.1	28.3	methine carbons
c	22.3	19.8921.76	mmmm methyl pentad
d	21.3	16.77-17.16	mmrr methyl pentad
e	20.0	14.36-15.35	rrmm methyl pentad

[a]Solvent 1,2,4-trichlorobenzene:benzene-d_6 (9:1 volume ratio), temperature 100°C

[b]Reference 45.

[c]Reference 42.

The signals of the methyl pentad were inadequately resolved, but compared well with results found by Ewen[46]. Ewen found that the isotactic portion of polypropylene, obtained with a catalyst like $Et(Ind)_2ZrCl_2$, followed the enantiomorphic-site control mechanism and that the polypropylene has the structure **(II)**, and calculated that stereochemical control is therefore based on the chirality of the catalyst.

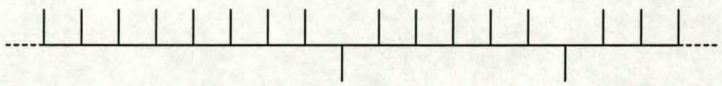

II

Structure **(II)** corresponds to stereosequences of isotactic meso (m) diads connected by pairs of syndiotactic racemic (r) diads. Figure 4.16 displays the ^{13}C NMR spectrum of the methyl region of the isotactic polypropylene polymer produced with catalyst $Et(Ind)_2ZrCl_2$ at 80°C. The resonance of the *mmmm* methyl stereochemical pentad at δ(22.3)ppm (c) is far more intense than the resonances of any other stereochemical pentads[44], hence the sample Mg37 is highly isotactic.

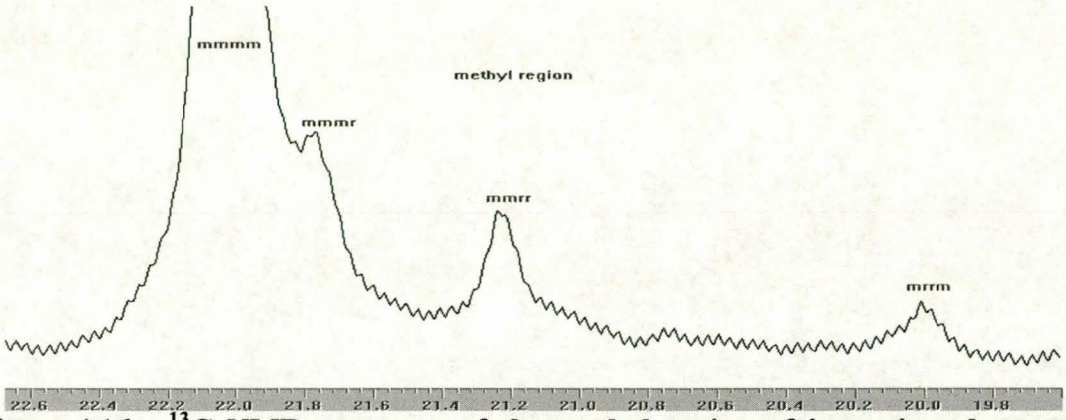

Figure 4.16. ^{13}C NMR spectrum of the methyl region of isotactic polypropylene (sample Mg37).

Solvent 1,2,4-trichlorobenzene:benzene-d_6 (9:1 volume ratio), temperature 100°C.

4.6.4.2 Propylene/1-pentene copolymers

With the introduction of 1-pentene into the polypropylene chain, more than the three signals of the polypropylene spectrum are visible in the ^{13}C NMR spectra of the copolymers due to the different new chemical environments. The chemical shifts, as well as multiplicities, could be determined by using the APT-pulse sequence, without great loss in sensitivity of the signals. In order to distinguish between the different carbon atoms, the ^{13}C signals were converted to negative and positive signals[47]. CH_3- and CH-carbon atoms are characterized by negative amplitudes, while the CH_2- and C-carbon atoms are characterized by positive amplitudes. Figure 4.17 shows the APT ^{13}C NMR spectrum of a propylene/1-pentene copolymer (Mg35).

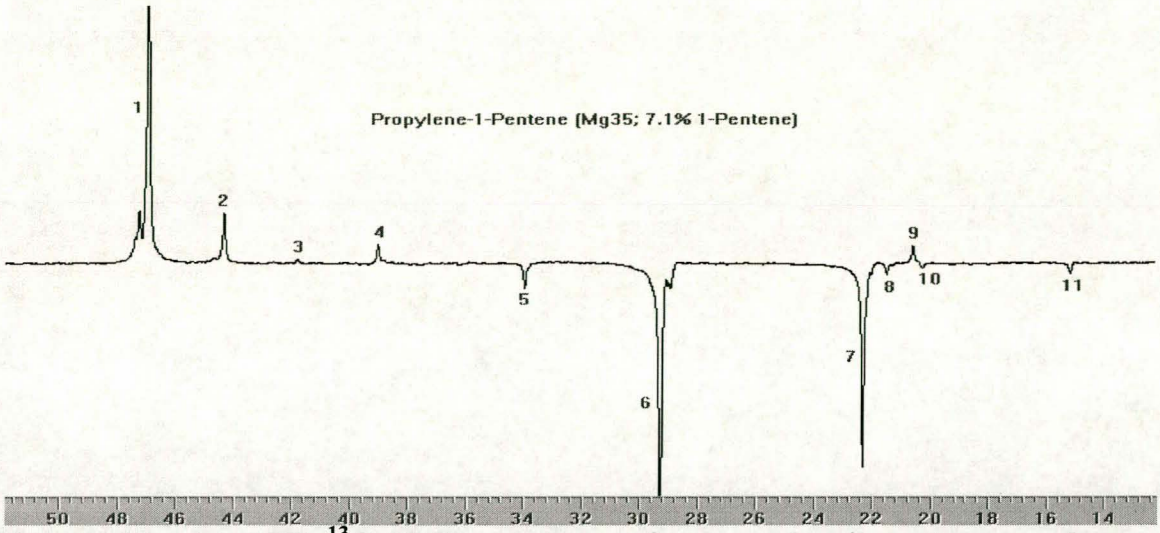

Figure 4.17. An APT ^{13}C NMR spectrum of a propylene/1-pentene copolymer (sample Mg35, 7.1% 1-pentene).

Solvent 1,2,4-trichlorobenzene:benzene-d_6 (9:1 volume ratio), temperature 100°C.

From this spectrum it can be seen that the signals numbered 5, 6, 7, 8, 10, and 11 have negative amplitudes and are resonances due to CH_3- and CH-carbon atoms. The rest of the signals have positive amplitudes and are due to CH_2- and C-carbon atoms. Figure 4.18 displays the ^{13}C NMR spectrum of the same propylene/1-pentene copolymer (Sample Mg35).

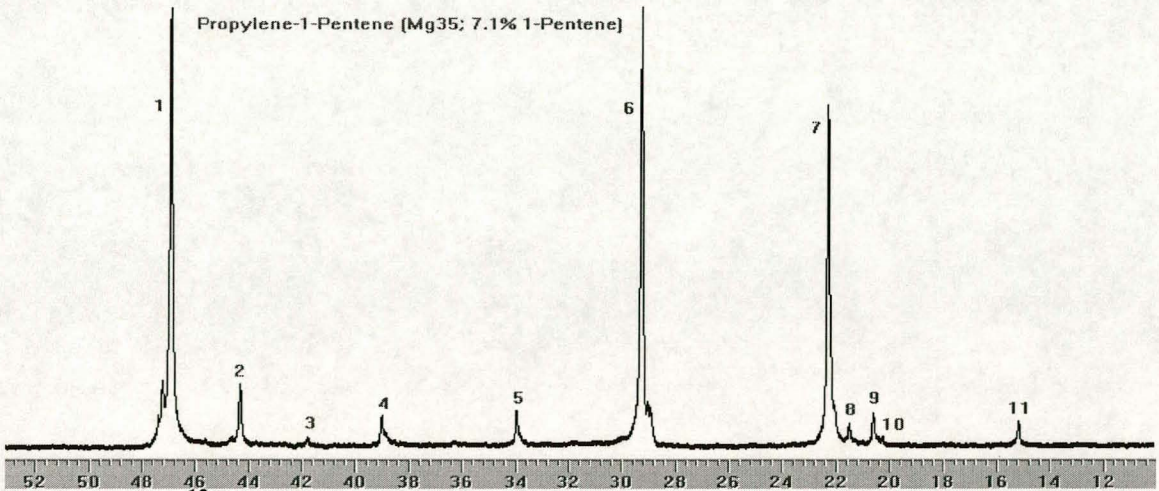

Figure 4.18. ^{13}C NMR spectrum of a propylene/1-pentene copolymer (sample Mg35, 7.1% 1-pentene).

Solvent 1,2,4-trichlorobenzene:benzene-d_6 (9:1 volume ratio), temperature 100°C.

To distinguish between the different C-atoms, the following numbering system was used, but these numbers do not necessarily correspond to a generally accepted nomenclature system (Figure 4.19).

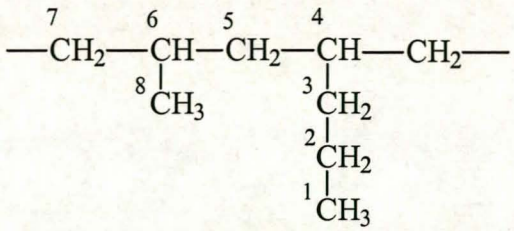

Figure 4.19. Carbon assignment scheme used in this study for propylene/1-pentene copolymers.

Possible assignments of the signals of propylene/1-pentene copolymers are given in Table 4.6.

Table 4.6. ^{13}C NMR signal assignments for propylene/1-pentene copolymers

Signal (see Figure 4.18)	δ(ppm)	Type of carbon	Assignment (see Figure 4.19)
1	46.95	CH_2	7
2	44.31	CH_2	5
3	41.78	CH_2	
4	38.95	CH_2	3
5	33.94	CH	4
6	29.28	CH	6
7	22.29	CH_3	8
8	21.48	CH/CH_3	
9	20.62	CH_2	2
10	20.27	CH/CH_3	
11	15.15	CH_3	1

Solvent 1,2,4-trichlorobenzene:benzene-d_6 (9:1 volume ratio), temperature 100°C.

The method used for the calculation of the amount of 1-pentene in each copolymer was obtained from Sasol[48]. The following equation was used:

$$[C_5] = \frac{0.5I(40-45ppm) + 0.5I(30-40ppm)}{I(40-50ppm) + I(25-30ppm) + 0.5I(30-30ppm)}$$

Results from ^{13}C NMR spectra of the propylene/1-pentene copolymers can be seen in Table 4.7.

Table 4.7 Integration of ^{13}C NMR signals, used to calculate the amount of 1-pentene incorporated in the propylene/1-pentene copolymers

Sample	Intensity of signals between δ(40 to 45)ppm	Intensity of signals between δ(30 to 40)ppm	Intensity of signals between δ(25 to 30)ppm	Intensity of signals between δ(40 to 50)ppm	Amount of 1-pentene incorporated [mol%]
Mg05	0.04	0.03	0.82	1.04	1.87
Mg02	0.05	0.09	0.73	1.05	3.84
Mg01	0.25	0.39	0.90	1.25	13.65
Mg36	2.9	2.3	55.6	70.1	2.5
Mg14	3.8	12.8	54.7	67.1	2.68
Mg34	10.4	10.4	49.0	64.8	8.7
Mg35	7.4	9.2	50.0	62.2	7.1
Mg41	0.01	0.01	0.86	1.01	0.5
Mg39	0.02	0.01	0.84	1.02	0.8
Mg38	5.0	6.3	55.0	68.0	4.48
Mg40	0.22	0.2	0.81	1.22	9.86

Solvent 1,2,4-trichlorobenzene:benzene-d_6 (9:1 volume ratio), temperature 100°C.

4.6.5. ^{13}C-Enriched end groups of polypropylene and propylene copolymers

Results of structural studies on the microstructure of ethylene copolymers[47, 49-56] have indicated that polymer molecular mass is controlled by various chain transfer reactions, mostly β-hydride transfer, but also β-alkyl transfer and chain transfer to aluminum. A study of the polymer sequence distribution gives a better understanding of the propagation step, while a study of the polymer end groups will give more information of the initiation and termination steps. Elucidation of polymer end groups includes the end groups that are saturated or unsaturated (and what type of double bond is present) and also the sequence of monomer units at the end groups[57].

The mechanism of the formation of the unsaturated end groups during polymerizations with metallocene catalysts is not well established, probably because the reaction is very sensitive to monomer, catalyst, cocatalyst, temperature, and other reaction conditions[58]. The dominant polymer end groups, found in low molecular mass polypropylenes produced by metallocene catalysts, such as $Et(Ind)_2ZrCl_2$, are the vinylidene group, resulting from β-hydride-elimination, and the *n*-propyl group, formed by initial insertion of propene into the resulting Zr-hydride. In sample Mg37, however, the end groups are not detectable by ^{13}C NMR spectroscopy, possibly due to their low concentrations. In sample Mg41, which is a copolymer with only 0.5% 1-pentene content, the proton signals of the vinylidene end group can easily be seen (Figure 4.20).

4.6.5.1 Vinylidene double bonds

The major unsaturated end groups are vinylidene groups[58, 59]. ^{1}H NMR spectroscopy indicates two different species of vinylidene groups. The major vinylidene signal is a pair of doublets at δ(4.74)ppm and δ(4.68)ppm (the splitting of each signal into a doublet is barely visible). The minor vinylidene signal is at slightly lower field, at δ(4.76)ppm. The minor vinylidene ^{1}H NMR signal area is 3-5% of the major vinylidene signal area. A very small amount of vinylidene end groups is observed by ^{1}H NMR spectroscopy but is absent in ^{13}C NMR spectroscopy of the propylene/1-pentene copolymer, sample Mg41.

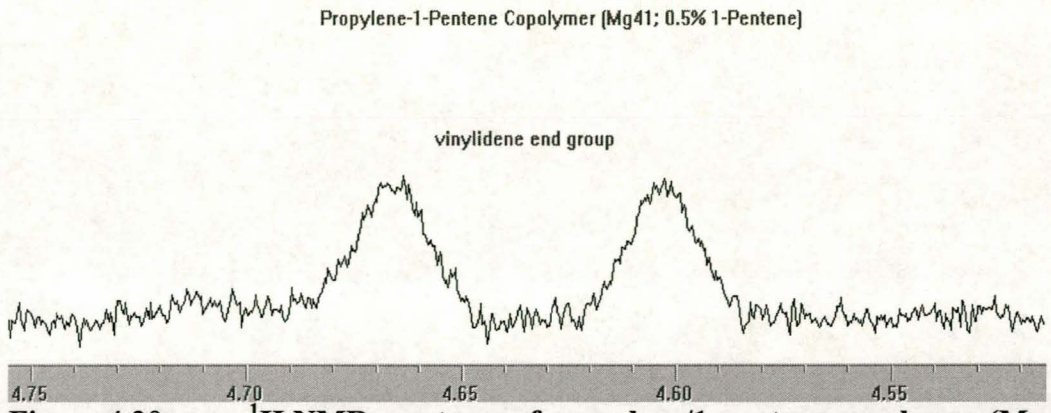

Figure 4.20. **^{1}H NMR spectrum of propylene/1-pentene copolymer (Mg 41, 0.5% 1-pentene).**

Solvent 1,2,4-trichlorobenzene:benzene-d_6 (9:1 volume ratio), temperature 100°C.

To confirm results, signals should be at δ(142.6)ppm and δ(109.3)ppm in the double bond region, and at δ(20.4)ppm in the methyl region, but they are not seen in this spectrum. The absence of vinylidene signals can be due to the fact that the polymerization was terminated by the addition of ethanol therefore saturating the double bonds. The chain ends will therefore consist mostly of saturated chain ends, with vinylidene ends in very low concentration. Figure 4.20 displays the ^{1}H NMR spectrum of a propylene/1-pentene copolymer with 0.5% 1-pentene incorporation (sample Mg41).

4.6.5.2 Saturated chain ends

If the polymerization is terminated with the addition of an alcohol or if hydrogen is present during copolymerization, the double bonds in the end groups will be saturated and the chain ends will consist of mostly saturated chain structures[59]. A complete interpretation of all saturated chain ends is difficult because of the effects of comonomer sequence placements, propylene tacticity, and propylene inversion, all acting together to produce a multitude of possible structures. Signals 3, 8 and 10, (Figure 4.18), could be due to end groups, but it is difficult to give precise assignments of these signals.

4.7 CONCLUSIONS

Low molecular mass propylene-1-pentene copolymers were obtained using the metallocene $Et(Ind)_2ZrCl_2$/MAO catalyst system. The weight-average molecular mass of the copolymers was quite low, in the range 19 000 to 49 010 g/mol. The melting temperatures and the percentage crystallinities of the propylene/1-pentene copolymers decreased when the 1-pentene content in the copolymer increased. An increase in the polymerization temperature lead to a decrease in the molecular mass of the copolymers. An increase in molecular mass was observed when the Al/Zr ratio was increased from 2 000:1 to 10 000:1.

The typical polymer end group in low molecular mass polypropylene and propylene/1-pentene copolymers produced by this catalyst system is the vinylidene group, resulting from β-H elimination. The low molecular mass of the propylene/1-pentene copolymers is ascribed to the catalyst $Et(Ind)_2ZrCl_2$[60]. The ligand substitution pattern generates different non-bonded interactions in the activation state, leading to chain transfer, and such non-bonded interactions determine the type and the rate of transfer reactions. To increase the molecular mass of the copolymers, a catalyst with a different ligand substitution must be used, for example the dimethylsilylene-briged 2,2'-dimethyl-4,4'-diaryl-substituted bis(indenyl) ziconocenes, developed by Brintzinger and coworkers[60] and Spaleck *et al*[61]. They found that the catalyst $Me_2Si(2\text{-}MeBenz[e]Ind)_2ZrCl_2$ polymerized polypropylene with high molecular mass, in the range of 140 000 g/mol.

4.8 REFERENCES

1. Reichert K.H., Meyer K.R., *Macromol. Chem.*, 1973, **169**, 163.
2. Sinn H., Kaminsky W., Vollmer H.-J., Woldt R., *Angew. Chem.*, 1980, **92**, 296.
3. Sinn H., Kaminsky W., *Adv. Organomet. Chem.*, 1980, **18**, 99.
4. Kaminsky W., Miri M., Sinn H., Woldt R., *Makromol. Chem. Rapid Commun.*, 1983, **4**, 417.

5. Kaminsky W., Buschermohle M., in *Recent Advances in Mechanistic and Synthetic Aspects of Polymerization*, Fontaille M. and Guyot A., eds., Reidel, New York, 1987, p.503.
6. Wild F.R.W.P., Zsolani L., Huttner G., and Brintzinger H.H., *J. Organomet. Chem.*, 1982, **232**, 233.
7. Wild F.R.W.P., Wasincionek M., Huttner G., and Brintzinger H.H., *J. Organomet. Chem.*, 1985, **288**, 63.
8. Kaminsky W., Külper K., Brintzinger H.H., Wild F.R.W.P., *Angew. Chem.*, 1985, **97**, 507.
9. Kaminsky W., *Angew. Makromol. Chem.*, 1986, **145/146**, 149.
10. Kaminsky W., in *Catalytic polymerization of Olefins*, Keii T., Soga K., Eds., Kodansha Elsevier Pub., Tokyo, 1986, p.293.
11. Ewen J.A., in *Catalytic polymerization of Olefins*, Keii T., Soga K., Eds., Kodansha Elsevier Pub., Tokyo, 1986, p. 271.
12. Chien J.C.W., He D., *J. Polym. Sci. Part A,* 1991, **29**, 1603.
13. Cheng H.N., Kakugo M., *Macromolecules*, 1991, **24**, 1724.
14. Pietikäinen P., Seppällä J.V., *Macromolecules*, 1994, **27**, 1325.
15. Lehtinen C., Löfgren B., *Eur. Polym. J.*, 1997, **33**, 115.
16. Naga N. Mizunuma K., Sadatoshi H., Kakugo M., *Macromolecules*, 1997, **30**, 2197.
17. Lehtinen C., Starck P., Löfgren B., *J. Polym. Sci: Part A: Polym. Chem.*, 1997, **35**, 307.
18. Kaminsky W., in *Transition Metal Catalyzed Polymerizations, Alkenes and Dienes*, Quirck, R.P., Ed., MMI Symposium Series, MMI Press: New York, 1983, **4**, Part A, 225.
19. Kaminsky W., Hahnsen H., *Advances in Polyolefins*, Seymour R.B., Cheng T., Eds., Plenum Press: New York, 1987, p. 361.
20. Dutscheke J., Kaminsky W., Lüker H., *Polymer Reactor Engineering, Influence of Reaction Engineering on Polymer Properties*, Reichert K.H., Geiseler W., Eds., Hanser Verlag: Munich, Germany, 1983, p.207.

21. Forlini F., Fan Zhi-Qiang, Tritto I., Lacatelli P., Sacchi M.C., *Macromol. Chem. Phys.*, 1997, **198**, 2397.
22. De Rosa C., Talarico G., Caporaso L., Auriemma F., Galimberti M., Fusco O., *Macromolecules*, 1998, **31**, 26, 9109.
23. Uozumi T., Soga K., Bello A., Perez E., Lacatelli P., Fan Z.Q., Zucchi D., *Polym. Bull.* 1996, **36**, 249-256.
24. Winter A., Dolle V., Rohrmann J., Spaleck W., Antberg M.,(Hoechst A-G), Eur. Patent Appl. EP433,986, *Chem. Abstr.*, **115**,233115z, 1991.
25. Wang, B.P. Ph.D. Dissertation, University of Massachusetts, Amherst, MA, 1988.
26. Starck P., Lehtinen C., Löfgren B., *Die Angew. Makromol. Chem.*, 1997, **249**, 115.
27. Kouvumäki J., Seppällä J.V. *Eur. Polym. J.*, 1994, **17**, 878.
28. Clark E.J., Hoffman J.D., *Macromolecules*, 1984, **30,** 1111.
29. Perez E., Benavente R., Bello A., Pere a J.M., Zucchi D., Sacchi M.C., *Polymer*, 1997, **38**, 11, 5411.
30. Sinn H., Kaminsky W., *Adv. Organomet. Chem.*, 1980, **18**, 99.
31. Kaminsky W. in *History of Polyolefins*. Seymour, R.B., Cheng T., eds. Plenum Press, New York, 1987, p. 275.
32. Kaminsky W., Schlobohm M., *Makromol. Chem., Macromol. Symp.*, 1986, **4**, 103.
33. Chien J.C.W., Wang W.P., *J. Polym. Sci., Part A: Polym. Chem. Ed.*, 1988, **26**, 3089.
34. Rieger B., Mu X., Mallin D.T., Rausch M.D., Chien J.C.W., *Macromolecules*, 1990, **23**, 3559.
35. Malmberg A, Kokko E., Lehmus P., Löfgren B., Seppällä J.V. *Macromolecules*, 1998, **31**, 8448.
36. Chien J.C.W., Rieger B., Martin H., *J. Polym. Sci., Part A: Polym. Chem.*, 1990, **28**, 2907.
37. (a)Kissin Y.V., *Adv. Polym. Sci.*, 1975, **15**, 91.
    (b)Kissin Y.V., Tsvetkova V.I., Chirkov M.M., *Dokl. Akad. Nauk SSSR*, 1963, **152**, 1162.

(c)Kissin Y.V., *Isospecific Polymerization of Olefins with Hetereogeneous Ziegler-Natta Catalysts*, Springer-Verlag, New York, 1985, p. 229.

(d)Kissin Y.V., Isvetkova V.I., Chirkov M.M., *Eur. Polym. J.*, 1972, **8**, 529.

38. Blitz J.P., McFaddin D.C., *J. Appl. Polym. Sci.*, 1994, **51**, 13-20.
39. McRae M., Maddams W., *Makromol. Chem.*, 1976, **177**, 449.
40. Usami T., Takayama S., *Polym. J.*, 1984, **16**, 731.
41. Maddams W., Woolmington J., *Makromol. Chem.*, 1968, **120**, 1665.
42. Grassi A, Zambelli A., Resconi L., Albizzati E., Mazzochi R., *Macromolecules*, 1988, **21**, 617.
43. Zambelli A., Dorman D.E., Brewster A.I.R., Bovey F.A., *Macromolecules*, 1973, **6**, 925.
44. The theoretical notation is that proposed by: Frisch I.L., Mallows C.L., Bovey F.A., *J. Chem. Phys.*, 1966, **45**, 156.
45. Asakura T., Nishiyama Y., Doi Y., *Macromolecules*, 1987, **20**, 616.
46. Ewen J.A., *J. Am. Chem. Soc.*, 1984, **106**, 6355.
47. Cheng H.N., *Macromolecules*, 1991, **24**, 4813.
48. Dawie Joubert, Principal Scientist, Sastech R&D, Polymer Research, Sasol Pty. Ltd., Sasolburg, Personal Communication.
49. Dechter J.J., Mandelkern L., *J. Polym. Sci., Polym. Phys. Ed.*, 1980, **18**, 1955.
50. Ray G.J., Spanswick J., Knox J.R., Serres C., *Macromolecules*, 1981, **14**, 1323.
51. Hsieh E., Randall J.C., *Macromolecules*, 1982, **15**, 353.
52. Kaminsky W., Schlobohm M., *Makromol. Chem. Macromol. Symp.*, 1986, **4**, 1897.
53. Kuroda N., Nishikitani Y., Matsuura K., Mitsuji M., *Macromolecules*, 1987, **188**, 1897.
54. Cheng H.N., *Polym. Bull.*, 1990, **23**, 589.
55. Kuroda N., Nishinori Y., Matsuura K., Ikegami N., *Macromolecules*, 1992, **25**, 2820.
56. Randall J.C., Rucker S.P., *Macromolecules*, 1994, **27**, 2120.
57. Rossi A., Odian G., Zhang J., *Macromolecules*, 1995, **28**, 1739.
58. Cheng H.N., Smith D.A., *Macromolecules*, 1986, **19**, 2065.

59. Rossi A., Odian G., Zhang J., *Macromolecules,* 1996, **29**, 7, 2331.

60. J ngling S., M lhaupt R., Stehling U., Brintzinger H.H., Fischer D., Langhauser F., *J. Polym. Sci., Part A.: Polym. Chem.*, 1995, **33**, 1305.

61. Spaleck W., K ber F., Winter A., Rohrmann J., Bachmann B., Antberg M., Dolle V., Paulus E.F., *Organometallics*, 1994, **13**, 954.

CHAPTER 5

High molecular mass propylene/1-pentene copolymers produced with the homogeneous catalyst *rac*-$Me_2Si(2\text{-}MeBenz[e]Ind)_2ZrCl_2$/MAO

Summary

Propylene was copolymerized with 1-pentene using the homogeneous MAO-activated *rac*-$Me_2Si(2\text{-}MeBenz[e]Ind)_2ZrCl_2$ catalyst at temperatures varying between 0°C and 80°C. The molecular masses of the copolymers produced were substantially higher than those produced with the catalyst $Et(Ind)_2ZrCl_2$. The weight-average molecular masses of the propylene/1-pentene copolymers varied between 427 800 g/mol and 633 500 g/mol and the molecular mass distributions between 2.5 and 3.4.

5.1 INTRODUCTION

Unlike the conventional heterogeneous multicenter Ziegler-Natta catalysts, single-site metallocene catalysts produce very uniform copolymers with narrow molecular mass distributions ($M_w/M_n \approx 2$) and the random incorporation of comonomers, including higher α-olefins as well as cycloolefins. Brintzinger[1] and Spaleck[2-4] discovered, almost simultaneously, that benzannelation and especially 2-methyl substitution of silylene-bridged *bis* (indenyl) zirconocenes lead to substantial increases in molecular masses. Several investigations concerning the influence of metallocene structures in ethene copolymerization were made[5-9]. The purpose of this study was to investigate the influence of temperature on the molecular mass of propylene/1-pentene copolymers when propylene and 1-pentene were copolymerized using the homogeneous MAO-activated *rac*-$Me_2Si(2\text{-}MeBenz[e]Ind)_2ZrCl_2$ (**MBI**). The molar masses, molar mass distributions, melting points, haze and microstructures of the products were determined.

5.2 EXPERIMENTAL

The experimental conditions were as described previously (Section 3.2) except that here the catalyst used was the homogeneous, MAO-activated *rac*-**$Me_2Si(2\text{-}MeBenz[e]Ind)_2ZrCl_2$** (see Figure 5.1). The catalyst was obtained from Prof. H.-H. Brintzinger, Fakultät für Chemie, Universität Konstanz, Germany, and used as received. Methylalumoxane (MAO) was commercially obtained from Aldrich as a 10 wt% solution in toluene and was used without further purification. It was stored under nitrogen.

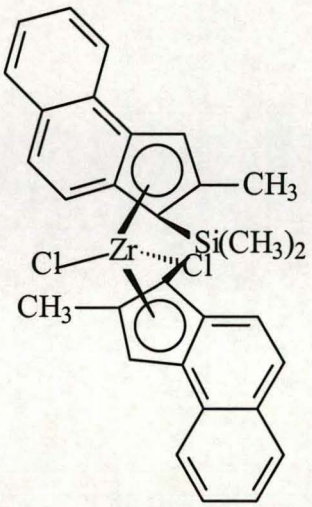

Figure 5.1. ***rac*-$Me_2Si(2\text{-}MeBenz[e]Ind)_2ZrCl_2$**

For studying the effect of temperature on the molecular mass of the copolymers the temperature of the reactions was varied from 8°C to 80°C. Typically, copolymerization was performed in toluene in the presence of the metallocene, (Figure 5.1) which was activated with methylalumoxane (MAO), using [Zr] = 8.2 μmol/L and [Al] = 50 mmol/L with [Al]:[Zr] = 6000:1. The abbreviations of the copolymers produced are as follows: a propylene/1-pentene copolymer prepared at 80°C is named as PP80. The reaction conditions are summarized in Table 5.1.

Table 5.1. Reaction conditions as selected for propylene/1-pentene copolymerization at different temperatures

Sample	Polymerization temperature Tp(°C)	1-Pentene (ml)	1-Pentene (g)[a]	Propylene (g)	Feed ratio (%)	Yield (g)
PP80	80	8	5.1	40.9	12.6	31.1
PP40	40	6	3.8	63.4	6.1	45.5
PP25	25	8	5.1	48.3	10.6	34.7
PP8	8	7	4.5	87.9	5.12	20.7

[a]Calculated by multiplying volume with density (density of 1-pentene 0.6429)

5.3 EQUIPMENT

5.3.1 Polymerization equipment

A 350 mL stainless-steel Parr autoclave was used for the propylene copolymerization. The reactor was equipped with a fitted polytetrafluroethylene (teflon) seal ring and a pressure gauge.

5.3.2 Analytical equipment

The copolymers were characterized by DSC, GPC, NMR- and IR-spectroscopy. A description of the equipment and the methods used has been given in Section 3.3.2.

5.4 SYNTHESIS OF COPOLYMERS

Polymerization was carried out in a 350 mL stainless steel pressure reactor fitted with a magnetic stirring bar. The system was first evacuated, flushed with nitrogen and then 30 mL toluene was injected. A Schlenk tube was filled with 1 mL (2mol/L) of MAO in 5 mL toluene. The catalyst (1 mL, 3.28×10^{-4} mol/L) was added to the Schlenk tube and preactivated for 5 min by standing at room temperature. The comonomer, 1-pentene, was added and then the catalyst/cocatalyst/comonomer mixture was introduced into the reactor, and the copolymerization initiated by introducing the monomer. The total volume of the reaction mixture was 40 mL in all the polymerizations. The reactor was placed in a temperature-controlled oil bath, set at the preselected temperature, and then charged with propylene at a pressure of 1 MPa.

After 3 hours the copolymerization was terminated and the copolymer produced precipitated in 200 mL ethanol, acidified with 10 mL 10 wt% aqueous HCl. The copolymer was filtered, then dried at room temperature under vacuum for 6 hours to a constant weight.

5.5 RESULTS AND DISCUSSION

The molar contents of the comonomers, molar mass, molar mass distribution and the melting points of these copolymers, as determined by GPC analyses, are presented in Table 5.2.

Table 5.2. Molar contents of the comonomers, molar mass, molar mass distribution and the melting points of propylene/1-pentene copolymers

Sample	Amount of 1-pentene (mol %)	Melting peak temperature T_m(°C)	Weight-average molecular mass M_w (g/mol)	Number-average molecular mass M_n (g/mol)	Viscosity-average molecular mass M_v (g/mol)	Molecular mass distribution M_w/M_n
PP80[a]	3.8	110.19	427 800	172 700	389 200	2.5
PP25	3.5	122.14	633 500	186 000	563 300	3.4
PP8	2.8	130.19	515 800	187 600	466 400	2.7
PP40	2.5	123.94	512 300	166 600	455 100	3.1

[a]See experimental section for polymerisation conditions.

5.5.1 Melting points

The copolymer with the lowest melting point was the copolymer with the highest amount of 1-pentene incorporated. A similar result was obtained when the ethylene-bridged catalyst was used, where the incorporation of 1-pentene into the polymeric chain creates a discontinuity that sharply reduces the crystallization tendency of the polymer. This results in a reduction in the rate of crystallization, a lower level of crystallinity, and a reduction in the melting point, all of which are related to the less perfect structure of the polymer chains. In Table 5.3 the amount of 1-pentene in the propylene/1-pentene copolymers, the melting points, heats of fusion and percentage crystallinities of the propylene/1-pentene copolymers are given.

Table 5.3. The 1-pentene amount, melting point, heat of fusion and percentage crystallinity of various propylene/1-pentene copolymers

Sample	1-Pentene amount copolymer (mol %)[a]	Offset of melting temperature (°C)	Melting peak temperature Tm (°C)	End of melting temperature (°C)	Heat of fusion ΔHm(J/g)	Crystallinity m_c/m_o[b] (%)
PP80	3.8	110	118	123	38.04	18.2
PP25	3.5	122	132	137	43.89	20.9
PP8	2.8	130	138	142	58.49	27.9
PP40	2.5[c]	123	134	138	55.06	26.3

[a]Content of comonomer in copolymer determined by ^{13}C NMR spectroscopy.

[b]Calculated from heat of fusion of samples and heat of fusion assuming, 209 J/g for enthalpy of perfectly crystalline polypropylene

[c]Error due to sensitivity of ^{13}C NMR spectroscopy.

The introduction of a comonomer (1-pentene) in a random copolymer of propylene is necessary to improve the optical properties of propylene. The resulting, less perfect, crystals are smaller and have a lower density than homopolymer spherulite crystals, and thus exhibit a lower refractive index as well as a smaller sphere of scattering. The difference in refractive index between the crystalline and amorphous phases is, therefore, lower, and light is refracted to a lower extent. The result is a product with lower haze and higher clarity, especially if artificial nucleating agents are used.

There are two ways in which the visibility of an object when viewed through an imperfectly specimen may be reduced, thus two criteria exist for transparency. Haze is used the most often for the characterization of the transparency of a plastic product. The second measure of transparency describes the degree to which fine detail is resolved, known as clarity. For the complete characterization of transparency, both must be determined, since they can change independently from each other[10]. Clarity is determined by the part of the incident light scattered at low angles, while haze by the part scattered at larger angles.

Haze is a measure of the milkiness of films and is caused by light being scattered by the surface roughness and inhomogeneities in the film. Haze is the total flux of light scattered within the angular range from 2.5 to 90° and normalized to the total transmitted flux. In all cases haze has been associated with scattering from the

surface rather than the bulk of films. The magnitude of surface roughness is related to the crystallization of the polymer. Rough film surfaces and high levels of haze are associated with high levels of crystallinity.

The introduction of heterogeneous nucleating agents into the polypropylene copolymer considerably improves the transparency of the product. By adding finely subdivided foreign material to the polymer sample, acting as heterogeneous nuclei, nucleation is observed in the polymer sample[11]. Nucleators cause the crystallization to begin at a higher temperature, with more initiation sites, leading to both more rapid development and higher levels of crystallinity in more numerous and, therefore, smaller, spherulites[12]. The nucleating agent decreases the average size of spherulites below the wavelength of visible light. With the propylene/1-pentene copolymers, which normally have quite large spherulites, the nucleating agent bis-benzylidene sorbitol (MILLAD 3905)[13, 14] was used to reduce the size of the spherulites and to improve the transparency of the films.

Preparation of films:

0.2 g of the propylene/1-pentene copolymer was mixed with 0.002g of the heat stabilizer (Irganox B225) and 0.002g of the MILLAD 3905 nucleating agent. The heat stabilizer Irganox B225 consists of Irganox 1010 and Irgafos 168 in a 1:1 ratio. The structures of Irganox and Irgafos are shown in Figure 5.2.

Chemical compounds that inhibit or retard the oxidative degradation of polymers are referred to as 'antioxidants'. Thermal antioxidants for polypropylene are chemical agents that stabilize the polymer against the effects of high temperature. Inhibition of thermal oxidation can be achieved by the use of low levels (usually 0.05-0.25 wt%) of antioxidants which are incorporated during the fabrication process. Antioxidants are classified according to their mode of action when interrupting the overall oxidation process. Sterically hindered phenols for example Irganox 1010 (chain-breaking donor, (CB-D) antioxidants) are among the most important processing antioxidants for polypropylene. Irganox 1010 acts by donating a hydrogen atom to the reactive peroxyl radical, hence reducing it to a hydroperoxide and forming a much less reactive antioxidant radical (a hindered phenoxyl radical). The latter can terminate by

further reaction with a second peroxyl radical, hence does not continue the kinetic chain (Figure 5.3).

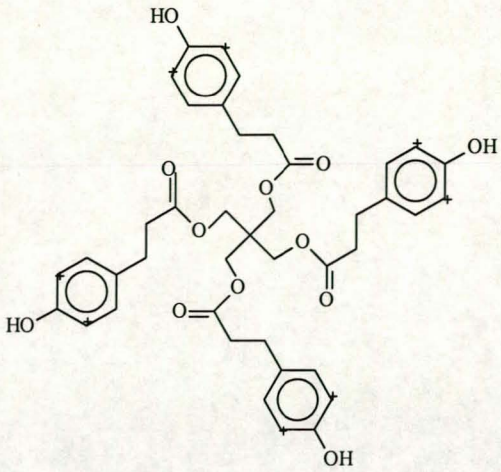

Irganox 1010

Molecular weight = 1178 g/mol

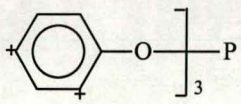

Irgafos 168

Molecular weight = 647 g/mol

Figure 5.2. Antioxidants used in the preparation of propylene/1-pentene films: Irganox 1010 and Irgafos 168.

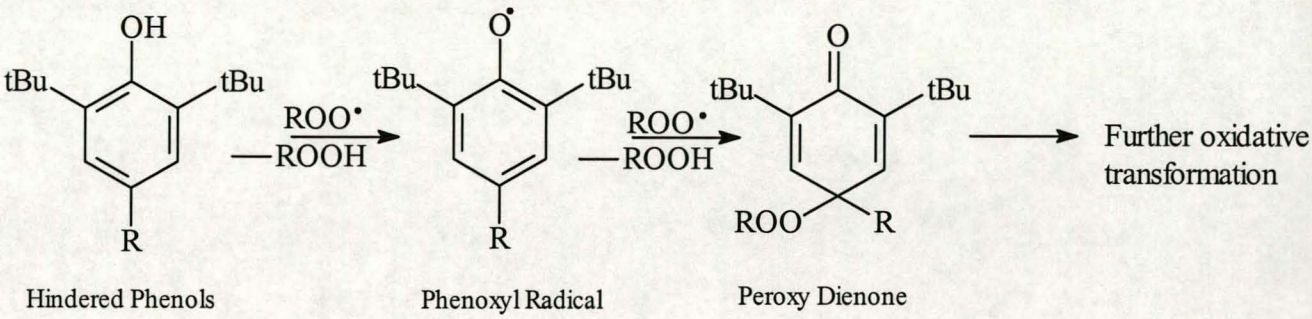

R=(—$CH_2CH_2CO_2CH_2)_4C$, Irganox 1010

Figure 5.3. Chain-breaking antioxidant reactions of hindered phenols.

Unfortunately, many hindered phenols impart various degree of color to the polymer, the extent of which depends on their chemical structure. To minimise

discoloration, peroxidolytic antioxidants (eg. phosphites) can be mixed with the hindered phenols during processing. Phosphites reduce hydroperoxides to alcohols with a 1:1 stoichiometry and are therefore referred to as 'stoichiometric peroxide decomposers (PD-s)', see Figure 5.4.

$$(RO)_3P + ROOH \longrightarrow ROH + (RO)_3P{=}O$$

Figure 5.4. Reactions of phosphites with hydroperoxide and water.

Table 5.4 shows the haze and transmittance results obtained for the polypropylene/1-pentene copolymers.

Table 5.4. Haze and transmittance results for propylene/1-pentene copolymers produced with *rac*-$Me_2Si(2\text{-}MeBenz[e]Ind)_2ZrCl_2$

Sample	Amount of 1-pentene (mol %)	Thickness	Haze (%)	Transmittance (%)
PP80	3.8	40μ	19.0	90.8
PP25	3.5	50μ	10.8	91.7
PP40	2.5	30μ	19.0	91.5
PP40	2.5	50μ	25.0	89.6
PP40	2.5	65μ	32.3	89.9

The haze values obtained for samples PP80, PP25 and PP40 correspond very well with haze values obtained in the experimental laboratorium of Sasol, Sastech. Their haze values are between 5-30%[15]. Sample PP25 showed the lowest haze value (10%) and the highest transmittance (91.7%). When the haze values are compared to commercial values of haze (which are lower than 3%)[13], they are much higher (10-30%). This can be due the surface roughness of the films. The propylene/1-pentene films were pressed on a heat press, where difficulties were experienced due to the small amount (0.2 g) of the samples that was used to press the films. The thinner the films, the more important the role of the film roughness on the haze. This can also be seen from sample PP40 where an increase in the film thickness, resulted in an increase in the haze. The high haze value obtained for sample PP40 can be due to bad quality of the film, the film surface was not as good as those of samples PP80 and PP25.

The differential scanning calorimetry (DSC) traces of samples PP80 and PP40, prepared at temperatures 80°C and 40°C, are shown in Figures 5.5 and 5.6.

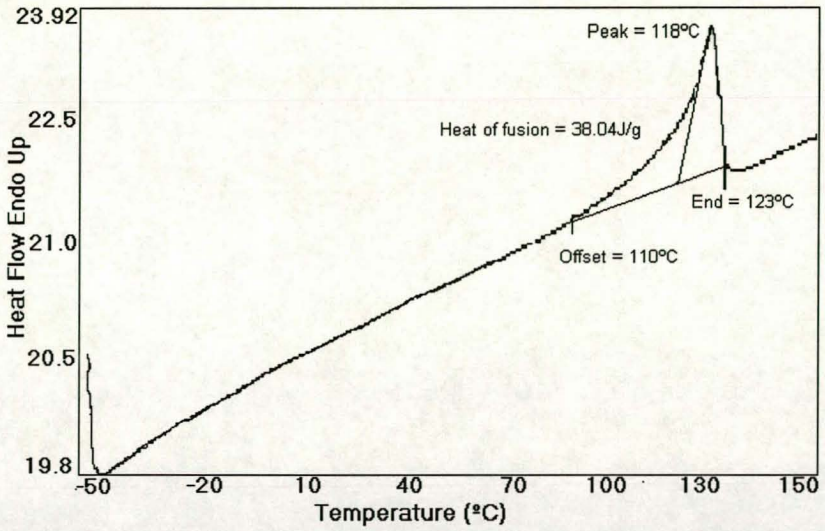

Figure 5.5. DSC trace of propylene/1-pentene copolymer (PP80), showing the melting endotherm (3.8 % 1-pentene).

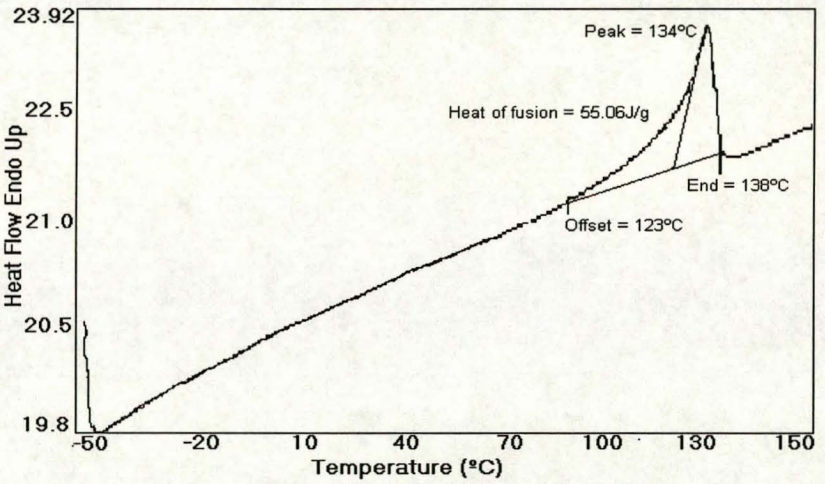

Figure 5.6. DSC trace of propylene/1-pentene copolymer (PP40), showing the melting endotherm (2.5 % 1-pentene).

5.5.2 Molecular mass and molecular mass distribution

Molecular masses of copolymers produced with the metallocene $Me_2Si(2\text{-}MeBenz[e]Ind)_2ZrCl_2$ were much higher than those produced with the catalyst $Et(Ind)_2ZrCl_2$. The 2-methyl substitution of the indenyl, as well as the benz[e]indenyl ligand, favored the formation of higher molecular mass copolymers, without affecting the narrow molecular mass distributions (which remained narrow).

The molecular mass of the copolymer is controlled by various chain transfer reactions, mostly through β-hydride transfer, but also β-alkyl transfer and chain transfer to aluminum[16-18]. Low molecular mass polypropylenes, produced by a metallocene catalyst such as $Et(Ind)_2ZrCl_2$, result from faster β-hydride-elimination. It is reported that the methyl groups in the 2-position on the benz[e]indenyl ligand in **MBI** suppress chain transfer to the monomer, which would otherwise result from β-hydride transfer from the last monomeric unit of the polymer chain to the monomer[1]. This results in an increase in molecular mass. Schneider *et al.*[19] found that for the copolymerization of ethylene/1-octene with **MBI**, the 2-methyl substitution favors increase in the molecular mass, whereas benzannelation facilitates incorporation of 1-octene and random distribution of 1-hexyl short-chain branches along the chain.

The copolymer with the lowest viscosity-average molecular mass was obtained at the highest reaction temperature, i.e. 80°C. The molecular mass distributions of all the propylene/1-pentene copolymers were narrow, varying from only 2.5 to 3.4.

5.5.3 Photo-acoustic infrared spectroscopy (PAS-IR)

The infrared spectrum of a propylene/1-pentene sample (PP80) prepared with the metallocene $Me_2Si(2\text{-}MeBenz[e]Ind)_2ZrCl_2$ can be seen in Figure 5.7. In the propylene/1-pentene copolymers formed with the metallocene $Me_2Si(2\text{-}MeBenz[e]Ind)_2ZrCl_2$, the presence of n-propyl branches causes a vibration in the region 745-735 cm^{-1}. This vibration is much stronger in these copolymers than in those formed with the catalyst $Et(Ind)_2ZrCl_2$ (Figure 5.8). The vibration at 890 cm^{-1}, which has been assigned to the methyl rocking mode for branches larger than ethyl, might overlap with the vibration of the vinylidene end groups. In all the propylene/1-pentene copolymers formed with the silylene-bridged catalyst, the absorbence in this area was not as strong as in the ethylene-bridged copolymers.

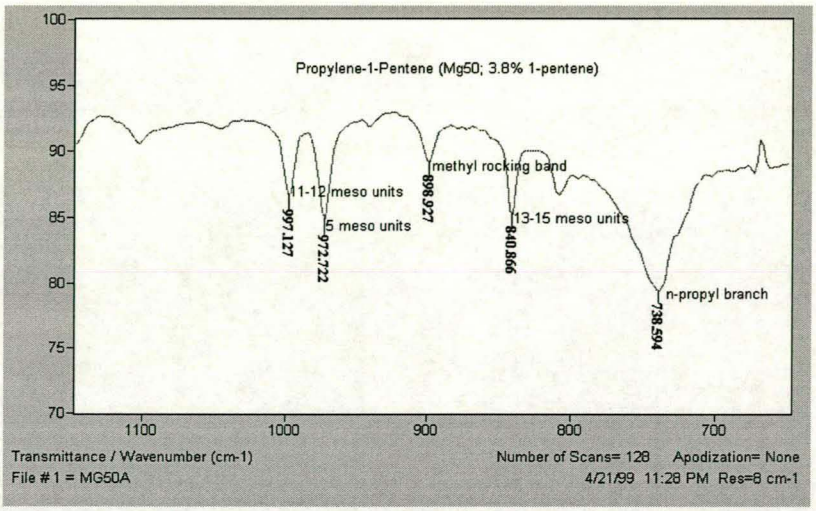

Figure 5.7. PAS-IR spectrum of propylene/1-pentene copolymer (PP80, 3.8% 1-pentene).

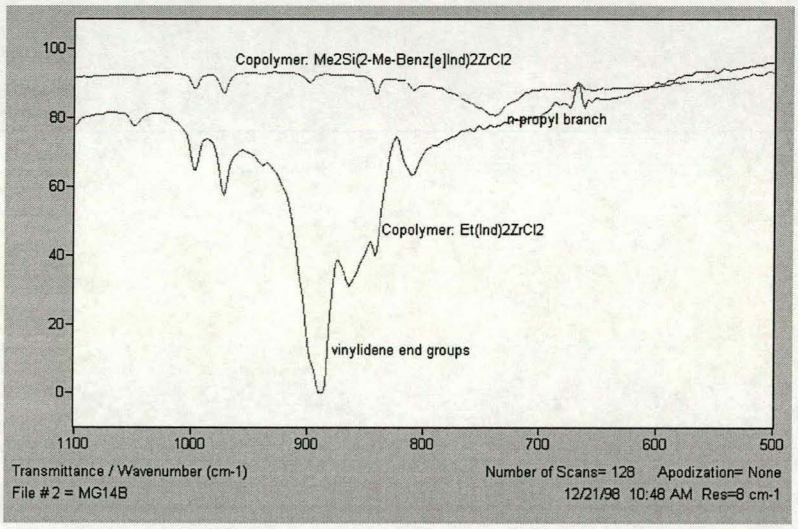

Figure 5.8. Comparison of PAS-IR spectra of two different propylene/1-pentene copolymers, prepared with the catalysts $Me_2Si(2\text{-}MeBenz[e]Ind)_2ZrCl_2$ (PP80, 2.8% 1-pentene) and $Et(Ind)_2ZrCl_2$ (Mg38, 4.4% 1-pentene).

The bands shown at 998 cm^{-1} and at 973 cm^{-1} were observed for meso sequence lengths of propylene, for 11 meso units and 5 meso units respectively. The band at 841 cm^{-1} was found for 13-15 meso units. There are very small bands that can be related to vibrations at 890 cm^{-1}, 910 cm^{-1} and 888 cm^{-1}, normally visible due to unsaturation, in the PAS-IR spectra of the propylene/1-pentene copolymers. This confirms the high molecular masses of the sample of the $Me_2Si(2\text{-}MeBenz[e]Ind)_2ZrCl_2$ catalyzed copolymer.

5.5.4 Microstructure of propylene/1-pentene copolymers

^{13}C NMR spectroscopy is the most powerful analytical method for the study of the microstructure of polyolefins. ^{13}C NMR spectroscopy was used to calculate the amount of 1-pentene incorporated in the copolymers. This was done by the same method as described in Chapter 4, Section 4.6.4. Propyl branches indicated the presence of the amount of 1-pentene incorporated in the copolymers. Figure 5.9 shows the ^{13}C NMR spectrum of sample PP80. (The chemical shifts are reported with respect to an internal 1,2,4-trichlorobenzene standard.)

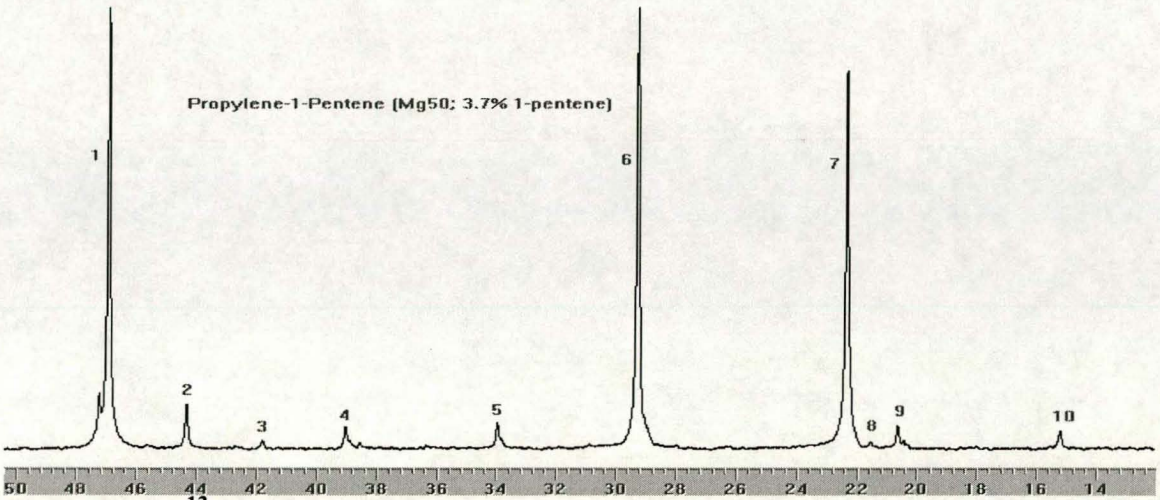

Figure 5.9. ^{13}C NMR spectrum of a propylene/1-pentene copolymer (sample PP80, 3.8% 1-pentene).

Solvent 1,2,4-trichlorobenzene:benzene-d_6 (9:1 volume ratio), temperature 100°C

To distinguish between the different C-atoms, the following numbering system was used (Figure 5.10). These numbers do, however, not necessarily correspond to any generally accepted assignment system.

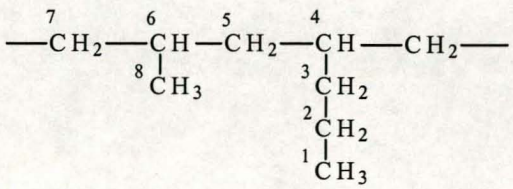

Figure 5.10. Carbon assignment scheme used for propylene/1-pentene copolymers.

The microstructure of the copolymer produced with the $Me_2Si(2\text{-}MeBenz[e]Ind)_2ZrCl_2$ catalyst system is the same as that produced with $Et(Ind)_2ZrCl_2$. The assignments of the signals in the ^{13}C NMR spectrum were therefore the same as those given in Section 4.6.4. The propylene/1-pentene copolymers produced with this catalyst system are highly isotactic as can be seen in Table 5.6.

Table 5.5. ^{13}C NMR signal assignments of the propylene/1-pentene copolymers produced with $Me_2Si(2\text{-}MeBenz[e]Ind)_2ZrCl_2$

Signal (refer Figure 5.9)	δ(ppm)	Type of carbon	Assignment (refer Figure 5.10)
1	46.95	CH_2	7
2	44.31	CH_2	5
3	41.78	CH_2	
4	38.95	CH_2	3
5	33.94	CH	4
6	29.28	CH	6
7	22.29	CH_3	8
8	20.62	CH_2	2
9	20.27	CH/CH_3	
10	15.15	CH_3	1

The amount of 1-pentene incorporated in the propylene/1-pentene copolymers and the amount of isotacticity in the propylene/1-pentene copolymers are shown in Table 5.6.

Table 5.6. The 1-pentene amount and the percentage isotacticity of the propylene/1-pentene copolymers, produced with $Me_2Si(2\text{-}MeBenz[e]Ind)_2ZrCl_2$, as calculated from ^{13}C NMR spectroscopy

Sample	1-Pentene amount (mol %)	mmmm[a]
PP80	3.8	95%
PP25	3.5	87%
PP8	2.8	87%
PP40	2.5	90%

[a]Area of the resonance of the methyl mmmm stereochemical pentad (percent with respect to the total area of the methyl resonance)

CHAPTER 6

Characterization of ethylene/1-pentene and propylene/1-pentene copolymers using CRYSTAF.

Summary

The short-chain branching distribution together with the molecular mass distribution of an olefin material determines its potential performance. The short-chain branching distribution (SCBD) of ethylene/1-pentene and propylene/1-pentene copolymers was measured by crystallization analysis fractionation (CRYSTAF). CRYSTAF is a relatively new technique useful for the analysis of the comonomer distribution in semi-crystalline polymers and, more specifically, for the analysis of the short-chain branching distribution (SCBD) in linear low density polyethylene (LLDPE). The technique is based on a step-wise precipitation approach. By monitoring the polymer solution concentration during crystallization, the cumulative and differential SCBD of the copolymer can be obtained without the need of physical separation of fractions. The new technique has been shown to provide similar results to temperature rising elution fractionation but in a shorter time.

6.1 INTRODUCTION

Analysis of the SCBD of a polyolefin is not a simple task. To achieve adequate resolution, fractionation of the polymer is required. The most common technique used to date to determine the SCBD of a copolymer has been temperature-rising elution fractionation (TREF). As a result of the operational complexity of TREF and the long analysis time involved, however, a new technique which performs the SCBD analysis in a simple manner and with shorter analysis time[1] has been developed.

The crystallization analysis fractionation (CRYSTAF) technique was first described by Monrabal[2] in 1994. Crystallization analysis fractionation is based on the approach to monitor the solution crystallization of a polymer that will allow the calculation of the overall SCBD. Both TREF and CRYSTAF fractionate on the basis

of crystallizability; TREF, however, does the crystallization on a packing and uses a dissolution (elution) step to perform the final fractionation. The CRYSTAF technique extracts this information directly during the crystallization process by looking to the solution concentration depression and no column packing is required. A CRYSTAF curve resembles that of temperature-rising elution fractionation (TREF) but in the former a correction due to the remaining noncrystallizable material after fractionation is taken into consideration. This fraction is referred to as the soluble fraction[6].

The analysis is carried out by monitoring the polymer concentration in the solution, while reducing the temperature, during the cooling crystallization. Aliquots of the solution are filtered and analyzed by an infrared detector. The entire process is similar to a classical stepwise fractionation by precipitation, with the exception that in this approach no attention is paid to the polymer precipitated but to the polymer that remains in solution[4]. The incorporation of comonomer into the polymer chain results in irregularities (side-chain branches) that modify the crystallizability of the polymer. Assuming random copolymerization, by using the proper experimental conditions and carrying out the crystallization in dilute solutions, the segregation of crystals should occur on the basis of comonomer incorporated, according to comonomer-branch content.

CRYSTAF can be used in quality control, when characterization of the short-chain branching of copolymers is required. With the short analysis time required and the simplicity of the analytical procedure full dissolution and crystallization-analysis and cleaning can be achieved in a relatively short time, making this a very attractive analytical method.

Ethylene/1-pentene copolymers, prepared with the catalyst $Et(Ind)_2ZrCl_2$/MAO, and propylene/1-pentene copolymers, prepared with the catalyst $Me_2Si(2\text{-}MeBenz[e]Ind)_2ZrCl_2$/MAO, were characterized by CRYSTAF. The copolymers varied in that they contained different amounts of comonomer (1-pentene) and had different molecular masses.

6.2 EXPERIMENTAL

The commercial CRYSTAF equipment was used to perform the CCD (chemical composition distributions) analyses. A Hewlett Packard 5890 II gas chromatograph oven was used for the crystallization temperature program. Crystallization was carried out in stainless steel reactors (60 mL volume) fitted with a stirrer, where dissolution and filtration takes place automatically. A dual wave length optoelectronic infrared detector was used together with a heated flow-through micro cell to measure the polymer concentration in solution at each sampling step during the crystallization. The microcell operates at 150°C and uses 3.5 μ as the measuring wavelength.

Sample concentrations of 0.1% w/v were typically used; for example, 30 mg of polymer in 30 mL of 1,2,4-trichlorobenzene solvent (commercial grade, redistilled). Typical crystallization rates were between 0.2°C/min and 0.70°C/min. Dissolution, crystallization, and cleaning is done in an automatic process which lasts between 1 and 6 hours (overall time), depending on the crystallization rate. Five samples can be analyzed simultaneously, in the same run.

The experimental method described here is similar to that described by Monrabal[3].

6.3 RESULTS AND DISCUSSION

CRYSTAF curves of copolymers produced by single-site metallocenes normally show narrow chemical composition distributions (CCD)[5]. In the ethylene/1-pentene copolymers produced by the ethylene-bridged catalyst, an increase in the amount of 1-pentene in the copolymer led to an increase in the short-chain branching and thus an increase in the CCD. Figures 6.1, 6.2 and 6.3 are CRYSTAF curves of polyethylene (Figure 6.1) and ethylene/1-pentene copolymers with different amounts of 1-pentene incorporated in the copolymer (Figures 6.2 and 6.3). Sample EtPn10 (see Figure 6.3) showed a bimodal CCD. The broad CCD appeared to be related to the molecular mass of the copolymer[5].

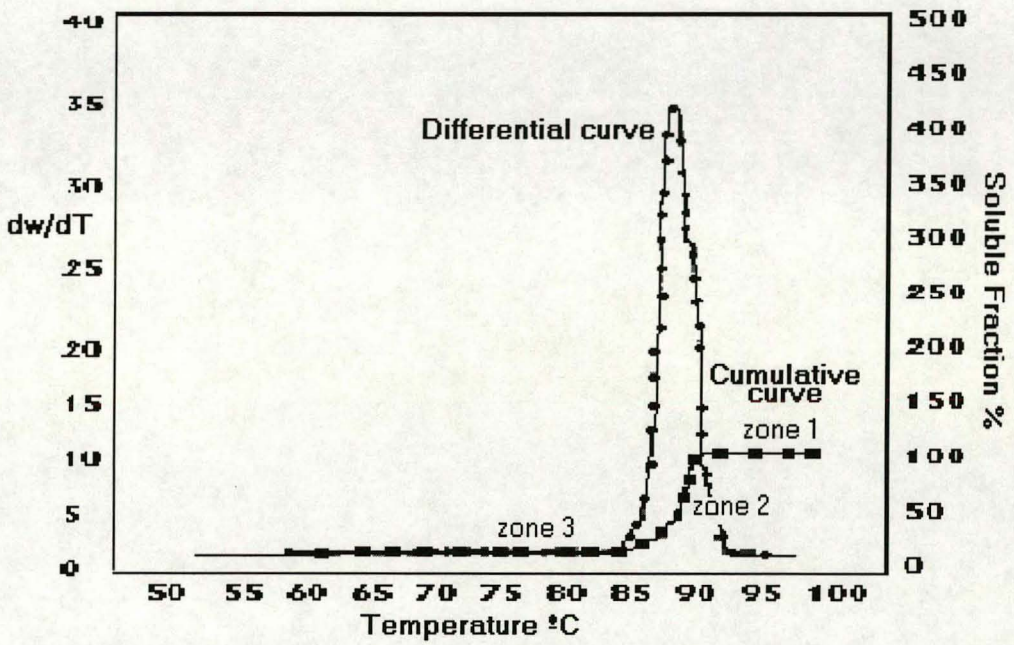

Figure 6.1. Cumulative (■■■) and differential (•••) SCBD of an ethylene homopolymer as obtained by crystallization analysis fractionation.

The first data points in the cumulative CRYSTAF curve, taken before any crystallization has taken place, provide a constant concentration equal to the initial polymer solution concentration (zone 1 in Figure 6.1). As the temperature is decreased, most of the crystalline fractions, composed of molecules with zero or few branches, will precipitate first, resulting in a steep decrease in the solution concentration (zone 2 in Figure 6.2). This is followed by precipitation of fractions of increasing branch content as the temperature continues to decrease (zone 3 in

Figure 6.3). The last data point (■), corresponding to the lowest temperature of the crystallization cycle, represents the fraction that has not crystallized (mainly highly branched material) and remains soluble. The top curve (■■■) in Figure 6.1 corresponds to the cumulative SCBD when the temperature scale is calibrated and transformed to the number of branches/1000 carbons. The first derivative of the cumulative curve is called the differential curve (•••) and can be associated with the SCBD as shown in Figure 6.1.

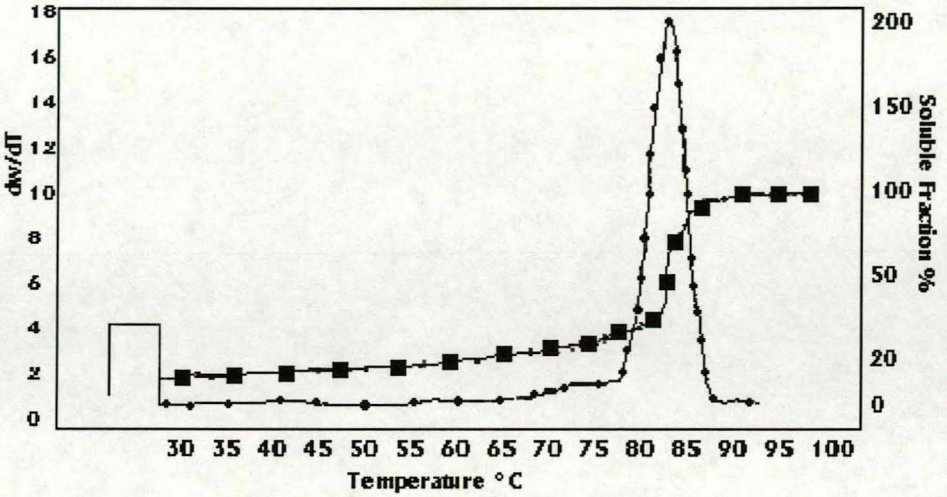

Figure 6.2. Cumulative (■■■) and differential (•••) SCBD of an ethylene/1-pentene copolymer (sample EtPn4, 5.2% 1-pentene) as obtained by crystallization analysis fractionation.

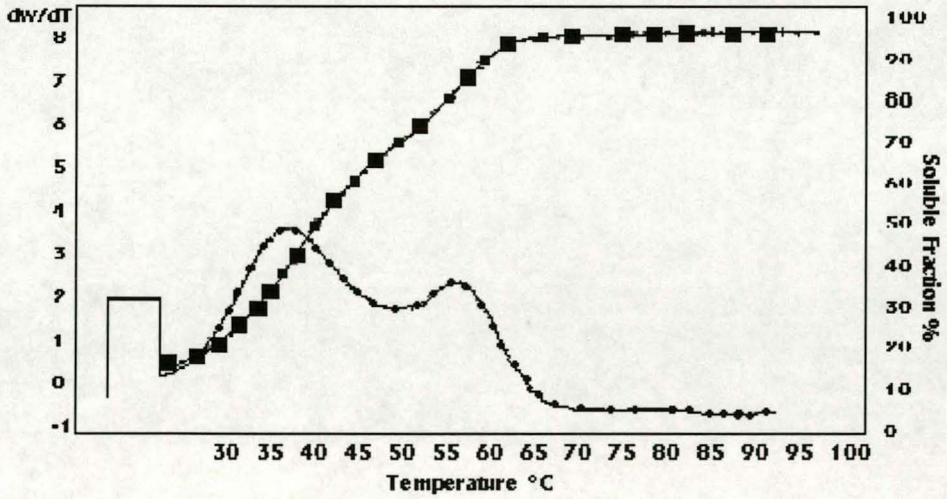

Figure 6.3. Cumulative (■■■) and differential (•••) SCBD of an ethylene/1-pentene copolymer (sample EtPn10, 2.6% 1-pentene) as obtained by crystallization analysis fractionation.

. The overall CRYSTAF results of the ethylene/1-pentene copolymers and the propylene/1-pentene copolymers are presented in Table 6.1.

Table 6.1. CRYSTAF results of the ethylene/1-pentene and propylene/1-pentene copolymers

Sample	1-Pentene (mol%)	Crystallization temperature T_c(°C)	Weight-average crystallization temperature T_w(°C)	Sigma (σ)	R
Ethylene/1-pentene copolymers					
EtPn0	0	86.7	85.7	6.2	1.0
EtPn4	5.2	77.2	66.6	17.1	1.1
EtPn10	2.6	42.6 and 58.6	47.3	10.2	1.0
EtPn20	45.3	42.3	32.3	6.4	1.0
Propylene/1-pentene copolymers					
PP80	3.8	43.1	42.4	1.5	1.0
PP25	3.5	55.1	54.6	5.9	1.0
PP8	2.8	59.8	57.2	8.7	1.0
PP40	2.5	56.7	53.9	8.2	1.0

Sigma and R are parameters defining the broadness of the CCD as per the formulas presented in appendix (Reference 2).

From Table 6.1 it can be seen that the crystallization temperature (T_c) decreases as the amount of 1-pentene incorporated in the ethylene/1-pentene copolymers and the propylene/1-pentene copolymers increases. The same effect is observed with the weight-average crystallization temperature (T_w). From these results we can conclude that a decrease in the crystallization temperature indicates an increase in the amount of branches in the copolymers. Sigma and R are parameters defining the broadness of the chemical composition distribution; therefore the high sigma values of EtPn4 (17.1) and EtPn10 (10.2) indicate a broader chemical composition distribution, when compared to samples EtPn0 (6.2) and EtPn20 (6.4). Although the sigma and R values define the broadness of the CCD, the soluble fraction at the last temperature of the crystallization gives an idea of the amount of short-chain branching in the copolymer. The soluble fractions left in the solution of the CRYSTAF experiments corresponds well with the molecular mass distribution results from GPC.

The soluble fraction values obtained from the ethylene/1-pentene CRYSTAF curves are compared to the molecular mass distribution values obtained from GPC analysis in Table 6.2.

Table 6.2 Comparison between the soluble fractions and the molecular mass distributions of the ethylene/1-pentene copolymers as determined by CRYSTAF and GPC analysis respectively.

Sample	1-Pentene content (mol %)	Soluble fraction (%)	M_w/M_n
EtPn0	0	0.4	3.1
EtPn10	2.6	12.1	2.01
EtPn4	5.2	23.0	4.23
EtPn20	45.3	89.7	7.4

The CRYSTAF results correspond well with the results obtained from GPC analysis. EtPn20 had an amount of 89.7% soluble fraction left in the polymer solution. The number of branches in the copolymer was therefore very high and the copolymer has a very broad SCBD. This result corresponds well with the broad molecular mass distribution of the copolymer as obtained from the GPC analysis where the polydispersity of the copolymer, sample EtPn20, was 7.4. EtPn0 had only a 0.4% soluble fraction, and therefore a narrow SCBD. The molecular mass distribution of the sample EtPn4, as obtained from GPC analysis, was 3.1. This also indicated uniform chains with narrow distribution. The differential CRYSTAF curve of sample EtPn10 (see Figure 6.3) shows two peaks, which corresponds well with the GPC curve which also show a bimodel curve for the distribution of molecular mass. When compared to that of the other samples, sample EtPn10 had a much higher number-average molecular mass.

Figures 6.4 and 6.5 show the CRYSTAF curves of the propylene/1-pentene copolymers (samples PP80 and PP8) obtained with the $Me_2Si(2\text{-}MeBenz[e]Ind)_2ZrCl_2$/MAO catalyst system.

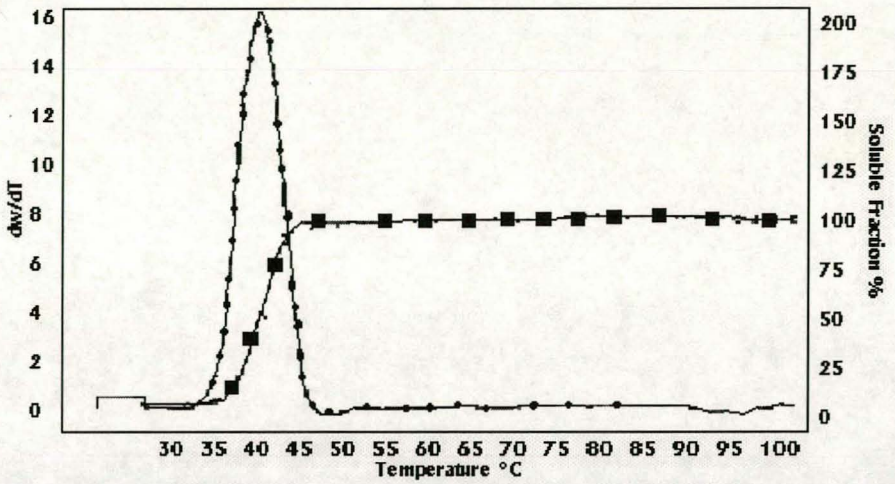

Figure 6.4. Cumulative (■■■) and differential (•••) SCBD of a propylene/1-pentene copolymer (sample PP80, 3.8% 1-pentene) as obtained by crystallization analysis fractionation.

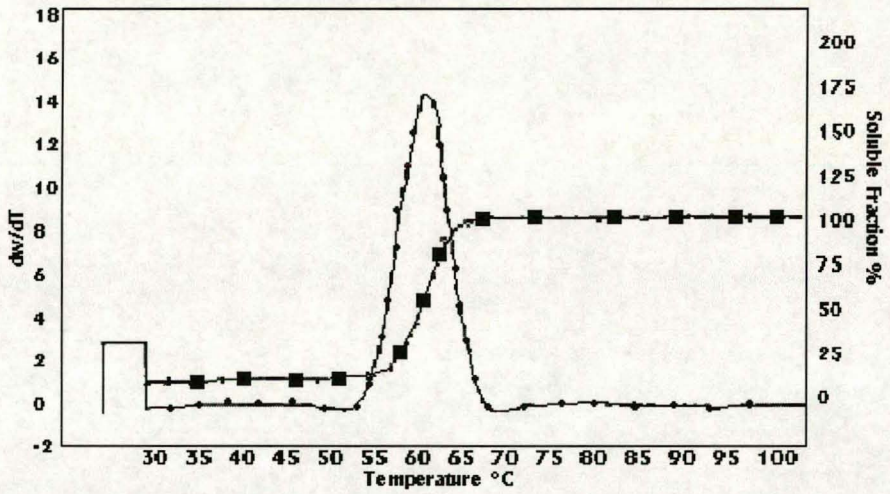

Figure 6.5. Cumulative (■■■) and differential (•••) SCBD of a propylene/1-pentene copolymer (sample PP8, 2.8% 1-pentene) as obtained by crystallization analysis fractionation.

As can be seen from the CRYSTAF curves, the metallocene catalyst $Me_2Si(2\text{-}MeBenz[e]Ind)_2ZrCl_2$ produced copolymers with narrow chemical composition distributions (CCD). If we compare the results obtained from CRYSTAF and the GPC analysis for the propylene/1-pentene copolymers

(see Section 5.5.2), the CRYSTAF curves confirm the narrow molecular mass distribution of the copolymers. Table 6.3 shows the CRYSTAF results and the results from the GPC analysis for the propylene/1-pentene copolymers.

Table 6.3. Comparison between the soluble fractions and the molecular mass results of the propylene/1-pentene copolymers as determined by CRYSTAF and GPC analysis respectively

Sample	1-Pentene content (mol %)	Soluble fraction(%)	Weight-average molecular mass M_w (g/mol)	Number-average molecular mass M_n (g/mol)	M_w/M_n
PP40	2.5	15.8	512 300	166 600	3.1
PP8	2.8	14.0	515 800	187 600	2.7
PP25	3.5	7.6	633 500	186 000	3.4
PP80	3.8	3.4	427 800	172 700	2.5

The CRYSTAF results in Table 6.3 do not correspond as well with the GPC analysis results when compared with that of Table 6.2. The soluble fraction values decrease as the amount of comonomer (1-pentene) increase. The reason for this could be that samples PP40 and PP8 showed a broader composition distribution than samples PP25 and samples PP80. The sigma values of samples PP40 (8.2) and PP8 (8.7) were much higher than that of PP80 (1.5) and PP25 (5.9). Although the copolymers PP40 and PP8 had a higher soluble fraction indicating a higher amount of comonomer in the copolymer, the same was not found from ^{13}C NMR results. Comparing the amount of 1-pentene in the propylene/1-pentene and ethylene/1-pentene copolymers, it can be seen that the increments in the amount of 1-pentene in the latter are much higher than that of the propylene/1-pentene copolymers.

A practical outcome of the use of CRYSTAF as an analytical method can be that it is possible to calibrate the type of results obtained with CRYSTAF, which could be used in the analysis of the short-chain branching of the copolymer of the same comonomer type. Plotting the crystallization temperature, T_c, vs. the comonomer wt % incorporated results in a relatively straight line. With the growing availability of

single-site type resins prepared with various types of comonomers, a calibration curve could be prepared for each comonomer type. The calibration curve could be used to convert the crystallization temperature scale to percentage of comonomer content or number of methyls per 1000 carbons. Unfortunately, there has been no CRYSTAF work done on propylene/1-pentene copolymers, except for this study, and a calibration curve for propylene/1-pentene copolymers must still be obtained. At this stage it can not be concluded how many methyls per 1000 carbons are present in the propylene/1-pentene copolymers.

6.4 CONCLUSIONS

The CRYSTAF analysis of various ethylene/1-pentene copolymers and propylene/1-pentene copolymers, produced by metallocenes, showed the homogeneity of their composition distribution. The CRYSTAF data correlated well with the amount of 1-pentene incorporated in the copolymer and the results obtained from GPC analysis. CRYSTAF can be used in quality control, as an online analytical technique, when characterization of the short-chain branching of copolymers in a specific batch is required.

6.5 APPENDIX

Weight and Number Average Parameters

$$T_w = \frac{\sum c_i \bullet T_i}{\sum c_i} \qquad T_n = \frac{\sum c_i}{\sum c_i / T_i}$$

Parameters to measure broadness of the CCD:

$$\sigma = \sqrt{\frac{\sum c_i (T_i^2 - T_w^2)}{\sum c_i}} \qquad R = (\frac{T_w}{T_n} - 1)$$

6.6 REFERENCES

1. Monrabal B., Jan van der Heuvel E., *International GPC Symposium '91*, p.415.
2. Monrabal B., *J. of Appl. Polym. Sci.*, 1994, **52**, 491.
3. Monrabel B., *Polym. ChAR, International GPC Symposium, '96*, p.50.
4. Monrabal B., *Polym. ChAR, Macromol. Symp.*, 1996, **110**, 81-86.
5. Monrabal B., Blavo L., Nieto J., Soares J.B.P., *J. Polym. Sci.: Part A., Polym. Chem.*, 1999, **37**, 89.
6. Lehtinen C., Starck P., Löfgren B., *J. Polym. Sci.; Part A: Polym. Chem.*, 1997, **35**, 307.

CHAPTER 7

Conclusions

This study was aimed at the production of branched polyolefins using metallocene catalysts.

The copolymerization of ethylene with 1-pentene was successfully carried out, under various conditions, using the isotactic stereorigid zirconium metallocene $Et(Ind)_2ZrCl_2$/MAO catalyst system. High molecular mass ethylene copolymers (M_w between 111 200 and 172 700g/mol) were obtained. The presence of propyl branches, as evident from ^{13}C NMR analysis, indicated that 1-pentene was easily incorporated into the ethylene polymeric chain. The molecular mass distributions of the ethylene copolymers were narrow, as expected from polymers polymerized using metallocene catalysts. An increase in the amount of 1-pentene incorporated in the copolymer resulted in a decrease in the melting point crystallinity of the copolymer.

Use of the isotactic stereorigid zirconium metallocene $Et(Ind)_2ZrCl_2$/MAO catalyst system did not lead to the successful polymerization of high molecular mass propylene/1-pentene copolymers as was evident from their GPC analysis. To overcome this problem, another metallocene system, the homogeneous *rac*-Me_2Si(2-MeBenz[e]Ind)$_2ZrCl_2$/MAO catalyst system, was used. The weight-average molecular mass of the propylene/1-pentene copolymers increased from 25 000 g/mol (as was obtained with the formally used ethylene-bridged catalyst) to 515 800 g/mol, while the molecular mass distribution remained narrow, between 2 to 4.

The following techniques were used to characterize the copolymers: differential scanning calorimetry (DSC), nuclear magnetic resonance (NMR) spectroscopy, gel permeation chromatography (GPC) and infrared (IR) spectroscopy, and a new technique called crystallization analysis fractionation, (CRYSTAF). Use of the latter method makes it possible to measure the short-chain branching distribution of copolymers.

Results of CRYSTAF analysis showed the narrow short-chain branching of the metallocene-catalyzed copolymers; these correlated well with the distribution results obtained by GPC analysis.

Ideas for future research

- As a result of the uniform catalytically active sites in a metallocene-based catalyst, it is possible to control molecular mass, stereoregularities, and comonomer incorporation without sacrificing the narrow molecular mass distributions. Small changes in the ligand structure of the metallocene catalyst can lead to copolymers with greatly varied properties. An examination of the effect of the ligand substitution pattern of the silylene-bridged catalyst, on the properties of ethylene/1-pentene and propylene/1-pentene copolymers, should be very interesting.

- Commercial polymerization processes require heterogenization of the metallocene-based catalyst. Such a modification is needed to avoid reactor fouling with finely dispersed polymer crystals, to prevent excessive swelling of polymers, and to produce polymer particles of a desired regular morphology. As most of the existing polymerization processes and plants run with heterogeneous catalysts, an investigation of supported catalysts for fluidized bed polymerization processes are important for industrial purposes. The supported catalyst can be prepared by reacting macroporous SiO_2 first with MAO and then with the metallocene catalyst.

- Metallocene-based catalysts are sensitive to catalytic poisons, such as water, oxygen, and alcohols, which immediately halt the polymerization reaction. The cocatalyst MAO acts as impurity scavenger and thereby increases the activity of the catalyst. A major improvement towards simpler and cheaper metallocene-based systems will be to use other cocatalysts instead of MAO. Boron compounds, such as $B(C_6F_5)_3$, NR_3H^+ $B(C_6F_5)_4^-$ and $PH_3C^+B(C_6F_5)_4^-$, in combination with metallocene dialkyls (Cp_2ZrMe_2), could be used as cocatalysts.

APPENDIX A
(DSC Curves)

Ethylene/1-pentene Copolymers

EtPn1
1.5% 1-pentene

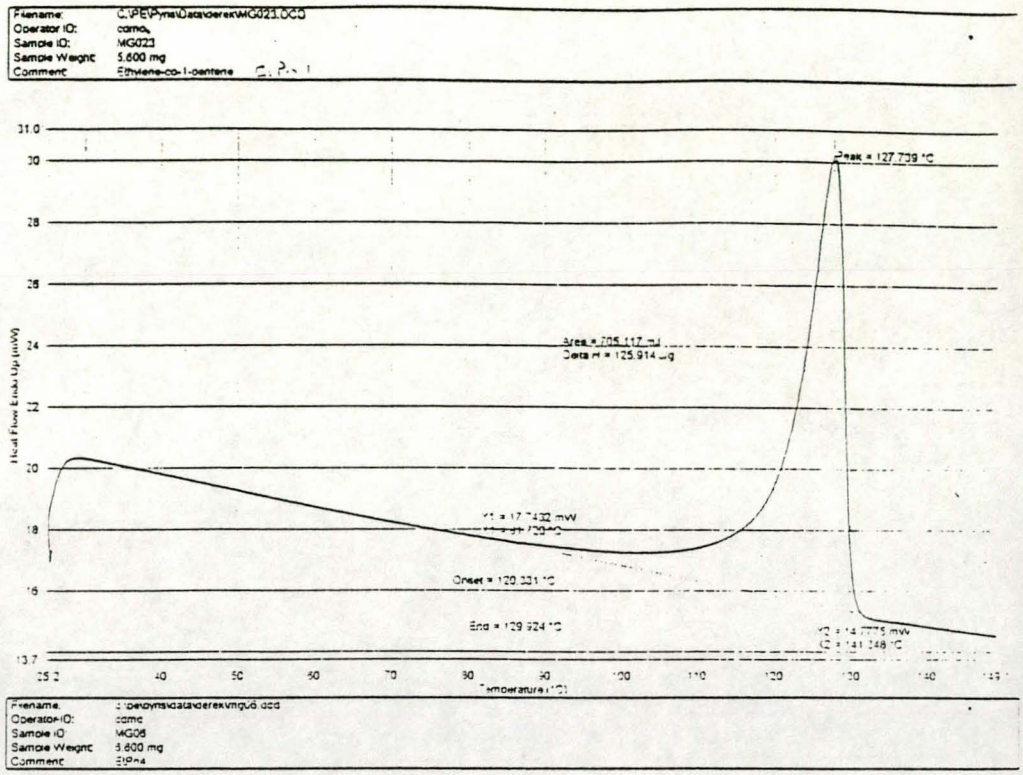

EtPn4
5.2% 1-pentene

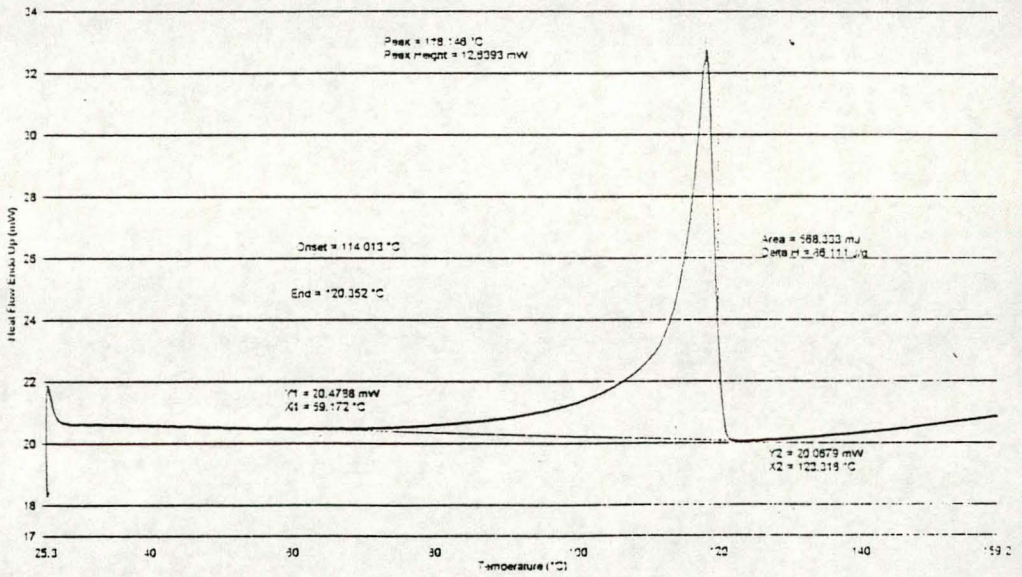

EtPn10
2.6% 1-pentene

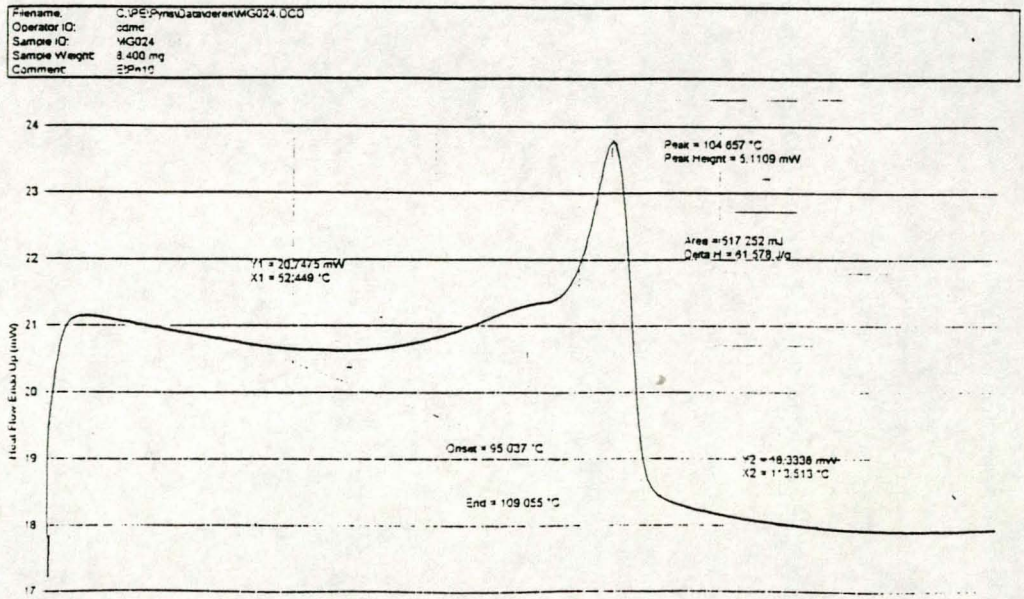

EtPn20
45.3% 1-pentene

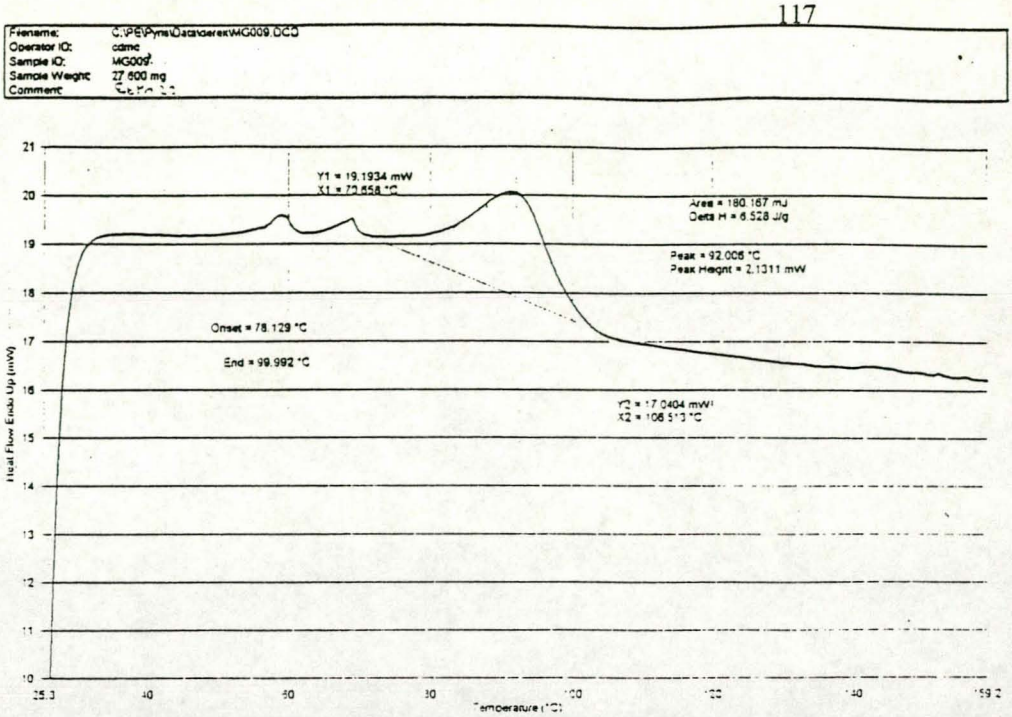

Propylene/1-pentene
Copolymers
Mg05
1.9% 1-pentene

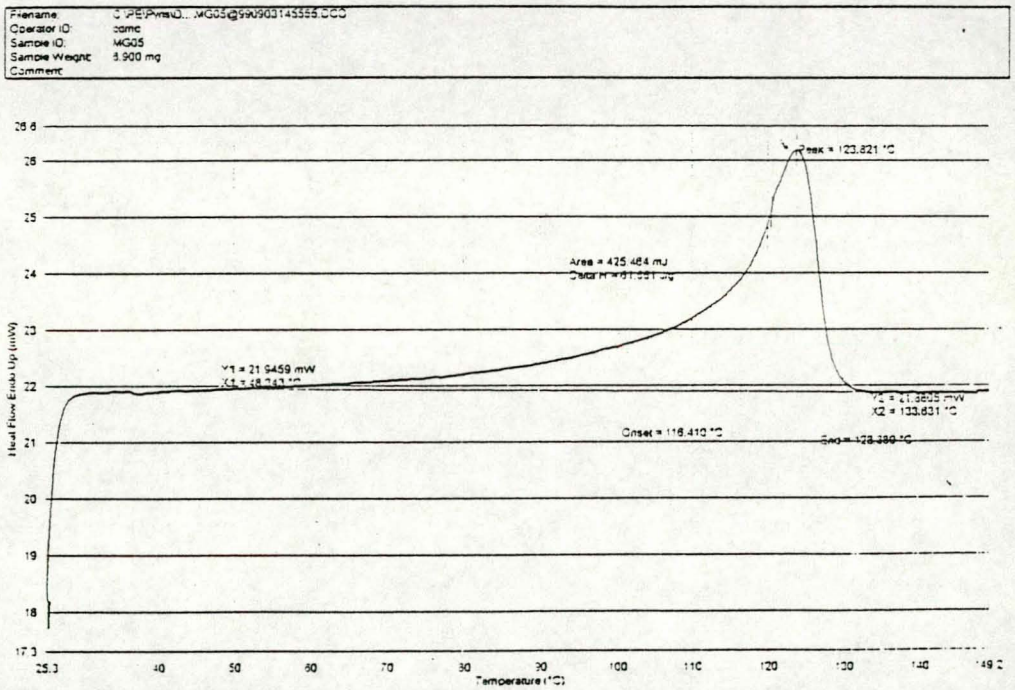

Mg02
3.8% 1-pentene

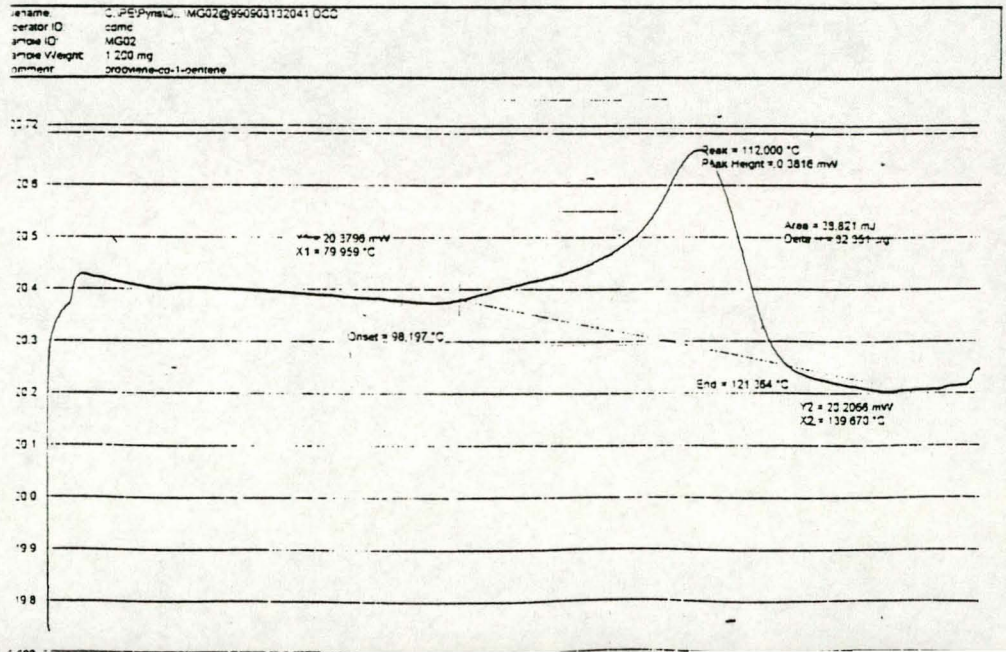

Mg01
13.7% 1-pentene

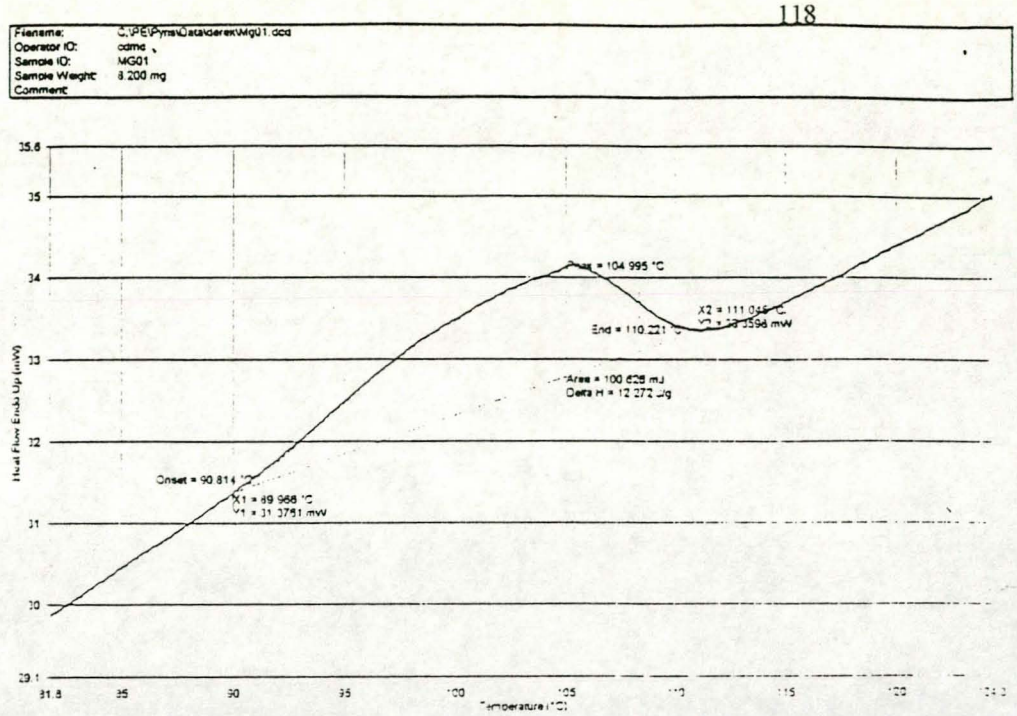

Mg33
0% 1-pentene

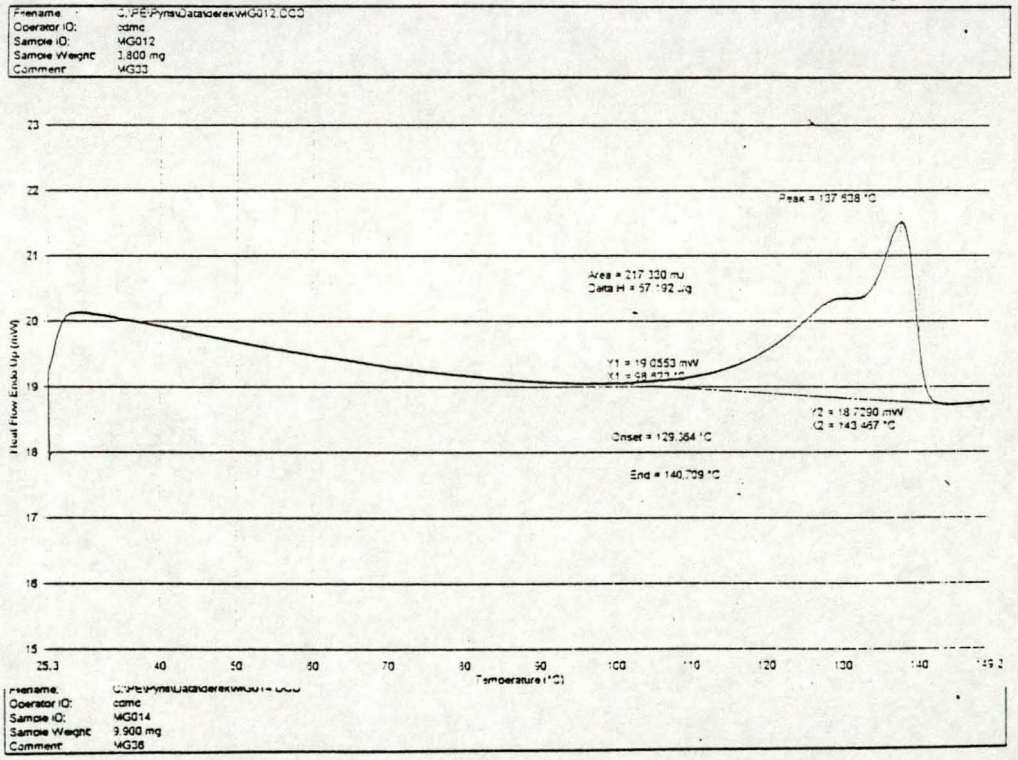

Mg36
2.1% 1-pentene

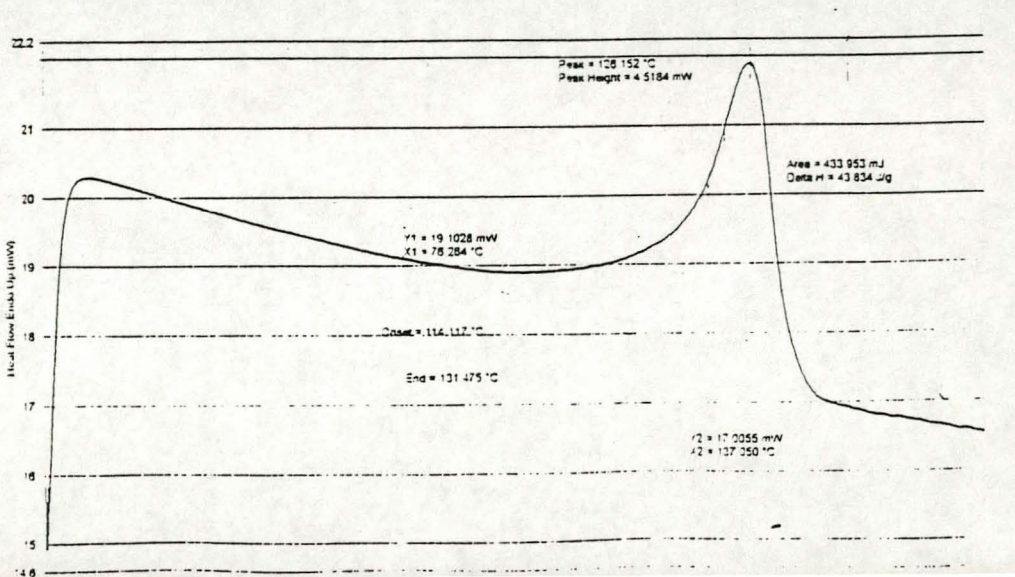

Mg14
2.7% 1-pentene

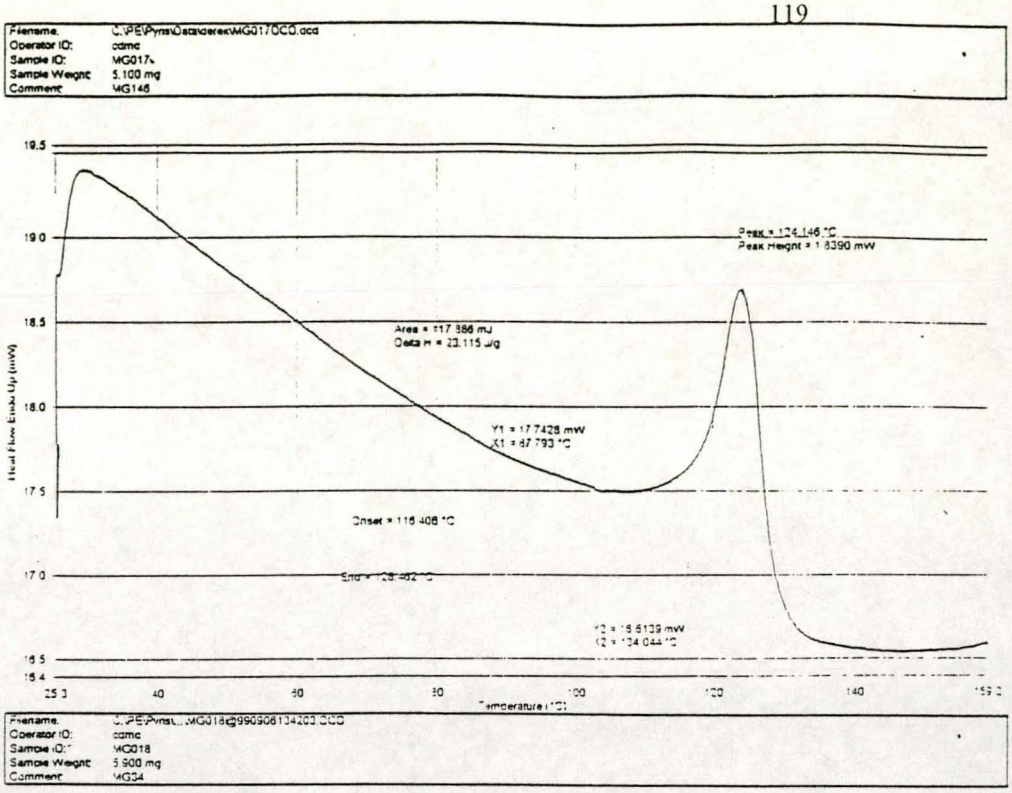

Mg34
8.7% 1-pentene

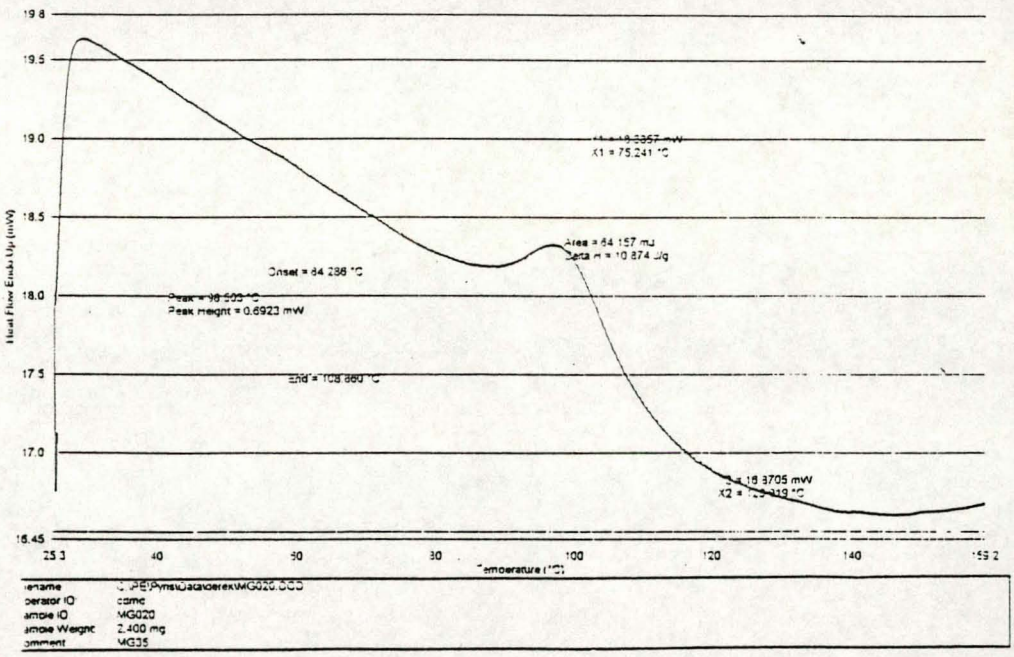

Mg35
7.1% 1-pentene

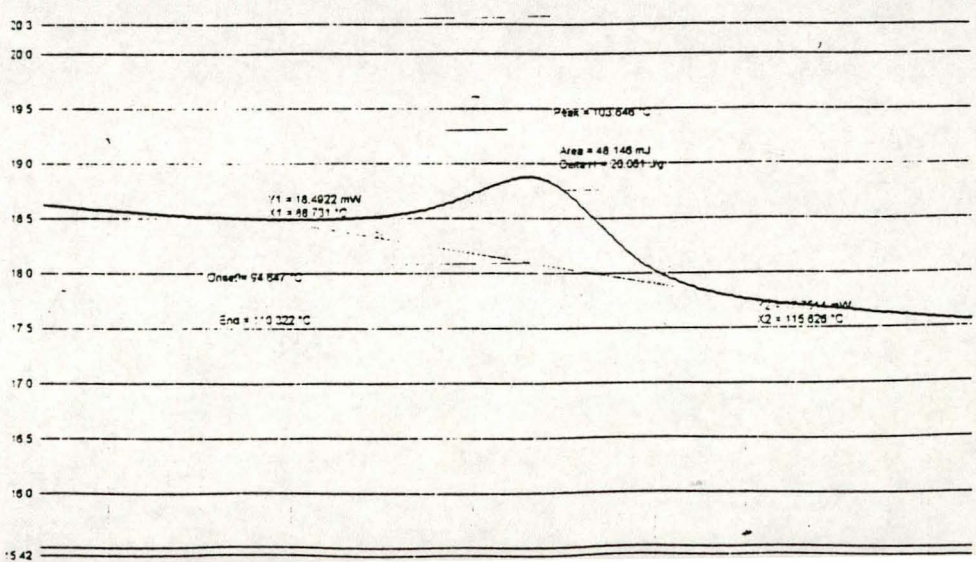

Mg37
0% 1-pentene

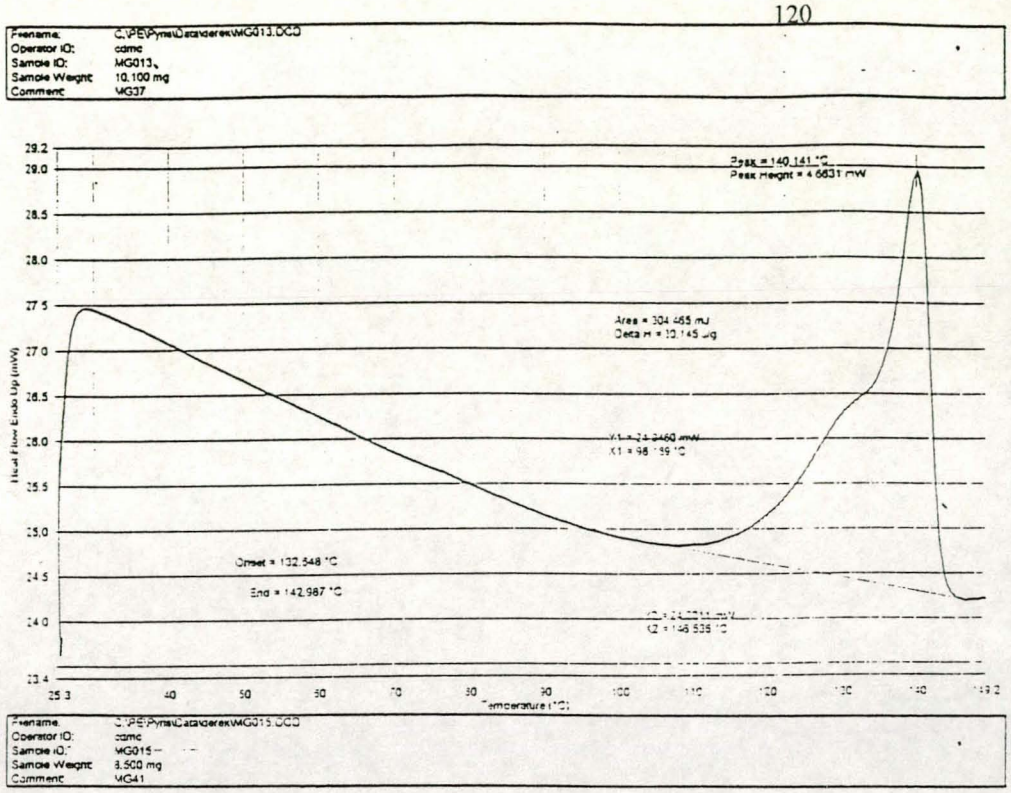

Mg41
0.5% 1-pentene

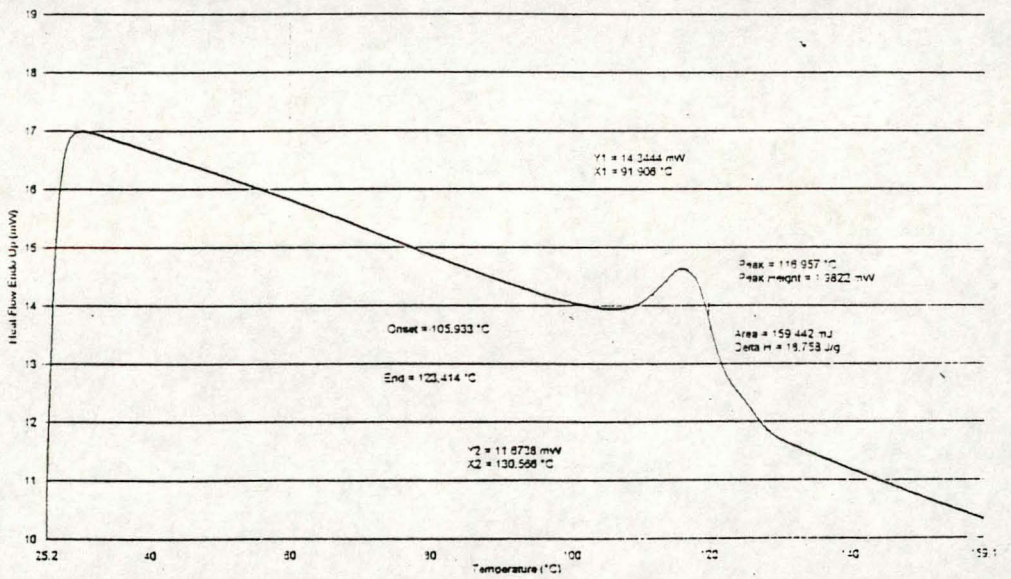

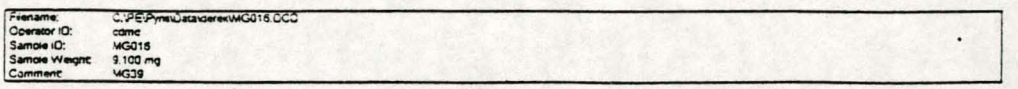

Mg39
0.8% 1-pentene

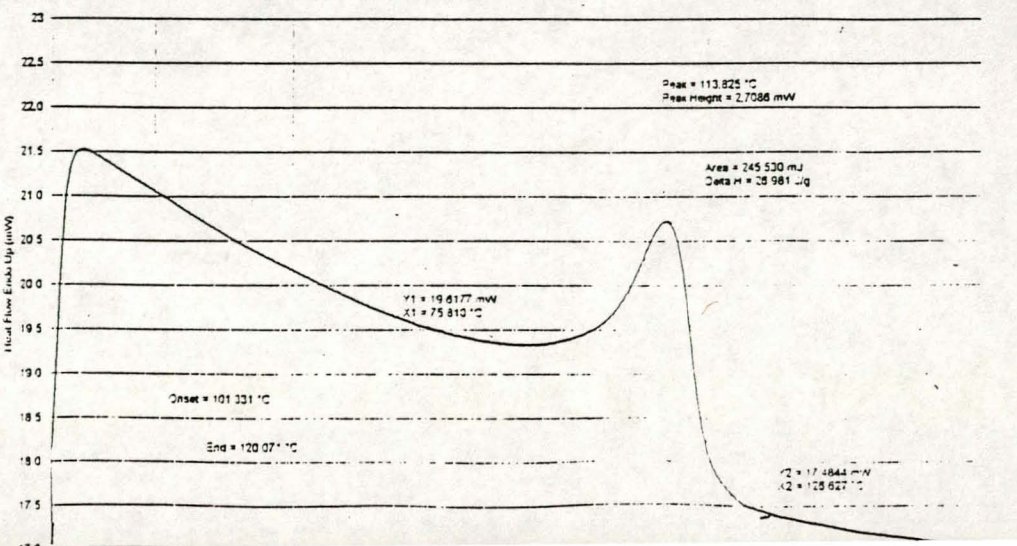

Mg38
4.4% 1-pentene

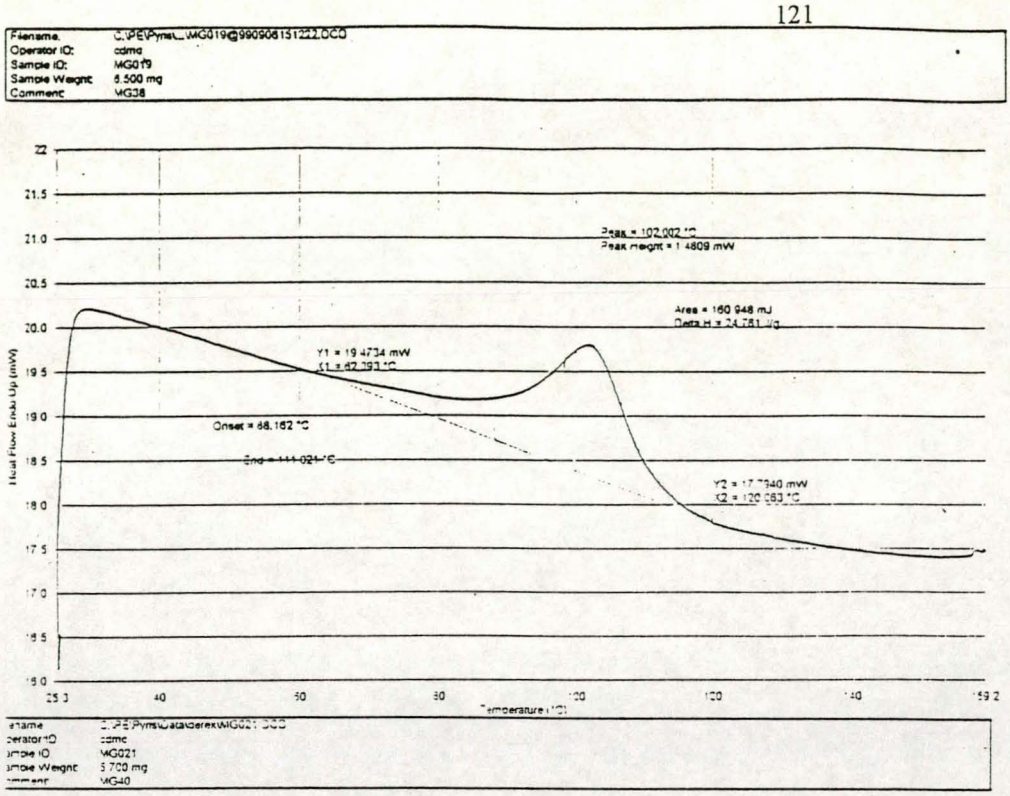

Mg40
9.9% 1-pentene

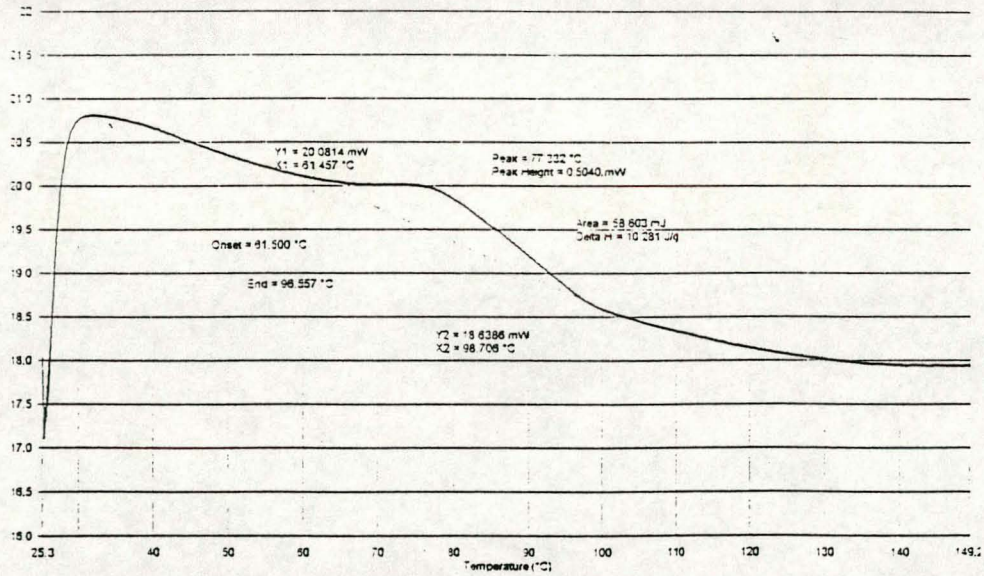

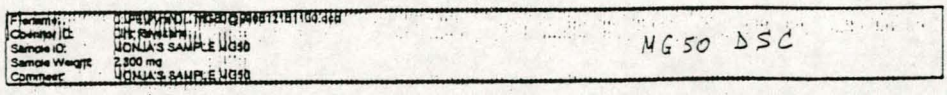

PP80
3.8% 1-pentene

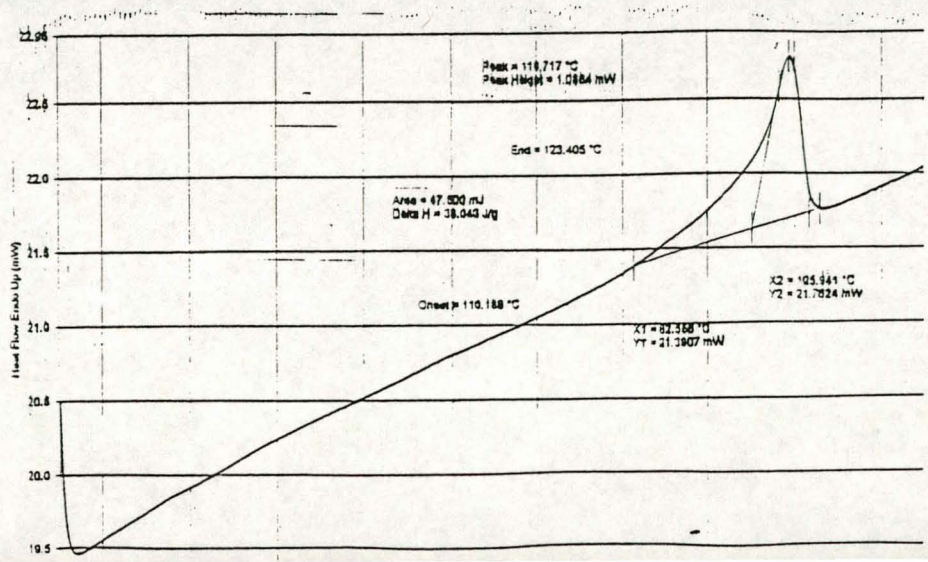

PP25
3.5% 1-pentene

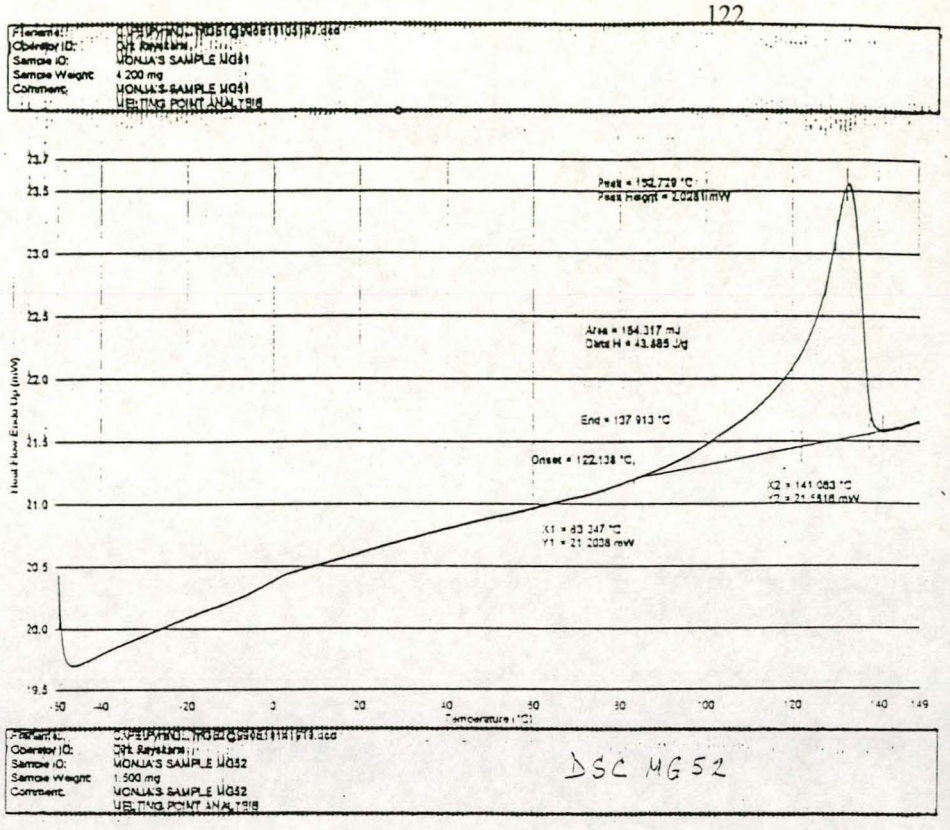

DSC MG52

PP8
2.8% 1-pentene

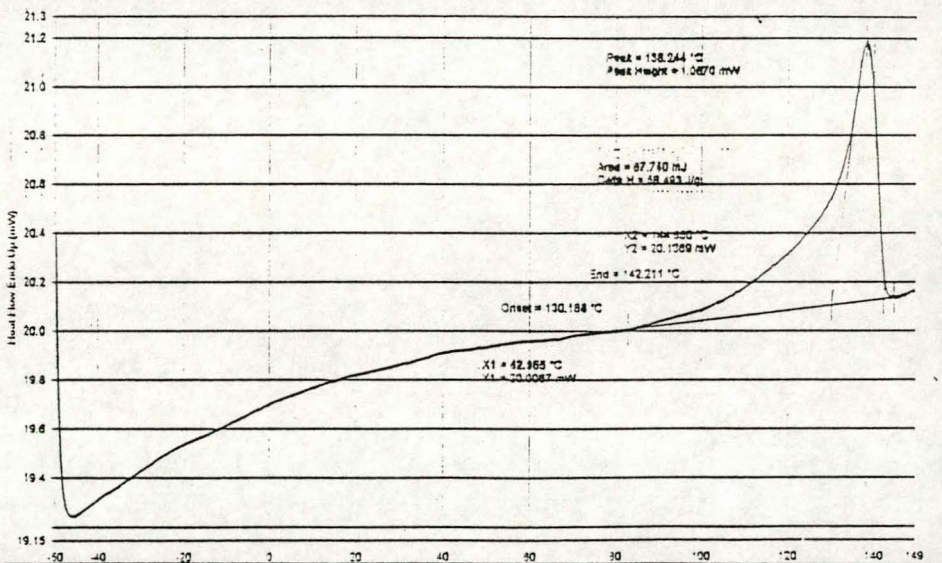

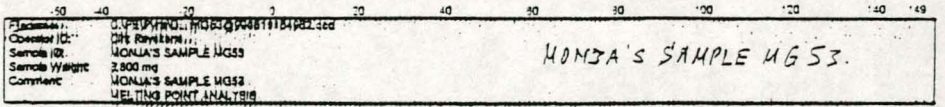

MONJA'S SAMPLE MG53.

PP40
2.5% 1-pentene

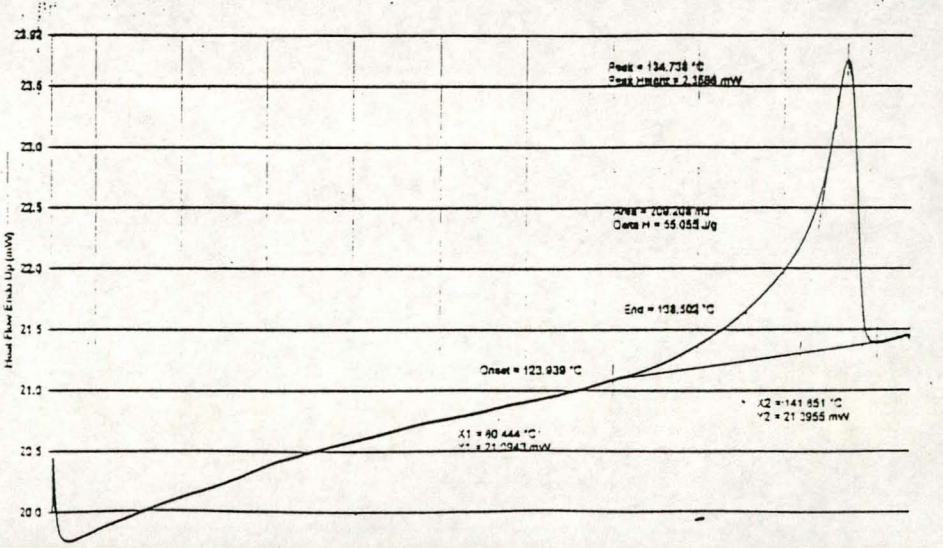

APPENDIX B
(GPC Curves)

Ethylene/1-pentene Copolymers

EtPn1

1.5% 1-pentene

RI 150C

$\overline{Mn}$:	3.665E+4	g/mol
$\overline{Mw}$:	1.264E+5	g/mol
$\overline{Mz}$:	2.700E+5	g/mol
$\overline{Mv}$:	1.131E+5	g/mol
$\overline{D}$:	3.449E+0	
[n]:	5.529E+1	ml/g
Vo :	3.301E+1	ml
Mo :	9.324E+4	g/mol
FI :	1.770E+1	ml*V
< 433	0.00	
w% :	100.00	
> 2669662	0.00	

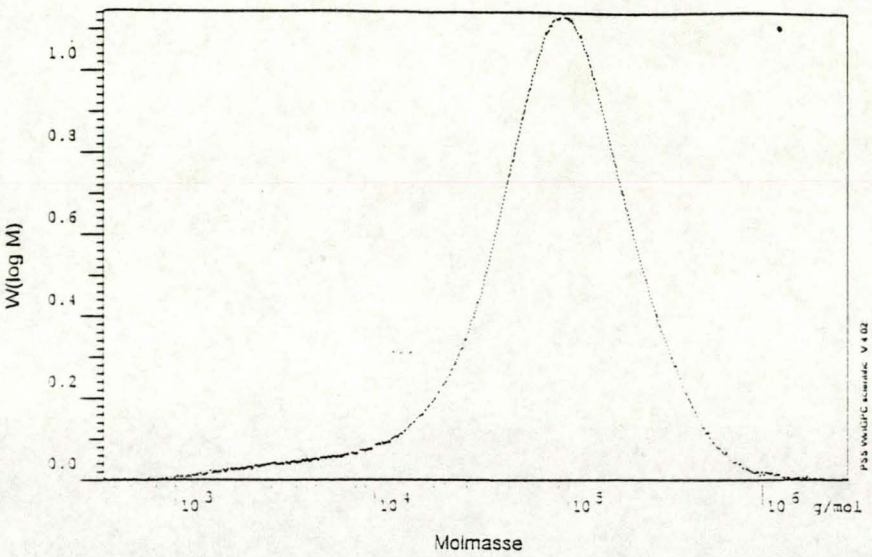

EtPn4

5.2% 1-pentene

RI 150C

$\overline{Mn}$:	1.626E+4	g/mol
$\overline{Mw}$:	1.112E+5	g/mol
$\overline{Mz}$:	2.506E+5	g/mol
$\overline{Mv}$:	9.746E+4	g/mol
$\overline{D}$:	4.234E+0	
[n]:	4.972E+1	ml/g
Vo :	3.787E+1	ml
Mo :	9.346E+4	g/mol
FI :	1.747E+1	ml*V
< 287	0.00	
w% :	100.00	
> 2326550	0.00	

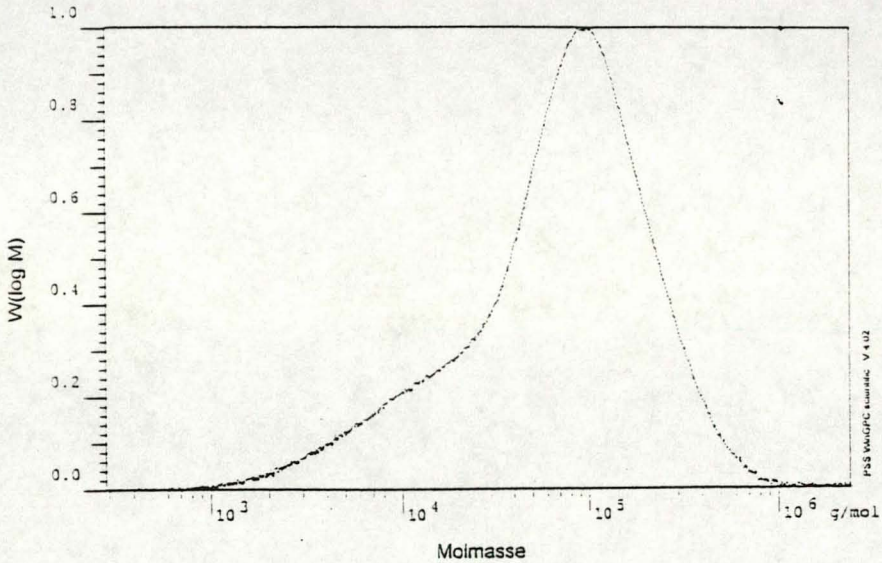

EtPn10

2.6% 1-pentene

RI 150C

$\overline{Mn}$:	6.243E+4	g/mol
$\overline{Mw}$:	1.272E+5	g/mol
$\overline{Mz}$:	2.538E+5	g/mol
$\overline{Mv}$:	1.160E+5	g/mol
$\overline{D}$:	2.037E+0	
[n]:	5.631E+1	ml/g
Vo :	3.312E+1	ml
Mo :	8.932E+4	g/mol
FI :	1.638E+1	ml*V
< 2022	0.00	
w% :	100.00	
> 2669662	0.00	

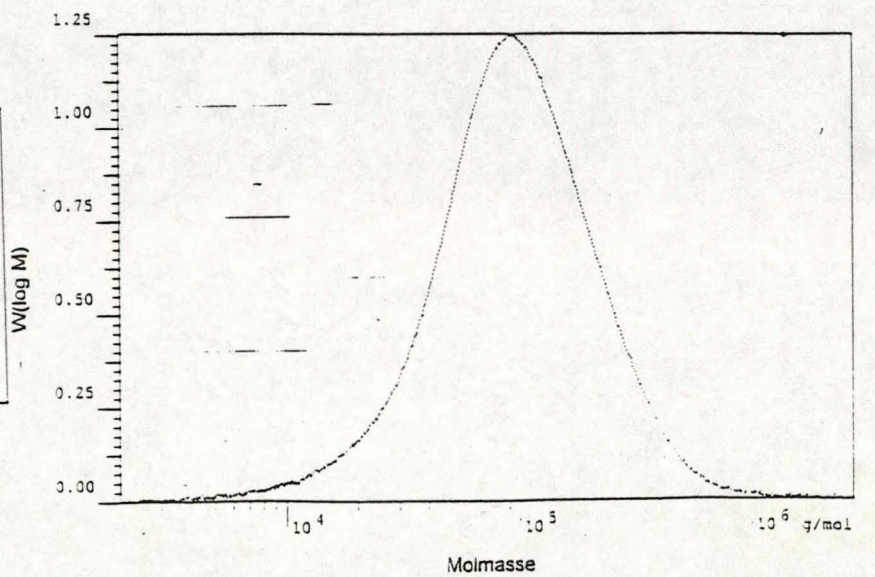

EtPn20
45.3% 1-pentene

RI 150C		
Mn :	2.626E+4	g/mol
Mw :	1.112E+5	g/mol
Mz :	2.506E+5	g/mol
Mv :	9.746E+4	g/mol
D :	4.234E+0	
[n]:	4.972E-1	ml/g
Vp :	3.787E+1	ml
Mp :	9.846E+4	g/mol
Fl :	1.747E-1	ml*V
< 287	0.00	
w% :	100.00	
> 2326550	0.00	

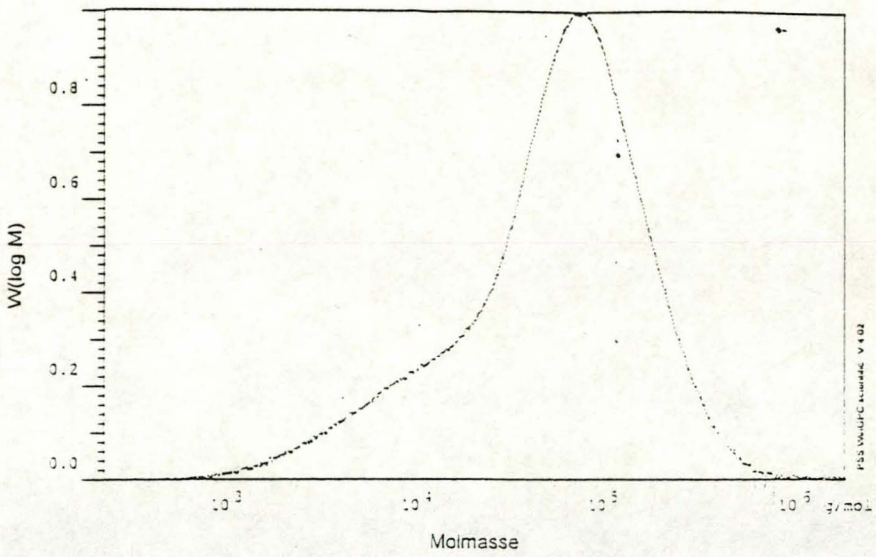

Propylene/1-pentene
Copolymers
Mg05
1.9% 1-pentene

RI 150C		
Mn :	7.222E+3	g/mol
Mw :	2.961E+4	g/mol
Mz :	5.116E+4	g/mol
Mv :	2.673E+4	g/mol
D :	4.100E+0	
[n]:	1.974E+1	ml/g
Vp :	4.108E+1	ml
Mp :	2.836E+4	g/mol
Fl :	1.708E-1	ml*V
< 85	0.00	
w% :	100.00	
> 253433	0.00	

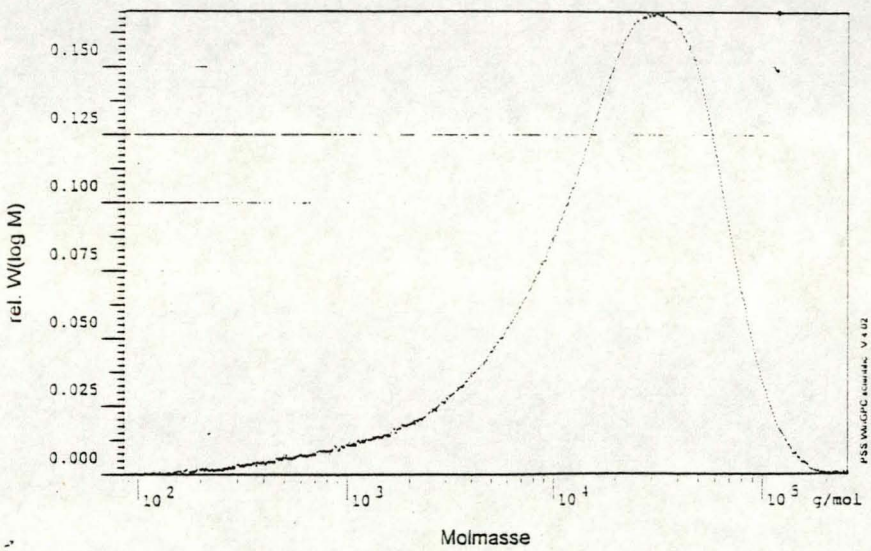

Mg02
3.8% 1-pentene

RI 150C		
Mn :	7.378E+3	g/mol
Mw :	2.665E+4	g/mol
Mz :	5.313E+4	g/mol
Mv :	2.361E+4	g/mol
D :	3.612E+0	
[n]:	1.806E+1	ml/g
Vp :	4.164E+1	ml
Mp :	2.282E+4	g/mol
Fl :	1.611E-1	ml*V
< 170	0.00	
w% :	100.00	
> 540533	0.00	

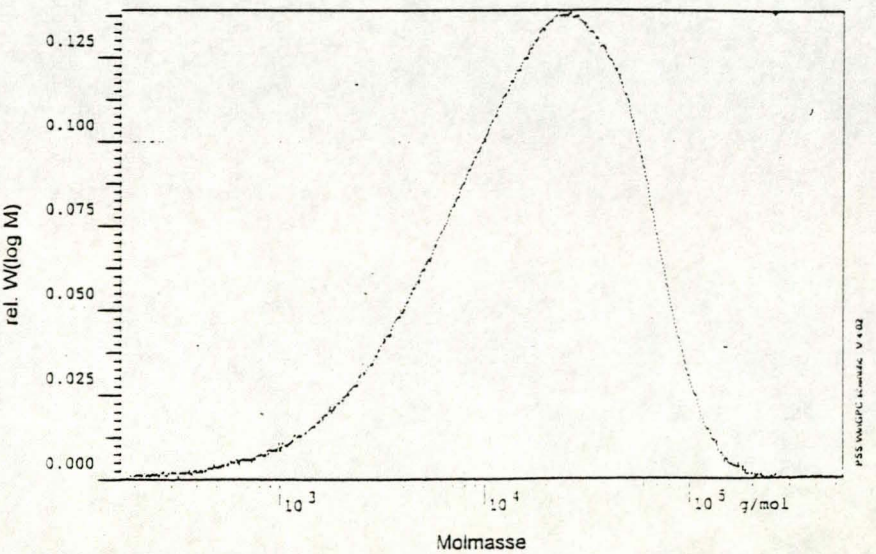

Mg01
13.7% 1-pentene

RI 150C		
Mn :	6.630E+3	g/mol
Mw :	3.098E+4	g/mol
Mz :	5.795E+4	g/mol
Mv :	2.769E+4	g/mol
D :	4.673E+0	
[n]:	2.025E+1	ml/g
Vo :	4.096E+1	ml
Mp :	2.373E+4	g/mol
FI :	1.719E-1	ml*V
< 70	0.00	
w% :	100.00	
> 662850	0.00	

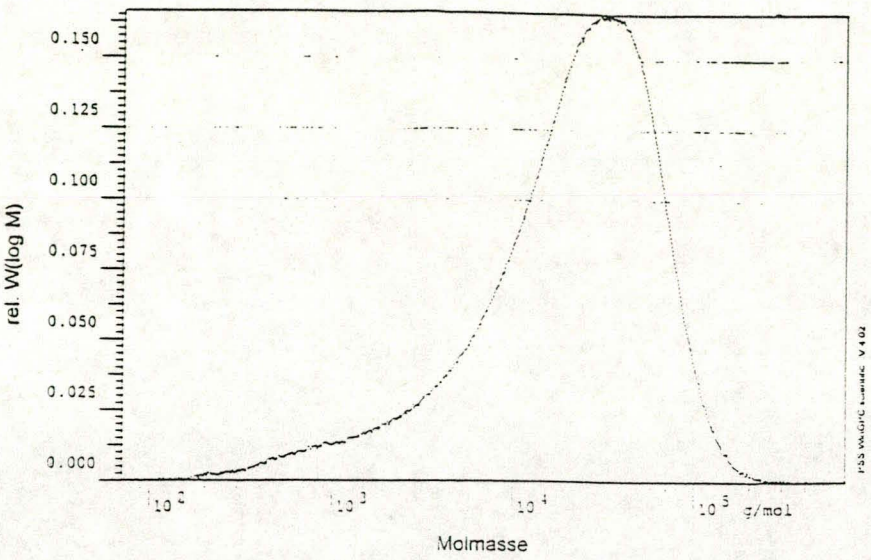

Mg33
0% 1-pentene

RI 150C		
Mn :	2.074E+4	g/mol
Mw :	4.705E+4	g/mol
Mz :	8.197E+4	g/mol
Mv :	4.300E+4	g/mol
D :	2.268E+0	
[n]:	2.772E+1	ml/g
Vo :	3.976E+1	ml
Mp :	4.728E+4	g/mol
FI :	1.470E-1	ml*V
< 893	0.00	
w% :	100.00	
> 554568	0.00	

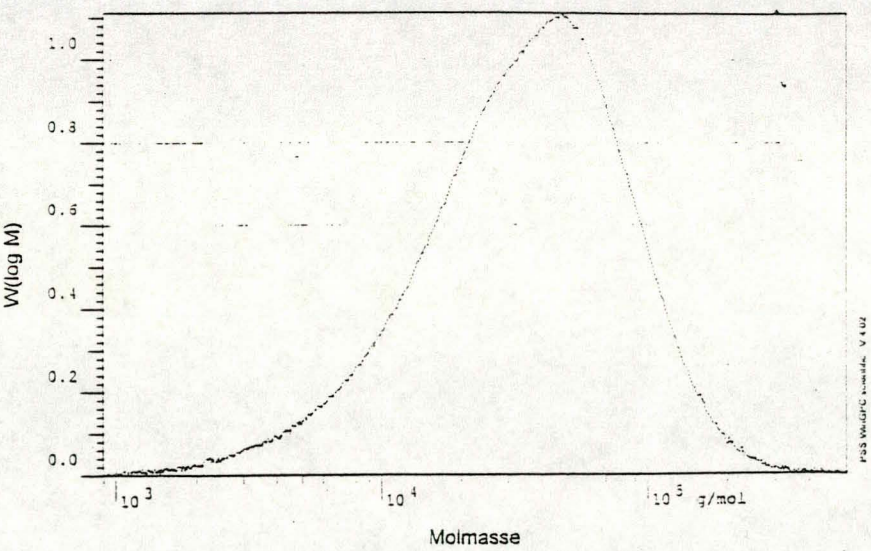

Mg36
2.1% 1-pentene

RI 150C		
Mn :	1.132E+4	g/mol
Mw :	3.405E+4	g/mol
Mz :	6.972E+4	g/mol
Mv :	3.038E+4	g/mol
D :	3.008E+0	
[n]:	2.163E+1	ml/g
Vo :	4.112E+1	ml
Mp :	2.800E+4	g/mol
FI :	1.576E-1	ml*V
< 123	0.00	
w% :	100.00	
> 571720	0.00	

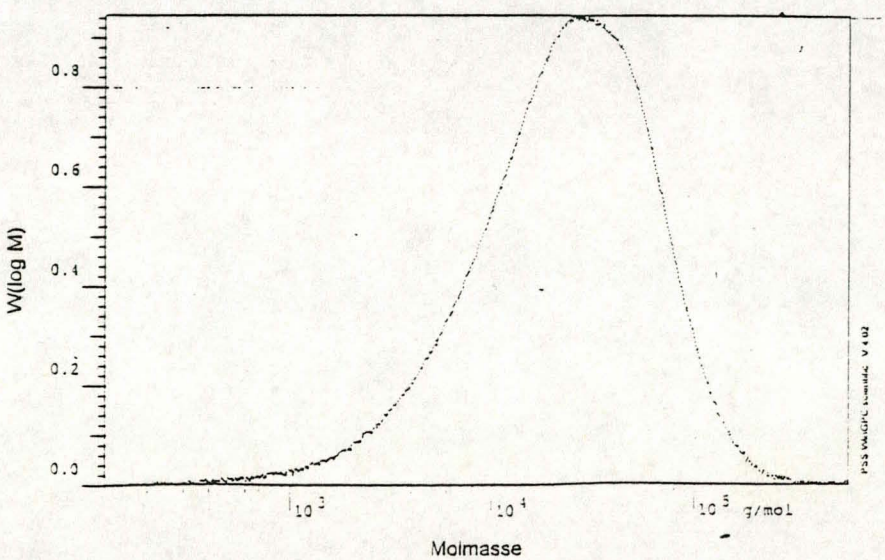

Mg14
2.7% 1-pentene

RI 150C

$\overline{Mn}$:	2.426E+4	g/mol
$\overline{Mw}$:	4.661E+4	g/mol
$\overline{Mz}$:	7.080E+4	g/mol
$\overline{Mv}$:	4.354E+4	g/mol
$\overline{D}$:	1.921E+0	
[n]:	2.797E+1	ml/g
Vp :	4.000E+1	ml
Mp :	4.951E+4	g/mol
FI :	1.570E-1	ml*V
< 618	0.00	
w% :	100.00	
> 692527	0.00	

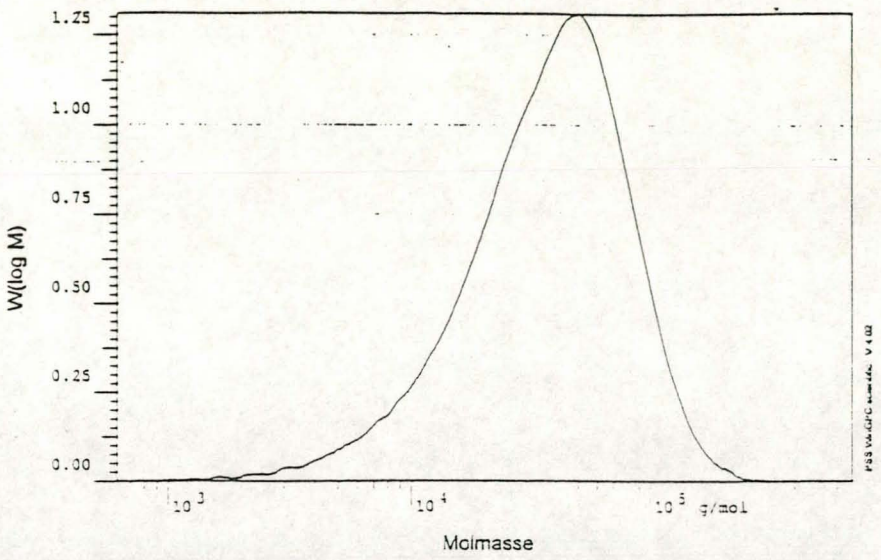

Mg34
8.7% 1-pentene

RI 150C

$\overline{Mn}$:	1.477E+4	g/mol
$\overline{Mw}$:	3.323E+4	g/mol
$\overline{Mz}$:	5.431E+4	g/mol
$\overline{Mv}$:	3.063E+4	g/mol
$\overline{D}$:	2.249E+0	
[n]:	2.176E+1	ml/g
Vp :	4.087E+1	ml
Mp :	3.074E+4	g/mol
FI :	1.517E-1	ml*V
< 300	0.00	
w% :	100.00	
> 360815	0.00	

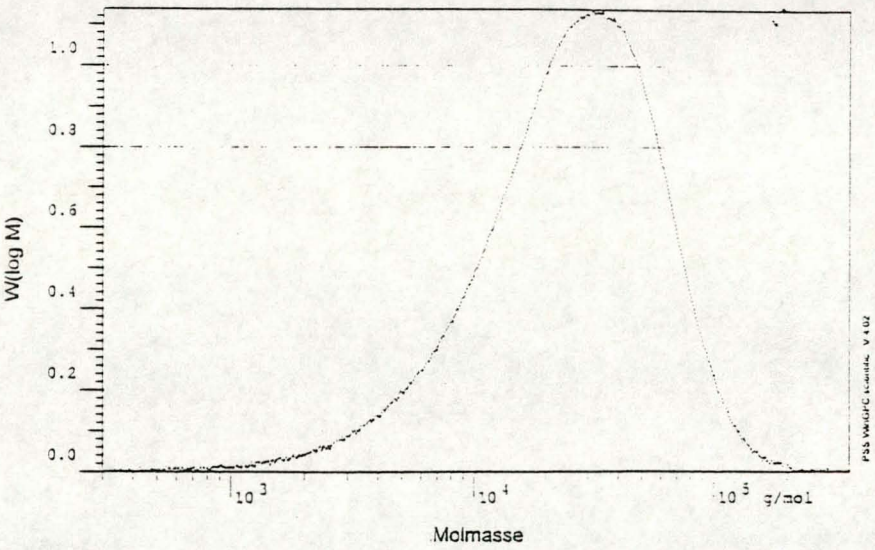

Mg35
7.1% 1-pentene

RI 150C

$\overline{Mn}$:	2.307E+4	g/mol
$\overline{Mw}$:	4.901E+4	g/mol
$\overline{Mz}$:	7.648E+4	g/mol
$\overline{Mv}$:	4.553E+4	g/mol
$\overline{D}$:	2.124E+0	
[n]:	2.888E+1	ml/g
Vp :	3.966E+1	ml
Mp :	4.917E+4	g/mol
FI :	1.590E-1	ml*V
< 320	0.00	
w% :	100.00	
> 655345	0.00	

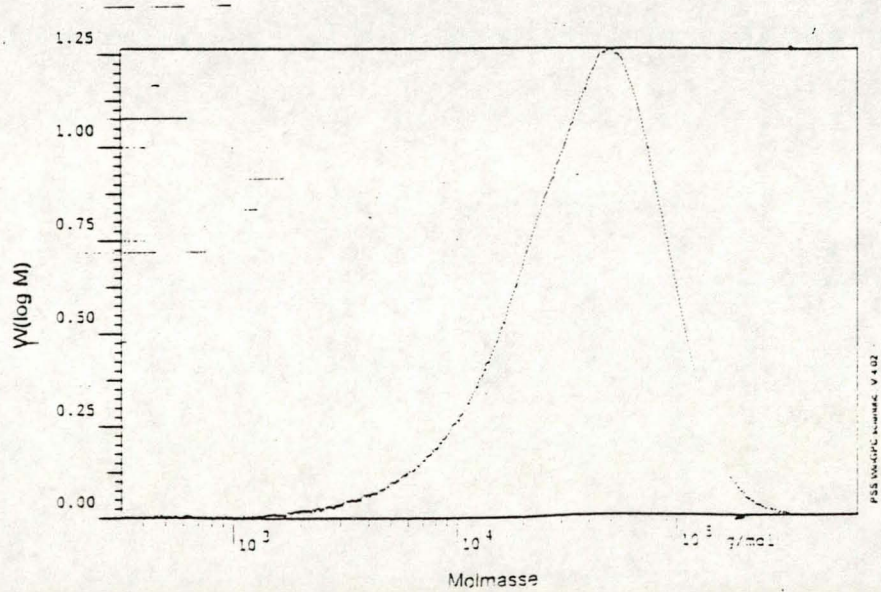

Mg37
0% 1-pentene

RI 150C		
$\overline{Mn}$:	2.649E+4	g/mol
$\overline{Mw}$:	5.730E+4	g/mol
$\overline{Mz}$:	9.604E+4	g/mol
$\overline{Mv}$:	5.277E+4	g/mol
$\overline{D}$:	2.163E+0	
[n]:	3.208E+1	ml/g
Vp :	3.938E+1	ml
Mp :	5.482E+4	g/mol
FI :	1.410E-1	ml*V
< 845	0.00	
w% :	100.00	
> 848467	0.00	

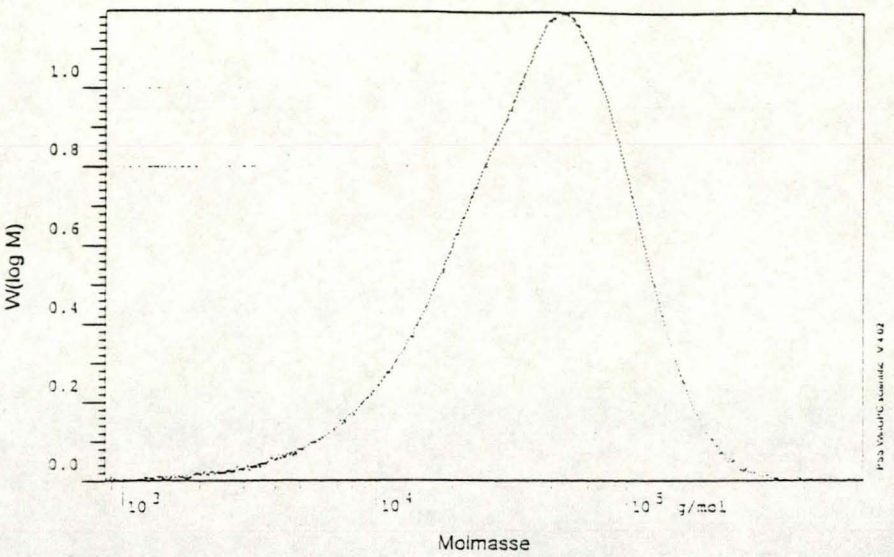

Mg41
0.5% 1-pentene

RI 150C		
$\overline{Mn}$:	4.158E+3	g/mol
$\overline{Mw}$:	1.923E+4	g/mol
$\overline{Mz}$:	5.327E+4	g/mol
$\overline{Mv}$:	1.609E+4	g/mol
$\overline{D}$:	4.625E+0	
[n]:	1.374E+1	ml/g
Vp :	4.370E+1	ml
Mp :	1.027E+4	g/mol
FI :	1.645E-1	ml*V
< 102	0.00	
w% :	100.00	
> 348805	0.00	

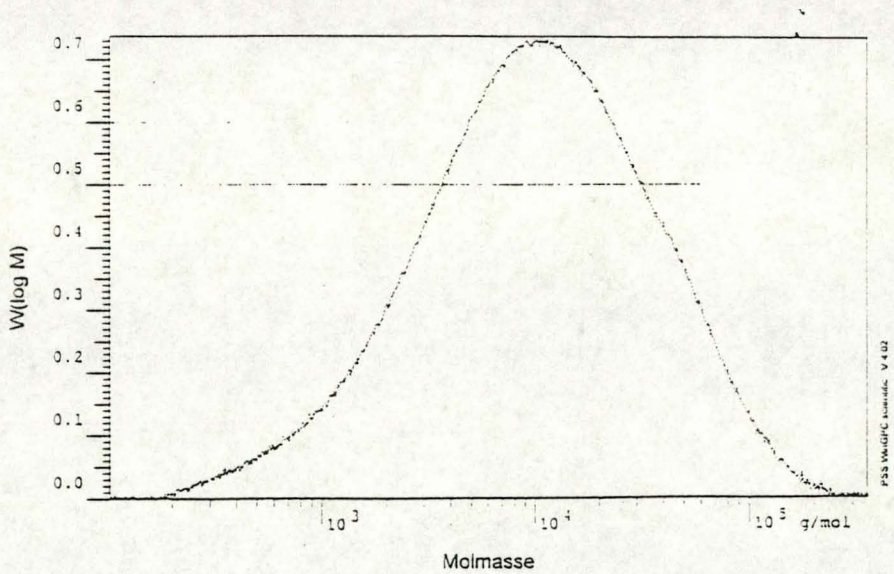

Mg39
0.8% 1-pentene

RI 150C		
$\overline{Mn}$:	8.778E+3	g/mol
$\overline{Mw}$:	2.271E+4	g/mol
$\overline{Mz}$:	4.784E+4	g/mol
$\overline{Mv}$:	2.047E+4	g/mol
$\overline{D}$:	2.587E+0	
[n]:	1.632E+1	ml/g
Vp :	4.216E+1	ml
Mp :	2.152E+4	g/mol
FI :	1.823E-1	ml*V
< 192	0.00	
w% :	100.00	
> 535710	0.00	

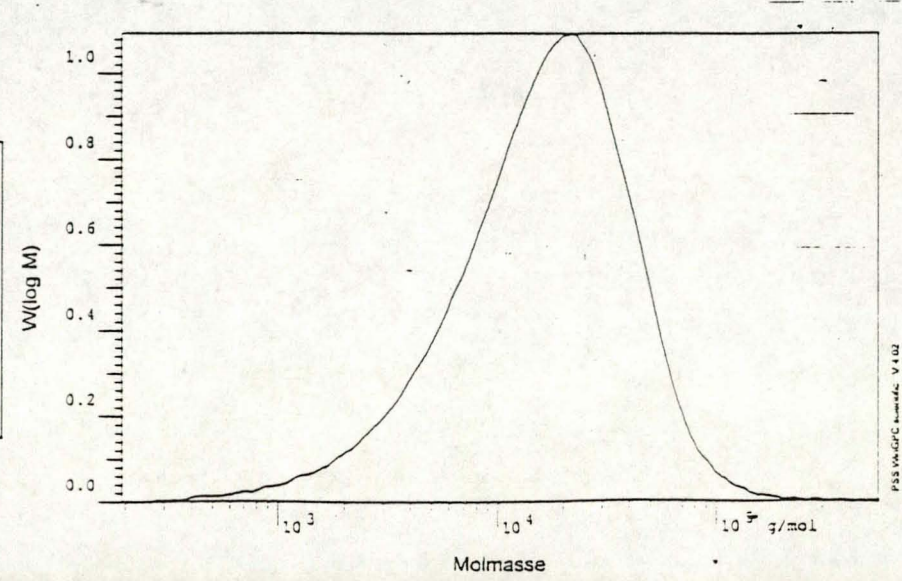

Mg38
4.4% 1-pentene

RI 150C		
$\overline{Mn}$:	7.406E+3	g/mol
$\overline{Mw}$:	2.403E+4	g/mol
$\overline{Mz}$:	4.689E+4	g/mol
$\overline{Mv}$:	2.154E+4	g/mol
D :	3.245E+0	
[n]:	1.692E+1	ml/g
Vo :	4.190E+1	ml
Mp :	2.069E+4	g/mol
Fl :	1.565E-1	ml*V
< 92	0.00	
w% :	100.00	
> 361892	0.00	

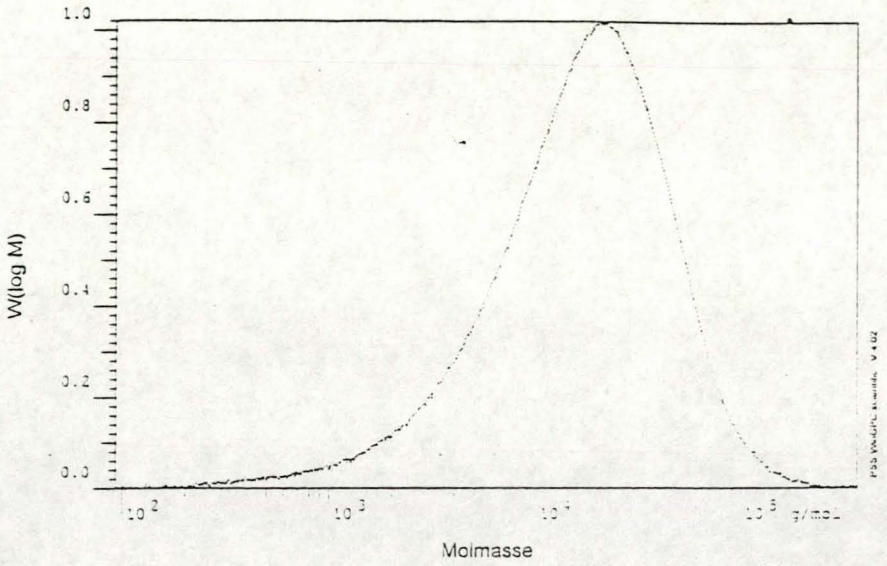

Mg40
9.9% 1-pentene

RI 150C		
$\overline{Mn}$:	9.952E+3	g/mol
$\overline{Mw}$:	2.559E+4	g/mol
$\overline{Mz}$:	4.965E+4	g/mol
$\overline{Mv}$:	2.320E+4	g/mol
D :	2.572E+0	
[n]:	1.784E+1	ml/g
Vo :	4.162E+1	ml
Mp :	2.307E+4	g/mol
Fl :	1.562E-1	ml*V
< 128	0.00	
w% :	100.00	
> 568704	0.00	

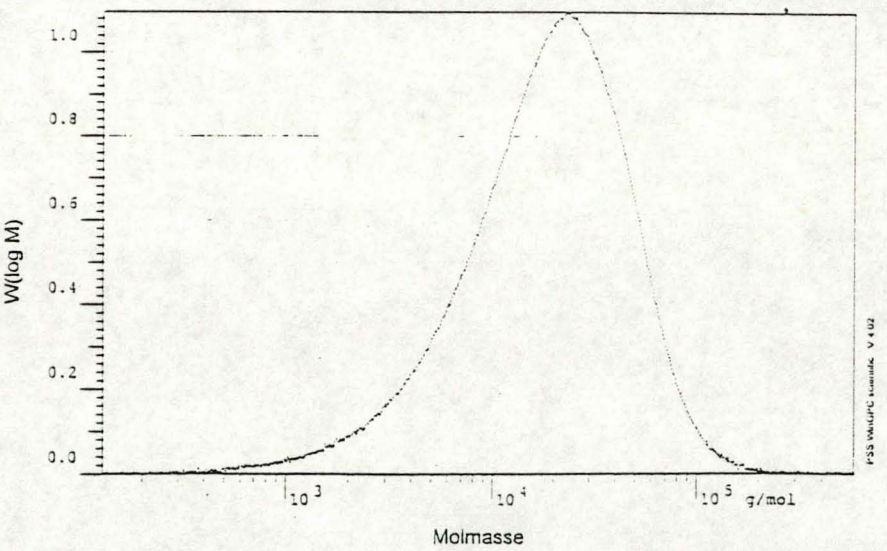

APPENDIX C
(IR Curves)

Ethylene/1-pentene
Copolymers
EtPn1
1.5% 1-pentene

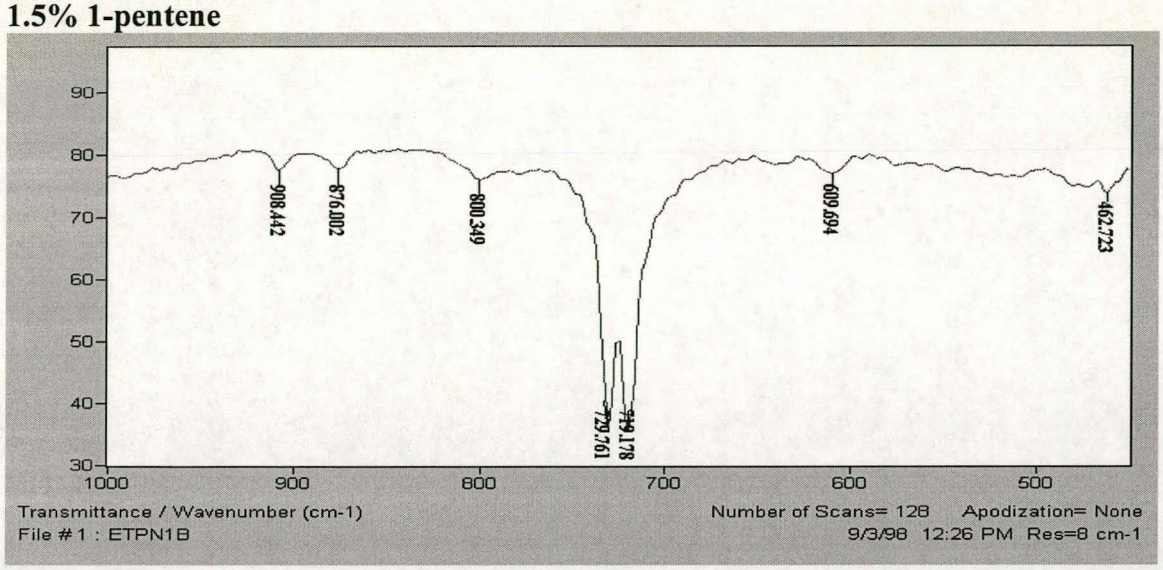

EtPn4
5.2% 1-pentene

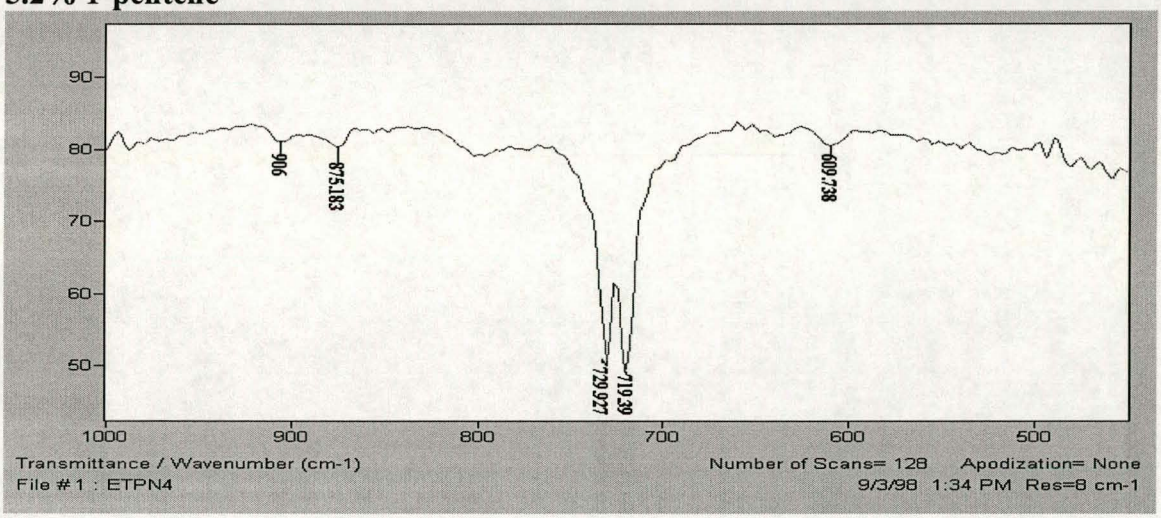

EtPn10
2.6% 1-pentene

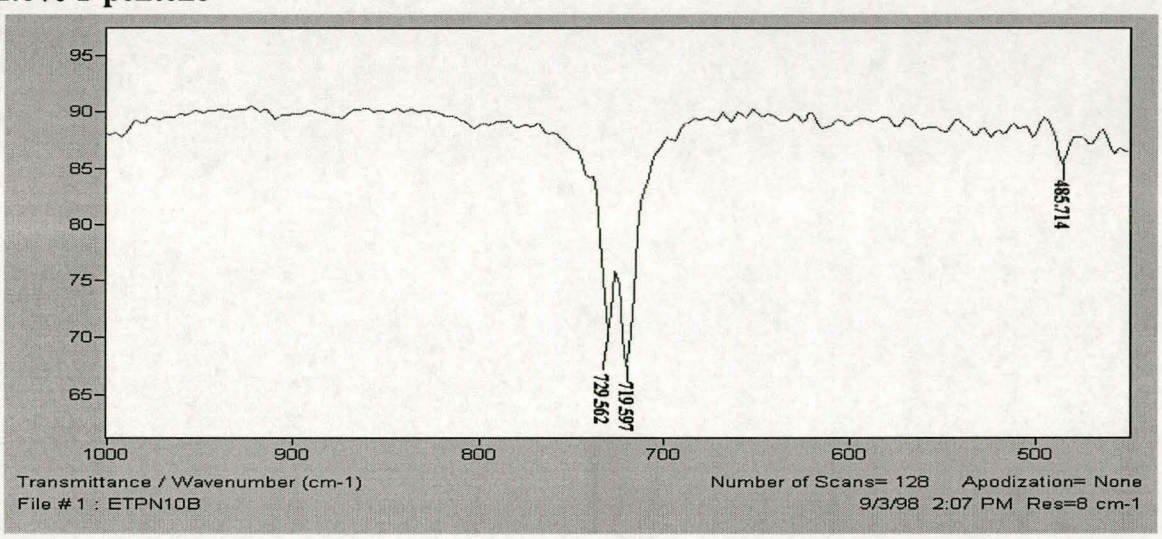

EtPn20
45.3% 1-pentene

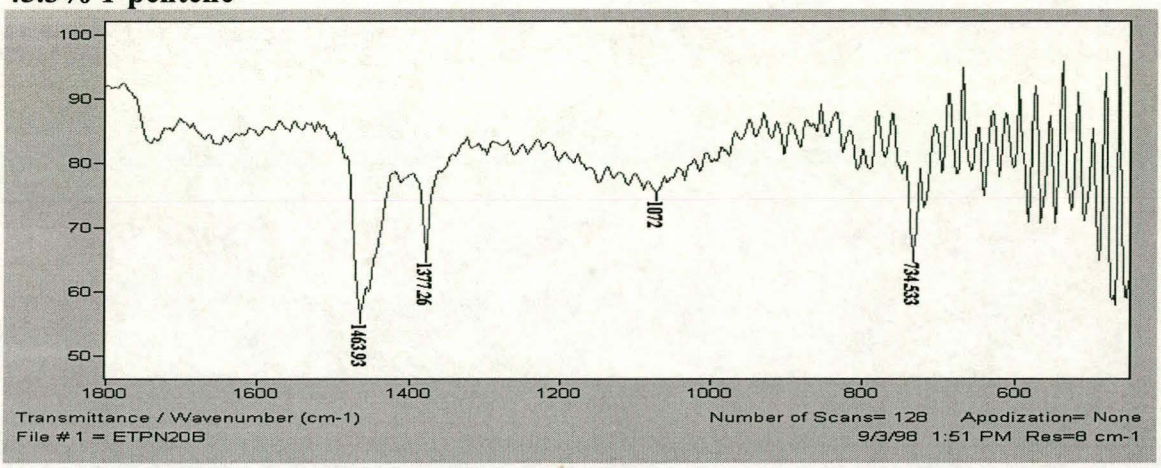

Propylene/1-pentene
Copolymers
Mg05
1.9% 1-pentene

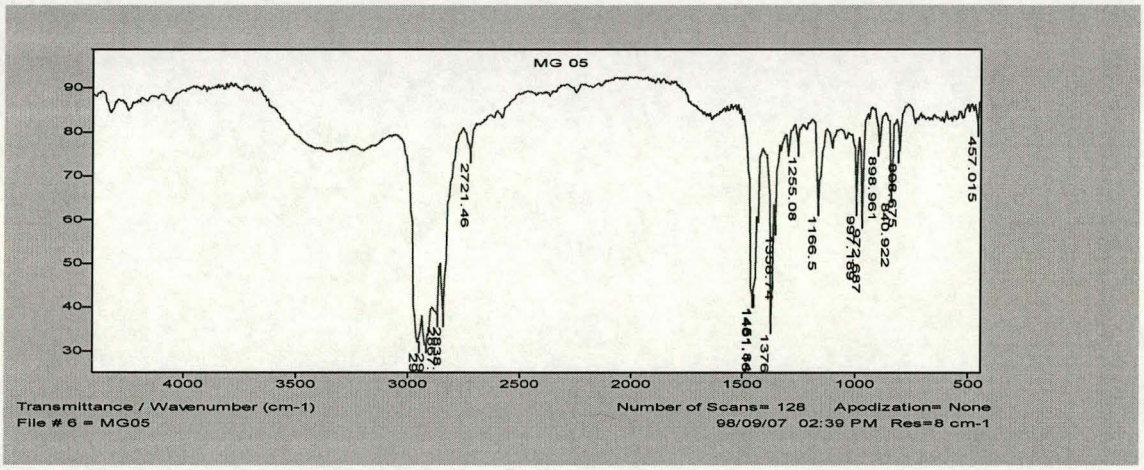

Mg02
3.8% 1-pentene

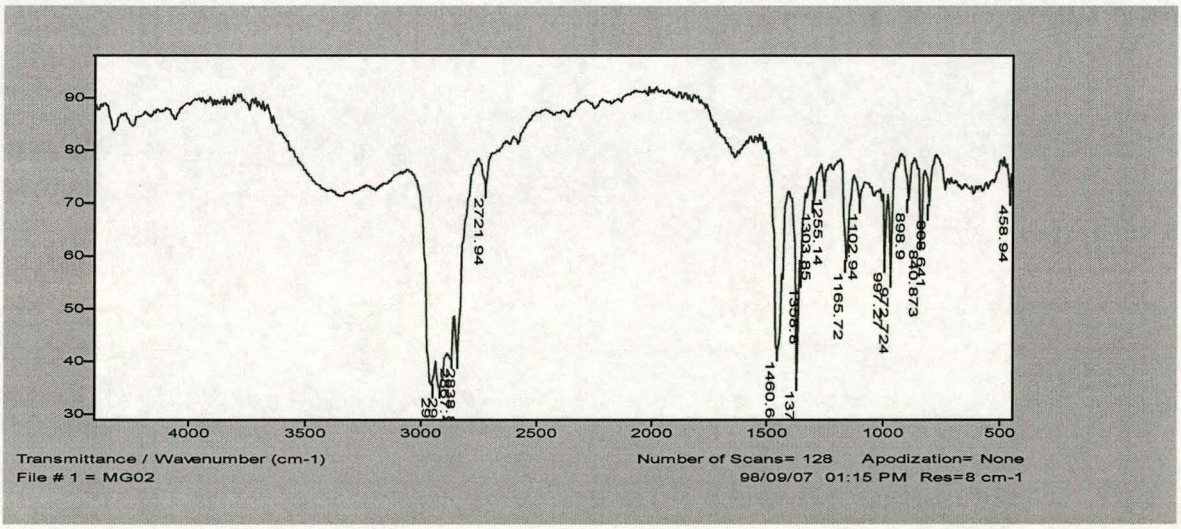

Mg01
13.7% 1-pentene

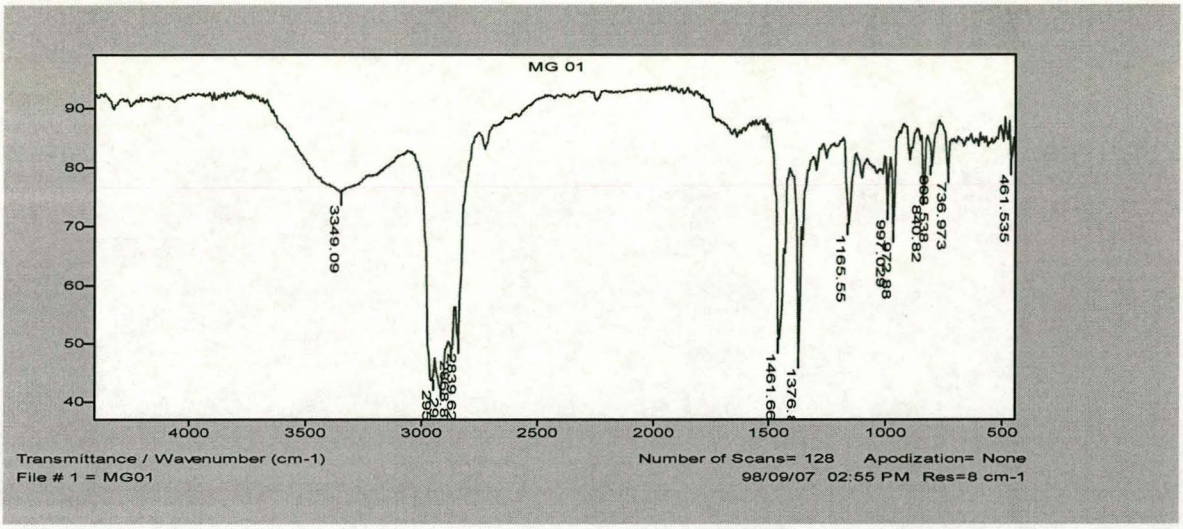

Mg33
0% 1-pentene

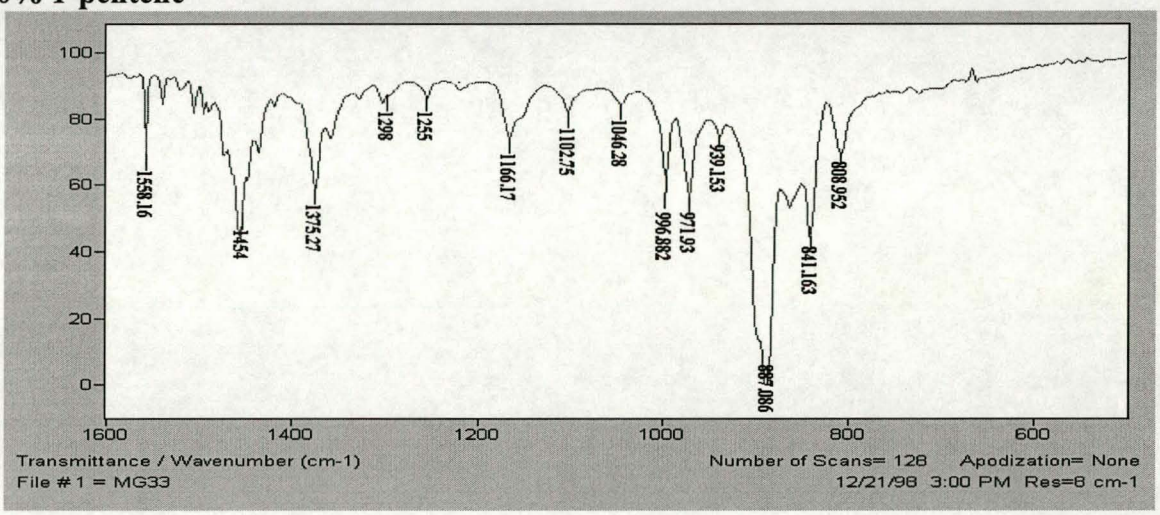

Mg36
2.1% 1-pentene

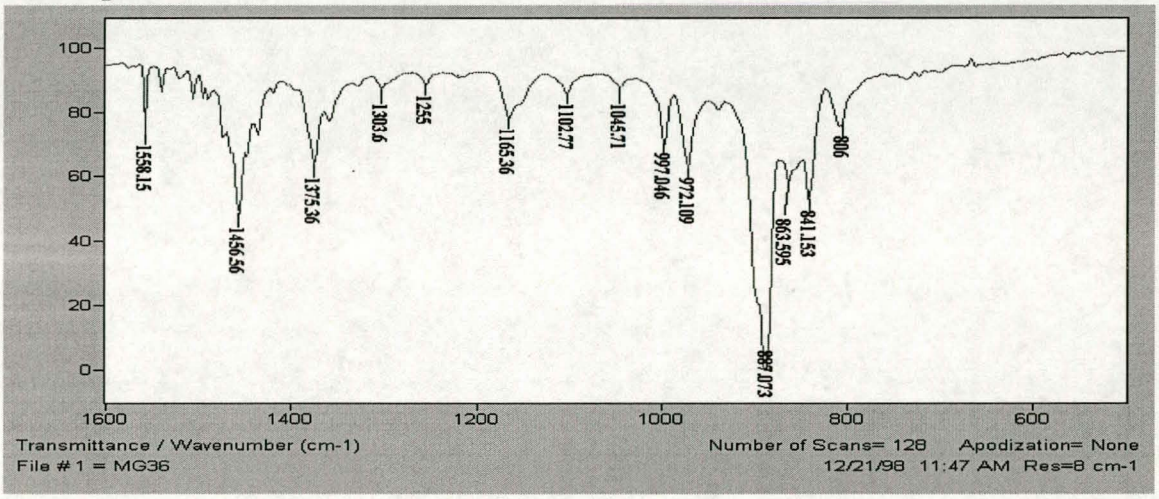

Mg14
2.7% 1-pentene

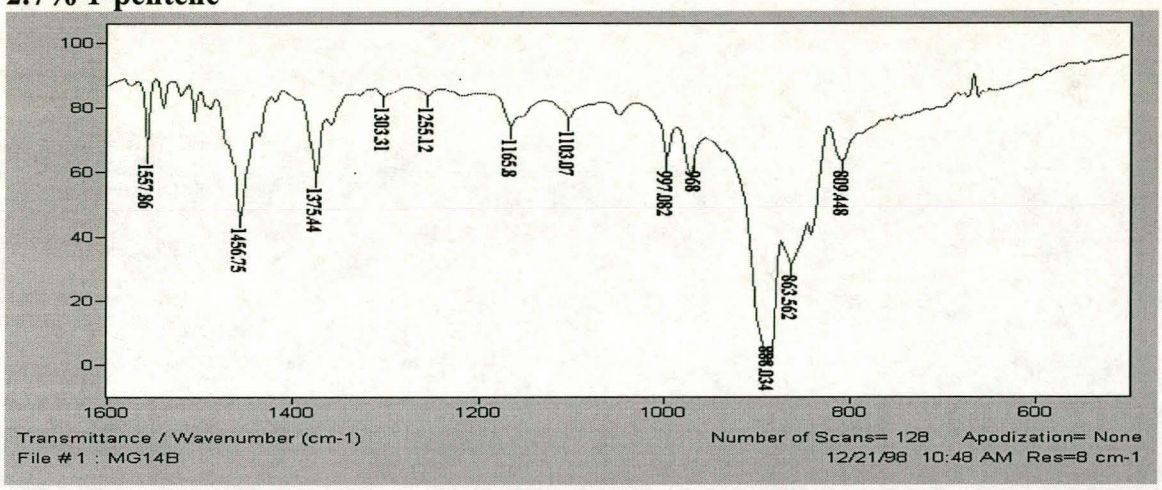

Mg34
8.7% 1-pentene

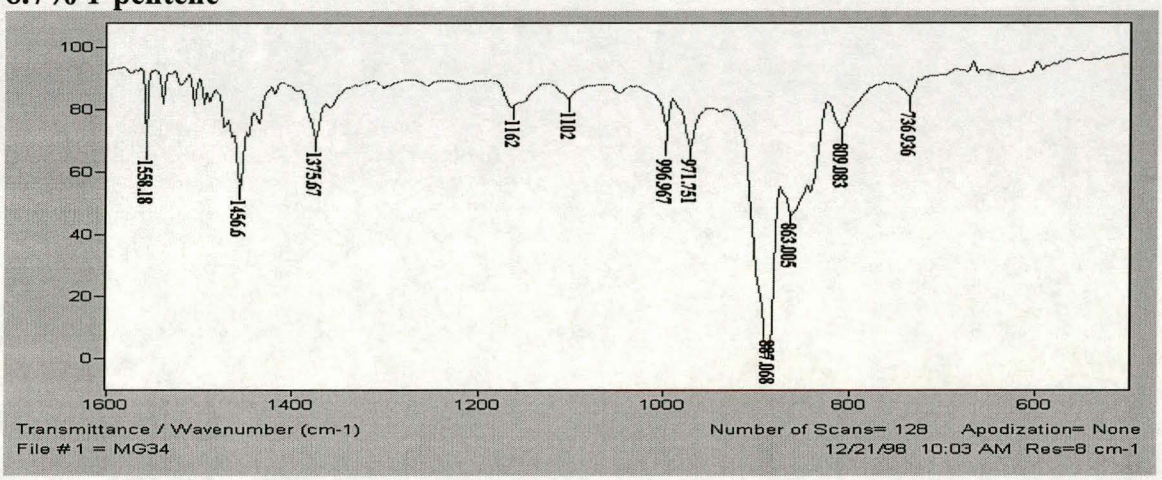

Mg35
7.1% 1-pentene

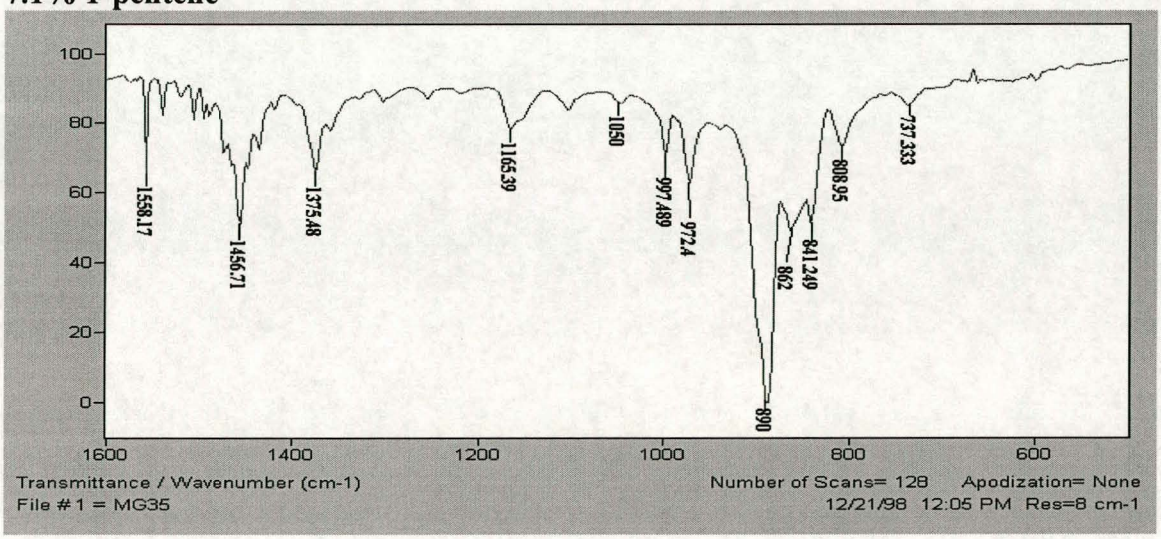

Mg37
0% 1-pentene

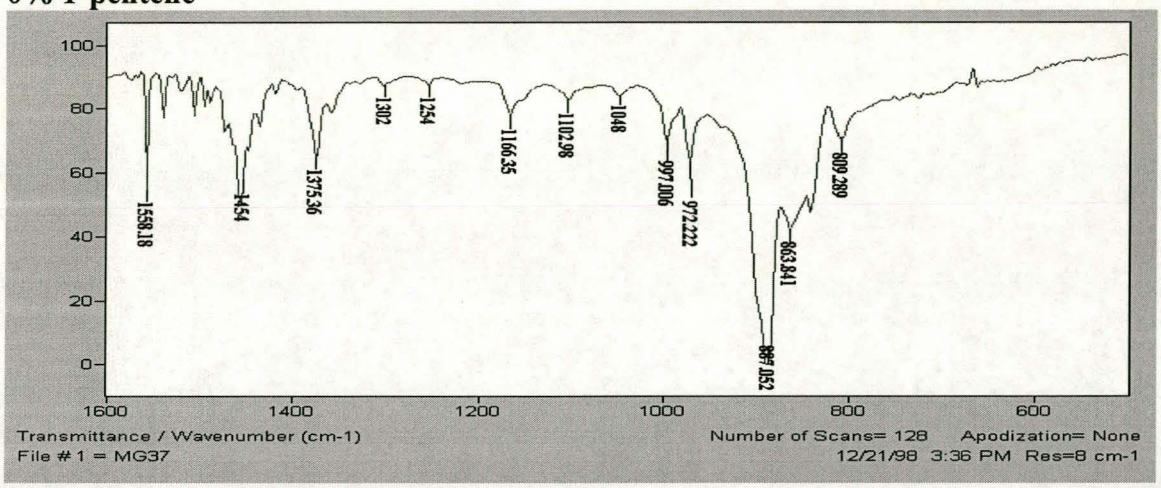

Mg41
0.5% 1-pentene

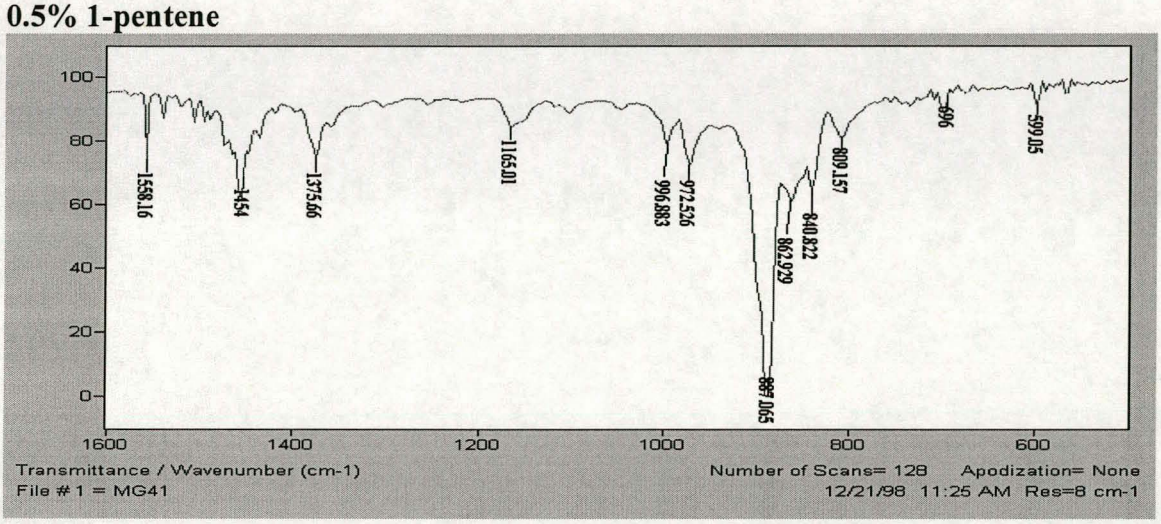

Mg39
0.8% 1-pentene

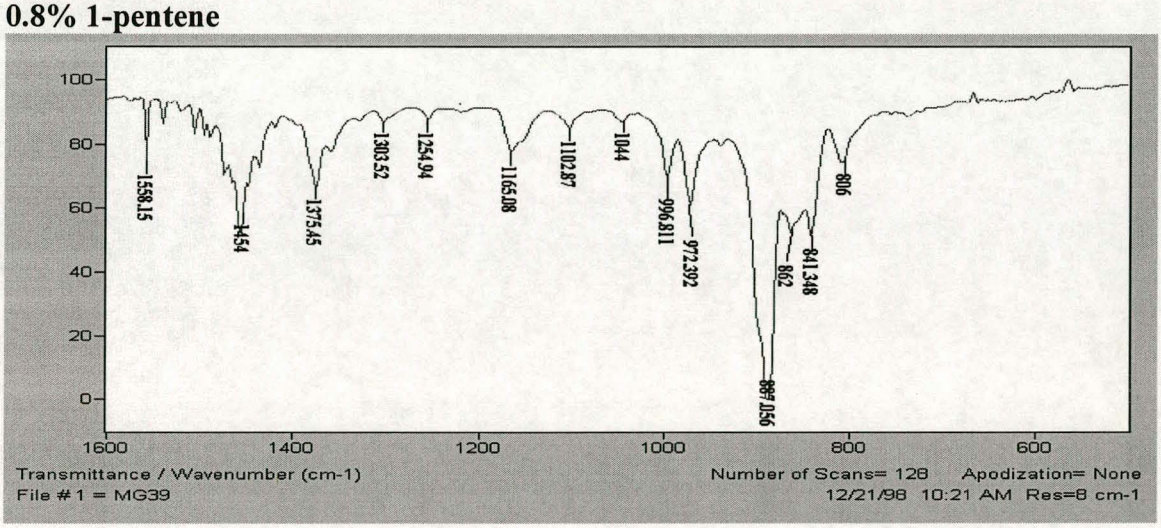

Mg38
4.4% 1-pentene

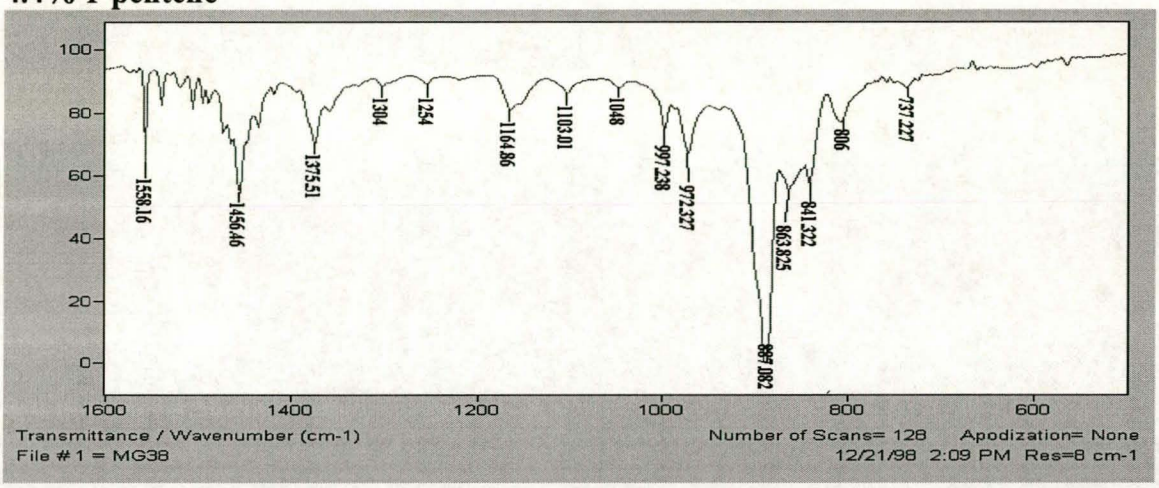

Mg40
9.9% 1-pentene

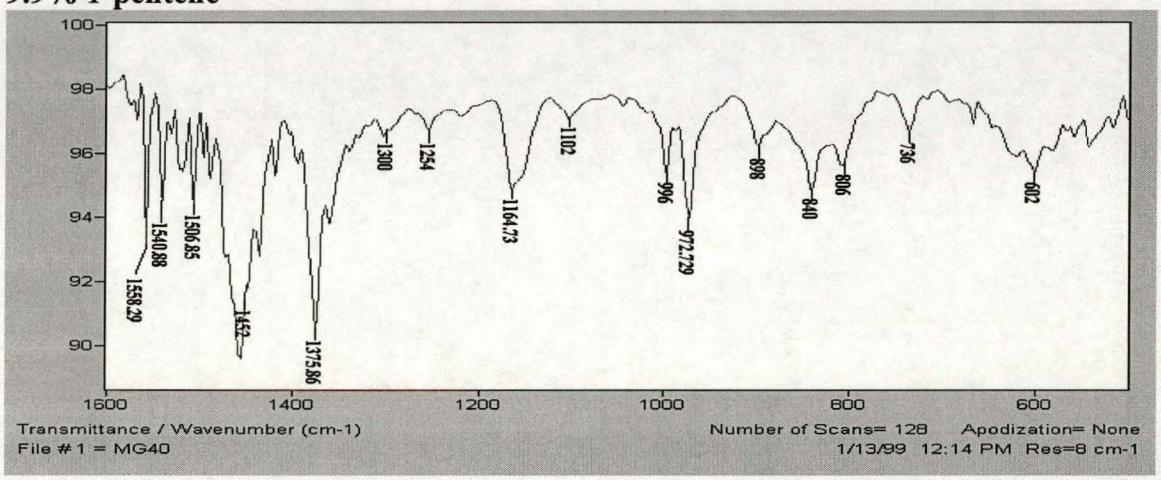

PP80
3.8% 1-pentene

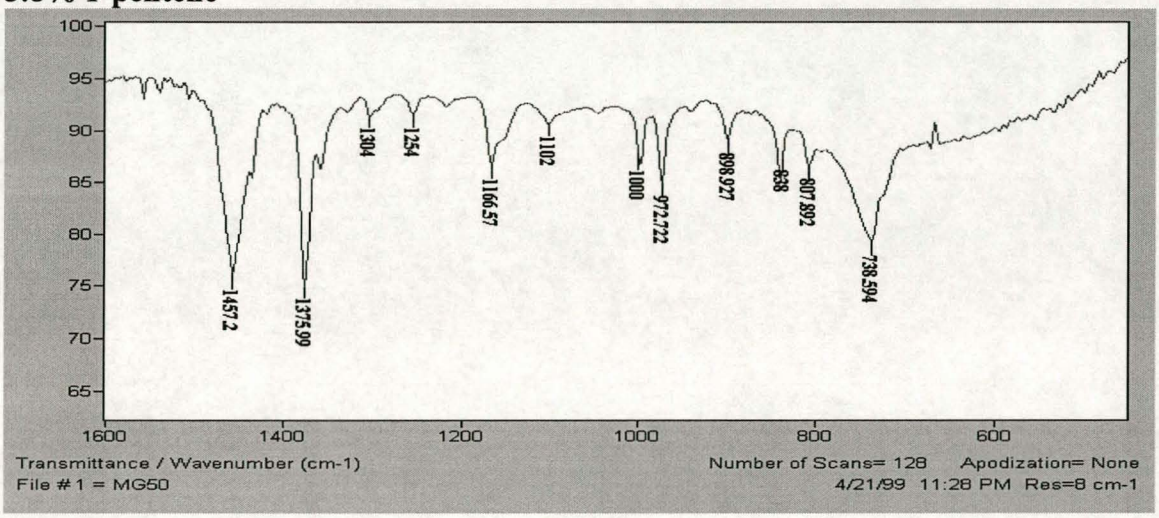

PP25
3.5% 1-pentene

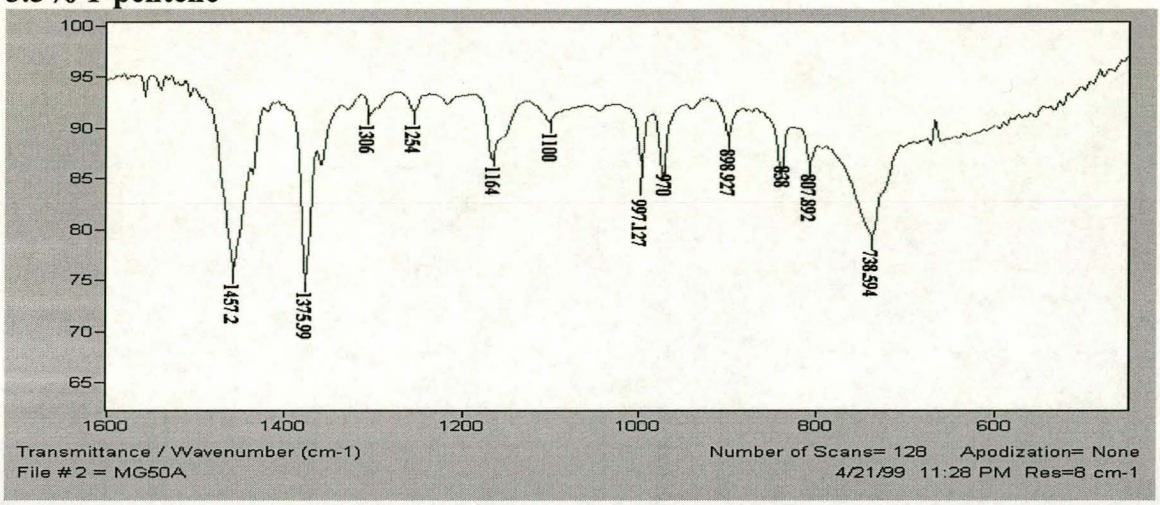

PP8
2.8% 1-pentene

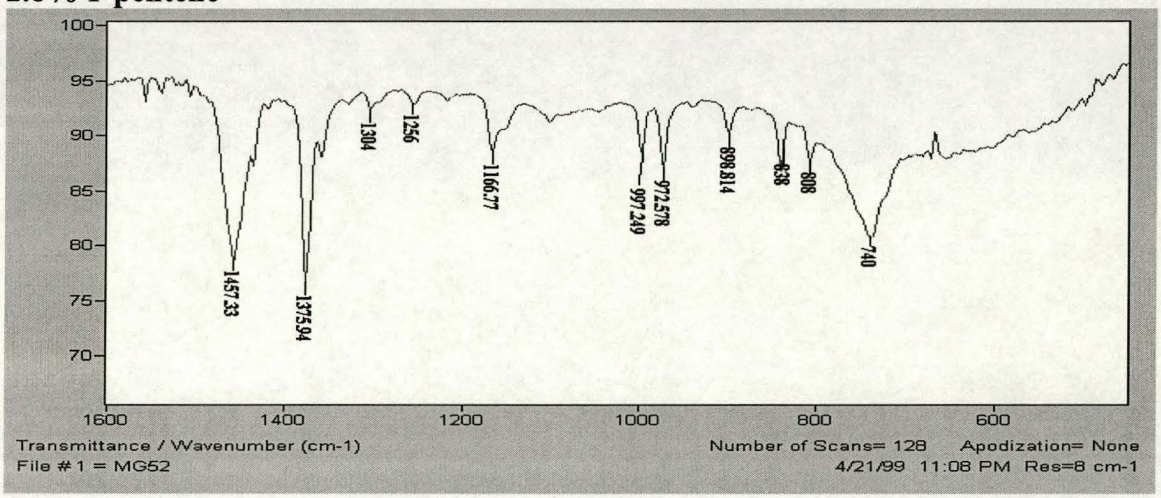

PP40
2.5% 1-pentene

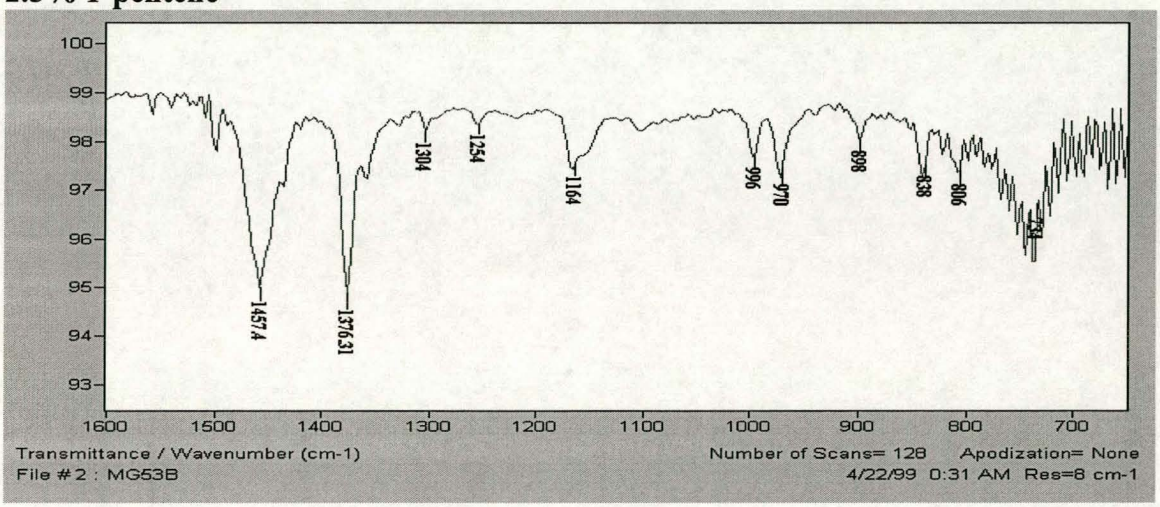

APPENDIX D
(^{13}C NMR Curves)

Ethylene/1-pentene
Copolymers
EtPn1
1.5% 1-pentene

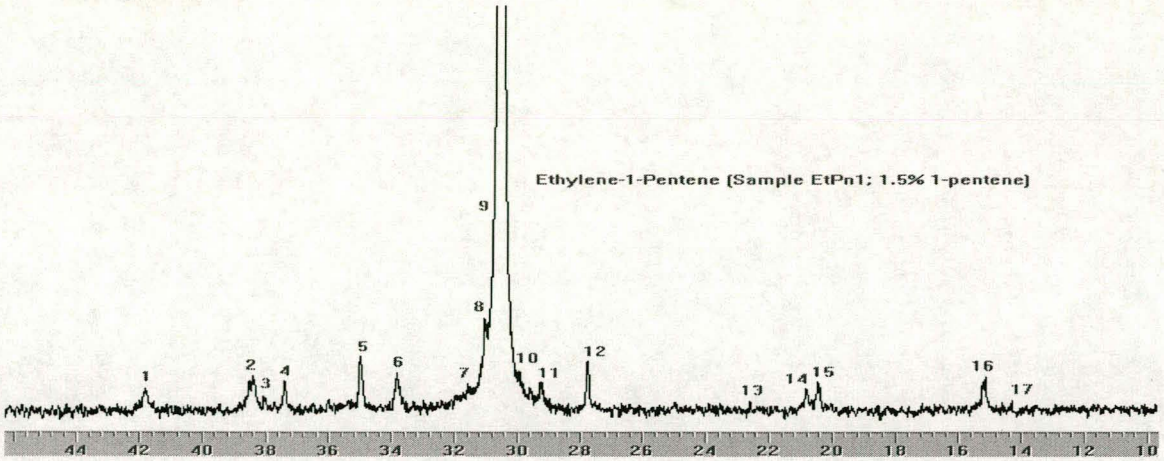

EtPn4
5.2% 1-pentene

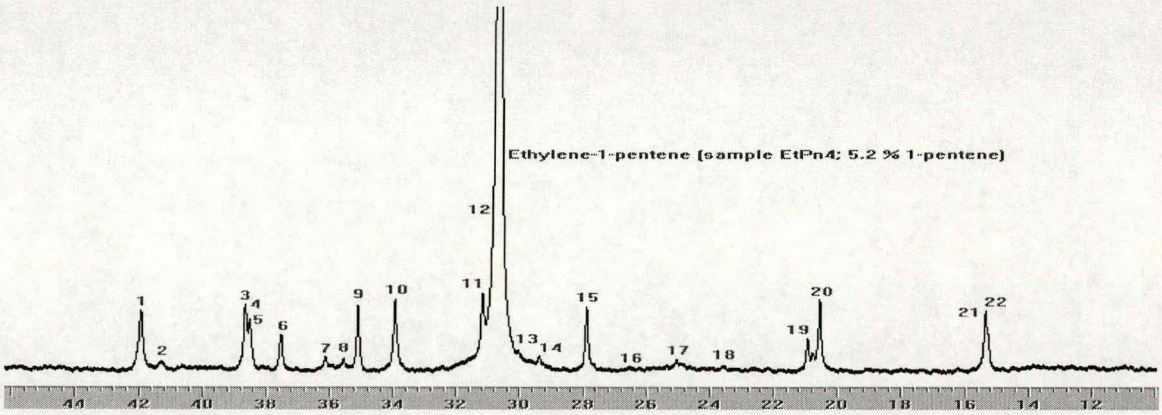

EtPn10
2.6% 1-pentene

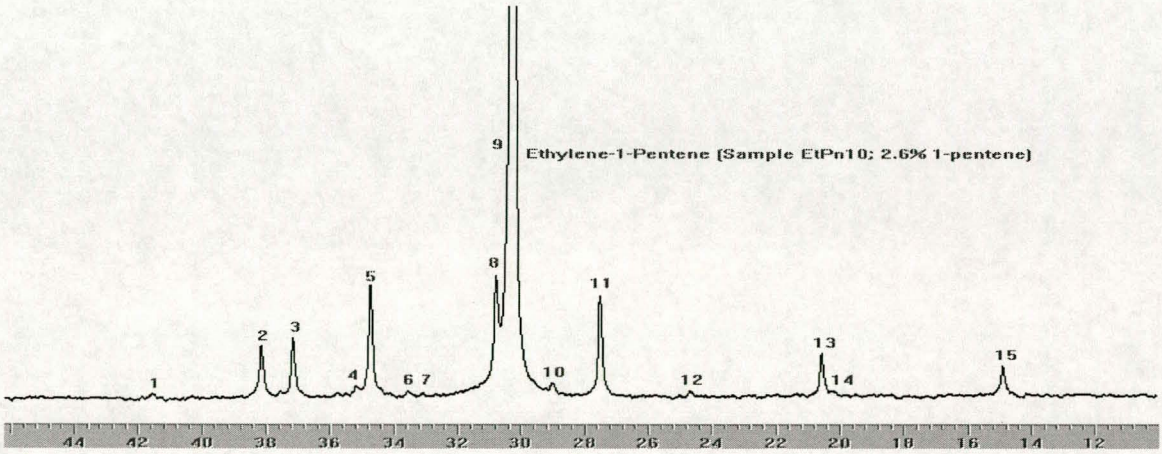

EtPn20
45.3% 1-pentene

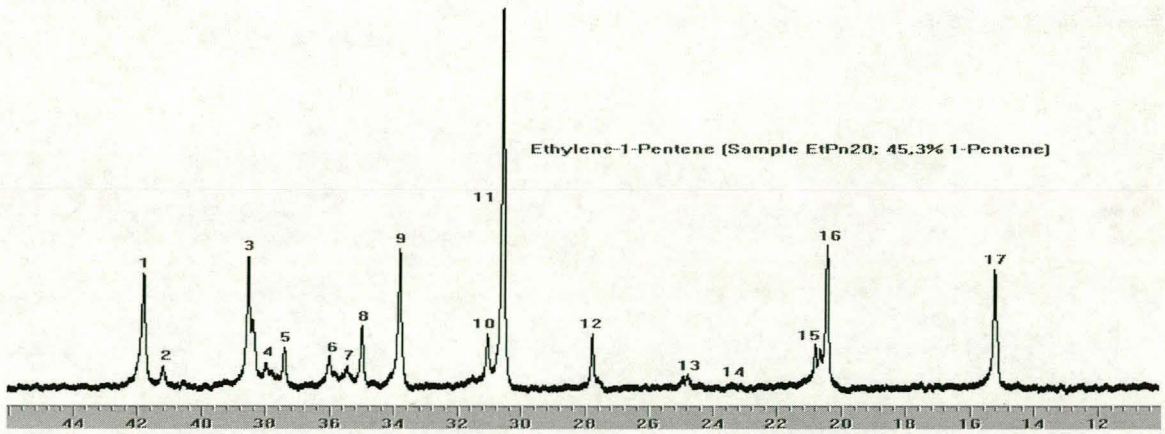

Propylene/1-pentene Copolymers

Mg05
1.9% 1-pentene

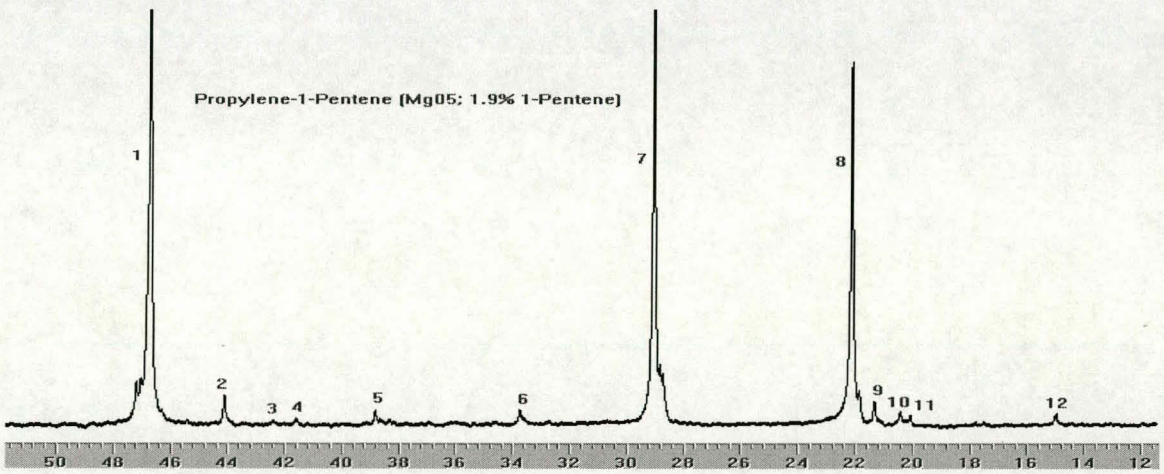

Mg04
3.8% 1-pentene

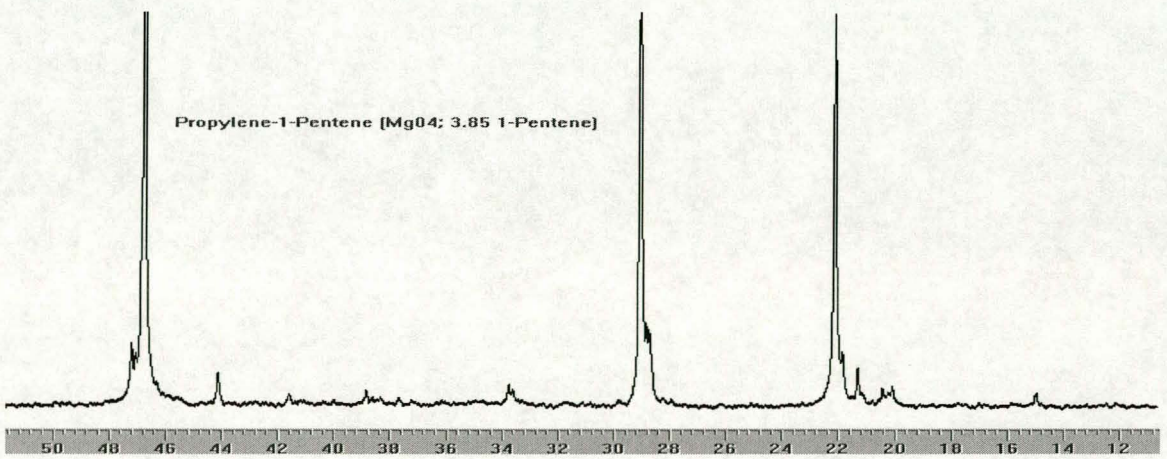

Mg01
13.7% 1-pentene

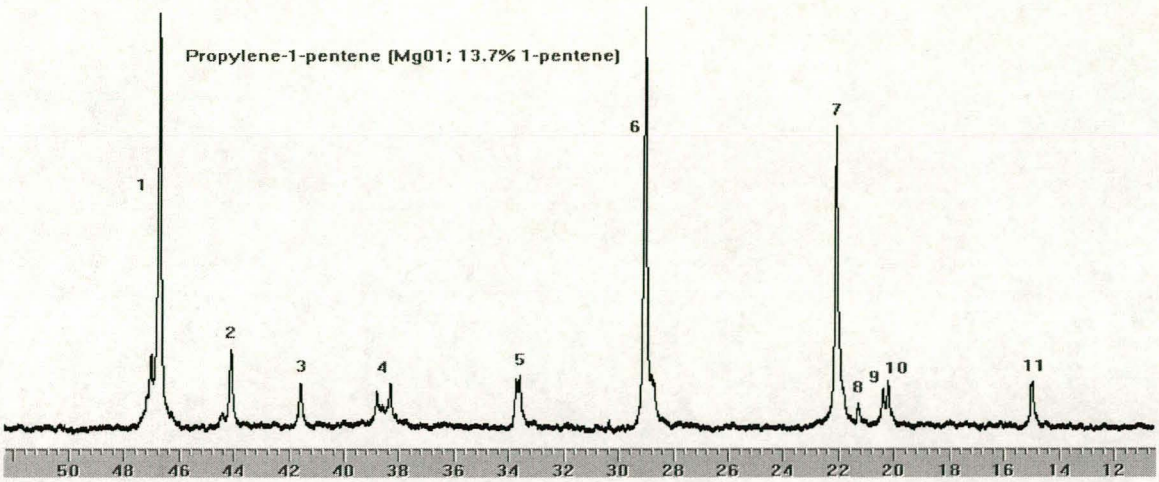

Mg14
2.7% 1-pentene

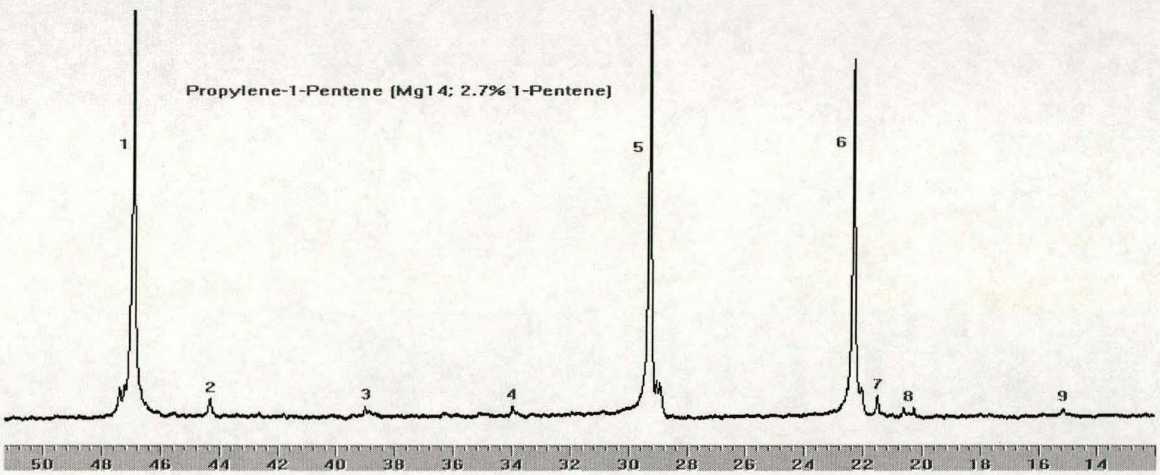

Mg34
8.7% 1-pentene

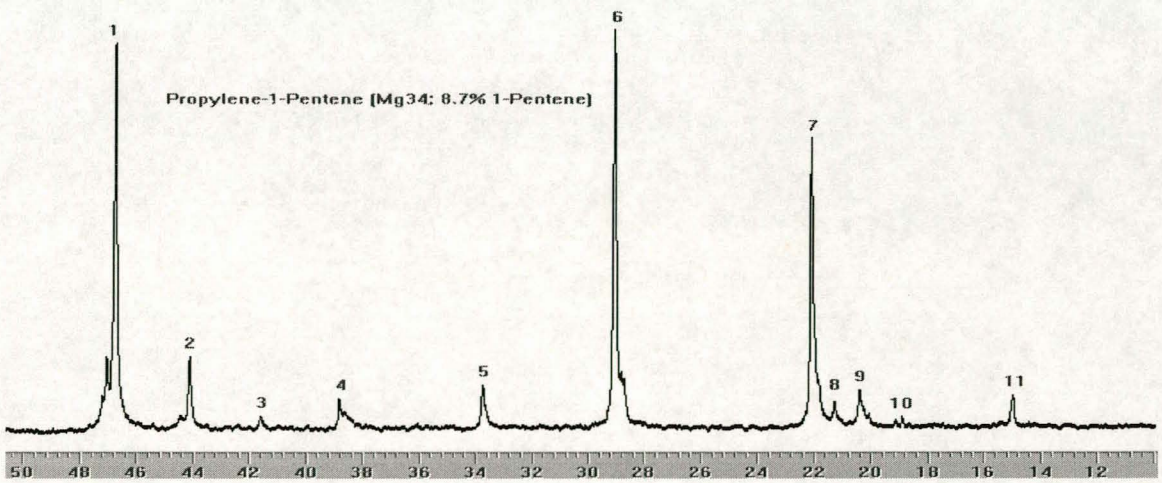

Mg35
7.1% 1-pentene

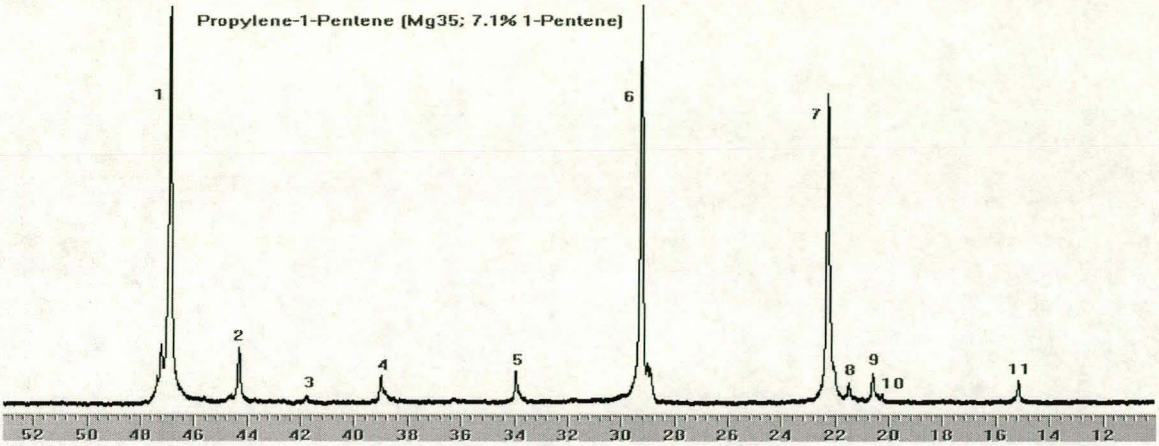

Mg37
0% 1-pentene

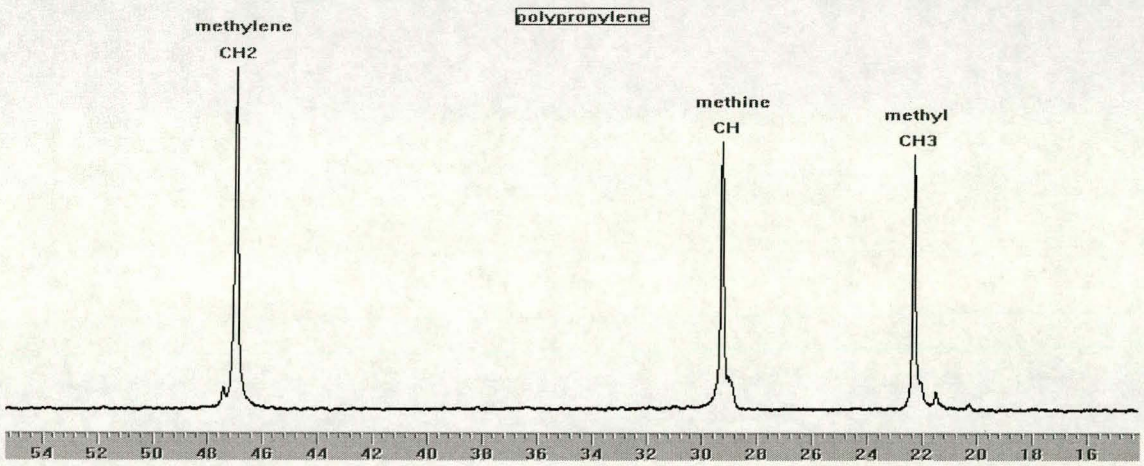

Mg41
0.5% 1-pentene

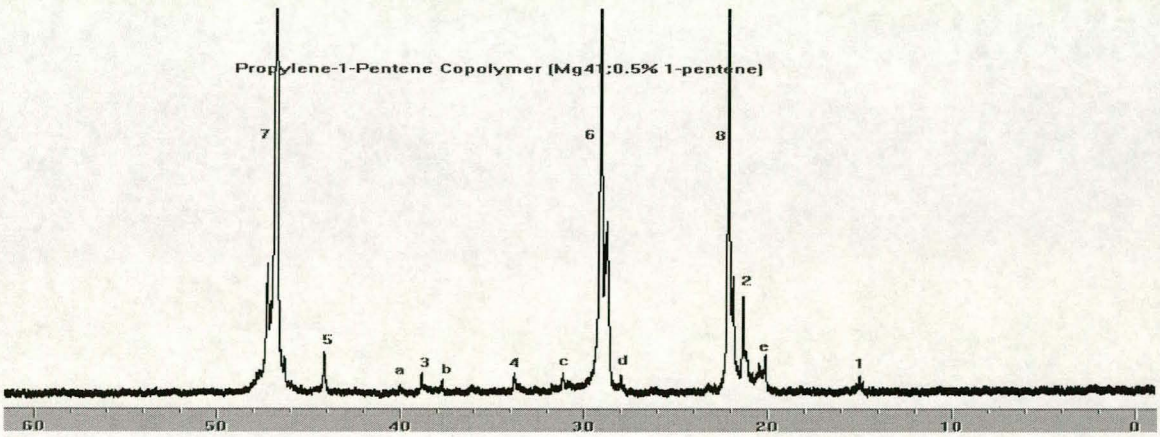

Mg39
0.8% 1-pentene

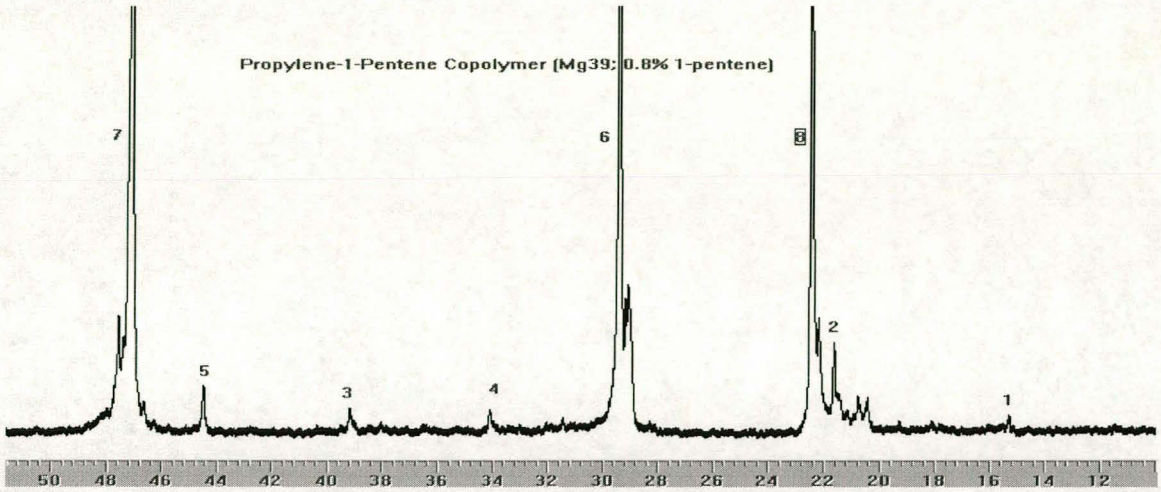

Mg38
4.4% 1-pentene

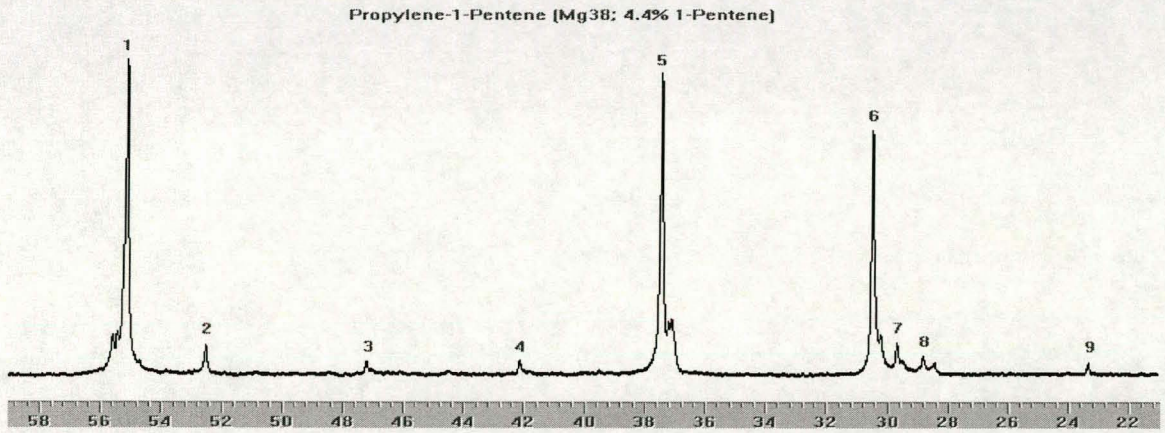

Mg40
9.9% 1-pentene

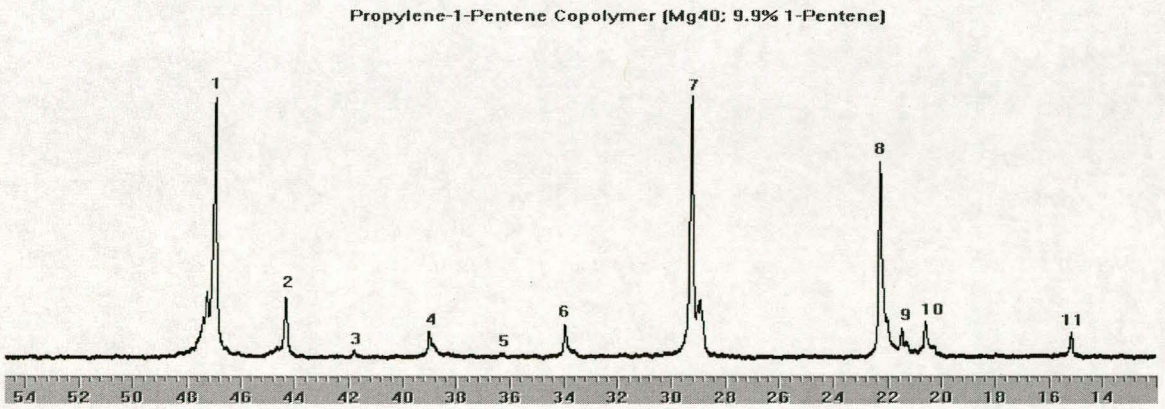

PP80
3.8% 1-pentene

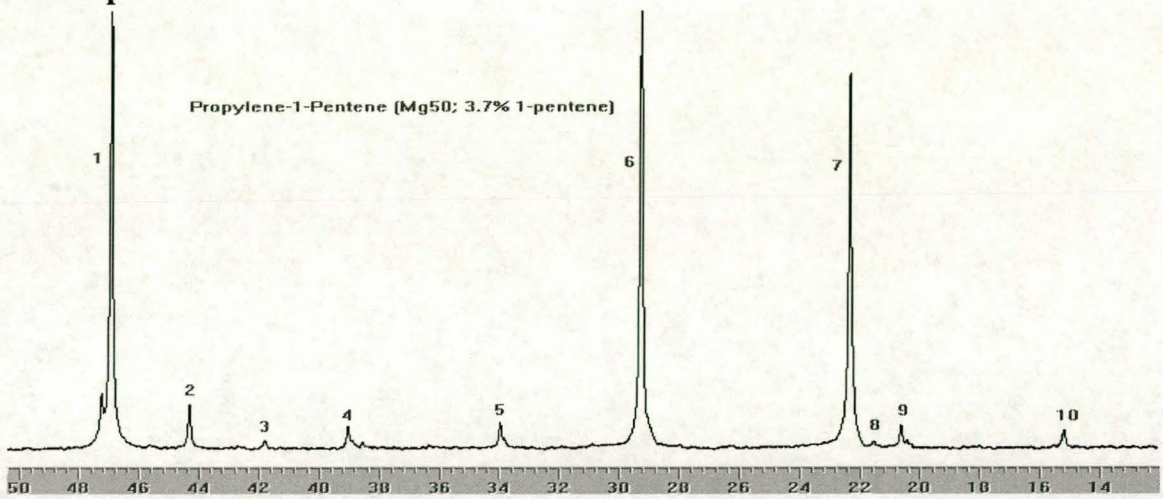

PP25
3.5% 1-pentene

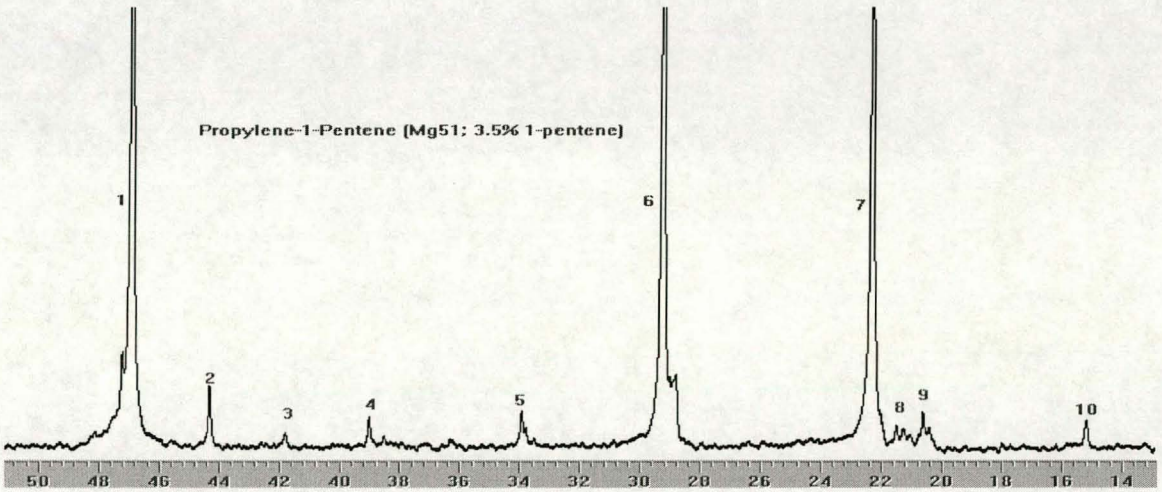

PP8
2.8% 1-pentene

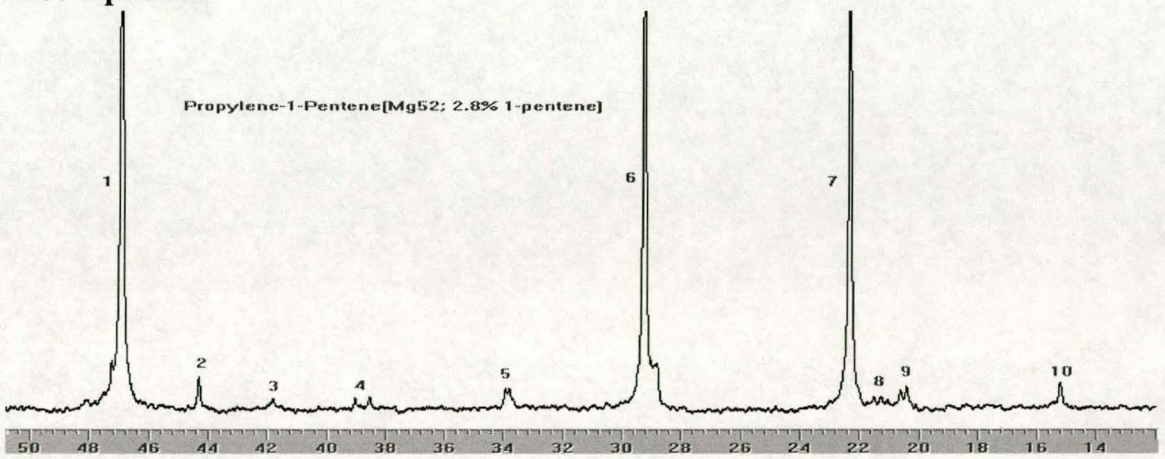

PP40
2.5% 1-pentene

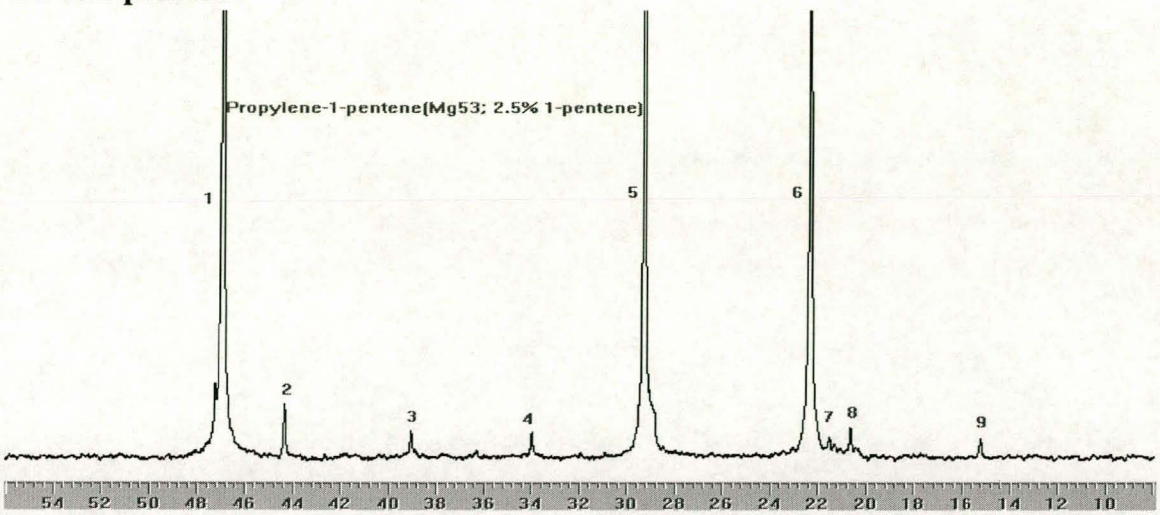

APPENDIX E
(CRYSTAF Curves)

Ethylene/1-pentene Copolymers

EtPn0
0% 1-pentene

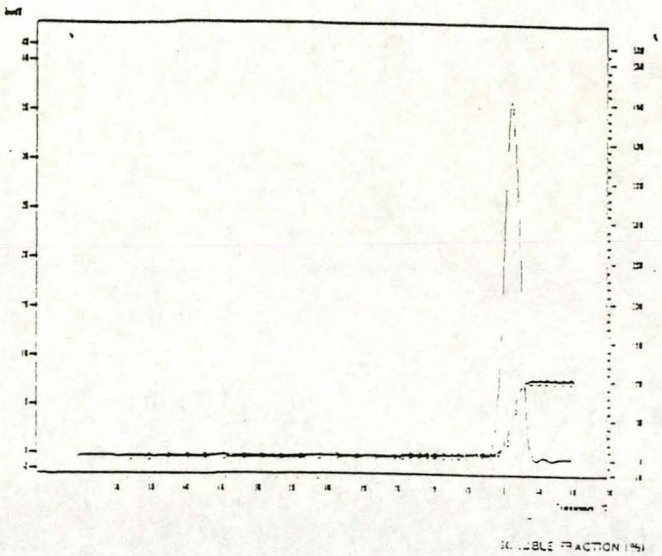

PEAK TEMP	59.9 °C	78.5 °C	81.0 °C	86.7 °C	Extrapolated 0.4
AREA	0.7 %	0.5 %	1.1 %	95.0 %	

ANALYSIS PARAMETERS Method: LLDPE0.1

	Dis.	Sep.	Cryst.	S.F.		
Rate	20.00	20.00	0.10	0.10	Volume	30.00
Temp.	160	95	70	30	Sample vol.	1.50
Time	60	45	0	0	Return vol.	1.10
# Samples			22	15	0 Waste vol.	2.00

Reactor : 1 Concentration 0.07 Detector: Smoothing:

Analyst : Rode/Brinkmann Two wavelengths T<70 T>70

Base line on 0.40 0.50

Sample statistics:

Tw : 95.7 °C r : 1.011 σ : 3.2 °C median : 96.7 °C

Tn : 94.7 °C R : 1.1 SCBI : 3.5 °C

EtPn4
5.2% 1-pentene

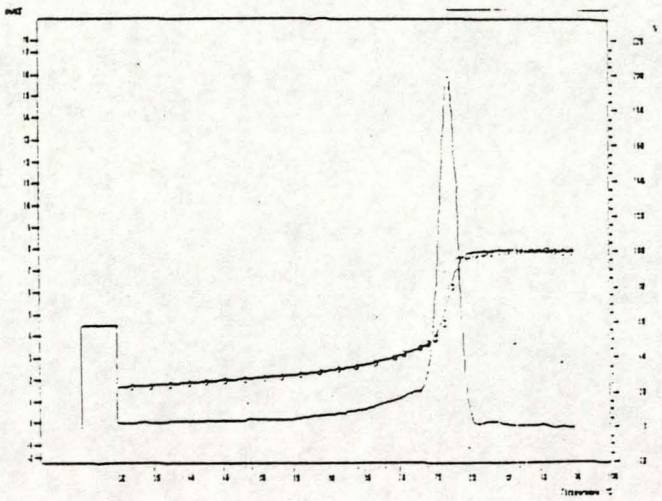

PEAK TEMP	33.6 °C	51.3 °C	77.2 °C	83.3 °C	Extrapolated 23.0
AREA	1.1 %	5.2 %	69.6 %	0.3 %	

ANALYSIS PARAMETERS Method: LLDPE0.1

	Dis.	Sep.	Cryst.	S.F.		
Rate	20.00	20.00	0.10	0.10	Volume	30.00
Temp.	160	95	70	30	Sample vol.	1.50
Time	60	45	0	0	Return vol.	1.10
# Samples			22	15	0 Waste vol.	2.00

Reactor : 3 Concentration 0.07 Detector: Smoothing:

Analyst : Rode/Brinkmann Two wavelengths T<70 T>70

Base line on 0.30 0.70

Sample statistics:

Tw : 56.6 °C r : 1.116 σ : 17.1 °C median : 75.0 °C

Tn : 59.6 °C R : 11.3 SCBI : 12.9 °C

EtPn10
2.6% 1-pentene

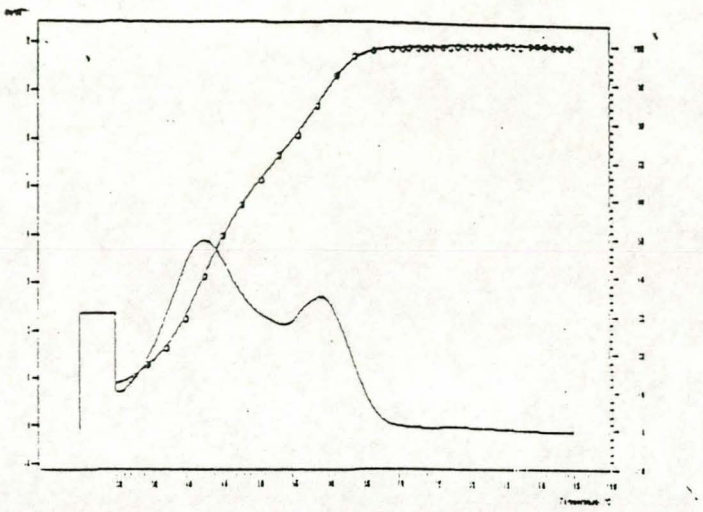

SOLUBLE FRACTION (%)

PEAK TEMP	42.6 °C	58.9 °C	0.0 °C	0.0 °C	Extrapolated	12.1
AREA	80.2 %	27.0 %	0.0 %	0.0 %		

ANALYSIS PARAMETERS Method: LLDPE0.1

	Dis.	Stag.	Cryst.		S.F.		
Rate	20.00	20.00	0.10	0.10		Volume	30.00
Temp.	160	95	70	30		Sample vol.	1.50
Time	60	45	0	0		Returned vol.	1.10
# Samples			22	15	0	Waste vol.	2.00

Reactor : 4 Concentration 0.07 Detector: Smoothing:

Analyst : Rode/Brinkmann Two wavelengths T<70 T>70

Baseline on 0.30 1.30

Sample statistics:

Tw : 47.1 °C r : 1.050 d : 10.2 °C median : 45.1 °C

Tn : 46.0 °C R : 5.0 SCBI 14.8 °C

EtPn20
45.3% 1-pentene

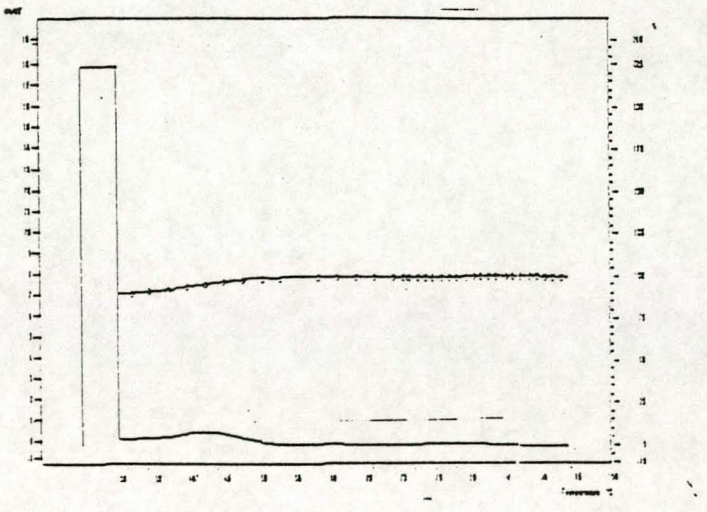

SOLUBLE FRACTION (%)

PEAK TEMP	42.3 °C	59.3 °C	78.4 °C	0.0 °C	Extrapolated	53.7
AREA	9.3 %	0.3 %	0.3 %	0.0 %		

ANALYSIS PARAMETERS Method: LLDPE0.1

	Dis.	Stag.	Cryst.		S.F.		
Rate	20.00	20.00	0.10	0.10		Volume	30.00
Temp.	160	95	70	30		Sample vol.	1.50
Time	60	45	0	0		Returned vol.	1.10
# Samples			22	15	0	Waste vol.	2.00

Reactor : 5 Concentration 0.07 Detector: Smoothing:

Analyst : Rode/Brinkmann Two wavelengths T<70 T>70

Baseline on 0.30 2.00

Sample statistics:

Tw : 32.3 °C r : 1.025 d : 8.4 °C median : 30.0 °C

Propylene/1-pentene Copolymers
PP80
3.8% 1-pentene

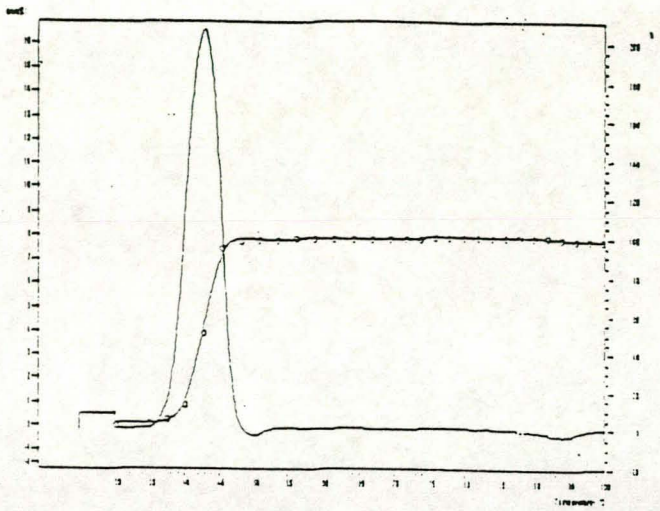

SOLUBLE FRACTION (%)

PEAK TEMP	43.1 °C	54.1 °C	83.6 °C	0.0 °C	Extrapolated	3.4
AREA	95.3 %	0.0 %	0.4 %	0.0 %	At : minutes	3.6

ANALYSIS PARAMETERS Method: PP-co-Pen

	Dis.	Stab.	Cryst.		S.F.		
Rate	20.00	20.00	0.10	0.10		Volume	30.00
Temp.	150	100	70	30		Sample vol.	1.50
Time	60	60	0	30		Returned vol.	1.10
# Samples			15	15	2	Waste vol.	2.00

Reactor : 2 Concentration 0.07 Detector: Smoothing:

Analyst : K.Rode, DKI Two wavelengths T<70 T>70

Base line on 1.00 2.00

Sample statistics:

Tw : 42.4 °C r : 1.004 σ 1.8 °C median : 42.7 °C

Tn : 42.3 °C R : 0.4 SCBI 11.1 °C

PP25
3.5% 1-pentene

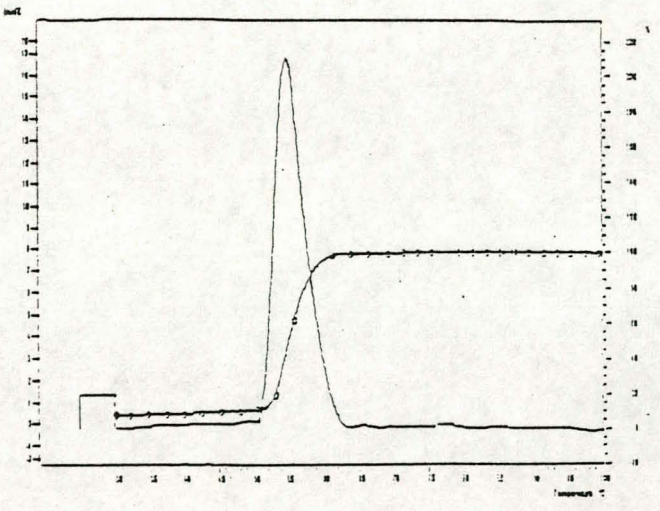

SOLUBLE FRACTION (%)

PEAK TEMP	43.3 °C	49.4 °C	58.1 °C	77.4 °C	Extrapolated	7.8
AREA	1.3 %	1.2 %	88.4 %	0.4 %	At : minutes	7.5

ANALYSIS PARAMETERS Method: PP-co-Pen

	Dis.	Stab.	Cryst.		S.F.		
Rate	20.00	20.00	0.10	0.10		Volume	30.00
Temp.	150	100	70	30		Sample vol.	1.50
Time	60	60	0	30		Returned vol.	1.10
# Samples			15	15	2	Waste vol.	2.00

Reactor : 1 Concentration 0.07 Detector: Smoothing:

Analyst : K.Rode, DKI Two wavelengths T<70 T>70

Base line on 0.20 0.30

Sample statistics:

Tw : 54.6 °C r : 1.019 σ : 3.0 °C median : 55.4 °C

Tn : 53.6 °C R : 1.9 SCB : 16.2 °C

PP8
2.8% 1-pentene

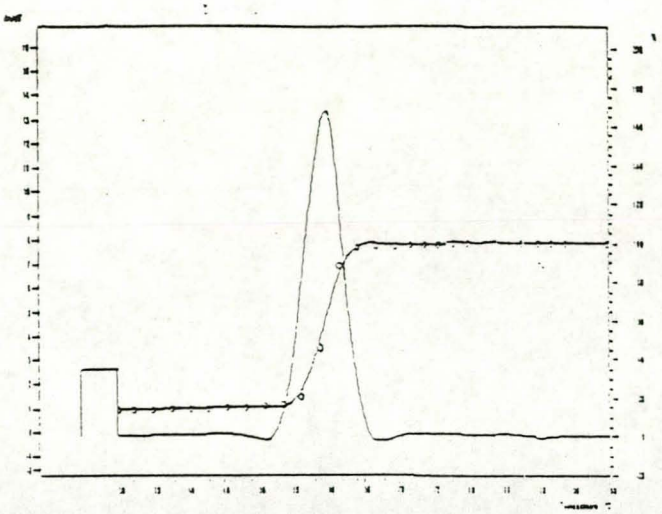

SOLUBLE FRACTION (%)

PEAK TEMP	19.2 °C	44.4 °C	59.8 °C	72.1 °C	Extrapolated	14.0
AREA	0.6 %	0.5 %	84.2 %	0.3 %	At 2 minutes	13.9

ANALYSIS PARAMETERS Method: PP-co-Pen

	Dis.	Stab.	Cryst.	S.P.		
Rate	20.00	20.00	0.10	0.10	Volume	30.00
Temp.	150	100	70	30	Sample vol.	1.50
Time	60	120	0	30	Returned vol.	1.10
# Samples			15	15	2	Wash vol.	2.00

Reactor : 2 Concentration 0.07 Detector: Smoothing:

Analyst : K.Rode, DKI Two wavelengths T<70 T>70

Baseline on 1.50 1.50

Sample statistics:

Tw : 57.2 °C r : 1.038 σ 3.7 °C median : 59.0 °C

Tn : 56.1 °C R : 3.8 SCDI 13.3 °C

PP40
2.5% 1-pentene

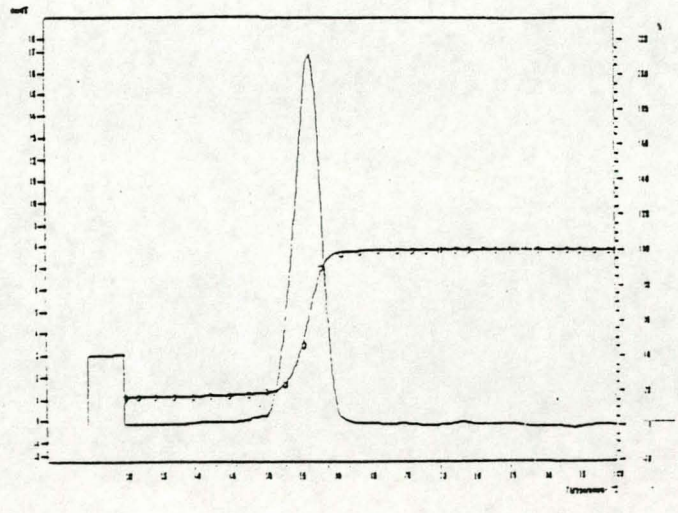

SOLUBLE FRACTION (%)

PEAK TEMP	42.1 °C	58.7 °C	64.5 °C	78.2 °C	Extrapolated	15.8
AREA	0.7 %	81.6 %	0.4 %	0.6 %	At 2 minutes	15.6

ANALYSIS PARAMETERS Method: PP-co-Pen

	Dis.	Stab.	Cryst.	S.P.		
Rate	20.00	20.00	0.10	0.10	Volume	30.00
Temp.	150	100	70	30	Sample vol.	1.50
Time	60	60	0	30	Returned vol.	1.10
# Samples			15	15	2	Wash vol.	2.00

Reactor : 1 Concentration 0.07 Detector: Smoothing:

Analyst : K.Rode, DKI Two wavelengths T<70 T>70

Baseline on 0.50 0.50

Sample statistics:

Tw : 53.9 °C r : 1.036 σ 6.2 °C median : 55.9 °C

Tn : 52.3 °C R : 3.6 SCDI 15.1 °C